Methods in Molecular Biology 1305

Springer Protocols

James Whelan
Monika W. Murcha *Editors*

Plant Mitochondria

Methods and Protocols

Humana Press

METHODS IN MOLECULAR BIOLOGY

Series Editor
John M.Walker
School of Life and Medical Sciences
University of Hertfordshire
Hatfield, Hertfordshire, AL10 9AB, UK

For further volumes:
http://www.springer.com/series/7651

Plant Mitochondria

Methods and Protocols

Edited by

James Whelan

La Trobe University, Bundoora, VIC, Australia

Monika W. Murcha

The University of Western Australia, Crawley, WA, Australia

Humana Press

Editors
James Whelan
La Trobe University
Bundoora, VIC, Australia

Monika W. Murcha
The University of Western Australia
Crawley, WA, Australia

Additional material to this book can be downloaded from http://extras.springer.com.

ISSN 1064-3745 ISSN 1940-6029 (electronic)
Methods in Molecular Biology
ISBN 978-1-4939-2638-1 ISBN 978-1-4939-2639-8 (eBook)
DOI 10.1007/978-1-4939-2639-8

Library of Congress Control Number: 2015937422

Springer New York Heidelberg Dordrecht London

Printed on acid-free paper

Humana Press is a brand of Springer
Springer Science+Business Media LLC New York is part of Springer Science+Business Media (www.springer.com)

Foreword

Highlights in Plant Mitochondrial Research

As someone who started their mitochondrial research in the 1970s, it is interesting to see how far the field has progressed in terms of methodologies and experimental approach and how our knowledge of the way mitochondrial function affects the entire cell's metabolism and gene networks has advanced. Table 1 illustrates the major milestones in this journey.

The late 1950s and 1960s were preoccupied with determining the seat of oxidative phosphorylation and associated metabolism within cells, and once that was more or less accepted, the next two decades were devoted to investigating the mitochondrial genome structure, the composition of the electron transport chain, the basic carbon and nitrogen metabolism associated with mitochondria, and, mainly in mammalian cells, the mechanism of ATP synthesis. This was an intensely competitive period in mitochondrial research, and conferences were often fiery and controversial (and fun, if you liked that sort of thing). The methods we used were quite indirect, mainly based around oxygen electrodes and spectrophotometric and fluorimetric assays. Experiments were imaginative and their interpretation often more so. Without direct proof of concept that is now available with gene knockout and editing technologies, we peered through the glass darkly and speculated widely. While the techniques available were indirect, they yielded results very quickly and if experiments were designed carefully and results analyzed rapidly, enough data for a paper could be generated in a few weeks of intense activity, spurred on by the knowledge that your competitors were doing the same. Try doing that today!

The world-wide cohort of plant mitochondrial researchers in this period was quite small, and the field lived very much in the shadow of photosynthesis—after all, mitochondria are found in all eukaryotes, and it was assumed that their function was much the same, while chloroplasts are unique to plants. A lot of the research into mitochondria in plants focused on their interaction with photosynthesis. The elucidation of the role of mitochondria in cellular oxidative stress and programmed cell death resulted in an explosion of mitochondrial research in mammals and a renewed interest in plant mitochondria. It also became apparent that the electron transport chain of plant mitochondria was quite different—and much more interesting—than their mammalian counterparts, and the scope of mitochondrial metabolism far greater in plants. The role of mitochondria in cytoplasmic male sterility highlighted how much their function could affect the plant, and the application of advanced transcriptomic and proteomic techniques illustrated the complexity of mitochondrial metabolism and its integration with other cellular pathways. It is now obvious that mitochondria are much more than ATP-synthesizing machines and are central to plant growth and development in many different ways. They also lie at the heart of the plant cell's oxidative stress networks, and manipulation of mitochondrial function may lead to enhanced tolerance to both biotic and abiotic stresses.

This is a timely book. It is, as far as I know, the only book devoted to mitochondrial methodology in plants and will be an important reference work for people in this field,

particularly those entering the field. The methodologies described here range from the biochemical, through molecular biology to bioinformatics. These are the techniques that have brought us to where we now stand in our understanding of mitochondria in plants and will be critical in continuing to take the field forward.

Adelaide, SA, Australia *David A. Day*

Table 1
Highlights in discoveries in plant mitochondrial research

Year	Discovery	Species	References
1904	First recorded observation of mitochondria in plants	*Nymphaea alba*	[1]
1925	Presence of cytochromes in plant mitochondria	Various vegetables (eschalots, potato, beans, leeks)	[2]
1929	Cyanide-resistant respiration observed	Sweet pea (*Lathyrus odoratus*)	[3]
1954	Synthesis of ascorbic acid by plant mitochondria	*Pisum Sativum*	[4]
1955	Cyanide insensitive respiration located to mitochondria	*Arum maculatum*	[5]
1970	Demonstration of malic enzyme in plant mitochondria	*Brassica oleracea*	[6]
1978–1989	Isolation of alternative oxidase and production of antibodies	*Arum maculatum*	[7–10]
1975–1981	Presence of pores in outer membrane	S*olanum tuberosum*, *Vigna radiata*	[11, 12]
1951–1962	Isolation of intact mitochondria	*Pisum sativum Spinacia oleracea* S*olanum tuberosum*	[13, 14]
1972–1982	Gradient purification of plant mitochondria	S*olanum tuberosum*, *Pisum sativum Vigna radiata*	[15–17]
1970–1974	Oxidation of External NAD(P)H	*Helianthus tuberosus*; *Brassica oleracea*	[18–21]
1972	Outer membrane NADH dehydrogenase	*Brassica oleracea*	[21–23]
1972–1976	Characterization of mitochondrial ribosomes	Various	[24, 25]
1977	Glycine oxidation located to mitochondria in plants	*Spinacia oleracea*	[26, 27]

(continued)

Table 1
(continued)

Year	Discovery	Species	References
1976–1980	Association of mitochondria with cytoplasmic male sterility	*Zea mays*	[28–30]
1981–1982	Detection of circular DNA molecules from mitochondria	*Nicotiana*, *Datura*, *Solanum*, *Phaseolus*, *Zea*, *Oenothera*	[28, 31–33]
1982	Discovery of chloroplast genome sequences in mitochondrial genome	*Zea mays*	[34]
1985	Cloning of first nuclear-located mitochondrial gene	*Nicotiana plumbaginifolia*	[35]
1985	Expression of "plastid"-type tRNAs in mitochondria	*Phaseolus vulgaris*	[36]
1986	Identification of first nonchromosomal stripe mutants	*Zea mays*	[37]
1987	Discovery of subgenomic DNA molecules	*Zea mays*	[38]
1987–1990	In vitro and in vivo protein import into mitochondria	*Vicia faba*, *Nicotiana tabacum*, *Nicotiana plumbaginifolia*, *Spinacia oleracea*	[39–42]
1989	RNA editing	*Arabidopsis thaliana*	[43–45]
1990–1992	Cloning of Glycine decarboxylase subunits	*Pisum sativum*	[46–50]
1992	In vivo import of tRNA	*Solanum tuberosum*	[51]
1992–1995	Membrane location and bifunctionality of a respiratory chain complex in plants	*Solanum tuberosum*, *Spinacia oleracea*	[52–55]
1992–2011	Purification of complex I	*Solanum tuberosum*, *Beta vulgaris*, *Arabidopsis thaliana*, *Vicia faba*	[56–59]
1992 and 1997	Sequencing of mitochondrial genome	*Marchantia* *Arabidopsis thaliana*	[60, 61]
1993	Elucidation of biochemical activation of alternative oxidase	*Glycine max*, *Vigna radiata*, *Sauromatum guttatum*	[62, 63]
1993–1995	Presence of genes encoding bacterial type cytochrome c maturation pathway	*Triticum aestivum* *Brassica napus*	[64, 65]
1993–2000	Ongoing gene transfer to the Nucleus	Various	[66–68]
1994	Genetic manipulation of alternative oxidase levels	*Nicotiana tabacum*	[69]
1995	Discovery of dual targeting of mitochondria and plastid proteins	*Pisum sativum*	[70]

(continued)

Table 1
(continued)

Year	Discovery	Species	References
1996	First receptor for protein import into plant mitochondria	*Solanum tuberosum*	[71]
1997	Fluorescent protein labeling of plant mitochondria	*Arabidopsis thaliana*	[72]
1997–2003	Autonomous antioxidant machinery in the mitochondrial matrix	*Arabidopsis thaliana*, *Pisum sativum*	[73, 74]
1997, 2000, 2009	Bacteriophage-type RNA polymerases in plant organelles	*Arabidopsis thaliana*	[75–77]
1998	Horizontal gene transfer	*Peperomia polybotyra*; *Various angiosperms*	[78, 79]
1999	Translocation of Cytochrome c in programmed cell death	*Cucumis sativus*	[80]
1999–2003	Cloning of Alternative NAD(P)H dehydrogenase genes	*Solanum tuberosum* *Arabidopsis thaliana*	[81, 82]
2000	Identification of the PPR family of protein	*Arabidopsis thaliana*	[83]
2000–2014	Mitochondrial dynamics, morphology, and controlling factors	*Arabidopsis thaliana*	[84–91]
2001–2014	Proteome characterization	*Arabidopsis thaliana*, *Solanum tuberosum*, *Oryza sativa*, *Triticum aestivum*, *Medicago truncatula*	[92–97]
2001–2008	Functional characterization of mitochondrial antioxidant defense systems	*Arabidopsis thaliana*	[98–100]
2002	Evidence for permeability transition	*Solanum tuberosum*	[101]
2002–2003	PPR involved in CMS restoration	*Petunia* *Raphanus sativus*	[102, 103]
2002–2006	Identification, characterization and crystallization of presequence peptidase for degrading mitochondrial presequences and other unstructured peptides	*Solanum tuberosum*, *Arabidopsis thaliana*	[104, 105]
2003	Identification of nuclear factors that control levels of subgenomic molecules	*Arabidopsis thaliana*	[106]
2003–2007	Identification of Biochemical properties of Type II NAD(P)H dehydrogenases	*Nicotiana sylvestris*, *Arabidopsis thaliana*	[107–109]
2003	Characterization of Supercomplexes of respiratory chain	*Arabidopsis thaliana*	[110]
2003	Association of enzymes of glycolysis with mitochondria	*Arabidopsis thaliana*	[111]

(continued)

Table 1
(continued)

Year	Discovery	Species	References
2003–2004	Respiratory complexes contain plant-specific subunits	*Arabidopsis thaliana* *Oryza sativa*	[112, 113]
2005	Oligomerization of ATP synthase induces curvature of the inner mitochondrial membrane	*Polytomella*	[114,115]
2005–2008	Identification of phenotype lesion resulting from absence of alternative oxidase	*Arabidopsis thaliana*	[116, 117,118]
2005	Carbonic anhydrase domain of complex I	*Arabidopsis thaliana*	[114, 115, 119, 120]
2006	In vitro import of tRNA into mitochondria	*Arabidopsis thaliana*	[121]
2006	Mitochondrial transformation	*Chlamydomonas reinhardtii*	[122]
2006–2012	Measurement of matrix physiology with genetically targeted fluorescent sensors	*Arabidopsis thaliana*	[123–125]
2006–2012	Plant-specific DNA-binding proteins involved in mitochondrial genome stability	*Arabidopsis thaliana*	[126–128]
2007	Demonstration that PPR protein required for splicing in mitochondria	Arabidopsis *thaliana*	[129]
2007	Isolation of highly pure mitochondria using free-flow electrophoresis	*Arabidopsis thaliana*	[130]
2008–2013	Identification of regulators of mitochondrial retrograde signaling	*Arabidopsis thaliana*	[131–134]
2009	Noncyclic mode of TCA cycle in the light	*Xanthium strumarium*	[135]
2009–2014	Characterization of posttranslational modifications of the mitochondrial proteome	*Arabidopsis thaliana*	[136–140]
2009	Demonstration that PPR protein required for editing in mitochondria	*Arabidopsis thaliana*	[141]
2010	Identification and characterization of a protein-only RNase P activity	*Arabidopsis thaliana*	[142]
2012	Mitochondrial pulsing	*Arabidopsis thaliana*	[143]
2012	Identification of first assembly factor for Complex I	*Arabidopsis thaliana*	[144]
2012	Identification of dual located protein in biogenesis and respiratory chain complexes	*Arabidopsis thaliana*	[145]
2012	Code for PPR protein recognition of RNA-binding sites	*Zea mays* *Arabidopsis thaliana*	[146]

(continued)

Table 1 (continued)

Year	Discovery	Species	References
2013	Link between mitochondria and plant immunity	*Arabidopsis thaliana*	[147]
2013	Identification, characterization, and crystallization of organellar oligopeptidase for degrading mitochondrial peptides	*Arabidopsis thaliana*	[148]
2013	Crystal structure of the alternative oxidase	[a]*Trypanosoma brucei brucei*	[149]
2013	Micro-respiratory measurements of tissues	*Arabidopsis thaliana*	[150]

[a]While clearly not a plant, as one of the distinguishing features of plant mitochondria is cyanide-insensitive respiration catalyzed by the alternative oxidase, the elucidation of the structure of the alternative oxidase provides an important platform to understand the activity and activation of the plant enzyme by a variety of organic acids.

References

1. Ernster L, Schatz G (1981) Mitochondria: a historical view. J Cell Biol 91:227–255
2. Keilin D (1925) On cytochrome, a respiratory pigment, common to animals, yeast, and higher plants. Proc R Soc Lond B Biol Sci 98:312–339
3. Genevois ML (1929) Sur la fermentation et sur la respiration chez les végétaux chlorophylliens. Revue Génétique Botanique 41:252–271
4. Mapson LW, Isherwood FA, Chen YT (1954) Biological synthesis of L-ascorbic acid: the conversion of L-galactono-gamma-lactone into L-ascorbic acid by plant mitochondria. Biochem J 56:21–28
5. James WO, Elliott DC (1955) Cyanide-resistant Mitochondria from the Spadix of an Arum. Nature 175:89. doi:10.1038/175089a175080
6. Macrae AR, Moorehouse R (1970) The oxidation of malate by cauliflower bud mitochondria. Eur J Biochem 16:96–102
7. Huq S, Palmer JM (1978) Isolation of a cyanide-resistant duroquinol oxidase from Arum maculatum mitochondria. FEBS Lett 95:217–220
8. Rich PR (1978) Quinol oxidation in Arum maculatum mitochondria and its application to the assay, solubilisation and partial purification of the alternative oxidase. FEBS Lett 96:252–256
9. Elthon TE, McIntosh L (1986) Characterization and solubilization of the alternative oxidase of Sauromatum guttatum mitochondria. Plant Physiol 82:1–6
10. Elthon TE, McIntosh L (1989) Monoclonal antibodies to the alternative oxidase of higher plant mitochondria. Plant Physiol 89: 1311–1317
11. Mannella CA, Bonner WDJ (1975) X-ray diffraction from oriented outer mitochondrial membranes. Detection of in-plane subunit structure. Biochim Biphys Acta 413:226–233
12. Mannella CA (1981) Structure of the outer mitochondrial membrane. Analysis of x-ray diffraction from the plant membrane. Biochim Biphys Acta 645:33–40
13. Miller A, Bonner J, Axelrod B, Bandurski RS (1951) Oxidative and phosphorylative activity of plant mitochondria. Proc Natl Acad Sci U S A 37:855–862
14. Wiskich JT, Bonner WD (1963) Preparation and properties of sweet potato mitochondria. Plant Physiol 38:594–604
15. Douce R, Christensen EL, Bonner WDJ (1972) Preperation on intact plant mitochondria. Biochim Biophys Acta 275: 148–160
16. Neuburger M, Journet E-P, Bligny R, Carde J-P, Douce R (1982) Purification of plant mitochondria by isopycnic centrifugationin density gradient of Percoll. Arch Biochem Biophys 217:312–323
17. Day DA, Neuburger M, Douce R (1985) Biochemical characterisation of chlorophyll-

free mitochondria from pea leaves. Aust J Plant Physiol 12:219–228
18. Cunningham WB (1964) Oxidation of externally added NADH by isolated corn root mitochondria. Plant Physiol 39:699–703
19. Coleman JO, Palmer JM (1971) Role of Ca(2+) in the oxidation of exogenous NADH by plant mitochondria. FEBS Lett 17: 203–208
20. Palmer JM, Passam HC (1971) The oxidation of exogenous reduced nicotinamide-adenine dinucleotide by plant mitochondria. Biochem J 122:16P–17P
21. Day DA, Wiskich JT (1975) Isolation and properties of the outer membrane of plant mitochondria. Arch Biochem Biophys 171:117–123
22. Moreau F, Lance C (1972) Isolement et propriétés des membranes externes et internes de mitochondries végétales. Biochimie 54: 1335–1348
23. Douce R, Manella CA, Bonner WD Jr (1973) The external NADH dehydrogenases of intact plant mitochondria. Biochim Biphys Acta 292:105
24. Leaver CJ, Harmey MA (1972) Isolation and characterization of mitochondrial ribosomes from higher plants. Biochem J 129:37P–38P
25. Leaver CJ, Harmey MA (1976) Higher-plant mitochondrial ribosomes contain a 5S ribosomal ribonucleic acid component. Biochem J 157:275–277
26. Woo KC, Osmond CB (1976) Glycine decarboxylation in mitochondria isolated from spinach leaves. Aust J Plant Physiol 3: 771–785
27. Moore AL, Jackson C, Halliwell B, Dench JE, Hall DO (1977) Intramitochondrial localization of glycine decarboxylase in spinach leaves. Biochem Biophys Res Commun 78:483–491
28. Levings CS 3rd, Pring DR (1976) Restriction endonuclease analysis of mitochondrial DNA from normal and Texas cytoplasmic male-sterile maize. Science 193:158–160
29. Warmke HE, Lee SL (1977) Mitochondrial degeneration in Texas cytoplasmic male-sterile corn anthers. J Hered 68:213–222
30. Forde BG, Leaver CJ (1980) Nuclear and cytoplasmic genes controlling synthesis of varient mitochondrial peptides in male sterile maize. Proc Natl Acad Sci U S A 77:418–422
31. Kolodner R, Tewari KK (1972) Pyysicochemical characterisation of mitochondrial DNA from pea leaves. Proc Natl Acad Sci U S A 69:1830–1834
32. Sparks RBJ, Dale RMK (1980) Characterisation of 3H-labelled supercolied mitochondrial DNA from tobacco suspension cultured cells. Mol Gen Genet 180: 351–355
33. Brennicke A (1980) Mitochondrial DNA from Oenothera berteriana. Plant Physiol 65:1207–1210
34. Stern DB, Lonsdale DM (1982) Mitochondrial and chloroplast genomes of maize have a 12-kilobase DNA sequence in common. Nature 299:698–702
35. Boutry M, Chua NH (1985) A nuclear gene encoding the beta subunit of the mitochondrial ATP synthase in Nicotiana plumbaginifolia. EMBO J 4:2159–2165
36. Marechal L, Guillemaut P, Grienenberger JM, Jeannin G, Weil JH (1985) Sequence and codon recognition of bean mitochondria and chloroplast tRNAsTrp: evidence for a high degree of homology. Nucleic Acids Res 13:4411–4416
37. Newton KJ, Coe EH (1986) Mitochondrial DNA changes in abnormal growth (nonchromosomal stripe) mutants of maize. Proc Natl Acad Sci U S A 83:7363–7366
38. Small I, Suffolk R, Leaver CJ (1989) Evolution of plant mitochondrial genomes via substoichiometric intermediates. Cell 58:69–76
39. Boutry M, Nagy F, Poulsen C, Aoyagi K, Chua NH (1987) Targeting of bacterial chloramphenicol acetyltransferase to mitochondria in transgenic plants. Nature 328: 340–342
40. Whelan J, Dolan L, Harmey MA (1988) Import of precursor proteins into Vicia faba mitochondria. FEBS Lett 236:217–220
41. Schmitz UK, Lonsdale DM (1989) A yeast mitochondrial presequence functions as a signal for targeting to plant mitochondria in vivo. Plant Cell 1:783–791
42. Whelan J, Knorpp C, Glaser E (1990) Sorting of precursor proteins between isolated spinach leaf mitochondria and chloroplasts. Plant Mol Biol 14:977–982
43. Covello PS, Gray MW (1989) RNA editing in plant mitochondria. Nature 341:662–666
44. Gualberto JM, Lamattina L, Bonnard G, Weil JH, Grienenberger JM (1989) RNA editing in wheat mitochondria results in the conservation of protein sequences. Nature 341: 660–662
45. Hiesel R, Wissinger B, Schuster W, Brennicke A (1989) RNA editing in plant mitochondria. Science 246:1632–1634
46. Kim Y, Oliver DJ (1990) Molecular cloning, transcriptional characterization, and sequencing of cDNA encoding the H-protein of the

mitochondrial glycine decarboxylase complex in peas. J Biol Chem 265:848–853

47. Macherel D, Lebrun M, Gagnon J, Neuburger M, Douce R (1990) cDNA cloning, primary structure and gene expression for H-protein, a component of the glycine-cleavage system (glycine decarboxylase) of pea (Pisum sativum) leaf mitochondria. Biochem J 268: 783–789
48. Bourguignon J, Macherel D, Neuburger M, Douce R (1992) Isolation, characterization, and sequence analysis of a cDNA clone encoding L-protein, the dihydrolipoamide dehydrogenase component of the glycine cleavage system from pea-leaf mitochondria. Eur J Biochem 204:865–873
49. Turner SR, Ireland R, Morgan C, Rawsthorne S (1992) Identification and localization of multiple forms of serine hydroxymethyltransferase in pea (Pisum sativum) and characterization of a cDNA encoding a mitochondrial isoform. J Biol Chem 267:13528–13534
50. Turner SR, Ireland R, Rawsthorne S (1992) Cloning and characterization of the P subunit of glycine decarboxylase from pea (Pisum sativum). J Biol Chem 267:5355–5360
51. Small I, Marechal-Drouard L, Masson J, Pelletier G, Cosset A, Weil JH, Dietrich A (1992) In vivo import of a normal or mutagenized heterologous transfer RNA into the mitochondria of transgenic plants: towards novel ways of influencing mitochondrial gene expression? EMBO J 11:1291–1296
52. Eriksson AC, Glaser E (1992) Mitochondrial processing peptidase: a general processing proteinase of spinach leaf mitochondria in a membrane-bound enzyme. Biochim Biophys Acta 1140:208–214
53. Eriksson AC, Sjoling S, Glaser E (1994) The ubiquinol cytochrome c oxidoreductase complex of spinach leaf mitochondria is involeved in both respiration and protein processing. Biochim Biophys Acta 1186:221–231
54. Braun HP, Emmermann M, Kruft V, Schmitz UK (1992) The general mitochondrial processing peptidase from potato is an integral part of cytochrome c reductase of the respiratory chain. EMBO J 11:3219–3227
55. Braun HP, Schmitz UK (1995) Are the 'core' proteins of the mitochondrial bc1 complex evolutionary relics of a processing protease? Trends Biochem Sci 20:171–175
56. Leterme S, Boutry M (1993) Purification and preliminary characterization of mitochondrial complex I (NADH: ubiquinone reductase) from broad bean (Vicia faba L.). Plant Physiol 102:435–443
57. Soole KL, Dry IB, Wiskich JT (1992) Partial purification and characterization of complex I, NADH:ubiquinone reductase, from the inner membrane of beetroot mitochondria. Plant Physiol 98:588–594
58. Klodmann J, Braun HP (2011) Proteomic approach to characterize mitochondrial complex I from plants. Phytochemistry 72: 1071–1080
59. Herz U, Schroder W, Liddell A, Leaver CJ, Brennicke A, Grohmann L (1994) Purification of the NADH:ubiquinone oxidoreductase (complex I) of the respiratory chain from the inner mitochondrial membrane of Solanum tuberosum. J Biol Chem 269:2263–2269
60. Oda K, Yamato K, Ohta E, Nakamura Y, Takemura M, Nozato N, Akashi K, Kanegae T, Ogura Y, Kohchi T et al (1992) Gene organization deduced from the complete sequence of liverwort Marchantia polymorpha mitochondrial DNA. A primitive form of plant mitochondrial genome. J Mol Biol 223:1–7
61. Unseld M, Marienfeld JR, Brandt P, Brennicke A (1997) The mitochondrial genome of Arabidopsis thaliana contains 57 genes in 366,924 nucleotides. Nat Genet 15:57–61
62. Millar AH, Wiskich JT, Whelan J, Day DA (1993) Organic acid activation of the alternative oxidase of plant mitochondria. FEBS Lett 329:259–262
63. Umbach AL, Siedow JN (1993) Covalent and noncovalent dimers of the cyanide-resistant alternative oxidase protein in higher plant mitochondria and their relationship to enzyme activity. Plant Physiol 103:845–854
64. Gonzalez DH, Bonnard G, Grienenberger JM (1993) A gene involved in the biogenesis of c-type cytochromes is co-transcribed with a ribosomal protein gene in wheat mitochondria [corrected]. Curr Genet 24:248–255
65. Bonnard G, Grienenberger JM (1995) A gene proposed to encode a transmembrane domain of an ABC transporter is expressed in wheat mitochondria. Mol Gen Genet 246:91–99
66. Brennicke A, Grohmann L, Hiesel R, Knoop V, Schuster W (1993) The mitochondrial genome on its way to the nucleus: different stages of gene transfer in higher plants. FEBS Lett 325:140–145
67. Kadowaki K, Kubo N, Ozawa K, Hirai A (1996) Targeting presequence acquisition after mitochondrial gene transfer to the nucleus occurs by duplication of existing targeting signals. EMBO J 15:6652–6661

68. Adams KL, Daley DO, Qiu YL, Whelan J, Palmer JD (2000) Repeated, recent and diverse transfers of a mitochondrial gene to the nucleus in flowering plants. Nature 408:354–357
69. Vanlerberghe GC, Vanlerberghe AE, McIntosh L (1994) Molecular genetic alteration of plant respiration (silencing and overexpression of alternative oxidase in transgenic tobacco). Plant Physiol 106:1503–1510
70. Creissen G, Reynolds H, Xue Y, Mullineaux P (1995) Simultaneous targeting of pea glutathione reductase and of a bacterial fusion protein to chloroplasts and mitochondria in transgenic tobacco. Plant J 8:167–175
71. Heins L, Schmitz UK (1996) A receptor for protein import into potato mitochondria. Plant J 9:829–839
72. Kohler RH, Zipfel WR, Webb WW, Hanson MR (1997) The green fluorescent protein as a marker to visualize plant mitochondria in vivo. Plant J 11:613–621
73. Chew O, Whelan J, Millar AH (2003) Molecular definition of the ascorbate-glutathione cycle in Arabidopsis mitochondria reveals dual targeting of antioxidant defenses in plants. J Biol Chem 278: 46869–46877
74. Jimenez A, Hernandez JA, Del Rio LA, Sevilla F (1997) Evidence for the presence of the ascorbate-glutathione cycle in mitochondria and peroxisomes of pea leaves. Plant Physiol 114:275–284
75. Hedtke B, Borner T, Weihe A (1997) Mitochondrial and chloroplast phage-type RNA polymerases in Arabidopsis. Science 277:809–811
76. Hedtke B, Borner T, Weihe A (2000) One RNA polymerase serving two genomes. EMBO Rep 1:435–440
77. Kuhn K, Richter U, Meyer EH, Delannoy E, de Longevialle AF, O'Toole N, Borner T, Millar AH, Small ID, Whelan J (2009) Phage-type RNA polymerase RPOTmp performs gene-specific transcription in mitochondria of Arabidopsis thaliana. Plant Cell 21:2762–2779
78. Adams KL, Clements MJ, Vaughn JC (1998) The Peperomia mitochondrial coxI group I intron: timing of horizontal transfer and subsequent evolution of the intron. J Mol Evol 46:689–696
79. Cho Y, Qiu YL, Kuhlman P, Palmer JD (1998) Explosive invasion of plant mitochondria by a group I intron. Proc Natl Acad Sci U S A 95:14244–14249
80. Balk J, Leaver CJ, McCabe PF (1999) Translocation of cytochrome c from the mitochondria to the cytosol occurs during heat-induced programmed cell death in cucumber plants. FEBS Lett 463:151–154
81. Rasmusson AG, Svensson AS, Knoop V, Grohmann L, Brennicke A (1999) Homologues of yeast and bacterial rotenone-insensitive NADH dehydrogenases in higher eukaryotes: two enzymes are present in potato mitochondria. Plant J 20:79–87
82. Michalecka AM, Svensson AS, Johansson FI, Agius SC, Johanson U, Brennicke A, Binder S, Rasmusson AG (2003) Arabidopsis genes encoding mitochondrial type II NAD(P)H dehydrogenases have different evolutionary origin and show distinct responses to light. Plant Physiol 133:642–652
83. Small ID, Peeters N (2000) The PPR motif - a TPR-related motif prevalent in plant organellar proteins. Trends Biochem Sci 25:46–47
84. Logan DC, Leaver CJ (2000) Mitochondria-targeted GFP highlights the heterogeneity of mitochondrial shape, size and movement within living plant cells. J Exp Bot 51: 865–871
85. Arimura S, Tsutsumi N (2002) A dynamin-like protein (ADL2b), rather than FtsZ, is involved in Arabidopsis mitochondrial division. Proc Natl Acad Sci U S A 99: 5727–5731
86. Logan DC, Scott I, Tobin AK (2003) The genetic control of plant mitochondrial morphology and dynamics. Plant J 36:500–509
87. Arimura S, Aida GP, Fujimoto M, Nakazono M, Tsutsumi N (2004) Arabidopsis dynamin-like protein 2a (ADL2a), like ADL2b, is involved in plant mitochondrial division. Plant Cell Physiol 45:236–242
88. Logan DC, Scott I, Tobin AK (2004) ADL2a, like ADL2b, is involved in the control of higher plant mitochondrial morphology. J Exp Bot 55:783–785
89. Scott I, Tobin AK, Logan DC (2006) BIGYIN, an orthologue of human and yeast FIS1 genes functions in the control of mitochondrial size and number in Arabidopsis thaliana. J Exp Bot 57:1275–1280
90. Taylor NL, Howell KA, Heazlewood JL, Tan TY, Narsai R, Huang S, Whelan J, Millar AH (2010) Analysis of the rice mitochondrial carrier family reveals anaerobic accumulation of a basic amino acid carrier involved in arginine metabolism during seed germination. Plant Physiol 154:691–704
91. Pan R, Jones AD, Hu J (2014) Cardiolipin-mediated mitochondrial dynamics and stress response in Arabidopsis. Plant Cell 26:391–409

92. Kruft V, Eubel H, Jansch L, Werhahn W, Braun HP (2001) Proteomic approach to identify novel mitochondrial proteins in Arabidopsis. Plant Physiol 127:1694–1710
93. Millar AH, Sweetlove LJ, Giege P, Leaver CJ (2001) Analysis of the Arabidopsis mitochondrial proteome. Plant Physiol 127: 1711–1727
94. Dubinin J, Braun HP, Schmitz U, Colditz F (2011) The mitochondrial proteome of the model legume Medicago truncatula. Biochim Biophys Acta 1814:1658–1668
95. Huang S, Taylor NL, Narsai R, Eubel H, Whelan J, Millar AH (2009) Experimental analysis of the rice mitochondrial proteome, its biogenesis, and heterogeneity. Plant Physiol 149:719–734
96. Jacoby RP, Millar AH, Taylor NL (2010) Wheat mitochondrial proteomes provide new links between antioxidant defense and plant salinity tolerance. J Proteome Res 9: 6595–6604
97. Salvato F, Havelund JF, Chen M, Rao RS, Rogowska-Wrzesinska A, Jensen ON, Gang DR, Thelen JJ, Moller IM (2014) The potato tuber mitochondrial proteome. Plant Physiol 164:637–653
98. Laloi C, Rayapuram N, Chartier Y, Grienenberger JM, Bonnard G, Meyer Y (2001) Identification and characterization of a mitochondrial thioredoxin system in plants. Proc Natl Acad Sci U S A 98:14144–14149
99. Finkemeier I, Goodman M, Lamkemeyer P, Kandlbinder A, Sweetlove LJ, Dietz KJ (2005) The mitochondrial type II peroxiredoxin F is essential for redox homeostasis and root growth of Arabidopsis thaliana under stress. J Biol Chem 280:12168–12180
100. Morgan MJ, Lehmann M, Schwarzlander M, Baxter CJ, Sienkiewicz-Porzucek A, Williams TC, Schauer N, Fernie AR, Fricker MD, Ratcliffe RG, Sweetlove LJ, Finkemeier I (2008) Decrease in manganese superoxide dismutase leads to reduced root growth and affects tricarboxylic acid cycle flux and mitochondrial redox homeostasis. Plant Physiol 147:101–114
101. Arpagaus S, Rawyler A, Braendle R (2002) Occurrence and characteristics of the mitochondrial permeability transition in plants. J Biol Chem 277:1780–1787
102. Bentolila S, Alfonso AA, Hanson MR (2002) A pentatricopeptide repeat-containing gene restores fertility to cytoplasmic male-sterile plants. Proc Natl Acad Sci U S A 99: 10887–10892
103. Koizuka N, Imai R, Fujimoto H, Hayakawa T, Kimura Y, Kohno-Murase J, Sakai T, Kawasaki S, Imamura J (2003) Genetic characterization of a pentatricopeptide repeat protein gene, orf687, that restores fertility in the cytoplasmic male-sterile Kosena radish. Plant J 34:407–415
104. Stahl A, Moberg P, Ytterberg J, Panfilov O, Brockenhuus Von Lowenhielm H, Nilsson F, Glaser E (2002) Isolation and identification of a novel mitochondrial metalloprotease (PreP) that degrades targeting presequences in plants. J Biol Chem 277:41931–41939
105. Johnson KA, Bhushan S, Stahl A, Hallberg BM, Frohn A, Glaser E, Eneqvist T (2006) The closed structure of presequence protease PreP forms a unique 10,000 Angstroms3 chamber for proteolysis. EMBO J 25: 1977–1986
106. Abdelnoor RV, Yule R, Elo A, Christensen AC, Meyer-Gauen G, Mackenzie SA (2003) Substoichiometric shifting in the plant mitochondrial genome is influenced by a gene homologous to MutS. Proc Natl Acad Sci U S A 100:5968–5973
107. Moore CS, Cook-Johnson RJ, Rudhe C, Whelan J, Day DA, Wiskich JT, Soole KL (2003) Identification of AtNDI1, an internal non-phosphorylating NAD(P)H dehydrogenase in Arabidopsis mitochondria. Plant Physiol 133:1968–1978
108. Michalecka AM, Agius SC, Moller IM, Rasmusson AG (2004) Identification of a mitochondrial external NADPH dehydrogenase by overexpression in transgenic Nicotiana sylvestris. Plant J 37:415–425
109. Geisler DA, Broselid C, Hederstedt L, Rasmusson AG (2007) Ca2+-binding and Ca2+-independent respiratory NADH and NADPH dehydrogenases of Arabidopsis thaliana. J Biol Chem 282:28455–28464
110. Eubel H, Jansch L, Braun HP (2003) New insights into the respiratory chain of plant mitochondria. Supercomplexes and a unique composition of complex II. Plant Physiol 133:274–286
111. Giege P, Heazlewood JL, Roessner-Tunali U, Millar AH, Fernie AR, Leaver CJ, Sweetlove LJ (2003) Enzymes of glycolysis are functionally associated with the mitochondrion in Arabidopsis cells. Plant Cell 15:2140–2151
112. Heazlewood JL, Howell KA, Millar AH (2003) Mitochondrial complex I from Arabidopsis and rice: orthologs of mammalian and fungal components coupled with plant-specific subunits. Biochim Biophys Acta 1604:159–169
113. Millar AH, Eubel H, Jansch L, Kruft V, Heazlewood JL, Braun HP (2004) Mitochondrial cytochrome c oxidase and

succinate dehydrogenase complexes contain plant specific subunits. Plant Mol Biol 56: 77–90

114. Dudkina NV, Eubel H, Keegstra W, Boekema EJ, Braun HP (2005) Structure of a mitochondrial supercomplex formed by respiratory-chain complexes I and III. Proc Natl Acad Sci U S A 102:3225–3229
115. Dudkina NV, Heinemeyer J, Keegstra W, Boekema EJ, Braun HP (2005) Structure of dimeric ATP synthase from mitochondria: an angular association of monomers induces the strong curvature of the inner membrane. FEBS Lett 579:5769–5772
116. Giraud E, Ho LH, Clifton R, Carroll A, Estavillo G, Tan YF, Howell KA, Ivanova A, Pogson BJ, Millar AH, Whelan J (2008) The absence of ALTERNATIVE OXIDASE1a in Arabidopsis results in acute sensitivity to combined light and drought stress. Plant Physiol 147:595–610
117. Fiorani F, Umbach AL, Siedow JN (2005) The alternative oxidase of plant mitochondria is involved in the acclimation of shoot growth at low temperature. A study of Arabidopsis AOX1a transgenic plants. Plant Physiol 139:1795–1805
118. Umbach AL, Fiorani F, Siedow JN (2005) Characterization of transformed Arabidopsis with altered alternative oxidase levels and analysis of effects on reactive oxygen species in tissue. Plant Physiol 139:1806–1820
119. Sunderhaus S, Dudkina NV, Jansch L, Klodmann J, Heinemeyer J, Perales M, Zabaleta E, Boekema EJ, Braun HP (2006) Carbonic anhydrase subunits form a matrix-exposed domain attached to the membrane arm of mitochondrial complex I in plants. J Biol Chem 281:6482–6488
120. Klodmann J, Sunderhaus S, Nimtz M, Jansch L, Braun HP (2010) Internal architecture of mitochondrial complex I from Arabidopsis thaliana. Plant Cell 22:797–810
121. Salinas T, Duchene AM, Delage L, Nilsson S, Glaser E, Zaepfel M, Marechal-Drouard L (2006) The voltage-dependent anion channel, a major component of the tRNA import machinery in plant mitochondria. Proc Natl Acad Sci U S A 103:18362–18367
122. Remacle C, Cardol P, Coosemans N, Gaisne M, Bonnefoy N (2006) High-efficiency biolistic transformation of Chlamydomonas mitochondria can be used to insert mutations in complex I genes. Proc Natl Acad Sci U S A 103:4771–4776
123. Jiang K, Schwarzer C, Lally E, Zhang S, Ruzin S, Machen T, Remington SJ, Feldman L (2006) Expression and characterization of a redox-sensing green fluorescent protein (reduction-oxidation-sensitive green fluorescent protein) in Arabidopsis. Plant Physiol 141:397–403
124. Schwarzlander M, Fricker MD, Muller C, Marty L, Brach T, Novak J, Sweetlove LJ, Hell R, Meyer AJ (2008) Confocal imaging of glutathione redox potential in living plant cells. J Microsc 231:299–316
125. Loro G, Drago I, Pozzan T, Schiavo FL, Zottini M, Costa A (2012) Targeting of Cameleons to various subcellular compartments reveals a strict cytoplasmic/mitochondrial Ca(2)(+) handling relationship in plant cells. Plant J 71:1–13
126. Zaegel V, Guermann B, Le Ret M, Andres C, Meyer D, Erhardt M, Canaday J, Gualberto JM, Imbault P (2006) The plant-specific ssDNA binding protein OSB1 is involved in the stoichiometric transmission of mitochondrial DNA in Arabidopsis. Plant Cell 18: 3548–3563
127. Cappadocia L, Marechal A, Parent JS, Lepage E, Sygusch J, Brisson N (2010) Crystal structures of DNA-Whirly complexes and their role in Arabidopsis organelle genome repair. Plant Cell 22:1849–1867
128. Janicka S, Kuhn K, Le Ret M, Bonnard G, Imbault P, Augustyniak H, Gualberto JM (2012) A RAD52-like single-stranded DNA binding protein affects mitochondrial DNA repair by recombination. Plant J 72:423–435
129. de Longevialle AF, Meyer EH, Andres C, Taylor NL, Lurin C, Millar AH, Small ID (2007) The pentatricopeptide repeat gene OTP43 is required for trans-splicing of the mitochondrial nad1 Intron 1 in Arabidopsis thaliana. Plant Cell 19:3256–3265
130. Eubel H, Lee CP, Kuo J, Meyer EH, Taylor NL, Millar AH (2007) Free-flow electrophoresis for purification of plant mitochondria by surface charge. Plant J 52:583–594
131. Giraud E, Van Aken O, Ho LH, Whelan J (2009) The transcription factor ABI4 is a regulator of mitochondrial retrograde expression of ALTERNATIVE OXIDASE1a. Plant Physiol 150:1286–1296
132. Ng S, Giraud E, Duncan O, Law SR, Wang Y, Xu L, Narsai R, Carrie C, Walker H, Day DA, Blanco NE, Strand A, Whelan J, Ivanova A (2013) Cyclin-dependent kinase E1 (CDKE1) provides a cellular switch in plants between growth and stress responses. J Biol Chem 288:3449–3459
133. Ng S, Ivanova A, Duncan O, Law SR, Van Aken O, De Clercq I, Wang Y, Carrie C, Xu L, Kmiec B, Walker H, Van Breusegem F,

Whelan J, Giraud E (2013) A membrane-bound NAC transcription factor, ANAC017, mediates mitochondrial retrograde signaling in Arabidopsis. Plant Cell 25:3450–3471

134. Ng S, De Clercq I, Van Aken O, Law SR, Ivanova A, Willems P, Giraud E, Van Breusegem F, Whelan J (2014) Anterograde and retrograde regulation of nuclear genes encoding mitochondrial proteins during growth, development, and stress. Mol Plant 7:1075–1093
135. Tcherkez G, Mahe A, Gauthier P, Mauve C, Gout E, Bligny R, Cornic G, Hodges M (2009) In folio respiratory fluxomics revealed by 13C isotopic labeling and H/D isotope effects highlight the noncyclic nature of the tricarboxylic acid "cycle" in illuminated leaves. Plant Physiol 151:620–630
136. Ito J, Taylor NL, Castleden I, Weckwerth W, Millar AH, Heazlewood JL (2009) A survey of the Arabidopsis thaliana mitochondrial phosphoproteome. Proteomics 9:4229–4240
137. Tan YF, O'Toole N, Taylor NL, Millar AH (2010) Divalent metal ions in plant mitochondria and their role in interactions with proteins and oxidative stress-induced damage to respiratory function. Plant Physiol 152:747–761
138. Havelund JF, Thelen JJ, Moller IM (2013) Biochemistry, proteomics, and phosphoproteomics of plant mitochondria from non-photosynthetic cells. Front Plant Sci 4:51
139. Konig AC, Hartl M, Boersema PJ, Mann M, Finkemeier I (2014) The mitochondrial lysine acetylome of Arabidopsis. Mitochondrion
140. Smith-Hammond CL, Hoyos E, Miernyk JA (2014) The pea seedling mitochondrial N-lysine acetylome. Mitochondrion
141. Zehrmann A, Verbitskiy D, van der Merwe JA, Brennicke A, Takenaka M (2009) A DYW domain-containing pentatricopeptide repeat protein is required for RNA editing at multiple sites in mitochondria of Arabidopsis thaliana. Plant Cell 21:558–567
142. Gobert A, Gutmann B, Taschner A, Gossringer M, Holzmann J, Hartmann RK, Rossmanith W, Giege P (2010) A single Arabidopsis organellar protein has RNase P activity. Nat Struct Mol Biol 17:740–744
143. Schwarzlander M, Logan DC, Johnston IG, Jones NS, Meyer AJ, Fricker MD, Sweetlove LJ (2012) Pulsing of membrane potential in individual mitochondria: a stress-induced mechanism to regulate respiratory bioenergetics in Arabidopsis. Plant Cell 24:1188–1201
144. Schertl P, Sunderhaus S, Klodmann J, Grozeff GE, Bartoli CG, Braun HP (2012) L-galactono-1,4-lactone dehydrogenase (GLDH) forms part of three subcomplexes of mitochondrial complex I in Arabidopsis thaliana. J Biol Chem 287:14412–14419
145. Wang Y, Carrie C, Giraud E, Elhafez D, Narsai R, Duncan O, Whelan J, Murcha MW (2012) Dual location of the mitochondrial preprotein transporters B14.7 and Tim23-2 in complex I and the TIM17:23 complex in Arabidopsis links mitochondrial activity and biogenesis. Plant Cell 24:2675–2695
146. Barkan A, Rojas M, Fujii S, Yap A, Chong YS, Bond CS, Small I (2012) A combinatorial amino acid code for RNA recognition by pentatricopeptide repeat proteins. PLoS Genet 8:e1002910
147. Huang Y, Chen X, Liu Y, Roth C, Copeland C, McFarlane HE, Huang S, Lipka V, Wiermer M, Li X (2013) Mitochondrial AtPAM16 is required for plant survival and the negative regulation of plant immunity. Nat Commun 4:2558
148. Kmiec B, Teixeira PF, Berntsson RP, Murcha MW, Branca RM, Radomiljac JD, Regberg J, Svensson LM, Bakali A, Langel U, Lehtio J, Whelan J, Stenmark P, Glaser E (2013) Organellar oligopeptidase (OOP) provides a complementary pathway for targeting peptide degradation in mitochondria and chloroplasts. Proc Natl Acad Sci U S A 110: E3761–E3769
149. Shiba T, Kido Y, Sakamoto K, Inaoka DK, Tsuge C, Tatsumi R, Takahashi G, Balogun EO, Nara T, Aoki T, Honma T, Tanaka A, Inoue M, Matsuoka S, Saimoto H, Moore AL, Harada S, Kita K (2013) Structure of the trypanosome cyanide-insensitive alternative oxidase. Proc Natl Acad Sci U S A 110: 4580–4585
150. Sew YS, Stroher E, Holzmann C, Huang S, Taylor NL, Jordana X, Millar AH (2013) Multiplex micro-respiratory measurements of Arabidopsis tissues. New Phytol 200: 922–932

Preface

The chapters to follow detail research and observations into plant mitochondria spanning over a century in time. However, this research intensified in the 1970s and has been continuing to the present day. The findings of mitochondrial research continually surprises the scientific community, whether it be the presence of cyanide-insensitive respiration to large genomes whose transcripts undergo specific editing, requiring at least hundreds of nuclear-encoded gene products to produce just 50 proteins. The ability to uncover these unique features is underpinned by the methodology that is used to investigate plant mitochondria, from morphology to detailed molecular mechanisms. With plant mitochondria representing a small proportion of the cell in terms of volume or protein content, the question of contamination is at the forefront of many studies into mitochondria. There are still many questions remaining which are made even more challenging due to the large variety of plants and tissues/organs that are used in studying plant mitochondria. However, this diversity is useful for plant mitochondrial research, and whilst plants display many similarities, it should not be forgotten that up to hundreds of millions of years of evolution separates plant lineages, and even species that are closely related may display substantial differences.

The chapters compiled in this collection outline a number of methods that are used to study mitochondria today, starting from the isolation of mitochondria to detailed analyses of RNA, protein, and enzymatic activities. The ability to visualize mitochondria in vivo with fluorescent protein tagging puts these activities in a spacial context, and the development of fluorescent probes to measure metabolites provides subcellular resolution that cannot be achieved by other means. The application of various omic techniques provides resolution of proteins and nucleic acids at orders of magnitude higher, unimaginable one or two decades ago. But despite the abundance of such data, there is still much to understand about how the mitochondrial machine works.

This collection of techniques does not cover all techniques; some are absent simply because they have been well documented elsewhere in recent times. What we have tried to achieve in these chapters is to have techniques written by researchers who have been actively involved in the development and continued use of these techniques. This is to ensure that they are relevant to researchers today and are accessible in that the authors can be contacted directly. In the philosophy of this series, we have tried to ensure a blow-by-blow account of these techniques so that they are accessible to beginners in the field as well as being useful to expert researchers who find themselves being pulled into the field of mitochondrial research as it links to so many important aspects of plant cell biology.

Most importantly this collection of methods could only be achieved due to the fact that these authors have taken the time and effort to prepare them. This is much appreciated, and hopefully writing 1 chapter and getting 19 in return is of some small benefit. Secondly, the editors would like to thank their colleagues and mentors, who have supported them

throughout their careers, allowing them to be in the position to be carrying out research into plant mitochondria with exceptional colleagues from all over the world. Finally, both editors would like to acknowledge the Australian Research Council (FT130100112, DP130102384, CE140100008) for their continual support to carry out plant mitochondrial research in their laboratories.

Bundoora, VIC, Australia — *James Whelan*
Crawley, WA, Australia — *Monika W. Murcha*

Contents

Contributors

Mary S. Albury • *Department of Biochemistry and Molecular Biology, School of Life Sciences, University of Sussex, Brighton, UK*

Isabel Aller • *INRES – Chemical Signalling, University of Bonn, Bonn, Germany*

Stefan Binder • *Molekulare Botanik, Universität Ulm, Ulm, Germany*

Rui M. Branca • *Clinical Proteomics Mass Spectrometry, Department of Oncology-Pathology, Science for Life Laboratory, Karolinska Institutet, Stockholm, Sweden*

Hans-Peter Braun • *Institute of Plant Genetics, Plant Proteomics, Leibniz Universität Hannover, Hannover, Germany*

Niall Brogan • *School of Biology and Environmental Science, University College Dublin, Dublin, Ireland*

Chris Carrie • *Department of Biology I, Botany, Ludwig-Maximilians-Universität München, Planegg-Martinsried, Germany*

Alex Costa • *Department of Biosciences, University of Milan, Milan, Italy*

Marina Cvetkovska • *Department of Biological Sciences, University of Toronto Scarborough, Toronto, ON, Canada; Department of Cell and Systems Biology, University of Toronto Scarborough, Toronto, ON, Canada*

David A. Day • *School of Biological Sciences, Flinders University, Adelaide, SA, Australia*

Anne-Marie Duchêne • *Institut de Biologie Moléculaire des Plantes, Université de Strasbourg, Strasbourg, France*

Owen Duncan • *Plant Energy Biology, Australian Research Council Centre of Excellence, University of Western Australia, Crawley, WA, Australia*

Sanjaya B. Ekanayake • *Department of Biology, University of Saskatchewan, Saskatoon, SK, Canada*

Catherine Elliott • *Department of Biochemistry and Molecular Biology, School of Life Sciences, University of Sussex, Brighton, UK*

Alisdair Fernie • *Max-Planck-Institut für Molekulare Pflanzenphysiologie, Potsdam, Germany*

Iris Finkemeier • *Plant Proteomics and Mass Spectrometry Group, Max-Planck-Institute for Plant Breeding Research, Cologne, Germany*

Richard Fly • *Institute for Plant Biotechnology, Stellenbosch University, Matieland, South Africa*

Mark D. Fricker • *Department of Plant Sciences, University of Oxford, Oxford, UK*

Elzbieta Glaser • *Department of Biochemistry and Biophysics, Arrhenius Laboratories for Natural Sciences, Stockholm University, Stockholm, Sweden*

Markus Hartl • *Plant Proteomics and Mass Spectrometry Group, Max-Planck-Institute for Plant Breeding Research, Cologne, Germany*

Shaobai Huang • *Plant Energy Biology, Australian Research Council Centre of Excellence, The University of Western Australia, Crawley, WA, Australia*

Momi Iwata • *Diamond-Membrane Protein Laboratory, Department of Life Sciences, Imperial College, London, UK*

Richard P. Jacoby • *Plant Energy Biology, Australian Research Council Centre of Excellence, Centre for Comparative Analysis of Biomolecular Networks (CABiN), The University of Western Australia, Crawley, WA, Australia*

Joanna Kacprzyk • *School of Biology and Environmental Science, University College Dublin, Dublin, Ireland*
Beata Kmiec • *Department of Biochemistry and Biophysics, Arrhenius Laboratories for Natural Sciences, Stockholm University, Stockholm, Sweden*
Ann-Christine König • *Plant Proteomics and Mass Spectrometry Group, Max-Planck-Institute for Plant Breeding Research, Cologne, Germany*
Stephan Krueger • *Botanical Institute II, University of Cologne, Cologne, Germany*
Szymon Kubiszewski-Jakubiak • *Plant Energy Biology, Australian Research Council Centre of Excellence, University of Western Australia, Crawley, WA, Australia*
Kristina Kühn • *Molekulare Zellbiologie der Pflanzen, Institut für Biologie, Humboldt Universität zu Berlin, Berlin, Germany*
Chun Pong Lee • *Department of Plant Sciences, University of Oxford, Oxford, UK*
James Lloyd • *Institute for Plant Biotechnology, Stellenbosch University, Matieland, South Africa*
David C. Logan • *UMR 1345 Institut de Recherche en Horticulture et Semences, Université d'Angers, Angers, France*
Laurence Maréchal-Drouard • *Institut de Biologie Moléculaire des Plantes, Université de Strasbourg, Strasbourg, France*
Benjamin May • *Department of Biochemistry and Molecular Biology, School of Life Sciences, University of Sussex, Brighton, UK*
Paul F. McCabe • *School of Biology and Environmental Science, University College Dublin, Dublin, Ireland*
Cyrille Megel • *Institut de Biologie Moléculaire des Plantes, Université de Strasbourg, Strasbourg, France*
Margaretha J. van der Merwe • *Plant Energy Biology, Australian Research Council Centre of Excellence, University of Western Australia, Crawley, WA, Australia*
Andreas J. Meyer • *INRES – Chemical Signalling, University of Bonn, Bonn, Germany*
A. Harvey Millar • *Plant Energy Biology, Australian Research Council Centre of Excellence, Centre for Comparative Analysis of Biomolecular Networks (CABiN), The University of Western Australia, Crawley, WA, Australia*
Anthony L. Moore • *Department of Biochemistry and Molecular Biology, School of Life Sciences, University of Sussex, Brighton, UK*
Monika W. Murcha • *Plant Energy Biology, Australian Research Council Centre of Excellence, University of Western Australia, Crawley, WA, Australia*
Reena Narsai • *Plant Energy Biology, Australian Research Council Centre of Excellence, Department of Botany, School of Life Science, La Trobe University, Bundoora, VIC, Australia*
Thomas Nietzel • *Plant Energy Biology Lab, INRES – Chemical Signalling, University of Bonn, Bonn, Germany*
Gaël Paszkiewicz • *UMR 1345 Institut de Recherche en Horticulture et Semences, Université d'Angers, Angers, France*
Theresa J. Reape • *School of Biology and Environmental Science, University College Dublin, Dublin, Ireland*
Aurélia Rolland • *UMR 1345 Institut de Recherche en Horticulture et Semences, Université d'Angers, Angers, France*
Thalia Salinas • *Institut de Biologie Moléculaire des Plantes, Université de Strasbourg, Strasbourg, France*

Peter Schertl • *Institute of Plant Genetics, Plant Proteomics, Leibniz Universität Hannover, Hannover, Germany*
Markus Schwarzländer • *Plant Energy Biology Lab, INRES – Chemical Signalling, University of Bonn, Bonn, Germany*
Yun Shin Sew • *Australian Research Council Centre of Excellence Plant Energy Biology, University of Western Australia, Crawley, WA, Australia*
Julia Shearman • *Department of Biochemistry and Molecular Biology, School of Life Sciences, University of Sussex, Brighton, UK*
Chevaun A. Smith • *School of Biological Sciences, Flinders University, Adelaide, SA, Australia*
Kathleen L. Soole • *School of Biological Sciences, Flinders University, Adelaide, SA, Australia*
Elke Stroeher • *Plant Energy Biology, Australian Research Council Centre of Excellence, University of Western Australia, Crawley, WA, Australia*
Lee Sweetlove • *Department of Plant Sciences, University of Oxford, Oxford, UK*
Nicolas L. Taylor • *Plant Energy Biology, Australian Research Council Centre of Excellence, Centre for Comparative Analysis of Biomolecular Networks (CABiN), The University of Western Australia, Crawley, WA, Australia*
Pedro F. Teixeira • *Department of Biochemistry and Biophysics, Arrhenius Laboratories for Natural Sciences, Stockholm University, Stockholm, Sweden*
Elodie Ubrig • *Institut de Biologie Moléculaire des Plantes, Université de Strasbourg, Strasbourg, France*
Greg C. Vanlerberghe • *Department of Biological Sciences, University of Toronto Scarborough, Toronto, ON, Canada; Department of Cell and Systems Biology, University of Toronto Scarborough, Toronto, ON, Canada*
Stephan Wagner • *Plant Energy Biology Lab, INRES – Chemical Signalling, University of Bonn, Bonn, Germany*
Yan Wang • *Plant Energy Biology, Australian Research Council Centre of Excellence, School of Life Science, La Trobe University, Bundoora, VIC, Australia*
James Whelan • *Plant Energy Biology, Australian Research Council Centre of Excellence, School of Life Science, La Trobe University, Bundoora, VIC, Australia*
Luke Young • *Department of Biochemistry and Molecular Biology, School of Life Sciences, University of Sussex, Brighton, UK*
Amr M. El Zawily • *Department of Biology, University of Saskatchewan, Saskatoon, SK, Canada; Faculty of Science, Damanhour University, Damanhour, Egypt*

Chapter 1

Isolation of Intact Mitochondria from the Model Plant Species *Arabidopsis thaliana* and *Oryza sativa*

Monika W. Murcha and James Whelan

Abstract

The study of mitochondrial composition, biogenesis, and metabolism requires the isolation of intact functional mitochondria, often in relatively large quantities sufficient for downstream biochemical and proteomic analysis. Here we describe techniques optimized for the isolation of functional mitochondria from a variety of tissues from the model monocot and dicot species Arabidopsis (*Arabidopsis thaliana*) and rice (*Oryza sativa*).

Key words Mitochondria, Organelle isolation, Density gradients, Arabidopsis, Rice

1 Introduction

Mitochondria are indispensible organelles essential for plant growth, development, and resistance to stress. Characterization of these processes requires the isolation of intact, respiratory active, and functional mitochondria for a multitude of biochemical assays, many of which are described in detail within this edition.

Traditionally, mitochondrial isolation procedures often focused on large heterotrophic organs such as potato tubers or cauliflower or photosynthetic tissues such as pea leaf and soybean cotyledons with several extensive reviews and specific methodology papers available [1–5]. With the complete sequencing of plant genomes, the model dicot, Arabidopsis (*Arabidopsis thaliana*), and monocot rice (*Oryza sativa*) are more widely used for biochemical studies in addition to the genetic studies that established these plants as models. The availability of mutant lines, antibodies, and tools for the generation of mutant germplasms, such as knockdown and over-expressing lines, offers many advantages to basic research. With modifications to plant growth and isolation procedures, sufficient quantities of pure, intact, and functional mitochondria can

James Whelan and Monika W. Murcha (eds.), *Plant Mitochondria: Methods and Protocols*, Methods in Molecular Biology, vol. 1305, DOI 10.1007/978-1-4939-2639-8_1,

be isolated from relatively small quantities from specific tissues from both Arabidopsis and rice. Here we present step-by-step methods for plant growth and mitochondrial isolation from Arabidopsis seedlings, rosettes and cell suspensions, and rice embryo, hypocotyl, and seedlings.

2 Materials

2.1 Arabidopsis Tissue Preparation

2.1.1 Soil-Grown Arabidopsis

1. 6 × 6 × 6 cm pots.
2. Soil mix consisting of vermiculture:peat moss:perlite mixed at a 1:3:1 ratio.

2.1.2 Plate-Grown Arabidopsis

Growing Arabidopsis on plates is useful for propagating enough tissue with minimal growth space. Additionally, plates can be easily treated prior to the isolation of mitochondria with a variety of stresses/compounds to induce/inhibit specific pathways and/or responses.

1. Murashige and Skoog (MS) media plates: 3 % (w/v) sucrose, 4.3 g/L MS powder, 0.5 g/L MES, 1 mL/L Gamborg B5 vitamins 1,000×, pH 5.7 (KOH), 7.5 g/L agar.
2. 3 % (v/v) Hydrochloride in sodium hypochlorite.
3. Glass non-vacuum desiccator.
4. 10 × 10 cm square petri dishes (*see* **Note 1**).
5. Surgical breathable tape (e.g., 2.5-cm width Leukopor).

2.1.3 Liquid-Grown Arabidopsis

Growing Arabidopsis in liquid is preferential when large amounts of mitochondria are required (3–5 mg). Additionally, seedlings can be treated continuously with a variety of compounds in solution.

1. Half-strength MS media: 1.5 % (w/v) sucrose, 2.15 g/L MS powder, 0.25 g/L MES, 0.5 mL/L Gamborg B5 vitamins (1,000×), pH 5.7 (KOH).
2. Orbital shaker.
3. 500-mL polycarbonate pots with polypropylene lid (e.g., Sarstedt cat. # 75.9922.811).
4. 3 % (v/v) concentrated HCl in sodium hypochlorite.
5. Glass non-vacuum desiccator.
6. Surgical breathable tape (e.g., 2.5-cm width Leukopor).

2.1.4 Arabidopsis Cell Suspensions

1. 250-mL Glass conical flasks.
2. 70 % (v/v) Ethanol.
3. Sterile 25-mL pipettes.
4. MS media: 3 % (w/v) sucrose, 4.3 g/L MS powder, 0.5 mg 1-naphthaleneacetic acid (NAA), 0.05 mg kinetin pH 5.7 (KOH).

2.1.5 Rice Coleoptiles and Seedlings

1. Rice dehusker (*see* **Note 2**).
2. Vermiculite.
3. Large 30 × 40 × 10-cm plastic trays with drainage holes.

2.1.6 Rice Embryos

1. Rice dehusker (*see* **Note 2**).
2. Rice growth media: 0.5 mM MES, 0.5 mM $CaCl_2$ pH 6.5, carbenicillin (6 mg/L) (*see* **Note 3**).
3. Sterile 250-mL conical flasks and air spargers (*see* **Note 4**).
4. Oxygen/nitrogen tank.

2.1.7 Mitochondrial Isolation Using Continuous Density Gradients

1. Large mortar and pestle.
2. Miracloth (e.g., Calbiochem Corp. Cat. # 475855) (*see* **Note 5**).
3. Beckman Coulter Avanti® J-E centrifuge with Beckman rotor JA25.5 or equivalent.
4. 50-mL centrifuge tubes (e.g., Nalgene polycarbonate Cat. # 3117-9500).
5. Fine-hair paintbrush.
6. 300-mL conical flask and funnel.
7. Gradient pourer with standard peristaltic pump.
8. Grinding buffer: 0.3 M sucrose, 25 mM tetrasodium pyrophosphate, 2 mM EDTA (disodium salt), 10 mM KH_2PO_4, 1 % (w/v) PVP-40, 1 % (w/v) bovine serum albumin (BSA), pH 7.5 (HCl). For 300 mL grinding media, 1.06 g sodium ascorbate and 0.74 g cysteine are added just prior to use.
9. 2× Wash buffer: 0.6 M sucrose, 20 mM TES, 0.2 % (w/v) BSA, pH 7.5 (NaOH) (*see* **Note 6**).
10. Light gradient solution.

	2 Gradients	**4 Gradients**
Wash buffer (2×)	17.5 mL	35 mL
Percoll	9.8 mL	19.6 mL
Double-deionized water	7.7 mL	15.4 mL

11. Heavy gradient solution.

	2 Gradients	4 Gradients
Wash buffer (2×)	17.5 mL	35 mL
Percoll	9.8 mL	19.6 mL
PVP-40 20 % (w/v)	7.7 mL	15.4 mL

2.1.8 Mitochondrial Isolation Using Discontinuous Density Gradients

1. Blender.
2. Miracloth (e.g., Calbiochem Corp. Cat. # 475855) (*see* **Note 5**).
3. Beckman Coulter Avanti® J-E centrifuge with Beckman rotor JA25.5 or equivalent.
4. 50-mL centrifuge tubes (e.g., Nalgene polycarbonate Cat. # 3117-9500).
5. Fine-hair paintbrush.
6. 300-mL conical flask and funnel.
7. Needle (21 gauge), 50-mL syringe, and retort stand.
8. Grinding buffer: 0.3 M mannitol, 50 mM tetrasodium pyrophosphate, 2 mM EDTA (disodium salt), 0.5 % (w/v) PVP-40, 0.5 % (w/v) BSA pH 8.0 (HCl). For 300 mL grinding media, add 0.74 g cysteine prior to use.
9. 2× Wash buffer: 0.6 M mannitol, 20 mM TES, 0.2 % (w/v) BSA, pH 7.5 (NaOH) (*see* **Note 6**).
10. Percoll gradients [2].

	Percoll	Water	Wash buffer (2×)
Percoll 21 % (v/v)	8.4 mL	11.6 mL	20 mL
Percoll 40 % (v/v)	4 mL	1 mL	5 mL
Percoll 16 % (v/v)	3.2 mL	6.8 mL	10 mL

2.1.9 Mitochondrial Isolation Using Continuous Density Gradients for Rice Embryos

1. Scalpel.
2. Small mortar and pestle.
3. Grinding buffer: 0.4 M mannitol, 50 mM tetrasodium pyrophosphate, 2 mM EGTA, 0.5 % (w/v) PVP-40, 0.5 % (w/v) BSA, 20 mM cysteine, pH 8.0 (HCl).
4. Wash buffer: 0.3 M mannitol, 10 mM TES, pH 7.5 (NaOH).
5. 10-mL ultracentrifuge tubes.
6. Percoll step gradient (*see* **Note 7**).

	40 % (v/v)	25 % (v/v)	15 % (v/v)
Wash buffer	1.2 mL	1.5 mL	1.7 mL
Percoll	800 µL	500 µL	300 µL

3 Methods

3.1 Tissue Growth Conditions and Tissue Preparation

3.1.1 Arabidopsis Seedlings Grown in Water Culture Pots

1. Water culture pots are prepared with 80 mL liquid MS media and sterilized by autoclaving.
2. Arabidopsis seeds are sterilized using the chlorine gas method: Place 100 mg of seed into a 1.5-mL microcentrifuge tube, and place open tube into a desiccator containing 50 mL sodium hypochlorite in a 100-mL beaker. Quickly add 3 mL of concentrated HCl to the bleach and close the lid; leave to sterilize for 6 h (*see* **Note 8**).
3. In a sterile laminar flow hood using sterile techniques, pour 100 mg of seed to each pot. Screw shut the lid and tape over the junction with medical tape.
4. Place the pots into standard plant growth conditions, shaking gently at 100 rpm to ensure that seed does not settle. For a standard mitochondrial isolation yielding 4–5 mg of mitochondria, ten pots will be required when mitochondria are isolated from 2-week-old plants.

3.1.2 Arabidopsis Seedlings Grown in Square Petri Dishes

1. Arabidopsis seed can be sterilized as described above in Subheading 3.1.1.
2. 300 mg of sterile seed can be sown evenly onto five large square MS agar plates and the lid taped up using medical tape (*see* **Note 9**).
3. Seeds are stratified for 48 h at 4 °C upon which they are placed under standard growth conditions for 2 weeks (*see* **Note 10**).
4. Tissue is collected by gently removing the whole seedlings from agar or washing the agar and plants through a sieve ensuring that all agar is removed. Excess water is gently squeezed out.

3.1.3 Arabidopsis Rosettes Grown in Soil

1. Arabidopsis seeds (non-sterile) are sprinkled onto pots containing soil within larger trays. Trays are stratified for 48 h at 4 °C prior to placing under optimal growth conditions. About 10 days after sowing, excess seedlings are removed from each pot and grown for a further 2 weeks. 100–200 pots are required for isolating 3–5 mg of mitochondria.
2. Tissue is removed by cutting the rosette from the stalk and gently rinsing excess soil.

3.1.4 Arabidopsis Cell Suspensions

1. Subculture cell suspensions every 7 days using sterile techniques in a laminar flow hood.
2. Subculture the cells by transferring 20–25 mL of the culture (depending on density) to an autoclaved flask containing 100 mL media. Minimize disturbance by pipetting gently into the liquid.
3. Shake the flasks in an orbital shaker at 100 rpm at 24 °C.

3.1.5 Rice Hypocotyl and Seedlings

1. Dehusk 50 mL of rice grain, and rinse to remove the husks.
2. Sow seeds onto a tray containing vermiculite (5 cm deep) and cover with 2 cm of vermiculite.
3. Soak tray in a larger tray filled with water to ensure that all vermiculite is wet.
4. Place into 26 °C growth chambers (with or without lights).

3.1.6 Rice Embryos

1. Dehusk 50 mL of rice grain, and rinse to remove the husks.
2. Sterilize rice grain with 5 % (v/v) sodium hypochloride for 5 min and rinse well with sterile water.
3. Submerge grains in rice growth media in sterile 250-mL flasks or sterile 500-mL polycarbonate pots and incubate at 30 °C for up to 48 h.
4. Bubble air or nitrogen continuously with spargers just below the growth media level.
5. Dissect embryos from the seed using sterile scalpels from 12 h post-imbibition.

3.2 Mitochondrial Isolation Using Continuous Gradients

This protocol is used for the isolation of intact mitochondria from Arabidopsis tissues grown in water cultures/pots, agar plates, and soil and for rice shoots and hypocotyls (Fig. 1). This protocol is adapted from [6]. All procedures following the grinding of the material are to be carried out at 4 °C.

1. Prepare the heavy and light gradient solutions in two 50-mL beakers.
2. Rinse the chambers and tubing of gradient pourer with water and check that all tubes are flowing at an even rate.
3. Place two 50-mL tubes on ice at a slight angle and tape tubing outlets to the inside of the tubes, so the gradient solution runs down the side of the tubes (*see* **Note 11**).
4. Ensure that the gradient pourer, tubing, and 50-mL tubes are free from water and that the connection between inner and outer chambers is closed.
5. Pour the light solution into outer chamber (chamber without tubing outlet).
6. Pour the heavy gradient solution into inner chamber (chamber with tubing outlet), place a small stirrer bar in the chamber, place gradient chambers on stirring block, and stir gently.
7. Set the peristaltic pump at a rate of 300 mL/h and allow the heavy solution to run until half is dispensed.
8. Slowly open the connection between the chambers (push black lever up halfway) and allow solution to mix.
9. Continue to run until all of the gradient mix has been dispensed from the chambers.

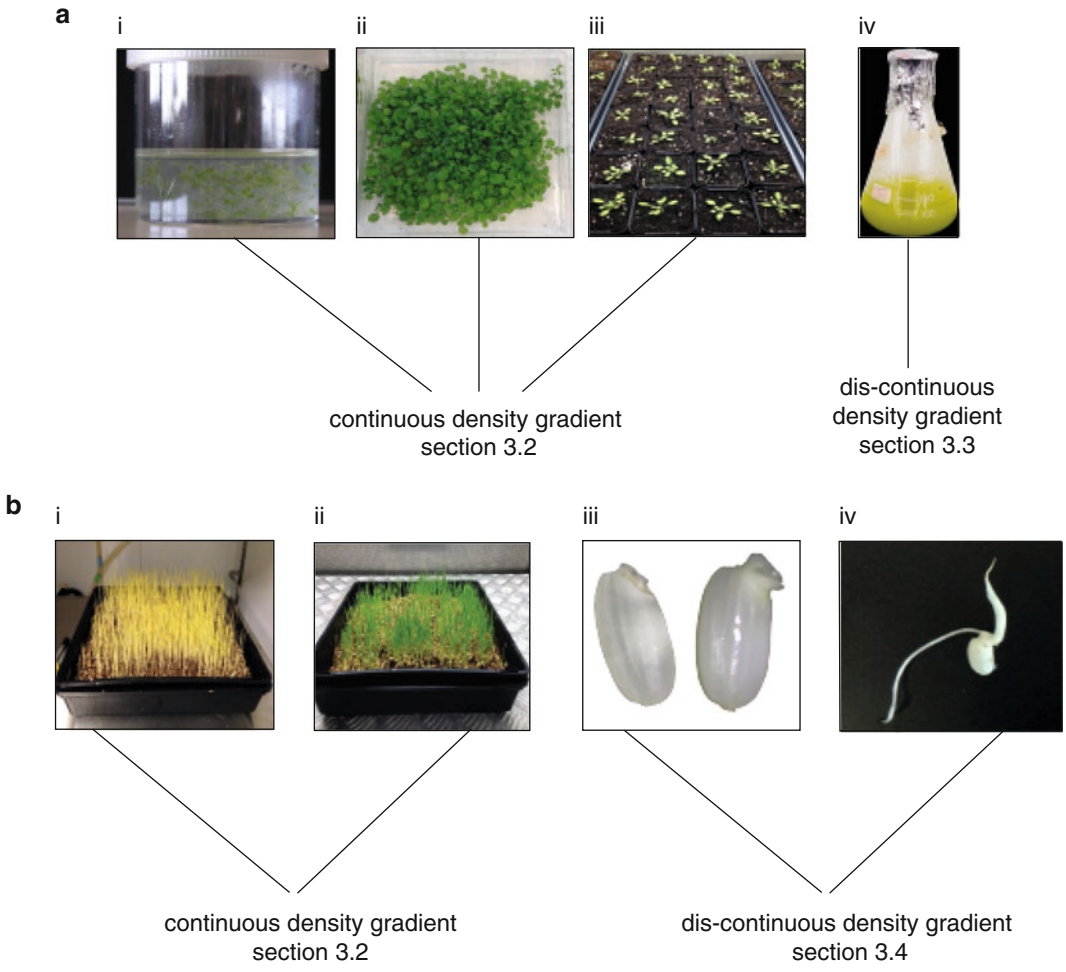

Fig. 1 Density gradient purification strategies for the isolation of plant mitochondria from (**a**) Arabidopsis seedlings grown by water culture (i), agar plates (ii), Arabidopsis rosettes grown in soil (iii), and Arabidopsis cell suspensions. (**b**) Rice hypocotyl (i), seedlings (ii), 1–2-day-old embryo (iii), and 2-week-old coleoptile (iv)

10. Keep the gradients on ice until ready to use in **step 11** (*see* **Note 12**).
11. Pour 75 mL of grinding medium onto a third of the plant material in a mortar and pestle, and grind well for several minutes (*see* **Note 13**).
12. Pour homogenate through four layers of Miracloth (pre-wet with grinding medium) into a 500-mL conical flask.
13. Repeat **step 11** twice using the remaining tissue.
14. Squeeze through the excess homogenate through the Miracloth, grind all of the pooled tissue again with the remaining grinding media, and filter again.
15. Transfer the filtered homogenate into 8 × 50-mL plastic centrifuge tubes on ice.

16. Centrifuge for 5 min at 2,450 × *g* at 4 °C.
17. Transfer the supernatant into new tubes and centrifuge for 20 min at 17,400 × *g* at 4 °C.
18. Remove the supernatant by aspiration (or gently pour off) and gently resuspend the pellets in residual buffer using a small paintbrush.
19. Add 10 mL of 1× wash buffer to each tube and combine four tubes into one (i.e., two tubes in total).
20. Repeat centrifugation **steps 16** and **17**.
21. Pool crude mitochondrial pellets and overlay two continuous PVP-40/Percoll gradients.
22. Balance tubes and centrifuge for 40 min at 40,000 × *g* at 4 °C with no brake.
23. Mitochondria should form a light yellow/grey band low in the tube (Fig. 2a).
24. Aspirate all solution 2 cm above the mitochondrial band and divide the remaining solution containing mitochondria into four tubes, filling each with 1× wash buffer. Centrifuge for 15 min at 31,000 × *g* at 4 °C with light brake (*see* **Note 14**).
25. Aspirate the supernatant off, pool all four mitochondrial pellets into two tubes, and add 1× wash buffer. Centrifuge at 18,000 × *g* for 15 min with soft brakes.
26. Aspirate supernatant off and remove the mitochondrial pellets in a minimum volume using a Pasteur pipette. Place the mitochondria into a 1.5-mL tube and keep on ice or store at –80 °C.

3.3 Mitochondrial Isolation: Discontinuous Density Gradients

This protocol is used for the isolation of intact mitochondria from Arabidopsis cell cultures and adapted from [7]. All procedures are to be carried out at 4 °C.

1. Filter 1 L of 7-day-old cell culture through four layers of Miracloth. This should yield about 100 g of cells.
2. Add 300 mL of grinding solution to the blender, add cells, and blend five times with 4-s bursts with 10-s intervals.
3. Filter the solution through four layers of Miracloth into a 500-mL conical flask.
4. Decant the cell extract into 50-mL tubes and centrifuge at 3,500 × *g* for 5 min.
5. Decant supernatant into new tubes and centrifuge at 18,000 × *g* for 15 min.
6. Prepare two Percoll gradients by layering 20 mL of 21 % (v/v) Percoll gradient solution over 5 mL of 40 % (v/v) Percoll gradient solution, and layering 10 mL of 16 % (v/v) Percoll gradient solution on the top; keep the gradients on ice (*see* **Note 15**).

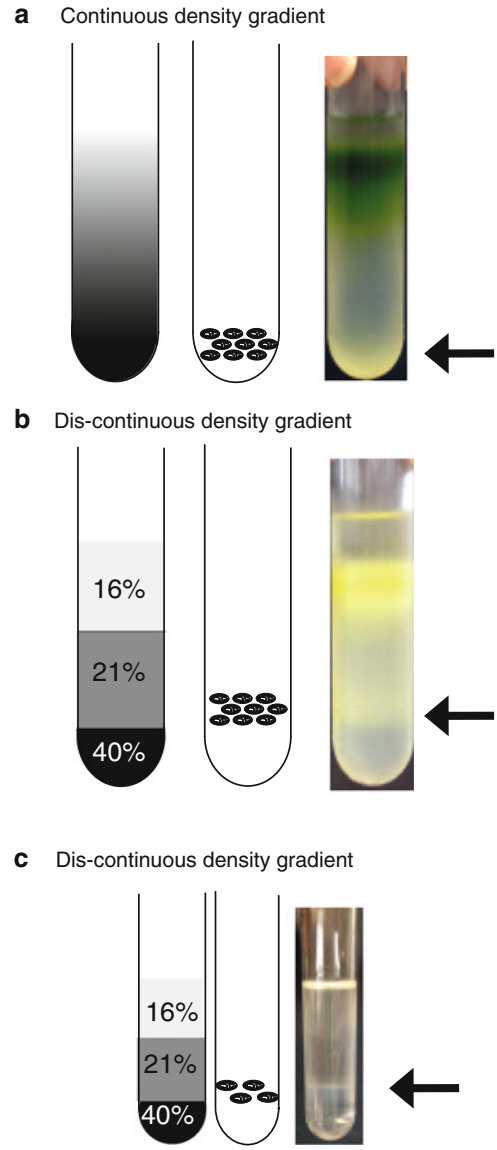

Fig. 2 Example of Percoll density gradients for the purification of mitochondria. (**a**) Continuous density gradient for Arabidopsis seedling and rice hypocotyl and seedling tissues. (**b**) Discontinuous density gradient for Arabidopsis cell suspension. (**c**) Discontinuous density gradient for rice embryo and coleoptiles. A model and photo of the banding patterns obtained following centrifugation. The positions of the mitochondrial bands are indicated with an *arrow*

7. Discard the supernatant and gently resuspend pellet with a fine-hair paintbrush. Pool the pellets into two tubes, fill with 1× wash buffer, and centrifuge at 1,000 × *g* for 5 min.
8. Decant the supernatant into two new tubes and centrifuge at 15,000 × *g* for 15 min.

9. Aspirate or gently pour off the supernatant and resuspend pellets in 2–3 mL of 1× wash buffer. Ensure that pellet is resuspended thoroughly.
10. Layer the two pellets using a Pasteur pipette over two Percoll gradients and centrifuge at 40,000 × *g* for 45 min without brake.
11. The mitochondrial band is located at the interface of the 21 % (v/v) and 40 % (v/v) Percoll layers (Fig. 2b). Aspirate the solution leaving 2 cm above the mitochondrial band and place into a new 50-mL tube.
12. Add 1× wash buffer, divide evenly between four 50-mL tubes, add 1× wash buffer, and centrifuge at 18,000 × *g* for 15 min with light brakes (*see* **Note 14**).
13. Aspirate the supernatant off, pool all four mitochondrial pellets into two tubes, and fill with 1× wash buffer. Centrifuge at 18,000 × *g* for 15 min with light brake.
14. Aspirate supernatant off and remove the mitochondrial pellets in a minimum volume using a Pasteur pipette. Place the mitochondria into a 1.5-mL tube and keep on ice or store at –80 °C.

3.4 Mitochondrial Isolation: Rice Embryos

The protocol is adapted from [8]. Embryos can be dissected from imbibed rice grains following 12-h imbibition (Fig. 1). Rice grains can be grown under anoxic or aerobic conditions. All procedures are carried out at 4 °C.

1. Dissect embryos from at least 200 rice grains using scalpel at room temperature.
2. Grind the embryos in a small precooled mortar and pestle using 3 mL of grinding buffer and transfer to a chilled microcentrifuge tube.
3. Centrifuge at 200 × *g* for 1 min at 4 °C. Remove the supernatant and gently layer onto the layered Percoll step gradients (1.5 mL per gradient).
4. Centrifuge the gradients at 34,000 × *g* for 30 min at 4 °C with the brakes off (*see* **Note 16**).
5. Mitochondria are visible as opaque bands at the 25–40 % (v/v) interface (Fig. 2c). The mitochondrial layer is removed using a flat-bottomed needle and transferred to a new 10-mL ultracentrifuge tube.
6. Add 1× wash buffer and centrifuge at 22,000 × *g* for 15 min at 4 °C.
7. Aspirate the wash buffer and transfer the mitochondrial pellet to a 1.5-mL microcentrifuge tube.
8. Add 1 mL 1× wash buffer, centrifuge at 200 × *g* for 1 min at 4 °C, transfer the supernatant (mitochondria) to a 1.5-mL microcentrifuge tube, and centrifuge at maximum speed for 15 min at 4 °C.

9. Remove the supernatant and determine total protein concentration of the mitochondrial pellet. Approximately 100–300 μg of rice embryo mitochondrial protein should be obtained using this protocol.

4 Notes

1. Larger and deeper plates are optimal to prevent MS media drying out and to provide sufficient growth space for plants.
2. Manual removal of the rice grain husk is required to ensure uniform germination.
3. Rice growth media can be made in large quantities with carbenicillin added prior to use.
4. Air is bubbled beneath the growth media surface.
5. Alternative materials such as disposable polypropylene stretcher sheets may be used (Medirite, Australia).
6. Certain downstream applications require the omission of BSA from the wash buffer in the final wash step.
7. Gradients are prepared by overlaying 2 mL each of 40 % (v/v), 25 % (v/v), and 15 % (v/v) Percoll solutions slowly in a 10-mL ultracentrifuge tube, being careful not to disturb the interfaces and layers.
8. If sterilizing overnight prepare 1.5 % (v/v) concentrated HCl in sodium hypochlorite.
9. For even distribution of seed, which is required for optimal growth, sprinkle seed by piercing several holes into the lid of the microcentrifuge tube and shake over the agar plate.
10. Condensation can easily occur if plates are overheated or inadequate ventilation is provided.
11. Test that solution is not dripping from the tube outlets with water.
12. The gradients can be prepared during the first 20-min centrifugation.
13. A small amount of fine sand can be used for fibrous material such as rice shoots.
14. It is essential to use at least four tubes for this wash step or else the Percoll concentration is too high and the mitochondria will fail to pellet.
15. Use a syringe and needle held up by a retort stand to prepare the gradients with each Percoll mix being poured into the syringe individually and allowed to run down the side of the tube. Alternatively the gradients can be prepared by pipetting though this needs to be done slowly and gently to ensure minimal disruption to the Percoll interfaces.
16. Light break may be applied.

References

1. Douce R, Moore AL, Neuburger M (1977) Isolation and oxidative properties of intact mitochondria isolated from spinach leaves. Plant Physiol 60:625–628
2. Eubel H, Heazlewood JL, Millar AH (2007) Isolation and subfractionation of plant mitochondria for proteomic analysis. Methods Mol Biol 355:49–62
3. Millar AH, Liddell A, Leaver CJ (2007) Isolation and subfractionation of mitochondria from plants. Methods Cell Biol 80:65–90
4. Neuburger M, Journet EP, Bligny R, Carde JP, Douce R (1982) Purification of plant mitochondria by isopycnic centrifugation in density gradients of Percoll. Arch Biochem Biophys 217: 312–323
5. Taylor NL, Stroher E, Millar AH (2014) Arabidopsis organelle isolation and characterization. Methods Mol Biol 1062:551–572
6. Day DA, Neuburger M, Douce R (1985) Biochemical-characterization of chlorophyll-free mitochondria from pea leaves. Aust J Plant Physiol 12:219–228
7. Millar AH, Sweetlove LJ, Giege P, Leaver CJ (2001) Analysis of the Arabidopsis mitochondrial proteome. Plant Physiol 127: 1711–1727
8. Howell KA, Millar AH, Whelan J (2006) Ordered assembly of mitochondria during rice germination begins with pro-mitochondrial structures rich in components of the protein import apparatus. Plant Mol Biol 60:201–223

Chapter 2

Determining Mitochondrial Transcript Termini for the Study of Transcription Start Sites and Transcript 5′ End Maturation

Stefan Binder and Kristina Kühn

Abstract

Mitochondrial gene expression in plants is considerably more complex than in animals or fungi. In plants, mitochondrial transcripts are generated from transcription initiation at numerous, poorly conserved promoters located throughout the mitochondrial genome. Most genes have more than one transcription start site. Posttranscriptional RNA 5′ end maturation contributes to the diversity of transcripts produced from each mitochondrial gene. Understanding transcriptional mechanisms and transcript maturation requires knowledge on transcription start sites and processing sites. This chapter describes two different, complementary experimental approaches for determining these sites in mitochondrial genomes through mapping of transcript 5′ ends. In order to distinguish 5′ ends deriving from transcription initiation, both strategies exploit the presence of triphosphates at these specific 5′ termini.

Key words Mitochondrial RNA, Transcription initiation, Transcript 5′ end maturation, Primary RNA, Processed RNA, Differential transcript 5′ end analysis, 5′-RACE, Primer extension

1 Introduction

Mitochondrial DNA in seed plants generally encodes up to 60 genes [1]. The expression of this genetic information is extraordinarily complex; it includes transcription and posttranscriptional processes like RNA editing, group II intron splicing, and maturation of 5′ and 3′ ends, as well as translation and most likely post-translational steps [2]. While all of these processes potentially influence gene expression, it is presently unknown how gene expression is controlled or even regulated in plant mitochondria. Further efforts are necessary to unravel the molecular mechanisms of plant mitochondrial gene expression.

The steady-state level of a transcript is a major quantitative determinant for the expression of the corresponding gene. Principally, the abundance of an RNA molecule is adjusted by two counterbalancing forces: the rate of RNA synthesis, i.e.,

James Whelan and Monika W. Murcha (eds.), *Plant Mitochondria: Methods and Protocols*, Methods in Molecular Biology, vol. 1305, DOI 10.1007/978-1-4939-2639-8_2,

transcription, and the rate of RNA degradation. In plant mitochondria, posttranscriptional modifications that can influence the stability of an RNA molecule are prevailing processes.

One or two bacteriophage-type RNA polymerases accomplish transcription in plant mitochondria [3]. These enzymes start RNA synthesis from loosely conserved promoters, and at least in vitro additional factors are not required for promoter recognition [2, 4–7]. Nevertheless, it is likely that in vivo one or several additional factors are involved in transcription initiation. To further characterize the initiation mechanism and proteins involved in this process, transcription initiation sites have to be identified. These sites coincide with the 5′ termini of primary RNAs and can thus be identified by mapping primary transcript 5′ ends, which are characterized by the presence of 5′ triphosphates (Fig. 1). This feature discriminates primary 5′ termini from 5′ ends that are posttranscriptionally generated and carry 5′ monophosphates. To date, the contributions of individual posttranscriptional processes to the stability of an RNA species are unknown. It appears though that formation of mature 3′ ends is tightly linked to transcript stability. For instance, the pentatricopeptide repeat (PPR) protein MTFS1 binds to the 3′-terminal part of the nad4 mRNA [8]. It is assumed that this prevents progression of one or two 3′–5′ exoribonucleases, thereby determining the mature 3′ extremity [9, 10]. In addition, 3′ poly(A) tracts have a profound influence on transcript stability. It has recently been found that oligo(A) tails, added by the poly(A) polymerase AGS1, target mitochondrial RNA for degradation by the a poly(A)-specific ribonuclease AHG2 [11].

A completely different mechanism generates the mature 5′ termini of plant mitochondrial RNAs. Unlike 3′ termini, 5′ ends are generated by endonucleolytic cleavage. Several RNA PROCESSING FACTORS, all of them PPR proteins, have been identified and were found to be required for the processing of one or several transcripts. Furthermore, proteins involved in 5′ processing are still unknown, and the importance of this maturation step for transcript stability and translation awaits clarification [12].

In this chapter we describe principal methods for RNA isolation and the identification of transcript 5′ termini, which have been optimized for the model organism Arabidopsis (*Arabidopsis thaliana*) but can be applied to other plant species. Special emphasis is laid on methods to distinguish between primary 5′ ends that originate from transcription initiation and secondary 5′ termini that are posttranscriptionally generated. The experimental discrimination between these ends depends on the presence of triphosphate groups at the primary 5′ ends. Two different approaches can be used for the identification of primary 5′ termini. One of these strategies involves the enzyme tobacco acid pyrophosphatase (TAP) and a differential 5′-RACE protocol (Subheading 3.2) [13]. An

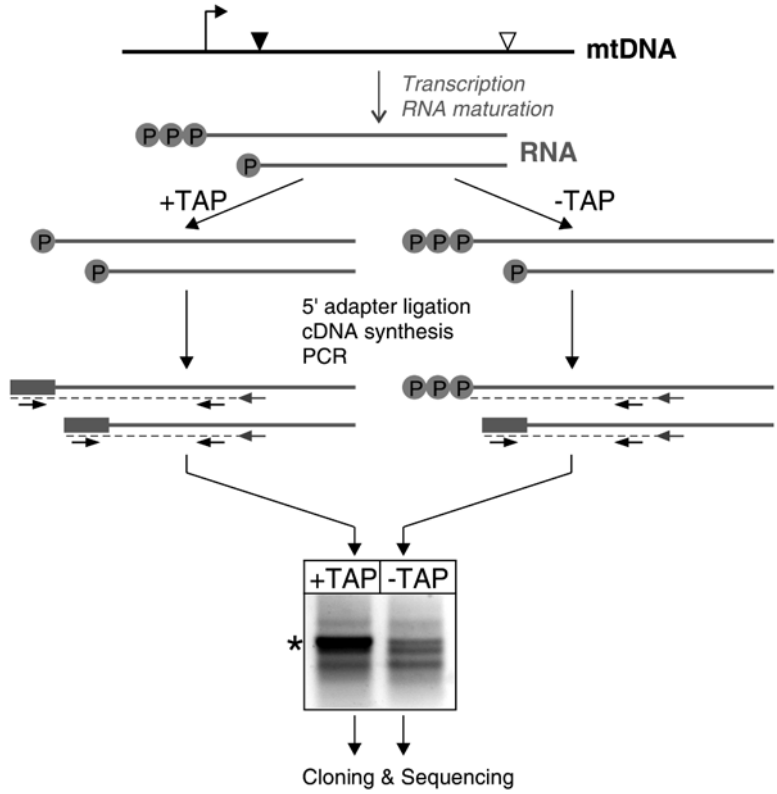

Fig. 1 Transcription initiation from mitochondrial promoters (*top*, promoter as *bent arrow*) generates primary transcript with 5′ triphosphates, whereas processing of these transcripts (5′ processing site as *black triangle*, 3′ processing site as *white triangle*) produces 5′ monophosphorylated transcripts. Differential 5′-RACE uses the enzyme TAP to discriminate between primary and processed 5′ ends. Transcripts are exposed to TAP to convert 5′ triphosphates to monophosphates (*left*), or not treated with TAP in a control experiment (*right*). An oligoribonucleotide adapter (*grey box*) is then ligated to the 5′ monophosphate ends, and cDNA (*grey dashed lines*) is synthesized using a primer complementary to the gene of interest (*small grey arrows*). Reverse-transcribed ligation products are amplified using a forward primer annealing to the linker sequence and a gene-specific reverse primer (*small black arrows*). RT-PCR products are analyzed by agarose gel electrophoresis, and products derived from primary transcripts (band indicated by an *asterisk*) are preferentially or exclusively amplified from TAP-treated samples

alternative strategy uses Terminator™ 5′-Phosphate-Dependent Exonuclease (TEX) (Subheading 3.3) combined with methods for 5′ end quantitation, such as primer extension (Subheading 3.4). Recent genome-scale transcriptomic studies on bacteria or chloroplasts combined TEX application with RNA sequencing for the genome-wide identification of transcription start sites [14–16].

The 5′-RACE strategy described under Subheading 3.2 for the mapping of mitochondrial primary transcript 5′ ends involves an initial treatment of total RNA with TAP (Fig. 1). This treatment will remove a pyrophosphate moiety from primary transcript 5′ ends, thus converting them to 5′ monophosphorylated molecules. This step is a prerequisite for the subsequent 5′ adapter ligation (*see* **Note 1**) to primary transcripts and amplification of 5′ ends by reverse transcription-polymerase chain reaction (RT-PCR) with adapter- and gene-specific primers (Fig. 1). Adapter ligation to processed 5′ ends does not require TAP treatment. Accordingly, 5′-RACE preceded by TAP treatment will amplify both primary and processed 5′ ends whereas 5′-RACE performed on untreated RNA will only capture processed 5′ ends. The comparison of 5′-RACE products obtained from TAP-treated or untreated RNA will thus identify primary transcripts, which are exclusively or preferentially amplified following TAP treatment (Fig. 1, *see* **Note 2**). Subsequent cloning of 5′-RACE products and sequencing across adapter ligation sites will determine transcript 5′ ends.

TEX used by the alternative strategy described under Subheadings 3.3 and 3.4 is a 5′–3′ exonuclease that digests RNA molecules with 5′ monophosphate ends. The enzyme does not degrade RNAs that have 5′ triphosphates, 5′ caps, or 5′ hydroxyl groups. Thus, TEX can be used to specifically enrich mitochondrial transcripts carrying 5′ triphosphates, which derive directly from transcription initiation.

For the identification of enriched (primary) or reduced (processed) 5′ termini it will be necessary to combine TEX treatment with a downstream procedure that allows the quantitative comparison of transcript termini between TEX-treated and untreated RNA preparations. The primer extension analysis protocol described under Subheading 3.4 has successfully been applied in previous studies for the identification of transcript 5′ ends enriched by TEX treatment [17, 18]. In contrast, we found that RT-PCR-based methods [e.g., 5′-RACE or circularized RNA-reverse transcription-polymerase chain reaction (CR-RT-PCR), Subheading 3.2] were not suitable.

The RNA preparation method described under Subheading 3.1 is based on acid guanidinium thiocyanate-phenol-chloroform extraction [19]. Unlike procedures using RNA binding to and subsequent elution from silica-based membranes, this method does not exclude the recovery of small RNAs. Earlier experimental studies of mitochondrial transcripts were done with RNA extracted from isolated mitochondria [20, 21]. However, the downstream procedures described under Subheadings 3.2 and 3.4 can be performed on total cellular RNA. While chromosome 2 of the Arabidopsis nuclear genome contains a large mitochondrial DNA insertion [22], it is generally assumed that this part of the nuclear genome does not contribute to transcripts measured for mitochondrial genes.

2 Materials

To avoid RNA degradation, ensure to use ribonuclease-free materials and solutions. Reaction tubes should be nuclease-free and nucleic acid-free. All described procedures require the use of ultrapure water (double-distilled and autoclaved, or Milli-Q quality, i.e., deionized, resin-filtered, and passed through a 0.22-μm membrane filter) for setting up enzymatic reactions or preparing solutions. Clean gloves should be worn at all times.

2.1 RNA Isolation and DNase Treatment

2.1.1 Equipment

1. Refrigerated microcentrifuge.
2. Bead mill (e.g., TissueLyser II from QIAGEN), including adapters for 1.5–2.0-mL reaction tubes and stainless steel beads (5 mm diameter, available from QIAGEN).
3. Ultraviolet-visible spectrophotometer (e.g., Nanodrop).
4. Electrophoresis chamber for horizontal agarose gel electrophoresis with gel tray, comb, and power supply.
5. Ultraviolet transilluminator.
6. Dewar flask for liquid nitrogen.

2.1.2 Materials, Reagents, and Solutions

1. Liquid nitrogen.
2. Reaction tubes (1.5 and 2.0 mL).
3. Reagent for acid guanidinium thiocyanate-phenol-chloroform extraction (e.g., TRIsure™ from Bioline, or TRIzol® from Life Technologies).
4. Phenol-chloroform-isoamyl alcohol (25:24:1), pH 5.0.
5. Chloroform.
6. Isopropanol.
7. Ethanol/3 M sodium acetate, pH 4.8 (30:1).
8. 70 % (v/v) ethanol.
9. RQ1 RNase-free DNase (Promega).
10. Materials and buffers for horizontal agarose gel electrophoresis.

2.2 Tobacco Acid Pyrophosphatase Treatment of RNA and Differential 5′-RACE

2.2.1 Equipment

1. Refrigerated microcentrifuge.
2. 37 °C incubator.
3. PCR cycler.
4. Electrophoresis chamber for horizontal agarose gel electrophoresis with gel tray, comb, and power supply.
5. Ultraviolet transilluminator.

2.2.2 Materials, Reagents, and Solutions

1. Reaction tubes (1.5 mL).
2. PCR tubes (0.2 mL).
3. Phenol-chloroform-isoamyl alcohol (25:24:1), pH 5.0.
4. Phenol-chloroform-isoamyl alcohol (25:24:1), pH 8.0.
5. Ethanol/3 M sodium acetate, pH 4.8 (30:1).
6. 70 % (v/v) Ethanol.
7. TAP (Epicentre Biotechnologies).
8. T4 RNA ligase (Epicentre Biotechnologies).
9. SuperScript® III reverse transcriptase (Life Technologies).
10. RiboLock™ RNase inhibitor (Thermo Scientific).
11. *Taq* DNA polymerase (e.g., DreamTaq from Bioline).
12. Oligoribonucleotide adapter (5′-GAU AUG CGC GAA UUC CUG UAG AAC GAA CAC UAG AAG AAA-3′, 10 pmol/μL).
13. RT oligonucleotide mix (Subheading 3.2), containing up to 12 different gene-specific primers (2 μM each).
14. Adapter-specific forward primer (5′-CGA ATT CCT GTA GAA CGA ACA CTA GAA G-3′).
15. Gene-specific reverse primers (Subheading 3.2).
16. dNTP mix (10 mM each dATP, dGTP, dCTP, and dTTP).
17. PCR product gel extraction kit (e.g., NucleoSpin® Gel and PCR Clean-up from Macherey-Nagel).
18. PCR cloning kit including vector and DNA ligase (e.g., pGEM®-T Vector System I from Promega).
19. Vector-specific primers for PCR amplification of cloned 5′-RACE products (e.g., 5′-ACG ACG TTG TAA AAC GAC GG-3′ and 5′-TTC ACA CAG GAA ACA GCT ATG AC-3′ when using pGEM®-T as cloning vector).
20. Chemically competent *Escherichia coli* cells (e.g., DH5α).
21. LB-agar plates with the antibiotic specified by the PCR cloning vector.
22. Materials and buffers for horizontal agarose gel electrophoresis.

2.3 Terminator™ 5′-Phosphate-Dependent Exonuclease Treatment (TEX) of RNA

1. Reaction tubes (1.5 mL).
2. TEX, Epicentre Biotechnologies.
3. RiboLock™ RNase inhibitor (Thermo Scientific).
4. Phenol-chloroform-isoamyl alcohol 25:24:1, pH 5.0.
5. Chloroform-isoamyl alcohol 24:1.
6. 3 M Sodium acetate, pH 4.8.
7. 100 % Ethanol.

8. 70 % (v/v) Ethanol.
9. 60 °C Incubator.
10. Refrigerated microcentrifuge.

2.4 Primer Extension Analysis

2.4.1 Oligonucleotide 5′ End Labeling

1. Reaction tubes (1.5 mL).
2. T4 polynucleotide kinase (PNK) and 10× T4 PNK buffer A (Thermo Scientific).
3. Oligonucleotide (20 μM).
4. [γ-^{32}P] ATP (10 μCi/μL) (Hartmann Analytic).
5. NAP-5 columns (GE Healthcare).
6. 37 °C Incubator.
7. Liquid scintillation counter (e.g., Tri-Carb 2800TR from Perkin Elmer).

2.4.2 Primer Extension Reaction

1. Reaction tubes (1.5 mL).
2. Murine Leukemia Virus Reverse Transcriptase (M-MLV RT) RNase (H-) point mutant and 5× reaction buffer (Promega).
3. RiboLock™ RNase inhibitor (Thermo Scientific).
4. dNTP mix (10 mM each dATP, dGTP, dCTP, and dTTP).
5. 1 M NaOH.
6. 1 M HCl.
7. Gen Elute™ PCR Clean-Up Kit (Sigma).
8. SpeedVac vacuum concentrator.
9. 72 °C/45 °C incubator or heating block.
10. Microcentrifuge.

2.4.3 Polyacrylamide Gel Electrophoresis

1. Glass plates, 0.2-mm spacer, and comb.
2. Vertical electrophoresis chamber for polyacrylamide gel electrophoresis (PAGE).
3. 40 % (w/v) Acrylamide stock solution (acrylamide/bisacrylamide 19:1).
4. Urea.
5. 10× TBE buffer (890 mM Tris-borate, 890 mM boric acid, 20 mM EDTA).
6. *N*,*N*,*N*′,*N*′-Tetramethylenediamine (TEMED).
7. 10 % (w/v) Ammonium persulfate (APS).
8. 3× PAGE sample solution [98 % (w/v) deionized formamide, 10 mM EDTA, a pinch of bromophenol blue, and a pinch of xylene cyanol].
9. pGEM® DNA Marker (Promega).
10. Whatman® 3MM paper.

3 Methods

3.1 RNA Isolation and DNase Treatment

It is important that all steps from tissue harvesting to TRIsure addition are performed rapidly, to avoid RNA degradation by ribonucleases present in the plant tissue. The tissue must remain deep-frozen between harvesting and TRIsure addition. All centrifugation steps are to be performed at 4 °C. Handle phenol-containing reagents and samples under a fume hood, and avoid contaminating gloves and equipment with traces of phenol (*see* **Note 3**). **Steps 1–5** will produce RNA that is sufficiently pure for many applications; however, for downstream applications described under Subheadings 3.2 and 3.4, we recommend further purification of the RNA as described in **steps 6–15**.

1. Harvest and transfer 100 mg of the tissue of interest into a 2-mL microcentrifuge tube containing one stainless steel bead. Close the tube tightly and rapidly snap-freeze the sample by transferring the tube into liquid nitrogen (*see* **Note 4**).
2. For tissue grinding using the bead mill, place the tube into a suitable precooled (−80 °C) tube holder and grind at 20 Hz for 1 min. Verify that the tissue has been thoroughly ground and a fine powder has been obtained; put the tube back into liquid nitrogen. If regrinding is required, ensure that the tissue, tube, and tube holder remain deep-frozen.
3. Remove the sample tube from liquid nitrogen and briefly shake the tube to collect all tissue powder at the bottom of the tube. Add 1 mL TRIsure reagent to the frozen tissue powder and mix the contents thoroughly during 30 s, using a vortex mixer at high speed. Leave the sample at room temperature for 5 min; then add 200 μL of chloroform. Following chloroform addition, keep the tube at room temperature for 2 min. Centrifuge the sample at 12 000 × *g* for 15 min.
4. Transfer the upper, RNA-containing aqueous phase into a new 1.5-mL microcentrifuge tube. Add 0.5 volume of isopropanol, mix, and incubate the sample on ice for 15 min in order to precipitate the RNA. Centrifuge the sample at 12 000 × *g* for 15 min to collect the precipitated RNA.
5. Wash the RNA pellet with 70 % (v/v) ethanol, recentrifuge the sample at 12 000 × *g* for 5 min, carefully remove all ethanol, and air-dry the pellet at room temperature (*see* **Note 5**). Dissolve the RNA in 200 μL of ultrapure water (*see* **Note 6**).
6. Add 200 μL of phenol-chloroform-isoamyl alcohol, pH 5.0, mix the contents of the tube using a vortex mixer at medium speed three times for 3 s, and centrifuge the sample at 12,000 × *g* for 8 min.

7. Transfer the upper, RNA-containing aqueous phase into a new 1.5-mL microcentrifuge tube, and repeat the phenol-chloroform-isoamyl alcohol extraction and centrifugation.
8. Transfer the upper phase into a new 1.5-mL microcentrifuge tube, add 200 μL of chloroform, and mix the contents of the tube in order to remove traces of phenol from the sample. Centrifuge the sample at 12,000 × *g* for 8 min.
9. Transfer the upper phase into a new 1.5-mL microcentrifuge tube. To precipitate the RNA, add 3 volumes of ethanol/3 M sodium acetate, pH 4.8 (30:1) and leave the sample at –20 °C for at least 1 h (preferably overnight). Collect the RNA by centrifugation (20,000 × *g* for ≥30 min).
10. Wash the pellet with 70 % (v/v) ethanol, recentrifuge the sample at 12,000 × *g* for 5 min, carefully remove all ethanol, and air-dry the pellet at room temperature (*see* **Note 5**). Once all ethanol has evaporated, resuspend the pellet in 30–60 μL of ultrapure water to obtain an RNA solution at a concentration of 0.5–2 μg/μL.
11. Use an ultraviolet-visible spectrophotometer to determine the concentration and purity of the RNA (*see* **Note 7**).
12. Treat an aliquot of the RNA with DNase I to remove residual genomic DNA (*see* **Note 8**). In a 1.5-mL reaction tube, mix 15 μg RNA, 10 μL RQ1 DNase (10 U), 10 μL 10× RQ1 reaction buffer (supplied with the enzyme), and ultrapure water to obtain a final volume of 100 μL. Incubate the reaction at 37 °C for 45 min, then add another 5 μL RQ1 DNase (5 U), and keep the reaction at 37 °C for another 45 min. Stop the reaction by adding 100 μL of phenol-chloroform-isoamyl alcohol, pH 5.0, mix the contents of the tube using a vortex mixer at medium speed three times for 3 s, and centrifuge the sample at 12,000 × *g* for 8 min.
13. Transfer the upper phase into a new 1.5-mL microcentrifuge tube, add 100 μL of chloroform, and mix the contents of the tube in order to remove traces of phenol from the sample. Centrifuge the sample at 12,000 × *g* for 8 min.
14. Transfer the upper phase into a new 1.5-mL microcentrifuge tube. To precipitate the RNA, add 3 volumes of ethanol/3 M sodium acetate, pH 4.8 (30:1) and leave the sample at –20 °C for at least 1 h (preferably overnight). Collect the RNA by centrifugation (20,000 × *g* for ≥30 min).
15. Wash the pellet with 70 % (v/v) ethanol, recentrifuge the sample at 12,000 × *g* for 5 min, carefully remove all ethanol, and air-dry the pellet at room temperature (*see* **Note 5**). Once all ethanol has evaporated, resuspend the pellet in 20 μL of ultrapure water to obtain an RNA solution at a concentration of 0.5–0.7 μg/μL.

16. Use an ultraviolet-visible spectrophotometer to determine the concentration and purity of the RNA. Inspect the RNA quality by horizontal non-denaturing agarose gel electrophoresis, using a 1.2 % (w/v) agarose gel and 1× TAE as running buffer. The RNA can be used immediately for downstream procedures or stored at −80 °C.

3.2 TAP Treatment of RNA and Differential 5′-RACE

1. In a 1.5-mL reaction tube, mix 5 μg RNA, 10 μL 10× TAP reaction buffer (supplied with the TAP enzyme), 2 μL TAP (10 U), 1 μL RiboLock RNase inhibitor (40 U), and ultrapure water to obtain a final volume of 100 μL. In a second tube, set up a control reaction with the same components but omitting the TAP enzyme. All subsequent steps will be performed simultaneously for both the +TAP and the −TAP sample. Incubate the reaction at 37 °C for 1 h, and then stop the reaction by adding 100 μL of phenol-chloroform-isoamyl alcohol, pH 5.0. Mix and centrifuge the samples at 12,000 × *g* for 8 min.
2. Transfer the upper phase into a new 1.5-mL microcentrifuge tube. To precipitate the RNA, add 3 volumes of ethanol/3 M sodium acetate, pH 4.8 (30:1) and leave the sample at −20 °C overnight. Collect the RNA by centrifugation (20,000 × *g* for ≥30 min). Wash the pellet with 70 % (v/v) ethanol, recentrifuge the sample at 12,000 × *g* for 5 min, carefully remove all ethanol, and air-dry the pellet at room temperature (*see* **Note 5**). If highly pure RNA was used, the RNA pellet may not be visible at this step.
3. Resuspend the pellet in 67 μL of ultrapure water. Add to the RNA 10 μL 10× T4 RNA ligase reaction buffer (supplied with the T4 RNA ligase enzyme), 10 μL T4 RNA ligase (50 U), 10 μL ATP (10 mM, supplied with the enzyme), 2 μL RiboLock RNase inhibitor (80 U), and 1 μL oligoribonucleotide adapter (10 pmol/μL) to obtain a final volume of 100 μL. Incubate the reaction at 37 °C for 1 h, and then stop the reaction by adding 100 μL of phenol-chloroform-isoamyl alcohol, pH 5.0. Mix and centrifuge the samples at 12,000 × *g* for 8 min.
4. Repeat **step 2**.
5. Resuspend the pellet in 29.5 μL ultrapure water. Transfer the RNA into a PCR tube and add 1 μL of preprepared RT oligonucleotide mix (*see* **Note 9**), containing up to 12 different gene-specific primers (2 μM each). Denature the RNA and primers at 65 °C for 5 min, and then immediately place the tubes on ice for 2 min. Add 2.5 μL of SuperScript® III reverse transcriptase (600 U), 10 μL 5× reaction buffer (supplied with the enzyme), 2.5 μL 0.1 M dithiothreitol (DTT, supplied with the enzyme), 2.5 μL dNTP mix (10 mM each dATP, dGTP,

dCTP, and dTTP), and 2 μL RiboLock RNase inhibitor (80 U) to obtain a final volume of 50 μL. In a PCR cycler, allow reverse transcription to proceed at 53 °C for 1 h; then inactivate the reaction through incubation at 70 °C for 15 min.

6. Add 50 μL of ultrapure water to the reaction and extract the cDNA with 100 μL of phenol-chloroform-isoamyl alcohol, pH 8. Mix and centrifuge the samples at 12 000 × *g* for 8 min.
7. Repeat **step 2**.
8. Dissolve the cDNA in 20 μL ultrapure water.
9. The products of reverse transcription are amplified in a first PCR step, using 1 μL of the cDNA as template, the adapter-specific forward together with a gene-specific reverse primer (Fig. 1 and *see* **Note 10**), and a standard *Taq* DNA polymerase (use according to the supplier's instructions).
10. Products amplified in the first PCR can be used as template for subsequent nested PCRs, using the adapter-specific forward primer and reverse primers annealing upstream of the first PCR reverse primer (*see* **Note 10**). Use a standard *Taq* DNA polymerase (according to the supplier's instructions) and 0.05–1 μL of the first PCR reaction as template.
11. RT-PCR products are analyzed by electrophoresis on 3 % (w/v) agarose gels (*see* **Note 11**), using 1× TAE as running buffer. Bands seen for +TAP and –TAP samples are excised from the gel and purified using a commercially available PCR product gel extraction kit (follow the supplier's instructions).
12. Ligate the purified products into a PCR cloning vector (set up the ligation reaction according to the supplier's instructions). Use the ligation reactions to transform chemically competent *Escherichia coli* cells, and grow transformants on LB-agar plates containing the antibiotic specified by the PCR cloning vector. One bacterial colony will correspond to one mitochondrial transcript molecule.
13. Amplify the cloned RT-PCR fragments by colony PCR, using a standard *Taq* DNA polymerase (following the supplier's instructions) and vector-specific primers flanking the insert. Use 1/10 of a colony PCR reaction for agarose gel electrophoresis, in order to confirm the insert size.
14. Transcript 5′ ends are identified by sequencing across adapter-transcript ligation sites (refer to a company providing standard DNA sequencing services). Per RT-PCR fragment, analyze the sequence of at least eight clones (equal to eight different colony PCR products). For heterogeneous or ambiguous transcript 5′ ends (*see* **Note 2**), sequencing of up to 40 clones for each +TAP and –TAP samples may be necessary to identify primary transcript 5′ ends.

3.3 Terminator™ 5′ -Phosphate-Dependent Exonuclease Treatment (TEX) of RNA

1. Prepare total cellular RNA from appropriate plant tissues as described under Subheading 3.1 or with the Spectrum Plant Total RNA Kit (Sigma). Generally, any RNA isolation procedure can be used; however, special care should be taken to minimize degradation of the RNA by contaminating ribonucleases.
2. For exonucleolytic digestion, add the following components to a total volume of 20 μL: 10 μg RNA in 16.5 μL ultrapure water, 2 μL 10× TEX reaction buffer A (supplied with the enzyme), 0.5 μL RiboLock RNase inhibitor (20 U), and 1 μL TEX (1 U) (*see* **Note 12**).
3. Mix gently and incubate for 30 min at 60 °C.
4. Add 180 μL of ultrapure water to adjust the total volume to 200 μL.
5. Add 200 μL of phenol-chloroform-isoamyl alcohol, pH 5.0, and mix on a vortex mixer.
6. Centrifuge the sample at 16,700 × *g* for 5 min at room temperature.
7. Carefully remove the upper aqueous layer (about 190 μL) and transfer into a new 1.5-mL reaction tube. Add 200 μL of chloroform-isoamyl alcohol (24:1) and mix the contents of the tube in order to remove traces of phenol from the sample. Centrifuge the sample at 16,700 × *g* for 5 min at room temperature.
8. Repeat **step 7**.
9. Finally remove the upper aqueous layer (about 190 μL) and transfer into a new 1.5-mL reaction tube. To precipitate the RNA, add 0.1 volume of 3 M sodium acetate, pH 4.8, and 2.5 volumes of 100 % ethanol.
10. Mix gently and incubate for 30 min at −80 °C (or overnight at −20 °C).
11. Centrifuge the sample at ≥16,700 × *g* for 30 min at 4 °C.
12. Discard the supernatant and wash the pellet twice with 400 μL 70 % (v/v) ethanol.
13. Dry the pellet at room temperature and resuspend in 16 μL ultrapure water.
14. The RNA can now be used for the primer extension reaction (Subheading 3.4).

3.4 Primer Extension Analysis

3.4.1 Oligonucleotide 5′ End Labeling

1. For the radioactive labeling of the primer, combine the following components to a total volume of 20 μL: 1 μL 20 μM oligonucleotide, 13 μL ultrapure water, 3 μL [γ-^{32}P] ATP (10 μCi/μL), 2 μL 10× T4 PNK buffer A (supplied with the PNK enzyme), and 1 μL PNK (10 U) (*see* **Note 3**).
2. Mix gently and incubate for 60 min at 37 °C.

3. Meanwhile prepare a NAP-5 column by adding twice 500 µL of ultrapure water. Discard the eluate.
4. Add 480 µL of ultrapure water to the PNK reaction and load the complete mixture onto the NAP-5 column.
5. Discard the flow-through, which contains non-incorporated [γ-^{32}P] ATP.
6. Add another 500 µL of ultrapure water onto the column and collect the eluate, which contains the labeled primer.
7. Use a scintillation counter to measure the incorporation of [γ-^{32}P] ATP. Approximately 200,000–300,000 cpm in 10 µL of the eluate is appropriate. The labeled oligonucleotide is now ready to be used in the primer extension reaction.

3.4.2 Primer Extension Reaction

1. Primer extension analysis of distinct mitochondrial transcripts can be carried out with total cellular RNA or with mitochondrial RNA preparations. Depending on the levels of individual transcripts, 25–50 µg of total RNA or 4–8 µg of mitochondrial RNA is used per reaction.
2. The extension reaction (i.e., single-strand DNA synthesis) is performed in a final volume of 25 µL. Mix 16.25 µL RNA in ultrapure water with 2 µL of labeled primer (300,000–450,000 cpm, *see* **Note 13**).
3. Incubate for at least 5 min at 72 °C and subsequently keep the sample on ice.
4. Add 5 µL 5× M-MLV RT reaction buffer (supplied with the enzyme), 0.75 µL RiboLock™ RNase inhibitor (30 U), and 1 µL M-MLV RT (H-) (200 U).
5. Mix gently with a pipette and incubate for at least 60 min at 45 °C. Meanwhile prepare a column of the Gen Elute™ PCR Clean-Up Kit (*see* **step 8**).
6. Stop the cDNA synthesis by adding 5 µL 1 M NaOH. Keep the reaction for 10 min at room temperature.
7. Add 5 µL 1 M HCl.
8. For purification of the extension products with the Gen Elute™ PCR Clean-Up Kit, insert the spin column into the provided collection tube. Add 500 µL column preparation solution (supplied with the kit) and spin for 30 s at 12,000 × *g*. Discard the eluate.
9. Add 5 volumes of the binding solution (supplied with the kit) to 1 volume of the extension reaction, mix with the pipette, and load onto the column.
10. Spin for 1 min at 12,000 × *g* and discard the eluate, but retain the collection tube.

11. Add 500 µL wash solution (supplied with the kit) to the column, centrifuge for 1 min at 12,000 × *g*, discard the eluate, and again retain the collection tube.
12. Centrifuge column again for 2 min at 12,000 × *g* to remove residual wash solution.
13. Insert column into a new collection tube, add 50 µL ultrapure water to the column, and incubate for 1 min at room temperature.
14. To elute the extension products, spin for 1 min at 12,000 × *g*. Repeat this step with another 50 µL of ultrapure water.
15. Reduce the volume to 8 µL in a SpeedVac and mix with 4 µL 3× PAGE sample solution. Extension products are now ready for electrophoresis.

3.4.3 Polyacrylamide Gel Electrophoresis of Primer Extension Products

1. Clean the glass plates and assemble with the spacers.
2. For a medium-size 6 % (w/v) polyacrylamide gel (16 × 24 cm), mix the following components in a beaker (*see* **Note 14**): 12.62 g urea, 3 mL 10× TBE buffer, 4.5 mL 40 % (w/v) acrylamide stock solution, and ultrapure water to a final volume of about 28 mL.
3. Stir the solution until the urea is dissolved. Now adjust with ultrapure water to a final volume of 30 mL.
4. Add 22.5 µL TEMED and 112.5 mL 10 % (w/v) APS, briefly mix, and cast the gel. Insert a comb at the top of the gel to create sample wells.
5. After about 1 h, the gel is fully polymerized and can be used for electrophoresis.
6. Remove the spacer at the bottom of the gel and place the gel in the appropriate electrophoresis chamber.
7. Add electrophoresis buffer (1× TBE) and remove air at the bottom of the gel and in the sample wells.
8. Apply an electric field (~13 W) for about 30 min. Make sure that you connect the lower electrode to the anode.
9. Stop the power and use a Pasteur pipette to wash the sample wells with electrophoresis buffer.
10. To resolve any secondary structures incubate the extension products for 5 min at 72 °C and subsequently store them on ice. This step should be performed at the end of **step 8**.
11. Now load the samples and a labeled pGEM® DNA marker onto the gel and again apply the power.
12. Run the gel for about 90 min (~13 W). The duration of the electrophoresis may vary and depends on the size range that has to be resolved.

13. Stop electrophoresis and carefully remove the gel from the chamber. Make sure that you collect radioactive solutions and discard them into the appropriate waste.
14. Use a knife to remove the upper plate.
15. Place a Whatman® 3MM paper on the gel and gently press until the gel sticks to paper.
16. Remove the gel with the paper, wrap in foil (e.g., Saran wrap), and expose to an X-ray film in an appropriate exposition cassette.

4 Notes

1. While the differential 5′-RACE protocol presented here uses ligation of transcript 5′ ends to an oligoribonucleotide adapter, it is also possible to set up the RNA ligation without this adapter and perform CR-RT-PCR, which amplifies cDNAs made from head-to-tail ligated transcripts and uses a forward primer annealing upstream of the transcript 3′ end instead of an adapter-specific forward primer [23]. Advantages of the CR-RT-PCR procedure are that (1) it does not require the rather expensive oligoribonucleotide and (2) it provides information on transcript 3′ ends. Advantages of using a defined 5′ adapter are that (1) RT-PCR products are less complex and 5′ ends will be easier to analyze, and (2) the ligation reaction may be more efficient.
2. Application of this 5′-RACE procedure for mitochondrial transcript 5′ end mapping has shown that results can be ambiguous, with little difference seen between +TAP and –TAP electrophoretic product patterns for primary transcripts [6, 7]. In many cases, this is because primary and processed transcript ends differ by very few nucleotides. These differences can usually be resolved by sequencing a sufficiently large number of cloned 5′ ends for both TAP-treated and untreated samples. In other cases, ambiguities arise from the instability of 5′ triphosphates, with both primary and monophosphorylated transcripts mapping to the same nucleotide. This was found to be the case for several mitochondrial transcripts encoding subunits of the ATP synthase in Arabidopsis [7]. While it has previously been possible to detect residual triphosphorylated primary transcripts through in vitro capping by guanylyl transferase [7], this enzyme is no longer commercially available. An alternative experimental strategy to confirm such ambiguous primary 5′ ends would be to demonstrate activity of the corresponding promoter in an in vitro transcription assay [7, 24, 25].

3. Prior to mixing or centrifuging TRIsure- and phenol-containing samples, ensure that lids of reaction tubes are tightly closed. Prior to opening reaction tubes containing TRIsure or phenol, verify that the inside of the lid is free of any liquid. It is possible to very briefly (i.e., 3 s) spin down the contents of the tube to clear the lid.
4. The tissue can be processed immediately or stored at −80 °C until tissue disruption. Storage periods exceeding 2 months are not recommended.
5. It is important not to overdry the RNA pellet as overly dry RNA can be very difficult to resuspend. While the RNA dries, observe the pellet regularly and add ultrapure water to the pellet immediately once it becomes transparent.
6. The RNA obtained here will still contain substantial contaminants, including protein and DNA. It can be further purified through optional **steps 6–15**, used immediately for downstream procedures that do not require highly pure RNA or stored at −80 °C until further use. Further purification of the RNA will, however, decrease yield.
7. At this point, it is highly recommended to inspect the RNA quality by non-denaturing agarose gel electrophoresis on a 1.2 % (w/v) agarose gel, using 1× TAE as running buffer. The RNA can be used immediately for downstream procedures or stored at −80 °C.
8. In our hands, DNase I treatments performed in solution as described here have been more efficient than DNase I treatments of RNA bound to silica membranes.
9. Gene-specific primers for reverse transcription (RT primers) should be designed in a way so that they anneal downstream of the start codon (for mRNAs) or the mature RNA 5′ end (for mRNAs and tRNAs). We recommend designing RT primers with a melting temperature between 54 and 60 °C according to [26]. In one reverse transcription reaction, we have previously used up to 12 different RT primers for different mitochondrial genes, allowing the subsequent 5′-RACE analysis of 12 different genes from a single cDNA preparation.
10. Gene-specific reverse primers should be designed in a way so that they will be compatible with the adapter-specific forward primer. They can anneal immediately upstream of the RT primer or may even be identical with the RT primer. We have previously used the first RT-PCR as template for different nested PCRs, in order to allow us to map several different 5′ ends for one gene from one cDNA preparation. Because small products are favored over larger products during PCR amplification, it is usually not possible to capture all 5′ ends for a given gene in the same PCR reaction. To map upstream 5′

ends, it will usually be necessary to design gene-specific reverse primers annealing upstream of downstream 5′ ends.

11. Products amplified by this 5′-RACE strategy are usually only between 50 and 500 bp long and thus require high agarose concentrations for optimum resolution by electrophoresis. Although special agarose is available for separating small fragments, standard agaroses exist that will serve the purpose (e.g., Agarose Standard DNA Grade from EUROMEDEX) and are less expensive. Gene-specific reverse primers should be designed in a way so that 500 bp product size is not exceeded. This will allow you to characterize a cloned 5′-RACE product by performing a single sequencing reaction per clone (Subheading 3.2, **step 14**), which will be important for keeping sequencing costs to a minimum.
12. When analyzing low-abundant transcripts, it is possible to scale up all reaction components up to a total volume of 60 μL.
13. If necessary reduce the volume of the labeled primer in a SpeedVac vacuum concentrator.
14. Make a mark at 30 mL on the glass beaker.

Acknowledgements

We thank Birgit Stoll and Katrin Stoll for their kind help with the manuscript. Work in our laboratories is supported by grants from the Deutsche Forschungsgemeinschaft to S.B. (Bi 590/9-2 and Bi 590/10-2) and from the ECFP7 to K.K. (PCIG12-GA-2012-333747).

References

1. Kubo T, Newton KJ (2008) Angiosperm mitochondrial genomes and mutations. Mitochondrion 8:5–14
2. Gagliardi D, Binder S (2007) Expression of the plant mitochondrial genome. In: Logan DC (ed) Plant Mitochondria. Blackwell Publishing Ltd., Oxford, UK, pp 50–96
3. Liere K, Weihe A, Börner T (2011) The transcription machineries of plant mitochondria and chloroplasts: composition, function, and regulation. J Plant Physiol 168:1345–1360
4. Fey J, Marechal-Drouard L (1999) Compilation and analysis of plant mitochondrial promoter sequences: an illustration of a divergent evolution between monocot and dicot mitochondria. Biochem Biophys Res Commun 256:409–414
5. Kühn K, Bohne AV, Liere K et al (2007) Arabidopsis phage-type RNA polymerases: accurate in vitro transcription of organellar genes. Plant Cell 19:959–971
6. Kühn K, Richter U, Meyer EH et al (2009) Phage-type RNA polymerase RPOTmp performs gene-specific transcription in mitochondria of Arabidopsis thaliana. Plant Cell 21: 2762–2779
7. Kühn K, Weihe A, Börner T (2005) Multiple promoters are a common feature of mitochondrial genes in Arabidopsis. Nucleic Acids Res 33:337–346
8. Haili N, Arnal N, Quadrado M et al (2013) The pentatricopeptide repeat MTSF1 protein stabilizes the nad4 mRNA in Arabidopsis mitochondria. Nucleic Acids Res 41:6650–6663
9. Perrin R, Lange H, Grienenberger JM et al (2004) AtmtPNPase is required for multiple aspects of the 18S rRNA metabolism in *Arabidopsis thaliana* mitochondria. Nucleic Acids Res 32:5174–5182
10. Perrin R, Meyer EH, Zaepfel M et al (2004) Two exoribonucleases act sequentially to process mature 3′-ends of atp9 mRNAs in

Arabidopsis mitochondria. J Biol Chem 279: 25440–25446

11. Hirayama T, Matsuura T, Ushiyama S et al (2013) A poly(A)-specific ribonuclease directly regulates the poly(A) status of mitochondrial mRNA in Arabidopsis. Nat Commun 4:2247
12. Binder S, Stoll K, Stoll B (2013) P-class pentatricopeptide repeat proteins are required for efficient 5′ end formation of plant mitochondrial transcripts. RNA Biol 10:1511–1519
13. Bensing BA, Meyer BJ, Dunny GM (1996) Sensitive detection of bacterial transcription initiation sites and differentiation from RNA processing sites in the pheromone-induced plasmid transfer system of *Enterococcus faecalis*. Proc Natl Acad Sci U S A 93: 7794–7799
14. Mitschke J, Georg J, Scholz I et al (2011) An experimentally anchored map of transcriptional start sites in the model cyanobacterium Synechocystis sp. PCC6803. Proc Natl Acad Sci U S A 108:2124–2129
15. Sharma CM, Hoffmann S, Darfeuille F et al (2010) The primary transcriptome of the major human pathogen Helicobacter pylori. Nature 464:250–255
16. Zhelyazkova P, Sharma CM, Forstner KU et al (2012) The primary transcriptome of barley chloroplasts: numerous noncoding RNAs and the dominating role of the plastid-encoded RNA polymerase. Plant Cell 24:123–136
17. Jonietz C, Forner J, Holzle A et al (2010) RNA PROCESSING FACTOR2 is required for 5′ end processing of nad9 and cox3 mRNAs in mitochondria of Arabidopsis thaliana. Plant Cell 22:443–453
18. Stoll B, Stoll K, Steinhilber J et al (2013) Mitochondrial transcript length polymorphisms are a widespread phenomenon in Arabidopsis thaliana. Plant Mol Biol 81:221–233
19. Chomczynski P, Sacchi N (1987) Single-step method of RNA isolation by acid guanidinium thiocyanate-phenol-chloroform extraction. Anal Biochem 162:156–159
20. Binder S, Brennicke A (1993) A tRNA gene transcription initiation site is similar to mRNA and rRNA promoters in plant mitochondria. Nucleic Acids Res 21:5012–5019
21. Binder S, Brennicke A (1993) Transcription initiation sites in mitochondria of *Oenothera berteriana*. J Biol Chem 268:7849–7855
22. Lin X, Kaul S, Rounsley S et al (1999) Sequence and analysis of chromosome 2 of the plant Arabidopsis thaliana. Nature 402:761–768
23. Forner J, Weber B, Thuss S et al (2007) Mapping of mitochondrial mRNA termini in Arabidopsis thaliana: t-elements contribute to 5′ and 3′ end formation. Nucleic Acids Res 35:3676–3692
24. Binder S, Hatzack F, Brennicke A (1995) A novel pea mitochondrial in vitro transcription system recognizes homologous and heterologous mRNA and tRNA promoters. J Biol Chem 270:22182–22189
25. Rapp WD, Stern DB (1992) A conserved 11 nucleotide sequence contains an essential promoter element of the maize mitochondrial *atp1* gene. EMBO J 11:1065–1073
26. Breslauer KJ, Frank R, Blocker H et al (1986) Predicting DNA duplex stability from the base sequence. Proc Natl Acad Sci U S A 83: 3746–3750

Chapter 3

Mitochondrial Run-On Transcription Assay Using Biotin Labeling

Kristina Kühn

Abstract

RNA synthesis and different posttranscriptional processes shape the transcriptome of plant mitochondria. It is believed that mitochondrial transcription in plants is not stringently controlled, and that RNA degradation has a major impact on mitochondrial steady-state transcript levels. Nevertheless, the presence of two RNA polymerases with different gene specificities in mitochondria of dicotyledonous species indicates that transcriptional mechanisms may provide a means to control mitochondrial steady-state RNA pools and gene expression. To experimentally assess transcriptional activities in mitochondria, run-on transcription assays have been developed. These assays measure elongation rates for endogenous transcripts in freshly prepared mitochondrial extracts. The mitochondrial run-on transcription protocol described here has been optimized for the model plant Arabidopsis (*Arabidopsis thaliana*). It uses mitochondria prepared from soil-grown Arabidopsis plants and employs nonradioactive labeling for the subsequent detection of run-on transcripts.

Key words Mitochondria, RNA polymerase, Transcriptome, Transcription activity, Run-on transcription assay, Biotin labeling, Slot-blot hybridization, Arabidopsis

1 Introduction

Mitochondrial biogenesis and function depend on the correct expression of mitochondrial genes. Mitochondrial genomes code for subunits of the protein complexes that form the oxidative phosphorylation (OXPHOS) system [1]. In land plants, they additionally contain genes required for cytochrome *c* maturation. Except for mitochondrial ribosomal RNA genes and genes for a subset of mitochondrial transfer RNAs (tRNAs) and ribosomal proteins, all components of the mitochondrial gene expression machinery are encoded in the nucleus and must be imported into the organelle [2].

Mitochondrial genomes are transcribed by nucleus-encoded RNA polymerases of the T3/T7 bacteriophage type [3]. Whereas monocotyledonous plants possess only one mitochondrial transcriptase, two RNA polymerases are present in mitochondria of eudicotyledonous species. In Arabidopsis (*Arabidopsis thaliana*),

James Whelan and Monika W. Murcha (eds.), *Plant Mitochondria: Methods and Protocols*, Methods in Molecular Biology, vol. 1305, DOI 10.1007/978-1-4939-2639-8_3,

these enzymes are named RPOTm and RPOTmp. RPOTm is exclusively found in mitochondria while RPOTmp is present in both mitochondria and plastids [4–6]. Recent analyses of Arabidopsis plants with an inactivated *RPOTm* or *RPOTmp* gene showed that RPOTm is essential for plant viability and can transcribe all mitochondrial genes; in contrast, RPOTmp transcribes only a subset of mitochondrial genes and is particularly important for the biogenesis of OXPHOS Complexes I and IV [7]. Substantially more work is needed to elucidate the physiological importance of this division of labor between two mitochondrial RNA polymerases in dicots, and to compare transcriptional mechanisms in dicots and monocots. It is to date unknown if plant mitochondrial RNA polymerases require transcriptional cofactors or function without the aid of auxiliary proteins [8].

A comprehensive set of methods is available for studying mitochondrial transcription. Plant mitochondrial promoters and their recognition by RPOT enzymes have been studied in various species through in vitro transcription assays, using mitochondrial extracts or recombinant RNA polymerases as a source of transcriptional activity [9–15]. Transcription start sites and promoters have been mapped on plant mitochondrial genomes by determining the 5′ ends of newly initiated transcripts [7, 16, 17]. Steady-state mitochondrial transcript levels, as determined by QRT-PCR or RNA gel blot hybridization, have been compared with transcriptional activities measured through run-on transcription assays [7, 18, 19]. Such comparisons have been used to assess the impact of transcriptional processes, as opposed to posttranscriptional processes and transcript stability, on steady-state RNA levels. Following initial applications of many of these techniques for the study of other plant species, most methods were later optimized for the model organism Arabidopsis.

Studying mitochondrial transcription in Arabidopsis has several advantages: Large mutant collections, including mutants disrupted in mitochondrial RNA polymerases and potential transcriptional cofactors, are readily available, and the complete genome sequence, including the mitochondrial genome, is known. This chapter describes a mitochondrial run-on transcription assay optimized for Arabidopsis plants. The procedure uses biotin labeling instead of the conventionally used radionucleotide labeling and has already been applied to compare transcriptional rates for different mitochondrial genes between Arabidopsis wild-type plants and RPOTmp-deficient plants [7]. Biotin has also been used as label for nuclear run-on transcription [20] but remains to be tested for chloroplast run-on assays [21].

Mitochondrial run-on transcription experiments require the isolation of intact mitochondria. Following lysis of the organelles and addition of nucleotides, including labeled ribonucleotides, the in vitro extension of transcripts already initiated in vivo is measured over a short period of time. Limiting the run-on period will ensure

that the accumulation of labeled transcripts is primarily determined by transcriptional activity and that the impact of posttranscriptional processes is negligible. Labeled transcripts synthesized during this period are quantified through hybridization to filter-immobilized gene-specific probes and subsequent detection of the label. Thus, mitochondrial run-on experiments require four major procedures: preparation of membranes with immobilized mitochondrial gene probes (described under Subheading 3.1), isolation of mitochondria (Subheading 3.2), synthesis of labeled mitochondrial run-on transcripts (Subheading 3.3), and hybridization of transcripts to filter-immobilized probes and quantitation of labels (Subheading 3.4).

2 Materials

All described procedures require the use of ultrapure water for preparing solutions or setting up enzymatic reactions. When handling RNA, ensure to use ribonuclease-free materials and solutions to avoid RNA degradation. Reaction tubes should be nuclease-free and nucleic acid-free. Clean gloves should be worn at all times.

2.1 Preparation of Slot-Blot Membranes

2.1.1 Equipment

1. PCR cycler.
2. Microfiltration apparatus for slot- or dot-blotting (e.g., MilliBlot-S from Millipore or PR648 Slot Blot Blotting Manifold from Hoefer).
3. Vacuum line or vacuum pump.
4. UV–Vis spectrophotometer (e.g., Nanodrop).
5. Refrigerated microcentrifuge.
6. Heating block.
7. UV crosslinker.

2.1.2 Materials, Reagents, and Solutions

1. Reaction tubes (1.5 mL).
2. PCR tubes (0.2 mL).
3. Whatman® 3MM paper.
4. Positively charged nylon membrane (e.g., from Roche Applied Science).
5. Standard *Taq* DNA polymerase (e.g., DreamTaq from Bioline), dNTPs, primers, and Arabidopsis cDNA for probe amplification.
6. PCR product purification kit (e.g., NucleoSpin® Gel and PCR Clean-up from Macherey-Nagel).
7. 10 M NaOH.
8. 0.5 M NaOH.
9. DNA loading dye: 30 % (v/v) glycerol, 0.25 % (w/v) bromophenol blue, 0.25 % (w/v) xylene cyanol.
10. 2× SSC solution: 0.3 M NaCl, 0.03 M Na-citrate.

2.2 Isolation of Mitochondria from Arabidopsis Plants

2.2.1 Equipment

1. POLYTRON® Batch Disperser (Kinematica).
2. Centrifuge (e.g., Avanti J-26XP from Beckman Coulter) with fixed-angle rotor for 50-mL tubes (e.g., JA 25.50 from Beckman Coulter).
3. Potter-Elvehjem tissue homogenizer (30 mL capacity, 0.1–0.15-mm chamber clearance).
4. Vacuum line or vacuum pump.
5. Spectrophotometer.

2.2.2 Materials

1. 30–50 Arabidopsis plants with fully grown rosettes.
2. Nylon mesh (reusable).
3. Miracloth (disposable, e.g., from Calbiochem).
4. Funnel.
5. 50-mL high-speed polycarbonate round-bottom centrifuge tubes fitting the rotor.
6. Transfer pipettes.
7. Paintbrush.

2.2.3 Reagents and Solutions

Buffers can be prepared on the day before the isolation of mitochondria; however, cysteine and dithiothreitol (DTT) should only be added to the extraction buffer immediately before use. For the gradient buffer it is recommended to prepare a larger volume at once and store 50-mL aliquots of the buffer at –20 °C until use.

1. Extraction buffer: 0.3 M sucrose, 5 mM tetrasodium pyrophosphate, 10 mM KH_2PO_4, 2 mM EDTA, 1 % (w/v) PVP-40, 1 % (w/v) bovine serum albumin (BSA), 5 mM cysteine, 1 mM DTT; adjust the pH to 7.5 with orthophosphoric acid.
2. Wash buffer: 0.3 M sucrose, 1 mM EGTA, 10 mM MOPS-KOH, pH 7.2.
3. 5× Gradient buffer: 1.5 M sucrose, 50 mM MOPS-KOH, pH 7.2.
4. Percoll (from GE Healthcare).
5. Bradford assay solution.

2.3 Run-On Transcription and Labeling

2.3.1 Equipment

1. Refrigerated microcentrifuge.
2. 25 °C incubator.

2.3.2 Materials, Reagents, and Solutions

1. Reaction tubes (1.5 mL)
2. 2× Run-on buffer: 50 mM Tris–HCl pH 7.6, 80 mM KCl, 20 mM $MgCl_2$.
3. 100 mM DTT.

4. RNase inhibitor (40 U/μL).
5. Run-on NTP mix: 5 mM of each, ATP, GTP, UTP, and 3 mM CTP.
6. 10 mM biotin-CTP (e.g., biotin-14-CTP from Life Technologies).
7. STOP solution: 5 % (w/v) lauroylsarcosine sodium salt, 50 mM Tris–HCl pH 8.0, 25 mM EDTA.
8. Phenol-chloroform (5:1), pH 4.5.
9. Chloroform-isoamyl alcohol (24:1).
10. Ethanol/3 M sodium acetate, pH 5.2 (30:1).
11. 70 % (v/v) ethanol.

2.4 Membrane Hybridization and Signal Detection

2.4.1 Equipment

1. Hybridization oven.
2. Heating block.
3. Refrigerated microcentrifuge.
4. CCD camera (e.g., ImageQuant RT ECL Imager from GE Healthcare).
5. Analysis software (e.g., ImageQuant TL software from GE Healthcare).
6. Rocking shaker.

2.4.2 Materials, Reagents, and Solutions

1. Hybridization bottles.
2. Containers with lid for room-temperature incubations and washes.
3. Hybridization buffer: 250 mM NaH_2PO_4 pH 7.2, 7 % (w/v) sodium dodecyl sulfate (SDS), 2.5 mM EDTA.
4. 20× SSC solution: 3 M NaCl, 0.3 M Na-citrate (needed to prepare wash solutions I and II).
5. Wash solution I: 1× SSC, 0.5 % (w/v) SDS.
6. Wash solution II: 1× SSC, 0.5 % (w/v) SDS.
7. Chemiluminescent Nucleic Acid Detection Module (Thermo Scientific; including blocking buffer, stabilized streptavidin-horseradish peroxidase conjugate, 4× wash buffer, substrate equilibration buffer, luminol/enhancer solution, stable peroxide solution).
8. Plastic wrap.

3 Methods

3.1 Preparation of Slot-Blot Membranes

For the subsequent hybridization with mitochondrial transcripts (Subheading 3.4), gene-specific probes need to be immobilized on a membrane. It is advisable to blot probes at least in duplicates. To allow analyses of low-transcribed as well as highly transcribed

RNAs on the same membrane, probes should be blotted in excess (0.5 μg of DNA per spot). The use of a vacuum-driven microfiltration apparatus for slot-blotting will generate regular spots on a membrane and should be preferred over manual spotting. The following protocol describes procedures for producing one membrane with duplicate probe spots.

1. For each gene to be analyzed in the run-on experiment, produce a DNA probe by PCR amplification of a mitochondrial cDNA fragment. Probes should be between 200 and 500 bp long (*see* **Note 1**). Several PCR reactions may be necessary per probe to generate sufficient amounts of probe. Additionally, produce a control probe lacking mitochondrial sequences (e.g., a standard PCR product cloning vector), which will be needed to determine nonspecific background hybridization (Subheading 3.4, **step 17**).
2. Purify the probes using a PCR product purification kit according to the supplier's instructions.
3. Use a UV–Vis spectrophotometer to determine the DNA concentration for each probe. In a 1.5-mL reaction tube, supplement 1 μg of probe with ultrapure water to obtain a volume of 190 μL. Add 10 μL 10 M NaOH and mix the probe samples; spin them briefly in a microcentrifuge to collect all liquid at the bottom of the tube. The final NaOH concentration in the probe samples will be 0.5 M.
4. Denature the probes at 95 °C for 10 min in a heating block; then chill the probes on ice for 2 min and spin them briefly in a microcentrifuge at 4 °C.
5. Add 15 μL of chilled 0.5 M NaOH to each probe, to make up for evaporation and possible pipetting inaccuracy.
6. Add 0.3 μL of chilled DNA loading dye, to facilitate locating probe spots on the membrane after blotting.
7. While denaturing the probes (**step 4**), cut three sheets of Whatman® 3MM paper and a positively charged nylon membrane to fit the blotting area of the slot-blot apparatus. Wet the 3MM paper and membrane in ultrapure water and assemble the blotting apparatus with the membrane placed on top of the three 3MM papers. Remove excess liquid by applying a moderate vacuum.
8. Rehydrate the membrane with 100 μL of ultrapure water per well; ensure that the vacuum is not too strong (*see* **Note 2**). Keep the vacuum until the end of **step 12**. Should air bubbles on the membrane block suction, pipet the contents of the well up and down until the path has been cleared.
9. One minute after all water has passed through the membrane, add 100 μL of probe to each well. To generate duplicate probe spots, apply each probe to two neighboring wells.

10. One minute after all liquid has passed through the membrane, add 100 µL 0.5 M NaOH to each well.
11. Keep the vacuum for 3 min after all liquid has passed through the membrane.
12. Disassemble the blotting apparatus and mark the probe slot positions with pencil on the edge of the membrane.
13. UV-crosslink the probes to the moist membrane at 120 mJ/cm^2.
14. Wash the membrane twice for 5 min in 2× SSC solution; then dry and store the membrane at room temperature until hybridization (Subheading 3.4).

3.2 Isolation of Mitochondria from Arabidopsis Plants

This protocol describes a procedure that has been optimized for the isolation of mitochondria from soil-grown Arabidopsis plants harvested after 5–6 weeks of growth, prior to bolting (*see* **Note 3**). Mitochondria are isolated from plant extracts using a series of differential centrifugations and further purified on a Percoll density gradient. Plant extracts and mitochondria must remain cold (4 °C) throughout the procedure. It is strongly recommended to perform the tissue disruption in the cold room, using precooled equipment and materials. Outside the cold room, samples should always be kept on ice. All centrifugation steps are to be performed at 4 °C. Ensure to use the "low brake" setting for all centrifugations. For gradient centrifugation (**step 11**), use the "low acceleration" setting; all other steps can be performed with maximum acceleration.

1. Harvest the aerial parts of the plants to collect 40–60 g of tissue.
2. Transfer the tissue into the blending beaker and add 30 mL of extraction buffer per 10 g of tissue. Place the POLYTRON aggregate in the beaker and select a low- to medium-speed setting (*see* **Note 4**). Disrupt the tissue by homogenizing two times for 5 s, pause briefly to allow the foam to settle, and homogenize again for 10–15 s.
3. Place a funnel onto a 500-mL Schott bottle and line the funnel with a nylon mesh and two layers of Miracloth. Filter the tissue extract through the Miracloth and nylon mesh, and recover all liquid from the sediment in the Miracloth by squeezing the mesh and Miracloth firmly. Distribute the filtered extract into 50-mL centrifuge tubes.
4. Centrifuge the homogenate for 5 min at 2,500 × *g* to pellet cell debris and large cell organelles/organelle fragments (*see* **Note 5**). Mitochondria will remain in the supernatant.
5. Pour the supernatant into new 50-mL centrifuge tubes and centrifuge for 10 min at 20,000 × *g* to obtain a pellet of crude mitochondria.

6. Discard the supernatant and resuspend the pellet in a small volume of wash buffer, using a paintbrush (*see* **Note 6**). Transfer the suspension into a Potter-Elvehjem tissue homogenizer and disrupt any aggregates by passing the pestle up and down five times. Distribute the suspension into two 50-mL centrifuge tubes and fill the tubes with wash buffer.
7. Centrifuge the homogenate for 10 min at 3,000 × *g* to pellet cell debris and large cell organelles/organelle fragments. Mitochondria will remain in the supernatant.
8. Pour the supernatant into new 50-mL centrifuge tubes and centrifuge for 10 min at 20,000 × *g* to obtain a pellet of crude mitochondria.
9. Thoroughly resuspend each pellet in 0.7–1 mL wash buffer using a 1-mL micropipette to obtain a suspension of crude mitochondria. It is important that no aggregates remain.
10. Prepare two Percoll step gradients per 40–60 g of starting material. This should be done at the same time as **steps 4–9**, to ensure that gradients are ready for loading when **step 9** has been completed. Percoll step gradients are prepared in 50-mL tubes and will have the following layers, from bottom to top: 5 mL 50 %, 25 mL 25 %, and 5 mL 18 % Percoll in wash buffer. The 50 % Percoll solution for two gradients is prepared by mixing 3.3 mL water, 5.5 mL Percoll, and 2.2 mL 5× gradient buffer. The 25 % solution is made by mixing 30.3 mL water, 13.7 mL Percoll, and 11 mL 5× gradient buffer. The 18 % solution is made by mixing 6.8 mL water, 2 mL Percoll, and 2.2 mL 5× gradient buffer. To prepare the gradients, place 5 mL of the 50 % solution in a 50-mL tube. Carefully layer 25 mL of the 25 % solution on top, followed by a 5-mL layer of the 18 % solution (*see* **Note 7**).
11. Overlay the gradients with the mitochondrial suspension obtained after **step 9**. Use a balance to equilibrate the gradients pairwise by layering wash buffer on top. Centrifuge the gradients at 40,000 × *g* for 45 min. The mitochondrial fraction will form a whitish band located at the interface between the 50 and 25 % layers.
12. Use a vacuum line to carefully and thoroughly remove the green top part of the gradient without disturbing the mitochondrial band. Collect the mitochondrial band using a transfer pipette without disturbing the bottom 2–3 mL of the gradient, and transfer the mitochondria into a new 50-mL tube. Fill the tube with wash buffer, and centrifuge at 20,000 × *g* for 10 min.
13. After **step 12**, the mitochondrial pellet will still be very loose due to the presence of Percoll; be careful when removing most of the supernatant using a vacuum line. Keep 2–4 mL of supernatant per tube and resuspend the pellet by swirling. Fill the tube with wash buffer, and pellet the mitochondria by centrifugation at 20,000 × *g* for 10 min.

14. Repeat **step 13** to obtain a firm mitochondrial pellet. From 40 to 60 g of Arabidopsis leaf tissue you may expect a mitochondrial yield equalling 0.5–2 μg of protein. Thoroughly resuspend the pellet in 1 mL wash buffer (*see* **Note 8**) and determine the protein concentration of the mitochondrial suspension through a Bradford protein assay. The mitochondria can now be assayed for run-on transcription activity (Subheading 3.3).

3.3 Run-On Transcription and Biotin Labeling

Always use freshly prepared mitochondria for run-on experiments and immediately proceed to **step 1** once you have obtained the mitochondrial suspension (Subheading 3.2, **step 14**). Samples should be kept on ice during **steps 1–6**. Centrifugation should always be performed at 4 °C. Handle phenol-containing reagents and samples under a fume hood, and avoid contaminating gloves and equipment with traces of phenol.

1. Mitochondria equaling 200 μg of protein are required for one run-on transcription reaction. Transfer an aliquot of mitochondrial suspension that contains 200 μg of protein into a 1.5-mL reaction tube and spin down the mitochondria by centrifugation at 20,000 × *g* for 10 min.
2. While spinning down the mitochondria, prepare the run-on mix by combining the following components in a new 1.5-mL reaction tube: 28 μL ultrapure water, 50 μL 2× run-on buffer, 1 μL 100 mM DTT, and 1 μL RNase inhibitor (40 U).
3. Thoroughly remove the supernatant from the mitochondrial pellet obtained after **step 1**; avoid disturbing the pellet.
4. Resuspend the mitochondrial pellet in 80 μL run-on mix (prepared in **step 2**) using a micropipette. This step induces the hypotonic disruption of mitochondria and will lead to foaming of the sample. It is advised to initially resuspend the mitochondria in 30–50 μL run-on mix and add the remaining run-on mix once all mitochondrial aggregates have been dispersed.
5. Start the synthesis of labeled run-on transcripts by adding 10 μL run-on NTP mix and 10 μL biotin-CTP (10 mM) to the sample to obtain a final reaction volume of 100 μL. Briefly but thoroughly mix the components and incubate the reaction at 25 °C for 10 min. The final composition of run-on transcription reaction will be 20 mM Tris pH 7.6, 40 mM KCl, 10 mM $MgCl_2$, 1 mM DTT, 0.5 mM of each ATP, GTP and UTP, 0.3 mM CTP, 1 mM biotin-CTP, 40 U RNase inhibitor, and 2 μg/μL of mitochondrial protein.
6. Terminate the reaction by placing the sample on ice, adding 100 μL STOP solution, and mixing thoroughly with a micropipette.
7. To extract transcripts from the reaction, add 200 μL phenol-chloroform pH 4.5. Mix the contents of the tube using a vortex mixer at medium speed three times for 3 s, and centrifuge

the sample at 12,000 × *g* for 8 min. Transfer the upper, RNA-containing aqueous phase into a new 1.5-mL tube.

8. Repeat **step 7**.
9. Add 200 μL of chloroform-isoamyl alcohol and mix the contents of the tube in order to remove traces of phenol from the sample. Centrifuge the sample at 12,000 × *g* for 8 min.
10. Transfer the upper, RNA-containing aqueous phase into a new 1.5-mL tube. To precipitate the RNA, add 3 volumes of ethanol/3 M sodium acetate pH 5.2 (30:1) and leave the sample at −20 °C overnight. Collect the RNA by centrifugation (~20,000 × *g* for ≥30 min).
11. Wash the RNA pellet with 70 % (v/v) ethanol, recentrifuge the sample at 12,000 × *g* for 5 min, carefully remove all ethanol, and air-dry the pellet at room temperature (*see* **Note 9**). Once all ethanol has evaporated, resuspend the pellet in 50 μL of ultrapure water. The run-on transcript sample can be used immediately for membrane hybridization (Subheading 3.4) or stored at −80 °C (*see* **Note 10**).

3.4 Membrane Hybridization and Signal Detection

Following membrane hybridization and washes (**steps 1–7**), the procedure described here uses the Chemiluminescent Nucleic Acid Detection Module (Thermo Scientific) for the detection of biotinylated transcripts (**steps 8–15**). Solutions needed for biotin label detection are components of this kit. **Steps 8–15** are performed at room temperature. It is important that the membrane is not left to dry at any time during the procedure.

1. Place the membrane (produced as described under Subheading 3.1) in a hybridization bottle (*see* **Note 11**) and add 10 mL hybridization buffer. Place the hybridization bottle in a preheated hybridization oven and pre-hybridize the membrane at 58 °C for 1 h.
2. Denature the run-on transcripts (produced as described under Subheading 3.3) in a heating block at 95 °C for 5 min; then place the tube on ice for 2 min. Briefly spin down the contents of the tube at 4 °C.
3. Remove the hybridization bottle from the oven and reduce the volume of hybridization buffer to 2.5 mL. Add the denatured run-on transcripts into the hybridization buffer; close and swirl the bottle and place it in the hybridization oven. Allow the hybridization to proceed overnight at 58 °C.
4. Following hybridization, remove the buffer with the run-on transcripts; it can be stored at −20 °C and reused if necessary.
5. Add 25 mL wash solution I to the bottle and wash the membrane at 57 °C for 10 min in the hybridization oven; discard the used wash solution.

6. Repeat **step 5**.
7. Add 25 mL wash solution II to the bottle and wash the membrane at 57 °C for 10 min in the hybridization oven; discard the used wash solution.
8. While performing the membrane washes (**steps 5–7**), slowly warm the blocking buffer (Thermo Scientific) and the 4× wash buffer (Thermo Scientific) to 37–50 °C in a water bath until all precipitate has dissolved.
9. Following **step 7**, place the membrane in a container with a lid (e.g., a square petri dish) that has approximately the size of the membrane. To block the membrane, add 10 mL blocking buffer (*see* **Note 12**) to the container and incubate the membrane for 15 min on a rocking shaker.
10. Remove the blocking buffer and add 10 mL of new blocking buffer supplemented with 30 μL of stabilized streptavidin-horseradish peroxidase conjugate (Thermo Scientific). Incubate the membrane in the conjugate/blocking buffer solution for 15 min on a rocking shaker. During this step, prepare 1× Wash buffer by adding 40 mL of 4× wash buffer to 120 mL ultrapure water.
11. Place the membrane in a new container and rinse the membrane briefly with 20 mL 1× wash buffer.
12. Wash the membrane four times for 5 min each in 20 mL of 1× wash buffer on a rocking shaker.
13. In a new container, incubate the membrane in 20 mL substrate equilibration buffer (Thermo Scientific) for 5 min on a rocking shaker. During this incubation, mix 2 mL luminol/enhancer solution (Thermo Scientific) with 2 mL stable peroxide solution (Thermo Scientific) and to obtain the substrate working solution, which should be kept in the dark until use.
14. Remove the membrane from the substrate equilibration buffer and blot a corner of the membrane on a tissue to remove excess liquid. In a new container, cover the membrane with the substrate working solution. Incubate the membrane in the substrate for 5 min without shaking.
15. Remove the membrane from the substrate working solution and blot a corner of the membrane on a tissue to remove excess liquid. Wrap the moist membrane in plastic wrap, avoiding bubbles and wrinkles.
16. Expose the membrane to a CCD camera. For the subsequent quantitative analysis of the chemiluminescence signals it is imperative that the recorded signals are not saturated.
17. Quantify the signals using appropriate analysis software, and subtract the background signal measured for the slot-blotted nonspecific DNA from each gene-specific signal.

4 Notes

1. It is possible to test the specificity and suitability of a probe by labeling the probe and using it for the detection of the corresponding transcript by RNA gel blot hybridization. Chloroplast run-on transcription assays have also used single-stranded oligonucleotide probes instead of longer double-stranded DNA probes produced by PCR. Oligonucleotide probes have the advantage that they allow the detection of strand-specific transcriptional signals.
2. If water is added to a row of 12 wells, the first wells should be emptied just as the last wells have been filled. Applying a vacuum that is too strong may lead to irregular DNA distribution within one spot, which will lead to irregular signals and cause problems during signal quantitation (Subheading 3.4).
3. Mitochondria can be prepared from Arabidopsis plants using different methods of tissue disruption. The efficiency of a method varies depending on the type of tissue and strongly influences the final mitochondrial yield. Whereas Arabidopsis seedlings are best disrupted using a large granite mortar and pestle, adult plants can also be processed with a specialized blender, such as the POLYTRON® Batch Disperser used by the protocol described here. A Waring® blender will not sufficiently disrupt Arabidopsis tissue to release mitochondria from cells; however, a blender modified according to ref. 22 is suitable for isolating mitochondria from adult Arabidopsis plants. Poor mitochondrial yields are very often due to insufficient tissue disruption; they are rarely caused by loss of mitochondria due to damage during tissue disruption. For different mitochondrial isolation procedures, *see* Chapter 2 of this volume.
4. You may have to adjust the POLYTRON speed setting in order to optimize the yield of your mitochondrial preparation.
5. The two low-speed spins (**steps 4–7**) are critical for the mitochondrial yield. The speed has been set to ensure that (1) mitochondria remain in the supernatant during this step, and (2) larger cell components are efficiently removed. Depending on your starting tissue and the method of tissue disruption, you may have to slightly adjust the speed of the low-speed spins.
6. The pellet obtained after **step 5** is rather gluey and cannot be easily resuspended with a micropipette.
7. A procedure has been described to facilitate the preparation of a Percoll step gradient [23].
8. It will be easier to initially resuspend the mitochondrial pellet in a smaller volume (200–400 μL) of wash buffer. It is critical for the reliability of the subsequent Bradford assay that no mitochondrial aggregates remain. Be aware that mitochondria will

sediment in the tube. Before taking aliquots for the Bradford assay and for the run-on transcription reaction (Subheading 3.3, **step 1**), agitate the mitochondrial suspension by gently pipetting up and down a few times or by flicking the tube.

9. It is important to not overdry the RNA pellet as overly dry RNA can be very difficult to resuspend. While the RNA dries, observe the pellet regularly and add ultrapure water to the pellet immediately once it becomes transparent.
10. It is possible to verify the synthesis of labeled run-on transcripts by subjecting the RNA samples obtained at this step to denaturing polyacrylamide gel electrophoresis (PAGE), followed by RNA transfer onto a positively charged nylon membrane and detection of the immobilized biotinylated RNA as described under Subheading 3.4, **steps 8–16**.
11. If small hybridization bottles are not available it is also possible to use 50-mL conical bottom polypropylene tubes (e.g., Falcon® tubes). These tubes may have to be sealed with Parafilm to prevent leaking during pre-hybridization and hybridization.
12. Volumes indicated here for the buffers of the Chemiluminescent Nucleic Acid Detection Module are smaller than those recommended by the manufacturer. You may be able to even further reduce volumes; ensure however that the membrane is always uniformly covered by the buffer or solution.

Acknowledgement

Work in the laboratory of K.K. is supported by the EC FP7 (PCIG12-GA-2012-333747).

References

1. Kubo T, Newton KJ (2008) Angiosperm mitochondrial genomes and mutations. Mitochondrion 8:5–14
2. Hammani K, Giege P (2014) RNA metabolism in plant mitochondria. Trends Plant Sci 19:380–389
3. Liere K, Weihe A, Börner T (2011) The transcription machineries of plant mitochondria and chloroplasts: composition, function, and regulation. J Plant Physiol 168:1345–1360
4. Hedtke B, Börner T, Weihe A (1997) Mitochondrial and chloroplast phage-type RNA polymerases in Arabidopsis. Science 277: 809–811
5. Hedtke B, Börner T, Weihe A (2000) One RNA polymerase serving two genomes. EMBO Rep 1:435–440
6. Hedtke B, Legen J, Weihe A et al (2002) Six active phage-type RNA polymerase genes in *Nicotiana tabacum*. Plant J 30:625–637
7. Kühn K, Richter U, Meyer EH et al (2009) Phage-type RNA polymerase RPOTmp performs gene-specific transcription in mitochondria of Arabidopsis thaliana. Plant Cell 21: 2762–2779
8. Gualberto JM, Kühn K (2014) DNA-binding proteins in plant mitochondria: implications for transcription. Mitochondrion 19 Pt B: 323–328
9. Binder S, Hatzack F, Brennicke A (1995) A novel pea mitochondrial in vitro transcription system recognizes homologous and heterologous mRNA and tRNA promoters. J Biol Chem 270:22182–22189

10. Caoile AG, Stern DB (1997) A conserved core element is functionally important for maize mitochondrial promoter activity in vitro. Nucleic Acids Res 25:4055–4060
11. Dombrowski S, Hoffmann M, Guha C et al (1999) Continuous primary sequence requirements in the 18-nucleotide promoter of dicot plant mitochondria. J Biol Chem 274: 10094–10099
12. Hoffmann M, Binder S (2002) Functional importance of nucleotide identities within the pea atp9 mitochondrial promoter sequence. J Mol Biol 320:943–950
13. Kühn K, Bohne AV, Liere K et al (2007) Arabidopsis phage-type RNA polymerases: accurate in vitro transcription of organellar genes. Plant Cell 19:959–971
14. Rapp WD, Lupold DS, Mack S et al (1993) Architecture of the maize mitochondrial *atp1* promoter as determined by linker-scanning and point mutagenesis. Mol Cell Biol 13: 7232–7238
15. Rapp WD, Stern DB (1992) A conserved 11 nucleotide sequence contains an essential promoter element of the maize mitochondrial *atp1* gene. EMBO J 11:1065–1073
16. Holec S, Lange H, Kuhn K et al (2006) Relaxed transcription in Arabidopsis mitochondria is counterbalanced by RNA stability control mediated by polyadenylation and polynucleotide phosphorylase. Mol Cell Biol 26:2869–2876
17. Kühn K, Weihe A, Börner T (2005) Multiple promoters are a common feature of mitochondrial genes in Arabidopsis. Nucleic Acids Res 33:337–346
18. Giegé P, Hoffmann M, Binder S et al (2000) RNA degradation buffers asymmetries of transcription in Arabidopsis mitochondria. EMBO Rep 1:164–170
19. Okada S, Brennicke A (2006) Transcript levels in plant mitochondria show a tight homeostasis during day and night. Mol Genet Genomics 276:71–78
20. Patrone G, Puppo F, Cusano R et al (2000) Nuclear run-on assay using biotin labeling, magnetic bead capture and analysis by fluorescence-based RT-PCR. Biotechniques 29(1012–1014):1016–1017
21. Zubo YO, Börner T, Liere K (2011) Measurement of transcription rates in Arabidopsis chloroplasts. Methods Mol Biol 774:171–182
22. Kannangara CG, Gough S, Hansen B et al (1977) A homogenizer with replaceable razor blades for bulk isolation of active barley plastids. Carlsberg Res Commun 42:431–439
23. Meyer EH, Millar AH (2008) Isolation of mitochondria from plant cell culture. In: Posch A (ed) 2D PAGE: sample preparation and fractionation, vol 425. Humana, New Jersey, pp 163–169

Chapter 4

In Vitro RNA Uptake Studies in Plant Mitochondria

Szymon Kubiszewski-Jakubiak, Cyrille Megel, Elodie Ubrig, Thalia Salinas, Anne-Marie Duchêne, and Laurence Maréchal-Drouard

Abstract

During evolution, most of the ancestral genes from the endosymbiotic α-proteobacteria at the origin of mitochondria have been either lost or transferred to the nuclear genome. To allow the comeback of proteins and RNAs [in particular transfer RNA (tRNAs)] into the organelle, macromolecule import systems were universally established. While protein import processes have been studied into details, much less is known about tRNA mitochondrial import. In plants, part of the knowledge on the tRNA import process into mitochondria has been acquired thanks to in vitro import assays. Furthermore, the development of in vitro RNA import strategies allowed the study of plant mitochondrial gene expression. The purpose of this chapter is to provide detailed protocols to perform in vitro RNA uptake into potato (*Solanum tuberosum*) or Arabidopsis (*Arabidopsis thaliana*) mitochondria as well as approaches to analyze them.

Key words Mitochondria, tRNA import, Protein carrier, Translocation, VDAC, TOM/TIM machineries

1 Introduction

In plants, only part of the required transfer RNA (tRNA) population is encoded by the mitochondrial genome. Indeed, it is now well admitted that the missing tRNAs are encoded by nuclear genes and transported from the cytosol into the organelle [1, 2]. The mechanism governing tRNA targeting into mitochondria remains poorly understood. In addition to the question of selectivity and regulation of tRNA mitochondrial import, two other major aspects need to be addressed regarding tRNA import mechanism. First, we need to understand how some cytosolic tRNAs escape from channeling to cytosolic translation machinery in order to be targeted to the mitochondrial surface. Second, we need to understand how such large hydrophilic and polyanionic macromolecules (with a size of about 25 kDa) can be translocated through the

Szymon Kubiszewski-Jakubiak and Cyrille Megel have equally contributed to this chapter.

James Whelan and Monika W. Murcha (eds.), *Plant Mitochondria: Methods and Protocols*, Methods in Molecular Biology, vol. 1305, DOI 10.1007/978-1-4939-2639-8_4,

double-mitochondrial membranes to reach the mitochondrial matrix. Concerning this last point, the identification and characterization of protein factors involved in the tRNA mitochondrial membrane import channel(s) remain essential and the recent establishment of in vitro tRNA uptake systems into isolated plant mitochondria brought some light to this question. The first in vitro tRNA import assay was set up using isolated potato mitochondria. In this system, it is possible to import radiolabeled tRNA transcripts in an ATP-dependent manner without the need of any added protein factors [3]. Under these conditions, tRNA mitochondrial import was shown to involve components of the translocase of the outer mitochondrial membrane (TOM) complex for tRNA binding at the surface of mitochondria and the voltage-dependent anion channel (VDAC) for the translocation through the outer membrane [1]. In the absence of any available protocol to transform plant mitochondria, an important challenge was to introduce foreign RNAs into mitochondria. For that purpose, an additional in vitro RNA mitochondrial import system based upon the use of a protein carrier to introduce foreign RNAs into isolated plant mitochondria was established. This artificial carrier corresponds to an RNA-binding protein (the mouse dihydrofolate reductase, DHFR) fused to the pSu9 mitochondrial targeting sequence (which consists in the first 69 amino acids of subunit nine of the mitochondrial F_0-ATPase of *Neurospora crassa*). It was successfully used with isolated potato or Arabidopsis mitochondria. This shuttle system appears much more efficient as compared to the in vitro import assay without carrier protein. This RNA uptake process does not involve VDAC but components of the protein import machinery are likely implicated [4, 5]. Here, we present state-of-the-art protocols for potato and Arabidopsis mitochondria purification and in vitro RNA uptake systems. We also provide additional procedures on how to control the uptake.

2 Materials

Classical protocols of molecular biology, materials, as well as appropriate precautions are described in [6].

2.1 Potato Mitochondria Isolation

1. 45-μm nylon meshes.
2. Moulinex juice extractor (TYPE 140.2.03).
3. Centrifuges (e.g., Beckman Coulter Avanti® J-E centrifuge, Beckman rotors JA10.5 and JA25.5).
4. Centrifuge tubes (e.g., Beckman Coulter, 29 × 104 mm, 50 mL; Nalgene centrifuge bottle, 500 mL).
5. Dounce homogenizer (30 mL volume).
6. Potato tubers (*Solanum tuberosum*, var. Bintje—untreated).

7. 3× Grinding buffer pH 7.5: 0.9 M sucrose, 90 mM sodium pyrophosphate, 6 mM EDTA, 2.4 % (w/v) polyvinylpyrrolidone (PVP)-25000, 12 mM cysteine, 15 mM glycine, 0.9 % (w/v) bovine serum albumin (BSA, fatty acid free), 6 mM β-mercaptoethanol, pH adjusted with 37 % (v/v) HCl.
8. Washing buffer pH 7.2: 0.3 M sucrose, 10 mM potassium phosphate pH 7.5, 1 mM EDTA, 0.1 % (w/v) BSA, 5 mM glycine.
9. Percoll gradient solution: 0.3 M sucrose, 10 mM potassium phosphate pH 7.5, 1 mM EDTA, 0.1 % (w/v) BSA, 28 % (v/v) Percoll.

2.2 Arabidopsis Mitochondria Isolation

1. Mortar and pestle.
2. Miracloth (Calbiochem®).
3. Beckman Coulter Avanti® J-E centrifuge, Beckman rotor JA25.5.
4. Centrifuge tubes (e.g., Beckman Coulter, 29 × 104 mm, 50 mL).
5. Gradient pourer with peristaltic pump.
6. Murashige and Skoog (MS) medium plates: 30 g/L (w/v) sucrose, 4.3 g/L (w/v) MS powder, 0.5 g/L MES, 1 mL/L Gamborg B5 vitamins 1,000×, 7.5 g/L agar.
7. 3 % (v/v) Hydrochloride in sodium hypochlorite: Please note that adding concentrated hydrochloride to sodium hypochlorite causes an immediate formation of chlorine gas bubbles and it should be done in the following sequence: Place a beaker in a desiccator with 12.5 % (v/v) sodium hypochlorite, add concentrated hydrochloride, and close the desiccator immediately.
8. Grinding buffer: 0.3 M sucrose, 25 mM tetrasodium pyrophosphate, 2 mM EDTA (disodium salt), 10 mM KH_2PO_4, 1 % (w/v) PVP-40, 1 % (w/v) BSA, pH 7.5 with 37 % (v/v) HCl. Supplemented with 1.06 g sodium ascorbate and 0.74 g cysteine per 300 mL of grinding buffer added prior to use.
9. 2× Washing buffer: 0.6 M sucrose, 20 mM TES, 2 % (w/v) BSA, pH 7.5 with NaOH.
10. Light gradient solution: 1× washing buffer, 28 % (v/v) Percoll. For a 35 mL gradient, complete with water.
11. Heavy gradient solution: 1× washing buffer, 28 % (v/v) Percoll, 4.4 % (w/v) PVP-40. For a 35 mL gradient, complete with water.

2.3 Integrity Test

1. 2× Integrity buffer: 0.6 M sucrose, 20 mM potassium phosphate buffer pH 7.2, 20 mM KCl, 10 mM $MgCl_2$, 0.1 % (w/v) BSA. Store at −20 °C.
2. Stock solutions: 0.2 M KCN, 0.2 M ATP pH 7.5, 16 mM cytochrome c; 1 M sodium succinate.
3. Spectrophotometer (e.g., Shimadzu UV-1800, *see* **Note 1**).

2.4 RNA Transcript Synthesis

1. Any plasmid containing a tRNA gene sequence directly fused to a T7 RNA polymerase promoter at the 5′ terminus and including a *Bst*NI site at the 3′ terminus can be used as substrates to produce mature tRNA molecules (*see* **Note 2**). The *Bst*NI restriction site allows the synthesis of the CCA extremity of a mature tRNA. Classically, the corresponding construct containing Arabidopsis cytosolic $tRNA^{Ala}$ can be used [7].
2. Any gene of interest cloned in a vector containing a T7 RNA polymerase promoter (*see* **Note 3**).
3. Restriction enzyme *Bst*N1.
4. Transcription kit: RiboMAX™ Large Scale RNA Production Systems-T7 (Promega—France). Store at −20 °C. Alternatively, the SP6 System can be used (*see* **Note 3**).
5. rNTP stock solution: 2.5 mM each (ATP, GTP, CTP, and UTP), for the synthesis of non-labeled transcripts.
6. rNTP stock solution: 2.5 mM of ATP, GTP, CTP, and 0.5 mM UTP, for the synthesis of radiolabeled transcript.
7. [α^{32}P]UTP 10 μCi/μL, 3 μCi/pmol.
8. Glycogen (Thermo Scientific).
9. Sephadex G-50 (Sigma): To prepare Sephadex G-50, slowly add Sephadex G-50 to water in a 50-mL tube. Autoclave at 10 psi for 15 min. Store at 4 °C.

2.5 RNA Transcript Analysis (See Note 4)

2.5.1 Acrylamide Gel Electrophoresis for Analysis of tRNA Transcript Integrity and tRNA Uptake

1. Acrylamide 15 % (w/v), 7 M urea, 1× TBE (Tris 90 mM, 2.5 mM EDTA pH 8.3, 90 mM boric acid): To prepare 100 mL of stock solution add 37.5 mL of 40 % (w/v) acrylamide/bisacrylamide (ratio 19/1) to 42 g of urea and 20 mL of 5× TBE. Dissolve and complete with water to 100 mL and dissolve. Heating at 30–40 °C can be necessary. Store in the dark at room temperature.
2. Ammonium peroxodisulfate (APS): 10 % (w/v) solution in water. Store at 4 °C.
3. *N*,*N*,*N*′,*N*′-Tetramethylethylenediamine (TEMED). Store at 4 °C.
4. RNA loading buffer: 95 % (v/v) formamide, 20 mM EDTA, 0.05 % (w/v) xylene cyanol, 0.05 % (w/v) bromophenol blue.
5. Ethidium bromide solution (0.5 μg/mL).
6. Fixation solution: 10 % (v/v) ethanol, 20 % (v/v) acetic acid.
7. Mini protein electrophoresis system and power supply.
8. Autoradiography developing machine and/or Phosphorimager.

2.5.2 RT-PCR or cRT-PCR Analysis

1. T4 RNA ligase and supplemented with 10× T4 RNA ligase buffer.
2. 1 M sodium acetate solution pH 4.5 and ethanol absolute anhydrous.
3. Superscript™ III RT and supplemented 5× RT buffer (Invitrogen).
4. Stock solutions: Mix of dNTP (10 mM each), 100 μM DTT.
5. *Taq* polymerase and associated buffer.

2.6 In Vitro RNA Import Assay into Isolated Potato Mitochondria (Without Protein Carrier)

1. 2× Import buffer: 0.6 M mannitol, 20 mM HEPES-KOH pH 7.5, 40 mM KCl, 2 mM dithiothreitol (DTT), 2 mM malate, 2 mM NADH, 2 mM potassium phosphate buffer pH 7.5. Store as 2× concentrated aliquots at −20 °C. Each import reaction is supplemented with the following substrates to the final concentration of 40 μM ADP, 5 mM ATP pH 7.5, and 5 mM $MgCl_2$ in 1× import buffer. Prepare the mix fresh and store at 4 °C until use.
2. ^{32}P-labeled tRNA transcript (Subheading 2.4). The in vitro-synthesized transcript can be stored at −20 °C for 2 weeks.
3. RNase mix: 50 μg/mL RNase A from bovine pancreas (e.g., Roche), 375 U/L RNase T1 from *Aspergillus oryzae* (e.g., Roche), 0.3 M sucrose, 10 mM potassium phosphate buffer pH 7.5, 1 mM EDTA, 5 mM glycine. Prepare fresh and store at 4 °C.
4. STOP solution: 5 mM EDTA, 5 mM EGTA, 0.3 M sucrose, 10 mM potassium phosphate buffer pH 7.5, 5 mM glycine, 0.1 % (w/v) BSA. Prepare fresh and store at 4 °C.
5. RNA extraction buffer: 10 mM $MgCl_2$, 10 mM Tris–HCl pH 7.5, 1 % (w/v) sodium dodecyl sulfate (SDS). Store at room temperature.
6. Biophenol water saturated (for tRNA extraction).
7. 1 M Sodium acetate solution, pH 4.8 and ethanol absolute anhydrous.

2.7 In Vitro RNA Import Assay into Isolated Potato or Arabidopsis Mitochondria (in Presence of Protein Carrier)

1. 2× Potato import buffer: 0.6 M mannitol, 20 mM HEPES-KOH pH 7.5, 40 mM KCl, 2 mM DTT, 2 mM malate, 2 mM NADH, 2 mM potassium phosphate buffer pH 7.5. Store in 2× concentrated aliquots at −20 °C.
2. 2× Arabidopsis import buffer: 0.6 M sucrose, 100 mM KCl, 20 mM MOPS pH 7.4, 10 mM KH_2PO_4, 0.2 % (w/v) BSA. Store in 2× concentrated aliquots at −20 °C.
3. Import reaction mix: 1 mM $MgCl_2$, 1 mM methionine, 0.2 mM ADP, 0.75 mM ATP, 5 mM succinate, 5 mM DTT, 5 mM NADH, 5 mM GTP, pH 7.5 in 1× import buffer. Prepare fresh and store at 4 °C until use.

4. ^{32}P-labeled RNA transcript (Subheading 2.4). The in vitro-synthesized transcript can be stored at −20 °C for 2 weeks.
5. Recombinant pDHFR protein purified under native conditions [4, 8]. Store in aliquots at −80 °C.
6. RNase mix: 50 μg/mL RNase A, 375 U/mL RNase T1, 0.3 mM sucrose, 10 mM TES, 1 % (w/v) BSA. Prepare fresh and store at 4 °C.
7. STOP solution: 10 mM EDTA, 10 mM EGTA, 300 mM sucrose, 10 mM TES, 15 % (w/v) BSA. Prepare fresh and store at 4 °C.
8. RNA extraction buffer: 10 mM $MgCl_2$, 10 mM Tris–HCl pH 7.5, 1 % (w/v) SDS (for tRNA extraction). Store at room temperature.
9. Biophenol water saturated (for tRNA extraction).
10. Trizol (e.g., TRI-Reagent™, Sigma), for mRNA extraction.
11. 1 M Sodium acetate solution, pH 4.8 and ethanol absolute anhydrous.

3 Methods

3.1 Potato Mitochondria Isolation

The protocol is adapted from [9]. All steps are performed at 4 °C with prechilled material.

1. Wash, peal, and cut into pieces 1–2 kg of potato tubers. Then, homogenize them in a juice extractor. Collect and mix the juice in one-third volume of grinding buffer (e.g., for 500 mL of grinding buffer collect 1 L of potato juice).
2. Quickly filtrate the mixture through 45-μm nylon mesh in order to eliminate most starch and then centrifuge the solution at 1,600 × *g* for 10 min in order to pellet the cellular debris.
3. Recover the supernatant and centrifuge at high speed at 13,000 × *g* for 15 min in order to pellet mitochondria.
4. Discard the supernatant, keep the mitochondria pellets, and gently resuspend them in a few mL of washing buffer using a Dounce homogenizer. Complete to 100 mL of washing buffer.
5. Perform a second round of differential centrifugation (**steps 2** and **3**).
6. Resuspend the mitochondria pellets in the minimum volume of washing buffer (4–6 mL in total), combine in the same tube, and load equal volumes on 6× Percoll gradients (32 mL per tube). Centrifuge at 40,000 × *g* for 60 min. Gradients are self-formed during centrifugation.
7. Mitochondria appear as a large white yellowish band at the bottom third of the Percoll gradient. Discard the upper part by aspiration. Collect mitochondrial bands and transfer them

in 50-mL tubes. Dilute in 5–6 volumes of washing buffer and centrifuge at 12,000 × *g* for 10 min.

8. Wash twice mitochondrial pellets with 5–6 volumes of the washing buffer without BSA and centrifuge for 10 min at 10,000 × *g*. Finally, suspend mitochondria in 0.5 mL of washing buffer without BSA. At this stage, mitochondria are intact and mostly devoid of any contaminant. Their amount is evaluated by determining the protein concentration using Bradford Assay (Bio-Rad) [10]. Classically about 50–100 mg of mitochondrial proteins are obtained from 1 to 2 kg of potato tubers (*see* **Note 5**). Keep mitochondria at 4 °C until use.

3.2 Arabidopsis Mitochondria Isolation

The protocol is adapted from Chapter 2.

1. Sterilize Arabidopsis seeds. To do so, place aliquot of 50 µg of seeds into 1.5-mL microcentrifuge tubes in a desiccator. Place in the desiccator a beaker with 3 % (v/v) hydrochloride in sodium hypochlorite and incubate for 3 h. Sow the sterilized seed onto the MS plates (12 × 12 cm), one aliquot of seeds per plate. Four plates are sufficient for mitochondrial isolation. Stratify for 48 h at 4 °C in the dark and grow for 14 days in long-daylight conditions (16 h).
2. The day of the preparation, cast the 0–4.4 % (w/v) PVP gradients by mixing the heavy and light solutions using a gradient pourer and a peristaltic pump. For two gradients use 35 mL of the heavy and 35 mL of the light solutions (Chapter 2) and keep on ice until use.
3. Collect the tissue using tweezers ensuring that minimal MS media is collected. Alternatively a razor blade can be used to "shave" the seedling off the plate. All following steps must be carried out at 4 °C. Using a cold mortar and pestle, grind tissue in 300 mL of grinding buffer until you cannot see intact seedlings. Filter the homogenate through two layers of Miracloth into a cold conical flask. Regrind the tissue remaining after filtering.
4. Transfer homogenate to 6–8 prechilled 50-mL centrifuge tubes on ice and centrifuge for 5 min at 2,500 × *g*. Transfer the supernatant to fresh tubes.
5. Centrifuge the supernatant for 20 min at 17,500 × *g*. Discard the supernatant.
6. Gently resuspend the crude mitochondrial pellets in a few mL of grinding buffer, using a soft-haired paintbrush. Add 1 mL of cold wash buffer (1×). Combine the resuspended pellets into one and fill the tube with wash buffer (1×).
7. Repeat **steps 5–6**.
8. Gently resuspend the pellet in 2 mL of grinding buffer, using a paintbrush.

9. Layer the crude mitochondrial fraction over the two 0–4.4 % (w/v) PVP Percoll gradients using a prechilled Pasteur pipette. Centrifuge at 40,000 × *g* for 40 min at 4 °C with brakes off. Remove the upper layers of the gradient (chloroplasts and thylakoids). Collect the mitochondrial fraction (yellow band in the lower section of the gradient) (Chapter 2) and transfer to a fresh, prechilled tube.
10. Wash the mitochondrial fraction by filling the tube with 1× wash buffer. Centrifuge at 31,000 × *g* for 15 min at 4 °C with slow deceleration. Repeat this step once with wash buffer (1×) without BSA.
11. Collect the mitochondrial pellets, keep on ice, and use immediately for the import assay. Determine protein concentration using the Bradford Assay, and adjust accordingly with 1× wash buffer if two or more genotypes are to be assayed.

3.3 Integrity Test

The integrity of outer mitochondrial membrane is determined by testing the ability of fresh mitochondria to reduce exogenously added cytochrome c [11]. The cytochrome c reduction is measured by following the absorbance at 550 nm (A_{550}). In order to calculate the percentage of intact mitochondria, two different tests are necessary, one with isolated intact mitochondria (cytochrome c cannot enter mitochondria) and the second with disrupted mitochondria (cytochrome c can now reach the intermembrane space and be reduced).

1. Thaw the 2× integrity buffer and keep it at room temperature. Prepare a solution of 1× integrity buffer (1 mL is required per assay).
2. Perform the first assay with intact mitochondria. To 1 mL of 1× integrity buffer, add 5 μL of KCN solution, 5 μL of ATP solution, and 5 μL of cytochrome c. Mix and add purified mitochondria (100 μg equivalent proteins). Gently mix and follow the A_{550}. Acquire the baseline and at $t = 1$ min, add 10 μl sodium succinate solution. The A_{550} slightly goes up. The strongest the slope is, the lowest the amount of intact mitochondria is. Calculate the slope of the line (V_1).
3. Perform the second assay with disrupted mitochondria. Mix 0.5 mL water with 100 μg equivalent proteins of mitochondria. Mix gently and wait for 30 s. This osmotic shock allows the disruption of the outer mitochondrial membrane. Then, add 0.5 mL of 2× integrity buffer to restore isotonicity and perform the assay as above. Calculate the second slope (V_0).
4. The percentage of intact mitochondria corresponds to $\% = 100 \times (1 - V_1/V_0)$ (Fig. 1) (*see* **Note 6**).

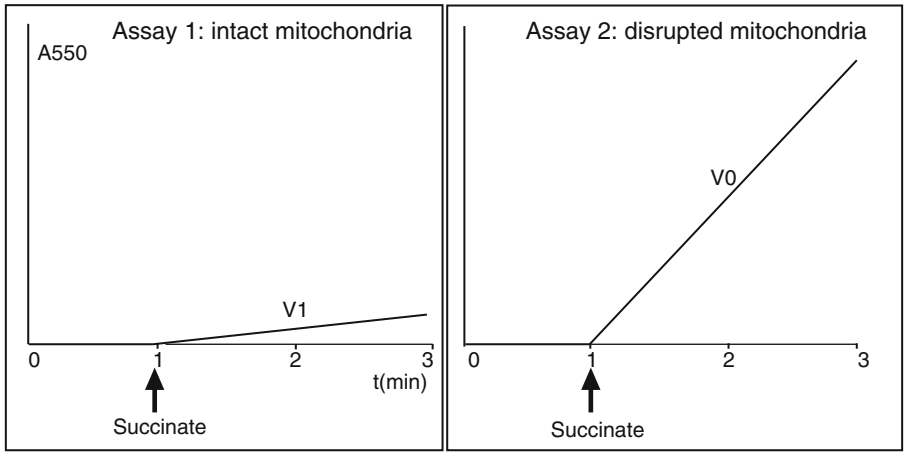

Fig. 1 Schematic representation of the two curves classically obtained when performing integrity assay based on cytochrome c reduction. On the *left*, the assay is performed with intact mitochondria (slope V_1) and on the *right*, the same assay is performed with disrupted mitochondria (slope V_0)

3.4 RNA Transcript Synthesis and Analysis

3.4.1 Transcript Synthesis

1. According to the manufacturer's protocol, linearize the plasmid (10 μg) construct containing a T7 (alternatively SP6) RNA promoter upstream of the gene of interest using either *Bst*NI (if the gene encodes a tRNA) or any restriction enzyme corresponding to a restriction site located downstream of the gene of interest. Make sure that there is no corresponding restriction site within the gene to be transcribed.
2. After linearization, perform an ethanol precipitation according to classical protocol. Dissolve the nucleic acid pellet in 10 μL of sterile water.
3. The Riboprobe Kit (Promega) is used to synthesize in vitro transcripts. The following transcription reaction mixture (50 μL) is incubated for 3 h at 37 °C: 1–5 μg of linearized plasmid, 10 μL of transcription buffer 5×, 10 μL rNTP mix (*see* **Note 7**), 5 μL enzymatic mix (T7 RNA polymerase, Recombinant RNasin® Ribonuclease Inhibitor, Recombinant Inorganic Pyrophosphatase), 1 μL of RNase inhibitor (40 U/μL).
4. Add 1 μL of DNase RQ1 (1 U/μL, Promega). Incubate for 15 min further at 37 °C.
5. If the transcription is performed in the absence of radioactivity, perform **steps 6–8**. If the transcript is synthesized in the presence of radiolabeled nucleotides, perform **step 9**.
6. Add 49 μL sterile water and 100 μL biophenol water saturated. Vortex for 30 s. Centrifuge at 10,000 × *g* for 10 min at room temperature.

7. Recover the aqueous phase and add 0.5 µL of glycogen, 0.1 volume of 1 M sodium acetate pH 4.5, and 2.5 volumes of ethanol. Mix by inverting the tube. Precipitate overnight at −20 °C.
8. Centrifuge at 16,100 × *g* for 30 min at 4 °C. Discard supernatant and leave the tube open for 10 min at room temperature. Dissolve the RNA pellet in 40 µL sterile water. Store at −80 °C.
9. If the transcription is performed in the presence of ^{32}P[UTP], separate the radiolabeled RNA transcript from unincorporated nucleotides by spin-column chromatography through Sephadex G-50. Store at −20 °C. The amount of incorporated radioactivity can be evaluated using a multipurpose scintillation counter (*see* **Note 8**).

3.4.2 Transcript Analysis

1. Assemble and cast the Bio-Rad Mini-PROTEAN® Tetra system. Prepare a 15 % (w/v) polyacrylamide gel by adding 70 µL of 10 % (w/v) APS and 3.5 µL of TEMED to 10 mL of the acrylamide stock solution. Pour the gel, immediately insert the comb, and let it polymerize for ~1 h.
2. Prepare RNA transcript for gel analysis by adding 1–2 volumes of RNA loading buffer to the RNA sample (1 µL is usually sufficient).
3. Load the sample(s) and RNA ladder (many are commercially available and provide wide range of RNA sizes) on the acrylamide gel. Run the gel at 150 V for ~80 min. Note that for long RNA (i.e., >500 nucleotides), analysis on agarose-formaldehyde gel is required. A protocol can be found in [6].
4. If the RNA transcript to be analyzed is not radiolabeled, stain the gel in a fresh solution of BET for 5 min. Visualize RNA band(s) under UV light and acquire photos. If the transcript to be analyzed is radiolabeled, pour the radioactive gel between two sheets of transparent plastic film and process the gel for autoradiography.

3.5 In Vitro RNA Import Assay (Without Protein Carrier)

The protocol was classically used for the import of radiolabeled tRNA [3]. It has not been developed so far to incorporate other types of RNAs.

1. Thaw the 2× import buffer, ATP, ADP, and $MgCl_2$ solutions and keep them on ice. Combine these solutions in the indicated concentrations (Subheading 2.6).
2. Thaw the ^{32}P-labeled tRNA on ice.
3. Add 100 µg freshly isolated mitochondria and gently flick the tube to mix. If you have several samples to prepare, keep them on ice till the addition of the transcript. Add 5 µL of tRNA transcript (10^5 cpm/assay). Note that the total volume of an import assay is classically 50 µL.

4. Incubate at 25 °C for 30 min. Stop the import reaction by putting the samples on ice.
5. Add 1 volume (50 μL) of freshly prepared RNase mix. Gently mix by pipetting and incubate on ice for 10 min (*see* **Note 9**).
6. Stop the RNase treatment by adding 0.8 mL of cold STOP solution, gently vortex, and centrifuge for 5 min at 7,000 × *g* (centrifugation can be done at room temperature). Eliminate the supernatant. Gently resuspend the mitochondrial pellet by pipetting with 1 mL of cold STOP solution and centrifuge for 5 min at 7,000 × *g*. Repeat this step once more. Eliminate the supernatant and keep the mitochondrial pellet on ice (*see* **Note 9**).
7. Add 100 μL of tRNA extraction buffer and immediately after 1 volume of water-saturated biophenol to the washed pellet (*see* **Note 10**). Rapidly vortex and let shake for 10 min. Centrifuge at maximum speed for 10 min at room temperature. Recover the aqueous phase.
8. Add 2.5 volumes of ethanol and 0.04 volume of 5 M NaCl and precipitate overnight. The following morning, centrifuge at 12,000 × *g* for 20 min at 4 °C. Discard the ethanol and leave the tube open for 10 min at room temperature. At this stage, RNA uptake must be analyzed. If the transcript is radiolabeled, analysis is performed by acrylamide gel electrophoresis (Subheading 3.7.1). If the transcript is unlabeled, reverse transcription-polymerase chain reaction (RT-PCR) or circularization RT-PCR (cRT-PCR) can be useful approaches (Subheadings 3.7.2 and 3.7.3).

3.6 In Vitro RNA Import Assay (with Protein Carrier)

This protocol has been successfully used for the import of tRNAs, precursor of tRNAs, and mRNAs into isolated potato mitochondria [4, 12]. We now have set up a similar protocol for Arabidopsis-isolated mitochondria.

1. Thaw the 2× import buffer (note that the import buffer differs depending on the plant species, potato, or Arabidopsis) and combine with $MgCl_2$, methionine, ATP, ADP, succinate, DTT, and NADH in the indicated concentrations (Subheading 2.7). The total volume of the import mix will be 100 μL (including the transcript and carrier protein added later on).
2. Thaw the in vitro-synthesized transcript on ice.
3. Add 100 μg of mitochondria to the import mix, and gently flick the tube to mix. Keep tubes on ice until all samples are prepared.
4. Add 5 μg of thawed recombinant pDHFR (*see* **Note 11**) and incubate on ice for 10 min.

5. Add either 5 μL of radiolabeled tRNA (10^5 cpm) or 2–5 μg of the transcript of interest (e.g., tRNA precursor, mRNA), and gently flick the tube to mix.
6. At this stage, all steps are as in Subheading 3.5 (from **step 4**).

3.7 RNA Uptake Analysis

If the uptake into isolated mitochondria concerns a radioactively labeled tRNA transcript, it is classically analyzed by electrophoresis through 7 M urea–15 % (w/v) polyacrylamide gel. If the RNA imported into isolated mitochondria corresponds to an unlabeled transcript, the uptake can be visualized using RT-PCR or cRT-PCR experiments as indicated below.

3.7.1 Acrylamide Gel Electrophoresis Analysis

The protocol is essentially the same as described in Subheading 3.4.2. The only difference is that due to the low amount of radiolabeled transcript imported into mitochondria, it is usually necessary, once the gel has run, to fix the gel before exposure. For that purpose, after BET staining (Subheading 3.4.2) and visualization under UV light (*see* **Note 12**), the gel is incubated under gentle agitation in 100 mL of fixation solution for 15 min. The gel is then placed on a Whatman® 3MM sheet and recovered by a plastic film. Dry the gel for 1 h at 80 °C in gel dryer using vacuum technology. Submit the gel to autoradiography or expose to a Phosphorimager plate overnight or longer if needed (up to 7 days).

Typical results showing differential efficiency of tRNA uptakes into isolated mitochondria in the absence or presence of the carrier protein pDHFR are presented in Fig. 2.

3.7.2 RT-PCR Analysis

The use of unlabeled transcript is essential when we want to analyze further molecular processes. Typically, we used a nonradioactive mRNA transcript to study the editing process of the RNA once it has reached the mitochondria [4].

1. Denature RNA (100–400 ng) for 5 min at 65 °C in the presence of 20 pmol of specific primer (the primer must be specific of the incorporated RNA and must not hybridize with endogenous RNA). Total volume is 13 μL.
2. Add 4 μL of 5× RT buffer, 1 μL DTT 100 mM, 1 μL RNase inhibitor (40 U/μL), and 1 μL dNTP mix.
3. Divide each sample into two equal amounts (i.e., 9.5 μL per tube); add 0.5 μL of Superscript® III in one of the tubes (RT+) and 0.5 μL of water in the other (RT–; negative control where no product should be visible after PCR amplification). Incubate for 1 h at 52 °C and inactivate the enzyme at 70 °C for 15 min.
4. The synthesized cDNA is then used as template for classical PCR amplification using two primers specific for the RNA of interest. PCR products are analyzed on agarose gel [6].

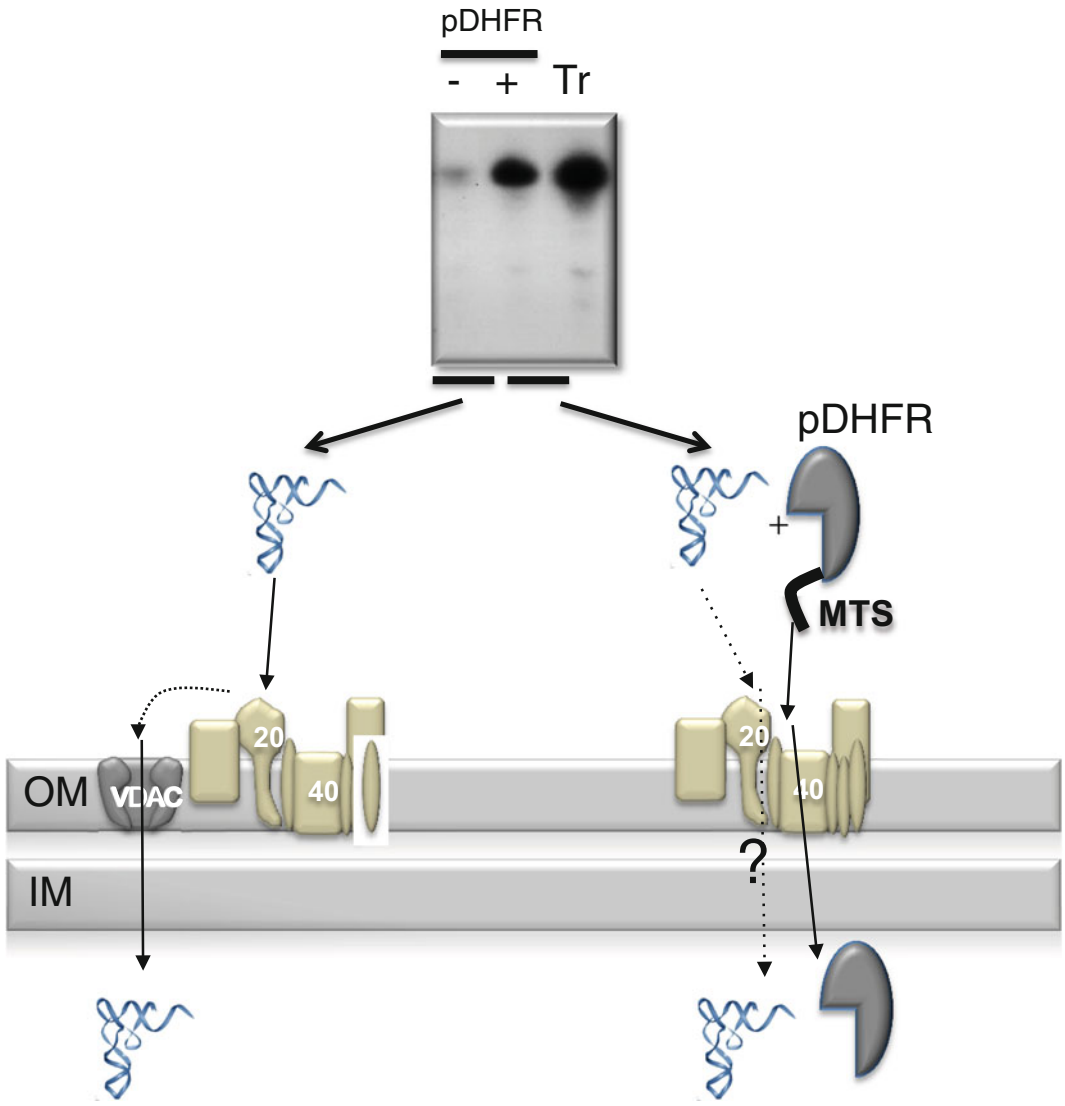

Fig. 2 *Top*: In vitro-transcribed ^{32}P-labeled cytosolic plant tRNA^{Ala} transcript (Tr) was incubated with isolated potato mitochondria in the absence (–) or in the presence (+) of pDHFR. Following standard import conditions as described in the text, mitochondria were RNase treated and RNAs were extracted. RNAs were then fractionated on a polyacrylamide gel and incorporated tRNA transcripts were visualized by autoradiography. *Bottom*: The two putative tRNA mitochondrial import pathways in the absence or presence of pDHFR, respectively, are depicted. Abbreviations: *MTS* mitochondrial targeting sequence, *VDAC* voltage-dependent anion channel, *TOM* translocase of the outer mitochondrial membrane

3.7.3 cRT-PCR Analysis

cRT-PCR is a very useful approach when you want to determine the 5′- and 3′-ends of an RNA. It consists in ligating 5′- and 3′-ends of linear RNA molecules and in performing RT-PCR to obtain products containing ligated 5′- and 3′-extremities of the RNA of interest. For example it has been successfully used to

identify the extremities of a processed precursor tRNA after incorporation into potato mitochondria [4]. The protocol described here has been adapted from [13].

1. Add 10 µL (0.5–1.5 µg) of RNA to 2.5 µL of 5× T4 RNA ligase buffer, 0.5 µL RNase inhibitor (40 U/µL), and 0.5 µL T4 RNA ligase. Complete to 25 µL with water.
2. Incubate at 37 °C for 1 h. Inactivate the enzyme at 65 °C for 15 min.
3. Add 25 µL of water, 0.1 volume of 1 M sodium acetate pH 4.5, and 2.5 volumes of ethanol. Mix and incubate for 1 h at –20 °C. Centrifuge at 12,000 × *g* for 20 min at 4 °C. Discard the supernatant and leave the tube open for 10 min at room temperature. Dissolve the RNA pellet in 10 µL sterile water.
4. Perform the RT-PCR steps with 4 µL of circularized RNA as described in Subheading 3.7.2.

4 Notes

1. A spectrophotometer allowing kinetic measurements is required.
2. The use of this strategy implies that the tRNA gene starts with at least one G residue (two Gs is even more favorable). If this is not the case, a ribozyme strategy can be used to synthesize tRNA transcript with a mature 5′ extremity. This approach is not developed here but can be found in [14].
3. Alternatively, the SP6 promoter and the SP6 RNA polymerase can be used. RiboMAX™ Large Scale RNA Production System-SP6 is also commercially available.
4. Gel electrophoresis on 15 % (w/v) polyacrylamide gel is convenient for tRNA analysis or for RNA fragments up to 200 nucleotides. To analyze longer RNA (from 200 to 500 nucleotides long RNAs), the acrylamide concentration can be reduced to 10–12 % (w/v). For longer RNA, formaldehyde agarose gel can be used [6]. For long RNA uptake analysis, we prefer to use RT-PCR experiments.
5. The protocol presented here allows the preparation of a huge amount of potato mitochondria. Ten times less mitochondria can be prepared by adapting volumes and centrifuge devices.
6. Integrity of isolated potato mitochondria is around 95–98 %. Integrity of Arabidopsis mitochondria is usually lower (80 %). If the integrity is not sufficient, RNA uptake experiments will be unsuccessful.
7. If the transcription is performed in the absence of radioactivity, use rNTP stock solution: 2.5 mM each (ATP, GTP, CTP, and UTP). If the transcript is synthesized in the presence of

radiolabeled nucleotides, use rNTP stock solution: 2.5 mM of ATP, GTP, CTP, and 0.5 mM UTP, and add 4 μL of [α^{32}P]UTP.

8. The work with radioactivity requires special security rules. Please ask your institute/laboratory for a full set of recommendations and for the specific room dedicated to radioactivity where you can perform your experiments.
9. This step is performed in order to eliminate all tRNA molecules remaining outside of mitochondria.
10. Add the water-saturated phenol immediately after adding the tRNA extraction buffer. The rapidity to which you perform this step is crucial as it avoids degradation of tRNAs imported into mitochondria. During this step mitochondria are lysed and imported tRNA molecules are no longer protected. Therefore the phenol extraction step must be quick to avoid any residual RNase activity. For long RNA such as mRNA, Trizol is directly added to the mitochondrial pellet and RNA extraction is done following instructions recommended by the provider (e.g., Sigma).
11. The recombinant pDHFR is aliquoted and kept at −80 °C. Once an aliquot is thawed, take what you need and freeze again the aliquot rapidly in liquid nitrogen.
12. This is an important step. Visualization of the endogenous mitochondrial RNAs allows checking the integrity of the mitochondria during the uptake (if mitochondria are not intact, then endogenous RNAs will be accessible to the added RNases and degraded). It also allows ensuring equivalent loading of RNAs recovered after extraction.

References

1. Salinas T, Duchêne AM, Delage L, Nilsson S, Glaser E, Zaepfel M, Maréchal-Drouard L (2006) The voltage-dependent anion channel, a major component of the tRNA import machinery in plant mitochondria. Proc Natl Acad Sci U S A 103:18362–18367
2. Duchêne AM, Pujol C, Maréchal-Drouard L (2009) Import of tRNAs and aminoacyl-tRNA synthetases into mitochondria. Curr Genet 55:1–18
3. Delage L, Dietrich A, Cosset A, Maréchal-Drouard L (2003) In vitro import of a nuclearly encoded tRNA into mitochondria of *Solanum tuberosum*. Mol Cell Biol 23:4000–4012
4. Sieber F, Placido A, El Farouk-Ameqrane S, Duchêne AM, Maréchal-Drouard L (2011) A protein shuttle system to target RNA into mitochondria. Nucleic Acids Res 39:e96
5. Sieber F, Duchêne AM, Maréchal-Drouard L (2011) Mitochondrial RNA import: from diversity of natural mechanism to potential applications. Int Rev Cell Mol Biol 2011(287): 145–190
6. Sambrook J, Russell DW (2001) Molecular cloning: a laboratory manual. Cold Spring Harbor Laboratory Press, New York, NY
7. Dietrich A, Maréchal-Drouard L, Carneiro V, Cosset A, Small I (1996) A single base change prevents import of cytosolic tRNA(Ala) into mitochondria in transgenic plants. Plant J 10:913–918
8. Rapaport D, Neupert W (1999) Biogenesis of Tom40, core component of the TOM complex of mitochondria. J Cell Biol 146:321–331
9. Pujol C, Bailly M, Kern D, Maréchal-Drouard L, Becker H, Duchêne AM (2008) Dual-targeted tRNA-dependent amidotransferase ensures both mitochondrial and chloroplastic Gln-tRNAGln synthesis in plants. Proc Natl Acad Sci U S A 105:6481–6485

10. Bradford MM (1976) A rapid and sensitive method for the quantitation of microgram quantities of protein utilizing the principle of protein-dye binding. Anal Biochem 72:248–254
11. Douce R (1985) Mitochondria in higher plants: structure, function and biogenesis. Academic, Orlando, FL
12. Placido A, Sieber F, Gobert A, Galerani R, Giegé P, Maréchal-Drouard L (2010) Plant mitochondria use two pathways for the biogenesis of tRNAHis. Nucleic Acids Res 38:7711–7717
13. Yokobori S, Paabo S (1995) Transfer RNA editing in land snail mitochondria. Proc Natl Acad Sci U S A 92:10432–10435
14. Fechter P, Rudinger J, Giege R, Theobald-Dietrich A (1998) Ribozyme processed tRNA transcripts with unfriendly internal promoter for T7 RNA polymerase: production and activity. FEBS Lett 436:99–103

Chapter 5

In Vitro and In Vivo Protein Uptake Studies in Plant Mitochondria

Owen Duncan, Chris Carrie, Yan Wang, and Monika W. Murcha

Abstract

The study of protein uptake into mitochondria is an important tool for investigating the subcellular distribution of proteins and the molecular mechanisms that determine location. Here we describe five techniques that allow the quantitative or qualitative monitoring of protein uptake into mitochondria using both in vitro and in vivo approaches.

Key words Mitochondria, Protein import, Fluorescent protein tagging, Radiolabeled precursor protein, Kinetic analysis, Assembly

1 Introduction

In the post-genomic era of research in biological science, one of the major challenges faced by researchers is to understand how the compartmentalization of eukaryotic cells affects the functioning of biochemical processes. A key piece of information in addressing this challenge is the knowledge of subcellular location of proteins. Interrogating databases such as the SUBcellular localization database for Arabidopsis proteins (SUBA) [1] and Rice DB [2] are ideal first steps to gain insights into the subcellular localization of a protein. These databases contain localization data derived from diverse sources and allow valuable cross referencing, allowing researchers to reach a "consensus" localization based on the existing literature and in silico targeting predictions. While these databases are constantly expanding, they remain incomplete; in the case of SUBA, fluorescent tagging data exists only for 2,477 proteins out of a possible greater than 35,000 proteins estimated to be encoded in the Arabidopsis (*Arabidopsis thaliana*) genome. Given the incomplete and often unreliable existing evidence for protein location, a variety of in vitro and in vivo approaches can be utilized, in combination, to determine the location of a protein within the cell, and specifically intraorganelle location for a protein in the mitochondrion.

James Whelan and Monika W. Murcha (eds.), *Plant Mitochondria: Methods and Protocols*, Methods in Molecular Biology, vol. 1305, DOI 10.1007/978-1-4939-2639-8_5,

In this chapter five techniques to characterize protein uptake into mitochondria are outlined. The first technique is an in vitro protein import assay to determine if a given protein has the ability to be imported into mitochondria. This technique can be modified to include the rupture of the outer membrane after the uptake assay followed by protease treatment, which can yield information as to the nature of the intraorganelle compartment of the target protein. The second technique is a protein import protocol that uses chemical amounts of tagged protein to determine the orientation and assembly of proteins into mitochondrial membranes using immunoblotting of tagged proteins. The third technique encompasses the analysis of protein uptake using blue native gel analysis. This protocol can determine if the protein of interest integrates and/or associates within a larger protein complex. The next protocol offers an orthogonal approach in determining the subcellular localization of a protein using fluorescent tagging of proteins. Finally, putative dual-targeting capabilities can be further confirmed by an in vitro simultaneous import assay for precursors predicted to be dual-targeted to both the mitochondria and chloroplasts.

2 Materials

2.1 Protein Import Assay-Radiolabeled Precursor Protein

2.1.1 Translation

1. T7 or SP6 rabbit reticulocyte lysate-coupled transcription-translation system.
2. Plasmid DNA containing the coding sequence of interest cloned downstream of a T7 or SP6 promoter. This plasmid should be prepared using a high-quality plasmid isolation kit to ensure high purity of isolated plasmid DNA.
3. RNase inhibitor.
4. L-^{35}[S]-methionine (1 mCi, 37 MBq).

2.1.2 Protein Import Assay

Prepare all solutions using sterile reverse osmosis water (SRO) water. Two-times strength (2×) protein import buffer can be prepared in bulk and stored at −20 °C in 50-mL aliquots. Similarly, valinomycin and Proteinase K (PK) solutions may be stored at −20 °C for up to 6 months. The import master mix should be prepared fresh prior to use. Stock solutions for the import master mix can be made prior to use and stored at −20 °C. These solutions can be thawed and reused with the exception of dithiothreitol (DTT).

1. 2× Import buffer: 0.6 M sucrose, 100 mM KCl, 20 mM MOPS-KOH pH 7.5, 10 mM KH_2PO_4, 0.2 % (w/v) bovine serum albumin (BSA).
2. 2 mL of Import master mix: To 1 mL of 2× import buffer add 2 μL of 1 M $MgCl_2$, 20 μL of 100 mM methionine, 4 μL of 100 mM ADP, 15 μL of 100 mM ATP, 20 μL of 500 mM

succinate, 20 µL of 500 mM DTT, 20 µL of 500 mM NADH, 20 µL of 100 mM GTP, 879 µL of SRO water.

3. Valinomycin solution: 1 mM valinomycin dissolved in ethanol, can be stored at −20 °C.
4. PK solution: 0.4 mg/mL.
5. Phenylmethanesulfonylfluoride (PMSF): 100 mM PMSF (*see* **Note 1**) dissolved in isopropanol.
6. Radiolabeled protein of interest.
7. Bradford protein assay reagent: Coomassie Plus™ (Bradford) Protein Assay.
7. SEH buffer: 250 mM sucrose, 1 mM EDTA, 10 mM HEPES-KOH pH 7.4.
8. HEPES-KOH: 20 mM HEPES-KOH, pH 7.4.
9. Sucrose solution: 2 M sucrose.
10. KCl solution: 3 M KCl.

2.1.3 Acrylamide Gel Electrophoresis

1. Separating buffer: 1.5 M Tris–HCl, pH 8.8.
2. Stacking buffer: 0.5 M Tris–HCl, pH 6.8.
3. 10× Running buffer: 0.25 M Tris, 1.92 M glycine, 1 % (w/v) sodium dodecyl sulfate (SDS).
4. 2× Sample buffer: 100 mM Tris–HCl pH 6.8, 4 % (w/v) SDS, 0.2 % (w/v) bromophenol blue, 20 % (v/v) glycerol, add 20 % (v/v) β-mercaptoethanol prior to use.
5. Coomassie staining solution: 10 % (v/v) glacial acetic acid, 40 % (v/v) ethanol, 1 % (w/v) Coomassie blue R-250. Stir overnight to ensure that all powder is dissolved.
6. Destaining solution: 15 % (v/v) glacial acetic acid, 30 % (v/v) ethanol, 2.5 % (v/v) glycerol.
7. Universal power supply: 100 V, 20 mA per gel, 4 h.
8. Gel dryer.
9. Gel electrophoresis system.
10. Phosphor-imager or X-ray-developing unit.
11. Phosphor-imaging plate or X-ray film.
12. Cassettes to hold phosphor-imaging plate or X-ray film.

2.2 Synthesis of Chemical Amounts of Precursor Protein

2.2.1 Protein Expression Using the Cell-Free System Rapid Translation System 500

1. DNA template (cDNA cloned into pIVEX vector of choice) 1 µg/µL. This plasmid should be prepared using a high-quality plasmid isolation kit.
2. Rapid translation system (RTS) ProteoMaster Instrument (Roche).
3. RTS 100 ProteoMaster-compatible reaction devices.
4. 1.5-mL RNase-free microcentrifuge tubes, calibrated pipettes, and filtered tips.

2.2.2 Import Reaction

1. 16 M urea (will solidify, therefore need to heat to 80 °C to dissolve prior to use).
2. Import master mix.

2.2.3 Immunodetection

1. Supported nitrocellulose membrane.
2. Semidry transblotter.
3. Chemiluminescence Western blotting kit.
4. Transfer buffer: 192 mM glycine, 25 mM Tris–HCl, 0.03 % (w/v) SDS, 20 % (v/v) methanol (pH should be 8.9–9 but do not adjust with HCl).
5. 10× Transfer buffer (TBS, Tris buffer saline): 1.5 M NaCl, 200 mM Tris–HCl pH 7.4.
6. 1× TBS-Tween: 100 mL 10× TBS, 900 mL reverse osmosis (RO) water, 1 mL Tween-20.
7. Ponceau stain: 0.1 % (w/v) Ponceau, 5 % (v/v) glacial acetic acid.

2.3 Blue Native (BN)-PAGE Buffers

1. Separating gel solutions

	Light solution	Heavy solution
RO water	13.73 mL	0 mL
Gel buffer (6×)	3.5 mL	3 mL
Acrylamide 40 % (w/v)	2.35 mL	7.42 mL
Bis-acrylamide 2 % (w/v)	1.42 mL	4.5 mL
Glycerol	0 mL	3.5 mL
Ammonium persulfate (APS) 10 % (w/v)	70 µL	50 µL
N,*N*,*N*′,*N*′-Tetramethylethylenediamine (TEMED)	7 µL	5 µL

2. Stacking gel solutions

	Stacking gel
RO water	10.1 mL
Gel buffer (6×)	2.5 mL
Acrylamide 40 % (w/v)	1.5 mL
Bis-acrylamide 2 % (w/v)	0.8 mL
APS 10 % (w/v)	65 µL
TEMED	7.5 µL

3. 5× Cathode buffer: 250 mM tricine, 75 mM bis-Tris–HCl pH 7, 0.1 % (w/v) Coomassie G-250.
4. 6× Anode buffer: 300 mM bis-Tris–HCl pH 7.0.
5. 6× Gel buffer: 1.5 M amino caproic acid, 150 mM bis-Tris–HCl pH 7.0.
6. 5 % Blue G: 750 mM amino caproic acid, 5 % (w/v) Coomassie G-250.
7. Digitonin extraction buffer: 30 mM HEPES-KOH pH 7.4, 150 mM K-acetate, 10 % (v/v) glycerol.
8. Universal power supply.
9. Cell electrophoresis system.
10. Gel dryer.
11. Gradient mixer.
12. Peristaltic pump.
13. Fixing buffer: 40 % (v/v) methanol, 10 % (v/v) glacial acetic acid.
14. Flatbed scanner.
15. Phosphor-imager or X-ray developing unit.
16. Phosphor-imaging plate or X-ray film.
17. Cassettes to hold phosphor-imaging plate or X-ray film.

2.4 Fluorescent Protein Targeting

1. 100 % Isopropanol.
2. 70 % (v/v) Ethanol.
3. 100 % Ethanol.
4. Sterile 50 % (v/v) glycerol.
5. RO water.
6. Green fluorescent protein (GFP) test/control plasmid ≥1 μg/μL.
7. Red fluorescent protein (RFP) control/test plasmid ≥1 μg/μL.
8. 1 μm gold microcarriers.
9. Macrocarriers.
10. PDS-1000/He Hepta system.
11. 1,100 psi rupture discs.
12. 2.5 M $CaCl_2$.
13. 100 mM Spermidine (free base).
14. Sterile Whatman® filter paper discs.
15. Osmoticum plates for Arabidopsis cell suspension.
16. Murashige and Skoog (MS) plates for other plant tissue.

17. Plant tissue:

    3–4-week-old Arabidopsis leaves.

    14-day-old Arabidopsis seedlings.

    Onion (*Allium cepa*) epidermal layers.

    Arabidopsis ecotype *Landsberg erecta* cell suspension.

2.5 Simultaneous Protein Uptake Assays Using Isolated Mitochondria and Chloroplasts

1. 2× Dual-import buffer: 0.6 M sucrose, 100 mM KCl, 30 mM HEPES-KOH pH 7.5, 10 mM KH_2PO_4, 0.4 % (w/v) BSA.
2. 2 mL of Dual-import master mix: To 1 mL of 2× dual-import buffer add 2 μL of 1 M $MgCl_2$, 20 μL of 100 mM methionine, 4 μL of 100 mM ADP, 15 μL of 100 mM ATP, 20 μL of 500 mM succinate, 20 μL of 500 mM DTT, 20 μL of 500 mM NADH, 20 μL of 100 mM GTP, 2 μL of 1 M K-acetate, 2 μL of 1 M $NaHCO_3$, and 875 μL of SRO water.
3. Thermolysin.
4. 0.1 M $CaCl_2$.
5. 0.5 M EDTA.
6. 60 W lamp and stand.
7. 400-μL Elongated microfuge tubes (Eppendorf).
8. Percoll.
9. 1× Wash buffer: 0.3 M sucrose, 15 mM HEPES-KOH pH 7.5, 5 mM KH_2PO_3, 0.2 % (w/v) BSA.

3 Methods

3.1 Protein Uptake Assay Using Radiolabeled Precursor Protein

3.1.1 Protein Translation

This protocol translates a precursor protein using a rabbit reticulocyte-coupled transcription and translation kit. Labeling with ^{35}[S]-methionine allows for visualization of the translated protein. If the protein of interest translates weakly, additional methionine residues may be added using site-directed mutagenesis to the N-terminus if the protein does not contain a cleavable N-terminal presequence or the C-terminus if it does. The addition of methionine residues does not usually affect the targeting ability [2]. Ensure that all the required training and safety procedures are carried out prior to the handling of radioactive isotopes.

1. Translation reaction for 400 μL of radiolabeled precursor protein is assembled on ice: 200 μL rabbit reticulocyte lysate (*see* **Note 2**), 16 μL reaction buffer, 8 μL 1 mM amino acid mix minus methionine, 8 μL RNA polymerase (SP6 or T7), 8 μL RNase inhibitor (40 U/μL), 4 μL ^{35}[S]-methionine, and 156 μL SRO water. Scale the reaction accordingly as required, but do not freeze–thaw the lysate more than once.

2. Aliquot the required amount of translation reaction mixture into a 1.5-mL tube containing the plasmid to be translated. For a 50 μL reaction you can use up to 2 μL of 200 ng/μL plasmid.
3. Gently mix reagents.
4. Incubate at 30 °C for 2 h.
5. Analyze 2 μL of the translation mixture by acrylamide gel electrophoresis.
6. Store the remaining translation reaction at –80 °C until needed.

3.1.2 Protein Uptake Assay

In vitro mitochondrial protein import assays can be used to determine if a target protein has the ability to be imported into mitochondria. The precursor protein is incubated with purified mitochondria in a buffer optimal for protein uptake. PK digestion is carried out to remove any non-imported proteins or proteins bound to the outer membrane but not imported. A second identical reaction is also carried out in the presence of valinomycin, an ionophore that dissipates the membrane potential and prevents the import of protein into or across the inner membrane and is used as a control for import. This procedure is utilized for proteins that are predicted to contain a targeting signal that is cleaved upon import by the mitochondrial processing peptidase. All procedures are carried out on ice, unless otherwise stated.

1. Pre-label 2-mL microcentrifuge tubes and place on ice.
2. Assemble the import master mix.
3. Divide the master mix into two tubes, adding 1 μL of 1 mM valinomycin per mL of import master mix to one tube.
4. Aliquot 180 μL of each master mix into a 2-mL microcentrifuge tube.
5. Add 100 μg of freshly isolated mitochondria to each tube. The volume should not be greater than 20 μL to avoid diluting the master mix; leave on ice for 3 min (*see* **Note 3**).
6. Add 10 μL of radiolabeled precursor protein to each import reaction and mix gently (*see* **Note 4**).
7. Incubate both reactions at 26 °C for 20 min, shaking at 350 rpm—i.e., shaking should be vigorous but not to cause contents to foam.
8. Place reactions on ice before dividing equally into two tubes (there should now be a total of four tubes). To one-half of each reaction (one with valinomycin and one without) add 8 μL of PK solution and mix gently.
9. Incubate for 30 min on ice.
10. To each tube containing PK add 1 μL of PMSF and mix gently.

11. Pellet the mitochondria in a precooled benchtop microfuge at 20,800 × *g* for 5 min at 4 °C.
12. Remove and discard supernatant taking care to avoid disturbing the mitochondrial pellet.
13. Resuspend the pellet in SDS-PAGE loading buffer and heat sample to 95 °C for 3 min for analysis by SDS-PAGE.
14. Samples can be loaded as shown in Fig. 1a, with 2 μL of the precursor protein alone loaded as a control in the first lane. A protein marker should also be loaded to determine the apparent molecular mass of the precursor and mature proteins.

3.1.3 Rupture of the Outer Membrane Following Import

Rupture of the outer mitochondrial membrane following protein uptake assays can be used to determine the intramitochondrial localization of the imported radiolabeled protein. This procedure is vital for confirming the import of precursor proteins that are inserted into the inner membrane and do not usually contain a cleavable presequence (such as Tim23-1, Fig. 1b). The rupture of the outer membrane by osmotic shock allows PK access to the intermembrane space (IMS) and inner membrane. Therefore outer membrane and IMS proteins are degraded. For inner membrane proteins there are two possibilities; if any part of an inner membrane protein is exposed to the IMS it may be cleaved to a lower molecular mass with outer membrane rupture and subsequent PK treatment (Tim23-1 from Fig. 1b is a good example); alternatively, if the protein is in the matrix or on the matrix side of the inner membrane the protein will still remain protease resistant even after outer membrane rupture. We recommend setting up the import reactions at twice the volumes described above (Subheading 3.1.2, **steps 1–11**) and splitting the samples with half of the reactions for

Fig. 1 (continued) γ-subunit presequence) [*note*: processing can still occur via mitochondrial processing peptidase (MPP) if the mitochondrial membrane structures were disrupted during isolation]; (*iv*) processed, imported protein (presequence has been cleaved and protein is protected from PK digestion); (*v*) the lack of imported PK-protected bands into valinomycin control reactions indicates that the import of this protein is dependent on the membrane potential across the inner membrane, suggesting a matrix or inner membrane location. (**b**) A typical five-lane import as described in (**a**) (*lanes 1–5*), with the rupture of the outer membrane after incubation of precursor protein with mitochondria and subsequent PK digestion (*lanes 6–9*). The example shown is for import of the translocase of the inner membrane subunit Tim23-1 (At1g17530.1). Tim23-1 does not contain a cleavable presequence; thus the import and subsequent inner membrane PK-protected portion are indicated in *lane 7* with an *asterisks* (*) (*note*: import occurs in a membrane potential-dependant manner as evidenced by the lack of radiolabeled protein in *lane 9*). (**c**) Determining the rate of import between mitochondria isolated from different genotypes. Using the alternative oxidase gene from *Glycine max* (uniprot Q07185) to program the translation lysate. Imports are conducted at various time points and PK treated allowing for the direct comparison of imported mature protein by quantification of band intensity. *p* precursor, *m* mature, *OM* outer membrane, *kDa* kilodaltons, *Pre* precursor, *Mit* mitochondria, *PK* proteinase, *Val* valinomycin, *WT* wild type

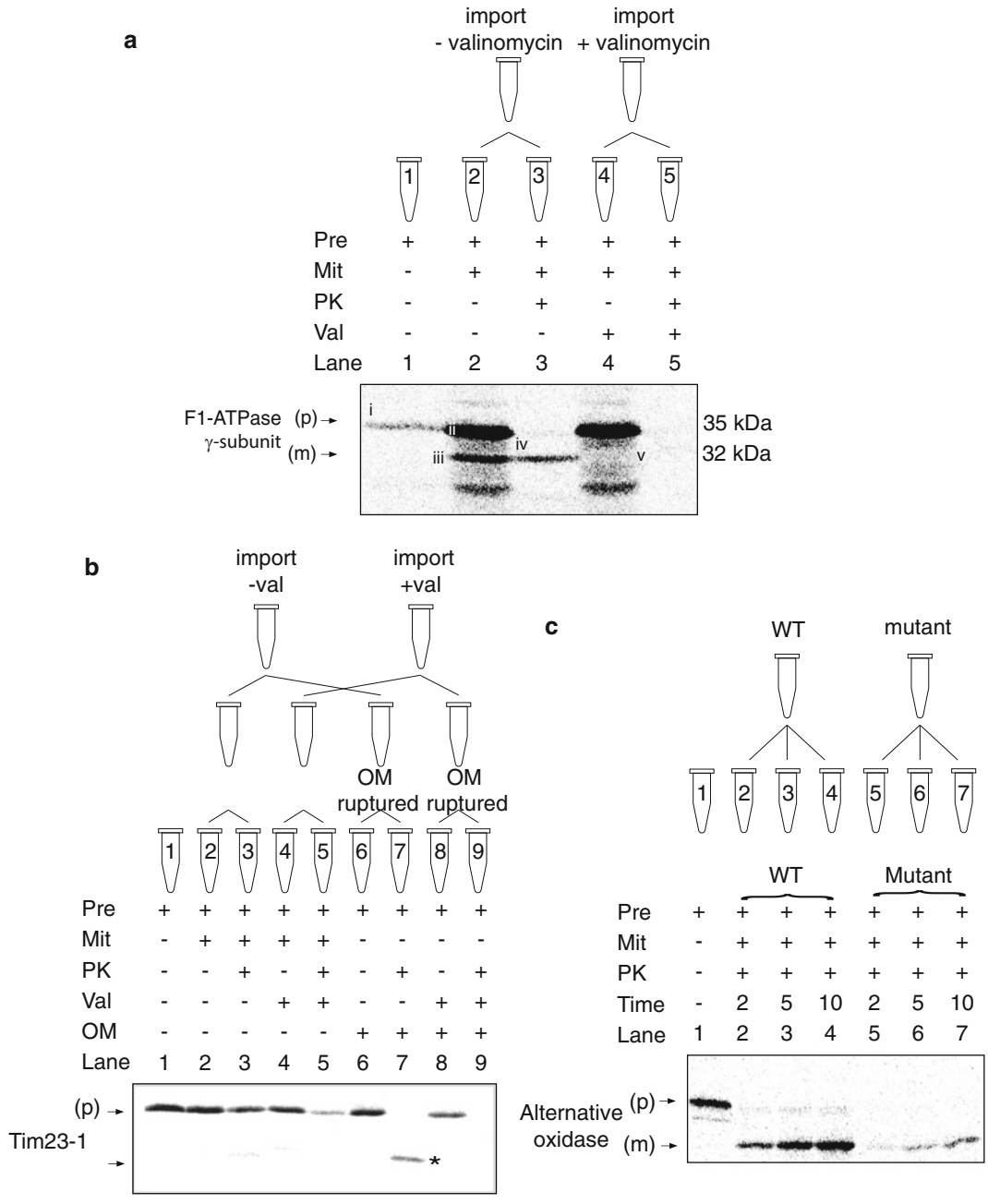

Fig. 1 Mitochondrial protein import assays. (**a**) A typical five-lane import used to determine the ability of a protein to be imported into isolated mitochondria. *Lane 1* contains radiolabeled precursor protein only. *Lane 2* contains the precursor protein incubated with isolated mitochondria under conditions that support import of proteins into mitochondria. *Lane 3*, same as lane 2 except with the addition of Proteinase K (PK) following incubation of precursor protein with mitochondria. *Lanes 4* and *5*, same as lanes 2 and 3 with the addition valinomycin to the import buffer which dissipates the membrane potential and prevents import into or across the inner membrane. The import of F_1-ATPase γ-subunit (At2G33040.1) as evidenced by the annotated bands: (*i*) precursor protein; (*ii*) precursor protein bound but not imported into mitochondria; (*iii*) processed mature form of F_1-ATPase γ-subunit (the apparent molecular mass has decreased indicating cleavage of the F_1-ATPase

PK digestion and the other half for outer membrane rupture followed by PK digestion (Fig. 1b). Rupture of the outer membrane and subsequent PK digestion is described below:

1. Remove supernatant and resuspend the mitochondrial pellet in 10 μL of SEH buffer gently by pipetting.
2. Add 155 μL of 20 mM HEPES-KOH, mix, and incubate on ice for 15 min.
3. Add 25 μL of 2 M sucrose and 10 μL of 3 M KCl, mix gently, and keep on ice.
4. Divide the sample into two microfuge tubes, and add 15 μL of PK to one.
5. Incubate both samples on ice for 30 min.
6. To the PK-treated samples add 1 μL of PMSF.
7. Pellet all samples and prepare for electrophoresis as described above (Subheading 3.1.2, **steps 11–14**).

3.1.4 Acrylamide Gel Electrophoresis Analysis

Gel electrophoresis is carried out by standard procedures as outlined in Sambrook et al. [3] using a large-format electrophoresis system, e.g., 16×16 cm. Following electrophoresis, gels are stained in Coomassie solution overnight and destained until the protein marker and protein bands are clearly visible. This procedure is important to verify equal protein loading prior to imaging. The gel is placed on Whatman® paper and the positions of the markers are penciled on the paper. The gel is covered with plastic film and the gel dried for 2 h at 80 °C in a gel dryer under vacuum. Expose the dried gel to a phosphor-imager plate overnight or longer if needed (up to 7 days). Alternatively the gel can be exposed to X-ray film.

3.2 Protein Uptake Assay Using Chemical Amounts of Precursor Protein

In vitro imports of chemical amounts of precursor can be useful for the subsequent detection of import by immunodetection. Recombinant proteins are expressed with N- and/or C-terminus-specific tags using a cell-free lysate system. This allows for the end-specific immunodetection of tags following protein uptake assays. This method is useful for determining the intramitochondrial location and orientation of precursor proteins following import [4].

3.2.1 Protein Expression Using a Cell-Free System (e.g., Roche RTS 100)

1. Reconstitute the lyophilized reagents according to the manufacturer's instructions or thaw previously reconstituted solutions (*see* **Note 5**).
2. Keep reconstituted reagents and working solutions on ice until use.
3. Set the RTS ProteoMaster (Roche) instrument to 24 °C and a shaking speed of 900 rpm for incubation of this reaction prior to assembly of the device.

4. In a 1.5-mL tube assemble the feeding solution containing 900 µL feeding mix, 80 µL amino acids, and 20 µL methionine.
5. In a 1.5-mL tube assemble the reaction solution containing 15 µL reaction mix, 4 µL amino acids, 1 µL methionine (*see* **Note 6**), 15 µL wheat germ or bacterial lysate, and 15 µL of circular DNA (2–4 µg).
6. Place the microplate on the workbench and insert one or more continuous-exchange cell-free (CECF) modules.
7. Pipette 1 mL of feeding solution into each of the (unlabeled) feeding compartments you will use in this run.
8. Carefully close the modules of the microplate with the adhesive film (supplied in the kit).
9. Insert the microplate into the RTS ProteoMaster instrument and set the instrument parameters to shaking speed: 900 rpm and temperature: 24 °C.
10. Remove the reaction mixture from the reaction chamber and store at –80 °C.
11. Determine protein expression by SDS-PAGE, followed by Coomassie staining and immunodetection (1 µL sample is sufficient for both methods). Use the β-glucuronidase (GUS) control vector supplied. A band with an apparent molecular weight of 68 kDa should be visible after the gel is stained with Coomassie brilliant blue and/or immunodetection using 6× histidine tag antibody (*see* **Note 7**).

3.2.2 Mitochondrial Protein Uptake Assays Using Chemical Amounts of Protein

1. Add 100 µg of freshly isolated mitochondria (ensuring that volume does not exceed 20 µL) into 180 µL import buffer, in a 15-mL polypropylene round-bottom test tube. Place on ice for 3 min.
2. Add 10 µL of hot (70 °C) 16 M urea to 10 µL of RTS reaction mix (recombinant protein) in a 1.5-mL tube and mix by pipetting several times (*see* **Note 8**).
3. Pipette the protein into the import master mix, place the tube at 26 °C, and rock gently.
4. After 40 min remove the import reaction and place 100 µL into cold 1.5-mL tubes of which one has PK added (10 µL of 0.4 mg/mL). Alternatively, the mitochondria may be pelleted at this stage and outer membranes ruptured as described in Subheading 3.1.3.
5. The import reactions are resolved by SDS-PAGE as described above in Subheading 3.1.2.
7. Transfer the gel to a polyvinylidene fluoride (PVDF) or nitrocellulose membrane according to standard protocols as outlined in Sambrook et al. [3].

8. Immunodetection can be carried out according to the manufacturer's instructions (*see* **Note 9**).
9. If the recombinant protein was also expressed with ^{35}[S]-methionine, the membrane can be dried for 1 h at 37 °C following immune detection and exposed to phosphor-imaging plate for 24–48 h or X-ray film.

3.3 Analysis of Assembly of Imported Protein into Membrane Complexes Using BN-PAGE

This protocol involves the import of radiolabeled protein into isolated mitochondria as previously described except that import is analyzed by BN-PAGE, allowing for the visualization of imported protein within larger protein complexes. A time course can be carried out to determine incorporation of radiolabeled protein into protein complexes in a time-dependant manner. Furthermore, incorporation of radiolabeled protein can be seen associating with smaller complex intermediate complexes, monomeric complexes, and supercomplexes allowing for a "chase" of import and assembly (Fig. 2).

3.3.1 Mitochondrial Protein Import Assay

1. In a 15-mL polypropylene round-bottom test tube, add 250 µg of freshly isolated mitochondria into 360 µL 1× import master mix and incubate on ice for 3 min. Add 25 µL of radiolabeled precursor protein and incubate for specified time ranging from 10 min to 3 h (time is dependent on protein and what complex(s) it may assemble or associate with) at 26 °C shaking at 350 rpm.

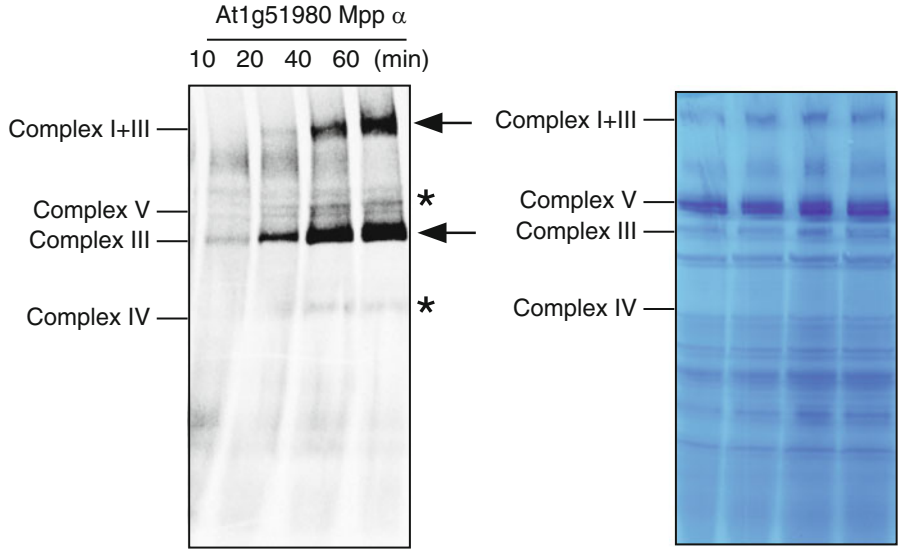

Fig. 2 BN-PAGE import analysis of Mpp-α into isolated mitochondria. The specific incorporation of radiolabeled protein into Complex III was observed initially followed by incorporation and assembly into the supercomplex I + III (indicated by the *arrows*). The intensity of incorporation increases in a time-dependant manner. Nonspecific incorporation of radiolabeled protein into Complex V and Complex IV is shown as indicated by *asterisk*. The Coomassie-stained gel is shown alongside with the respiratory chain complexes indicated

2. Centrifuge the whole import reaction in a 1.5-mL microcentrifuge tube at 20,000 × *g* for 10 min and remove the supernatant ensuring that the mitochondrial pellet is not disturbed.
3. The mitochondrial pellet can be stored at −80 °C or prepared directly for BN-PAGE analysis as described in Subheading 3.3.2.

3.3.2 Casting Acrylamide Gradient Gel

1. Preparation of the gradient gel is to be carried out at 4 °C with all devices (such as the gradient mixer and casting stand) cooled prior to use. All reagents (except glycerol) are to be cooled to 4 °C prior to use (*see* **Note 10**).
2. Push an injection needle through the rubber sealing from the bottom of the casting stand, so that it is placed between the glass plates. Using a long cannula attach the needle to the gradient pourer.
3. Using a peristaltic pump, pump 3 mL of RO water between the glass plates.
4. Prepare both the heavy and light solutions required for one gel (0.15 × 20 × 20 cm) as indicated in Subheading 2.3. This recipe forms 4–16 % (w/v) acrylamide gradient gel that resolves the protein mass range of 10 kDa–3 MDa. Place the solutions at −20 °C for 5 min to cool rapidly (*see* **Note 11**).
5. Add APS and TEMED (Subheading 2.3) into light and heavy solution, and mix well by inversion four times.
6. Pour the light solution into the first chamber of the gradient mixer, and the heavy solution into the second with the mixing valve closed.
7. Start pumping the light solution into the bottom of the plates at a low speed (0.3 mL/min). After 10 min or when the light solution reaches the same level as the heavy solution, open the valve between the two chambers, allowing the heavy solution to mix gently with light solution (*see* **Note 12**).
8. Speed up the pumping speed to 1 mL/min after 1/3 solution has been pumped into the plates. It is critical to ensure that no air bubbles are pumped into the gel (*see* **Note 13**).
9. Unplug the needle and allow the gel to polymerize at room temperature for 1 h.

3.3.3 Preparing the Stacking Gel

1. After polymerization, remove the water from the top of the gradient gel and prepare the stacking gel as described in Subheading 2.3.
2. Gently pour the stacking gel over the gradient gel and place a 1.5-mm 10-sample comb.
3. Allow the stacking gel to polymerize for 30 min at room temperature.

3.3.4 Solubilization of Mitochondrial Protein

1. Dissolve 5 % (w/v) digitonin in extraction buffer, vortex, and incubate at 75 °C for 5 min until dissolved. Place on ice for 15 min.
2. Resuspend the mitochondrial pellet with cold digitonin buffer and incubate for a further 20 min on ice (250 μg protein/25 μL digitonin buffer/1.25 mg digitonin).
3. Centrifuge at 20,800 × *g* at 4 °C for 20 min, collect the supernatant in a new tube, and add 5 % (w/v) Coomassie blue G-250 before loading to the gel. Do not load more than 50 μL per well.

3.3.5 Electrophoresis

1. A wide-format 1-D vertical electrophoresis cell is used for electrophoresis. Assemble the gels to the rig according to the manufacturer's instructions. Pour 1.2 L anode buffer into the tank and 350 mL cathode buffer on the top. Place the assembled tank at 4 °C.
2. Resolve the gel at 100 V with the current limited to 8 mA for 45 min, followed by 15 mA with the volts limited to 500 V for 7 h.
3. After electrophoresis, incubate the gel with 100 mL fixing buffer to destain the gel. Image the gel using a flatbed scanner for identification of the major respiratory chain complex locations.
4. Place the gel on Whatman® paper, dry for 1 h using a gel dryer, then expose the gel to a phosphor-imaging plate or X-ray film for up to 7 days, and develop the images as appropriate.

3.4 Fluorescent Protein Targeting

The transformation procedure has been adapted from the manual for the PDS1000 system from BioRad and describes the biolistic transformation of Arabidopsis cell culture, onion epidermal cells, and Arabidopsis tissue with fluorescent-tagged constructs (Fig. 3).

3.4.1 Protocol for Gold Preparation (PDS 1000 System)

1. Weigh out 0.03 g of 1-μm gold particles into a 1.5-mL microcentrifuge tube.
2. Pipette 1 mL 70 % (v/v) ethanol onto gold.
3. Vortex vigorously for 3–5 min and allow to settle/or spin down for 5 s in a microfuge.
4. Remove supernatant and add 1 mL of 100 % ethanol.
5. Allow particles to soak in 100 % ethanol for 15 min.
6. Quick spin, remove the supernatant, and discard (do not spin excessively as gold becomes hard to resuspend evenly).
7. Wash pellet with 1 mL 70 % (v/v) ethanol and then remove supernatant.

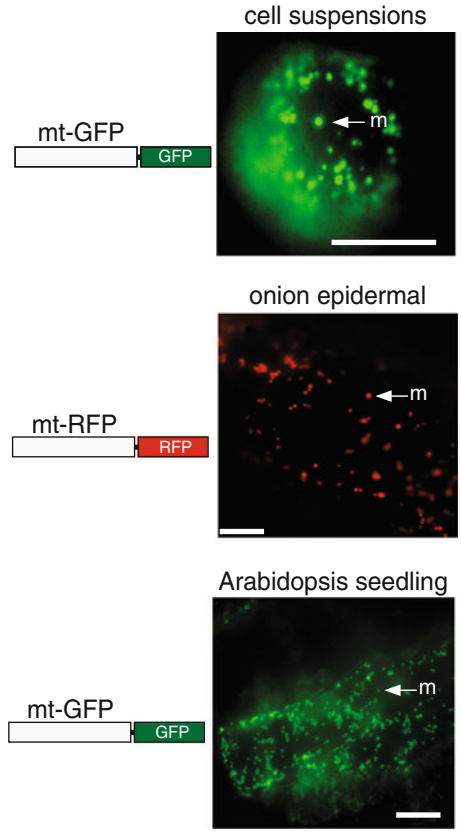

Fig. 3 Fluorescent protein targeting. Examples of mitochondrial (*m*) targeting in biolistically transformed Arabidopsis cell suspensions, onion epidermal tissue, and Arabidopsis seedling tissue. Scale bar indicates 20 μm. The ALTERNATIVE OXIDASE (*AOX*) of *Glycine max* (uniprot Q07185) was used to target green fluorescent protein (*GFP*) and red fluorescent protein (*RFP*) to the mitochondria

8. Repeat **step 7** twice more.
9. Wash pellet with 1 mL RO water, and remove supernatant.
10. Repeat **step 9** twice more.
11. Resuspend the gold particles in 500 μL 50 % (v/v) glycerol (ensure that the particles are resuspended evenly).
12. Aliquot gold solution into 50-μL aliquots for immediate use or storage at 4 °C.

3.4.2 Tissue Preparation Prior to Biolistic Transformation

1. Arabidopsis suspension cultures should be transformed 4–5 days after subculturing. Slowly pipette 2 mL of culture evenly onto a sterile Whatman® filter paper disc using a vacuum filter. Ensure an even coverage of the filter paper. Place the filter paper on osmoticum agar plates and incubate at normal growth conditions for 2 h.

2. Onions can be bought from a local supermarket preferably the same day as transformation. The onions are chopped into quarters and the individual layers separated and chopped further into 2 × 2 cm pieces. Using tweezers, gently peel the thin epidermal layer and place upside down directly onto an MS agar plate. Cover the whole plate with epidermal layers to ensure sufficient frequency of transformation.
3. For young Arabidopsis seedlings, germinate and grow seedlings on a round MS agar, ensuring that the plate is well covered. Use directly for transformation.
4. Arabidopsis leaf tissue can be transformed when 3–4 weeks old. Leaves from soil-grown Arabidopsis are excised and placed directly on MS agar plates immediately prior to transformation.

3.4.3 Precipitating DNA onto Macrocarriers

1. For each transformation to be performed, vortex a 50-μL aliquot of sterilized gold thoroughly and then add 5 μL of GFP test plasmid (at 1 μg/μL) and 5 μL of RFP control plasmid (at 1 μg/μL) (*see* **Note 14**).
2. While vortexing, quickly add 50 μL of 2.5 M $CaCl_2$ and 20 μL of 100 mM spermidine (*see* **Note 15**).
3. Close the lid on the microcentrifuge tube and continue vortexing for a further 1–2 min.
4. Allow gold particles to settle/quick spin (2–3 s) and remove and discard the supernatant.
5. Add 140 μL 70 % (v/v) ethanol, vortex, quick spin, and remove supernatant.
6. Add 140 μL 100 % ethanol, vortex, quick spin, and remove supernatant.
7. Add 56 μL 100 % ethanol.

3.4.4 Preparation of Macrocarriers for Biolistic Transformation

1. Place seven macrocarriers for each bombardment onto a piece of white A4 paper.
2. Resuspend the gold with the precipitated DNA by vortexing or pipetting.
3. Pipette 8 μL onto the center of each macrocarrier.
4. Allow the ethanol to evaporate before proceeding with the transformation.

3.4.5 Biolistic Transformation

1. Place the plate holder in the bottom most rack.
2. Turn on the gun, red switch on the gun chamber, and the switch on the vacuum pump.
3. Turn on the gas bottle. Pressure should be set to 1,300 psi if using 1,100 psi rupture discs.
4. Clean the gun and all parts with 70 % (v/v) ethanol.
5. Attach the hepta adaptor to the PDS-1000 unit.

6. Close the door and place under vacuum. When vacuum is at the 27 in./Hg position toggle the rocker switch to "hold," press the "fire" switch momentarily several times, and then release vacuum.
7. Remove hepta adaptor, place a rupture disc into the center of the hepta adaptor, and ensure that it is sealed (*see* **Note 15**).
8. Place macrocarriers coated with gold onto the hepta adaptor ring with a stopping screen and assemble (ensure that gold-coated side is facing down towards plant material).
9. Place the plate into plate holder just under gas head in the gun chamber.
10. Place plate with tissue to be transformed onto plate holder in gun chamber (without plate lid).
11. Close the door and toggle switch to "vac."
12. When the vacuum has reached 27 in./Hg, toggle the rocker switch to "hold" and press and hold the fire button until the rupture disc breaks.
13. Once fired, vent vacuum immediately.
14. Remove the rupture discs, macrocarriers, and plates from the gun chamber.
15. Repeat process for each plate to be transformed—gun chamber and all parts need to be cleaned with 70 % (v/v) ethanol if shooting different constructs.
16. Remove the rupture discs, macrocarriers, and plates from the gun chamber.
17. Spray all parts of the gun (especially hepta adaptor) with 70 % (v/v) ethanol and attach to the gun (*see* **Note 16**).
18. Close the gas bottle main valve.
19. Place under vacuum and press fire to bleed the lines. Do this until both gauges on the regulator read zero.
20. Turn off vacuum pump and gun.
21. Return transformed plates to dark growth chamber for 24–48 h before microscopy.

3.5 Simultaneous Protein Uptake Assays Using Isolated Mitochondria and Chloroplasts

The majority of precursor proteins are targeted specifically to their respective organelle though an increasing number of proteins are found to be also localized to both the mitochondria and chloroplasts [5]. Here we describe a simultaneous in vitro import assay developed to confirm the dual-targeting ability of proteins and to prevent the likelihood of mis-targeting [6]. Organelles are isolated independently (*see* Chapter 1 for mitochondrial isolation procedures and previously published procedures for chloroplast isolation [7, 8]), mixed, and incubated together in an import buffer that will support import into both organelle; following import uptake organelles are subsequently recovered using a Percoll gradient.

3.5.1 Simultaneous In Vitro Import Assay

1. Isolate mitochondria and chloroplasts from the tissue of choice (*see* **Note 17**).
2. Quantitate protein abundance (mitochondria) and chlorophyll content (chloroplasts) using methods of choice.
3. Keep organelles on ice until use.
4. Prepare 1× dual-import master mix.
5. In a 2-mL microcentrifuge tube pipette 100 μL 1× dual-import master mix, 50 μg mitochondria, and 20 μg chloroplasts. Keep on ice for 2 min (*see* **Note 18**).
6. Pipette 10 μL of radiolabeled precursor protein.
7. With the lids open, place the microfuge at 25 °C with gentle agitation under a bright lamp for 20 min (*see* **Note 19**).
8. Close the lids and place the reactions on ice.
9. Divide the reaction into two equal parts adding 4 μL of the 2 mg/mL thermolysin supplemented with 0.1 mM $CaCl_2$. Incubate on ice for a further 30 min.
10. Inhibit thermolysin activity by the addition of 1 μL of 1 M EDTA.
11. Load the sample onto a preprepared 4 % (v/v) Percoll gradient in an elongated microfuge tube (*see* **Note 20**).
12. Centrifuge for 30 s at 4,000 × *g* in a fixed-angle rotor microfuge at 4 °C.
13. Remove the mitochondrial band at the top of the gradient and place in a new 1.5-mL microcentrifuge tube containing 1 mL of 1× wash buffer.
14. Pellet the mitochondria by centrifugation at 20,800 × *g* for 5 min at 4 °C.
15. Remove the chloroplast pellet at the bottom of the gradient and place into a new 1.5-mL microcentrifuge tube containing 1 mL of 1× wash buffer.
16. Pellet the chloroplasts by centrifugation at 830 × *g* for 2 min at 4 °C.
17. The imports are analyzed by SDS-PAGE analysis as outlined in Subheading 3.1.4.

4 Notes

1. PMSF is not stable in aqueous solutions, so is best prepared shortly before use. This may require warming to 37 °C to dissolve the PMSF. Do not store PMSF on ice as it will precipitate out of solution. An alternative to PMSF is 4-(2-aminoethyl) benzenesulfonyl fluoride hydrochloride (Pefabloc) that is water soluble.

2. Proteins synthesized by the rabbit reticulocyte system can be added directly to the in vitro import reaction without the need for further purification. It is worth noting that this is not the case for the similar wheat germ kits. Proteins synthesized using this system, under the majority of circumstances, are not import competent and will not be imported into mitochondria using this protocol.
3. When the rate of protein import is to be compared between mitochondrial samples, in addition to the five-lane import described in Subheading 3, prepare 3 × 2-mL tubes per sample, each containing 90 μL of import master mix and 10 μL of precursor protein. These should be incubated at 26 °C alongside the other samples. One tube per mitochondrial sample should be removed at 2-, 5-, and 15-min time points to be treated with PK. It is important to note that these samples should not be left on ice but should be treated with PK immediately (Fig. 1c).
4. Minimizing the amount of time samples sit on ice in an import-competent state is critical to the reproducibility of this technique. One useful technique to minimize the amount of import occurring outside of the 25 °C incubation step is to carefully assemble the import reaction by layering the sucrose-rich mitochondria-containing solution into the bottom of the 2-mL tube, avoiding mixing with the import master mix, followed by pipetting the less dense rabbit reticulocyte lysate onto the top of the master mix. In this way, mixing of the mitochondria and precursor protein is avoided until the start of the 26 °C incubation period.
5. The RTS 500 unit may also be used, though unless a large amount of precursor protein is required, the small-scale RTS 100 is sufficient.
6. While the RTS kits provide "cold" methionine, radiolabeled ^{35}[S]-methionine may be added instead (Subheading 2.1.1). This allows protein import to be detected simultaneously via two methods, immunodetection of N- or C-terminal tags and detection of the radiolabeled protein via exposure of dried gel to a phosphor-imaging plate.
7. Recombinant protein can be purified and concentrated using standard procedures. In this case the precursor protein can be imported straight away without the need of additional 16 M urea.
8. Pipette the hot urea and precursor protein rapidly to prevent precipitation. Do not place on ice prior to addition to the import master mix.
9. For best result, incubate primary antibody (anti-6× histidine tag or anti-C-Myc) overnight at 4 °C on a gentle rocker.
10. It is critical to cool down all the devices and reagents before casting the gradient gel to prevent gel polymerization in the gradient mixer.

11. Different acrylamide concentrations can be chosen depending on the protein mass. Larger protein complexes can be resolved with lower acrylamide concentrations. 3–14 % (w/v) acrylamide gradient gel is sufficient for protein masses from 10 kDa up to 10 MDa.
12. When light and heavy solutions are pumped into plates, adjust the valve between two chambers to make sure that light solution and heavy solution stay at the same level, so that a linear gradient acrylamide gel can form in plates.
13. It is vital to ensure that no bubbles are pumped into the gel. Immediately stop pumping when all the solution has gone out of the mixer.
14. It is recommended that you purify your plasmids with a commercial midi-scale preparation kit of your choice. This ensures sufficient amounts of plasmid and its quality.
15. Spermidine must be free-base. It is best purchased as a powder and the entire contents of the bottle resuspended to the correct concentration. It is best aliquoted and then frozen at −20 °C. Once thawed, it should be used once and not refrozen.
16. Dipping the rupture disc first in isopropanol can help to insert and seal into the hepta-adapter.
17. To ensure that both organelles spend minimal amount of time on ice prior to the import assay, mitochondria and chloroplasts are isolated consecutively, with chloroplast isolation procedures initiated during the long gradient spin during the mitochondrial isolation procedure.
18. Ensure that the mitochondrial and chloroplastic volume added to the import buffer is kept to a minimum to prevent dilution of the substrates.
19. A lamp placed above the import reaction is required for light-driven ATP and NADH production essential for chloroplast protein import.
20. Gradients are prepared by pipetting 300 μL of 4 % (v/v) Percoll solution in 1 × wash buffer into an elongated microfuge tube. Gradients can be prepared earlier and kept on ice until required.

References

1. Tanz SK, Castleden I, Hooper CM, Vacher M, Small I, Millar HA (2013) SUBA3: a database for integrating experimentation and prediction to define the SUBcellular location of proteins in Arabidopsis. Nucleic Acids Res 41(Database issue):D1185–D1191
2. Narsai R, Devenish J, Castleden I, Narsai K, Xu L, Shou H, Whelan J (2013) Rice DB: an Oryza Information Portal linking annotation, subcellular location, function, expression, regulation, and evolutionary information for rice and Arabidopsis. Plant J 76:1057–1073

3. Sambrook JFEFMT (1989) Molecular cloning: a laboratory manual. Cold Spring Harbor Laboratory, Cold Spring Harbor, NY
4. Murcha MW, Elhafez D, Millar AH, Whelan J (2005) The C-terminal region of TIM17 links the outer and inner mitochondrial membranes in Arabidopsis and is essential for protein import. J Biol Chem 280:16476–16483
5. Carrie C, Small I (2013) A reevaluation of dual-targeting of proteins to mitochondria and chloroplasts. Biochim Biophys Acta 1833:253–259
6. Rudhe C, Chew O, Whelan J, Glaser E (2002) A novel in vitro system for simultaneous import of precursor proteins into mitochondria and chloroplasts. Plant J 30:213–220
7. Aronsson H, Jarvis RP (2011) Rapid isolation of Arabidopsis chloroplasts and their use for in vitro protein import assays. Methods Mol Biol 774:281–305
8. Taylor NL, Stroher E, Millar AH (2014) Arabidopsis organelle isolation and characterization. Methods Mol Biol 1062:551–572

Chapter 6

Plant Mitochondrial Proteomics

Nicolas L. Taylor and A. Harvey Millar

Abstract

Mitochondrial proteomics has significantly developed since the first plant mitochondrial proteomes were published in 2001. Many studies have added to our knowledge of the protein components that make up plant mitochondria in a wide range of species. Here we present two common and one emerging quantitative proteomic techniques that can be used to study the abundance of mitochondrial proteins. For this publication, we have described the methods as an approach to determine the amount of contamination in a mitochondrial isolation to contrast historical approaches that involved the use of use of antibodies to specific marker proteins or the measurement of activity of marker enzymes. However, these approaches could easily be adapted to carry out control versus treatment studies.

Key words Mitochondria, Proteomics, Mass spectrometry, Differential in-gel electrophoresis (DIGE), Spectral counting, Selected reaction monitoring (SRM) mass spectrometry

1 Introduction

Proteins are large macromolecules with a wide range of diverse primary structures, folding patterns, and modifications, and they are essential components of reactions, cascades, and pathways for a wide range of cellular processes. They are vital to mitochondrial function as they responsible for vast arrays of activities, including the generation and utilization of electrochemical gradients, the formation of structural or signal transducing molecules and the catalysis of reactions. Whilst the study of proteins of has existed since their naming in 1838 by Jöns Jacob Berzelius, developments towards the end of the last century in gel electrophoresis, mass spectrometry and bioinformatics has fostered a major shift from pure function driven protein biochemistry to systematic, holistic and high throughput analysis of proteins. This shift was accompanied by the introduction of the term "proteome" to describe the entire PROTEin complement expressed by a genOME, by a cell or tissue type [1]. The complexity of whole proteome analysis was discovered in the following years and a number of challenges were

James Whelan and Monika W. Murcha (eds.), *Plant Mitochondria: Methods and Protocols*, Methods in Molecular Biology, vol. 1305, DOI 10.1007/978-1-4939-2639-8_6,

revealed including the large dynamic range of abundant and minor proteins and the dynamic nature of the proteome in response to genetic or environmental parameters. The proteome was also shown to be several orders of magnitude more complex than the genome, due to the translation of splicing and editing variants and the addition of post-translational modifications (PTMs) to mature proteins. These challenges have led to a number of new areas of research and specialties including membrane proteomics, PTM specific phospho-, glyco-, and ubiquitin-proteomics, and subcellular proteomics.

Plant mitochondrial proteomics developed from the subcellular specialty and utilized traditional organellar isolation techniques developed decades earlier to reduce overall sample complexity and dynamic range by focusing on this subset of proteins. Mitochondrial proteins have been a focus of research for many years, and the first 2D separation of a mitochondrial protein was the α-subunit of the *Vicia faba* ATP synthase [2]; however, large-scale identification of proteins of the entire mitochondrial proteome separated by 2D gel electrophoresis (classical proteomics) could not occur until the availability of a complete genome sequence or large EST collections of the plant of interest. This occurred in 2000 with the release of the genome sequence of Arabidopsis (*Arabidopsis thaliana*) [3] and the back-to-back publications of the Arabidopsis mitochondrial proteome by Millar et al. and Kruft at al. [4, 5] a year later. This was quickly followed by an investigation in to the changes in the mitochondrial proteome during development in pea by Bardel et al. [6]. Following these initial studies and as the bioinformatics resources required to carry out large-scale analysis have matured, a number of studies have revealed the mitochondrial proteomes of a number of species including Arabidopsis [4, 5, 7–37], rice [38–45], wheat [46–48], maize [49, 50], barley [51], pea [6, 52] soybean [53–55], medicago [56], *Phaseolus vulgaris* [57], potato [58], and Chlamydomonas [59]. This was then followed by studies focussed on mitochondrial proteins that have been shown to vary in abundance in control versus abiotic treatments in whole tissue/organ studies and in mitochondrial specific studies including on salinity [32, 42, 47, 48, 60–65], anoxia [39, 55, 66], cold [35, 52, 54, 67–74], heat [75, 76], heavy metals [27, 77–79], and drought (osmotic) [52, 61, 80] treatments, and these have been reviewed in refs. [24, 81, 82]. Studies have also investigated changes in the mitochondrial proteome during plant development or in different tissues [6, 22, 26, 31, 32, 34, 37, 83], in response to biotic treatments [21, 84], and to identify mitochondrial proteins that have specific PTMs [23, 41, 85]. These surveys of mitochondrial proteomes have yielded a vast amount of information that has allowed us to better define what makes up a mitochondrial proteome, how it adapts to stress or changes during development, and these discovery type investigations have dominated the literature in the last 12 years.

More recently we have started to see the emergence of a new approach in quantitative mitochondrial proteomics known as Selected Reaction Monitoring (SRM) mass spectrometry and sometimes referred to as Mass Westerns [86] or targeted proteomics [87]. In this approach a triple quadropole (QqQ) mass spectrometer transmits a peptide precursor ion in Q1 that is then fragmented in q2 and a single peptide fragment ion is selected in Q3 for quantitation. The precursor and fragment ion pair is referred to as a transition and its abundance is used quantify the abundance of a protein. During a SRM experiment, sequential gating of precursor and product in a QqQ mass spectrometer allows millions of precursor/fragment ion combinations (transitions) to be assessed in complex peptide mixtures generated by proteolysis of protein extracts from isolated mitochondria. These targeted approaches are more reminiscent of the pure function driven protein biochemistry carried out prior to the proteomics revolution, in that they usually involve the quantitation of a predefined protein, or group of proteins prior to analysis. Using this approach a basic amino acid carrier involved in arginine metabolism [44] and subunits and assembly factors of succinate dehydrogenase [88] have been quantified and the amount of contamination by mitochondria in a cytosolic preparation was determined by quantifying the abundance of the mitochondrial ATP-β subunit [89]. To examine the utility of this approach for studying the abundance of mitochondrial proteins we recently investigated the abundance of two isoforms of the tricarboxylic acid (TCA) cycle, aconitase (mACO1) and malate dehydrogenase (mMDH1), and two lower abundance isoforms for the same enzymatic steps, mACO2 and mMDH2 [33, 90]. We quantified peptides of each of the isoforms, in wild-type and knockout plants, and in the case of mMDH, in double knockout and complemented plants. The SRM analysis demonstrated that this approach is a sensitive and reliable method to distinguish between similar isoforms of mitochondrial proteins where traditional antibodies are unable to do so.

Here we present two traditional and one contemporary quantitative proteomic approaches that can be used to study the abundance of mitochondrial proteins. We have framed these methods here as approaches for assessing the degree of contamination in mitochondrial preparations; however, they could easily be adapted to control versus treatment experiments as well. The use of antibodies to specific marker proteins or the measurement of activity of marker enzymes has traditionally been used to determine the degree of contamination in mitochondrial fractions. The techniques outlined below add to this basic knowledge of the amount of contamination by either identifying contaminating proteins, estimating the amount an individual protein contaminates the sample, allowing the reclassification of previously considered mitochondrial proteins as contaminants or contaminants as mitochondrial proteins and

the identification of colocalized proteins. They can also help to distinguish between the presence of mitochondrial and non-mitochondrial isoforms of proteins.

2 Materials

2.1 Differential In-Gel Electrophoresis (DIGE)

There are two main gel-based methods to separate the plant mitochondrial proteins for DIGE analysis. Blue native-sodium dodecyl sulfate-polyacrylamide gel electrophoresis (BN-SDS-PAGE) DIGE is well suited to profile the composition of individual electron transport chain (ETC) complexes, and detailed procedures of BN-SDS-PAGE [91] and BN-SDS-PAGE-DIGE [92] are available and will not be covered here. 2D-isoelectric focusing (IEF)-SDS-PAGE is a highly reproducible platform that is commonly used for mitochondrial proteomic analysis, and the combination of DIGE and 2D-IEF-SDS-PAGE (2D-IEF-SDS-PAGE-DIGE) provides a powerful tool to define contaminants when comparing two mitochondrial isolation procedures.

2.1.1 Mitochondrial Precipitation and Resuspension

1. Acetone.
2. Microfuge such Eppendorf 5430 or equivalent.
3. Lysis buffer 1: 8 M urea, 4 % (w/v) CHAPS, 40 mM Tris (*see* **Note 1**).

2.1.2 CyDye Labeling

1. CyDyes Cy5, Cy3, and Cy2 (GE Healthcare Life Sciences).
2. Dimethylformamide (DMF) (water-free).
3. 10 mM Lysine.
4. Vortex and microfuge.
5. Lysis buffer 2: 8 M urea, 4 % (w/v) CHAPS, 40 mM Tris, 72 mM dithiothreitol (DTT) (*see* **Note 1**).

2.1.3 Isoelectric Focusing (IEF)

1. Rehydration buffer: 8 M urea, 2 % (w/v) CHAPS, 0.05 % (w/v) bromophenol blue. Just prior to use add 0.5 % (v/v) IPG buffer (pH 3-10 NL, GE Healthcare Life Sciences) and 18 mM DTT (*see* **Note 1**).
2. Vortex and microfuge such as using an Eppendorf 5430 or equivalent.
3. Ettan ceramic strip holder or equivalent (GE Healthcare Life Sciences) for IEF equipment being used.
4. Immobiline DryStrips 3-10NL 240 mm (GE Healthcare Life Sciences) or equivalent.
5. IPG cover fluid (GE Healthcare Life Sciences) or mineral oil equivalent.
6. Ettan IPGphor 3 (GE Healthcare Life Sciences) or equivalent.

2.1.4 Transferring and Setting IEF Strips onto SDS-PAGE

1. 12 % SDS-PAGE gel solution: 375 mM Tris–HCl, pH 8.8, 0.1 % (w/v) SDS, 0.36 % (w/v) bisacrylamide, 12 % (w/v) acrylamide, with 0.1 % (w/v) APS 0.04 % (v/v) *N*, *N*, *N′*, *N′*-tetramethylethylenediamine (TEMED) added just before use.
2. Forceps.
3. Equilibration buffer: 50 mM Tris–HCl (pH 8.8), 6 M urea, 2 % (w/v) SDS, 26 % (v/v) glycerol, 0.05 % (w/v) bromophenol blue. DTT (65 mM) or iodoacetamide (IAA) (135 mM) added freshly before use.
4. Rinse solution: 1.5 M Tris–HCl pH 8.8, 1 % (w/v) SDS.
5. IPG fixing solution: 375 mM Tris–HCl, pH 8.8, 1 % (w/v) SDS, 0.5 % (w/v) agarose, 0.5 % (w/v) bromophenol blue.

2.1.5 Gel Scanning and Software Analysis

1. Software analysis packages such as DeCyder 2D Software (GE Healthcare Life Sciences), Delta 2D (DECODON).

2.1.6 Determination of Proteins Abundance on 2D-IEF-SDS-PAGE-DIGE

1. V-bottom 96-well plate made of polypropylene such as Greiner Bio-One (651201) and sealing film such as Nunc (232702) or equivalent.
2. Destain solution: 50 % (v/v) acetonitrile (ACN), 10 mM NH_4HCO_3.
3. Orbital shaker.
4. Dry block heater.
5. Digestion solution: 12 μg/mL trypsin, 10 mM NH_4HCO_3, 0.0012 % trifluoroacetic acid (TFA) (*see* **Notes 2** and **3**).
6. 37 °C heating oven.

2.1.7 Protein Identification on 2D-IEF-SDS-PAGE-DIGE by MALDI-MS/MS

1. MALDI TOF/TOF MS such as the Bruker UltraFlex III or equivalent.
2. Peptides extracted from a protein spot as outlined in Subheading 3.1.6.
3. MALDI mass spectrometry calibration standards.
4. LCMS grade ACN, water, TFA and ammonium phosphate (monobasic) ($NH_4H_2PO_4$).
5. Machine specific MALDI plate.
6. Saturated α-cyano-4-hydroxycinnamic acid (CHCA) matrix solution. Take 150 μL of 90 % (v/v) ACN, 0.1 % (v/v) TFA add a small spatula of CHCA, vortex and then sonicate for 15 min. If all of the matrix is solubilized, then add more CHCA and repeat sonication until undissolved matrix is visible (saturated). Centrifuge at 10,000 × *g* for 5 min to pellet undissolved matrix (*see* **Note 4**).
7. Matrix solution (600 μL). This contains 516 μL 95 % (v/v) ACN, 0.1 % (v/v) TFA, 27 μL saturated CHCA solution, 6 μL 10 % (v/v) TFA, and 6 μL 100 mM $NH_4H_2PO_4$.

2.1.8 Protein Identification on 2D-IEF-SDS-PAGE-DIGE by ESI-MS/MS

1. Electrospray ionization-quadrupole-time-of-flight-mass spectrometer (ESI-Q-TOF-MS) such as an Agilent Technologies 6550 or equivalent.
2. Peptides extracted from a protein spot as outlined in Subheading 3.1.6.
3. LCMS grade ACN, water and formic acid (FA).
4. C18 column (*see* **Note 5**).

2.2 Gel Free Peptide Fractionation and Identification to Determine Mitochondrial Purity

This approach requires electrospray ionization (ESI) tandem mass spectrometer with an online cap/nano HPLC.

2.2.1 Sample Preparation

1. Resuspension solution: 8 M urea, 50 mM NH_4HCO_3, 5 mM DTT, pH 8.0.
2. Vortex.
3. IAA stock solution: 100 mM IAA.
4. Dilution buffer: 50 mM NH_4HCO_3, pH 8.0.
5. Digestion solution: 1 μg/μL trypsin in 1 mM $CaCl_2$.
6. FA.
7. C18 spin columns (such as Pierce C18 spin columns, Thermo Scientific) or C18 embedded tips (such as ZipTips, Merck Millipore).
8. Charging and elution solution: 70 % (v/v) ACN, 0.1 % (v/v) FA (LCMS grade).
9. Equilibration and washing solution: 2 % (v/v) ACN, 0.1 % (v/v) FA (LCMS grade).
10. Vacuum centrifuge.

2.2.2 Sample Fractionation and Mass Spectrometry

1. Peptides extracted from a mitochondrial sample as outlined in Subheading 3.2.1.
2. ESI-Q-TOF-MS such as an Agilent Technologies 6550 or equivalent.
3. LCMS grade ACN, water, and FA.
4. C18 column (*see* **Note 5**).

2.2.3 Data Analysis

1. Microsoft Excel is useful but not essential as is statistical package such as Analyze-it (www.analyze-it.com), an add-in for Microsoft Excel.

2.3 SRM Mass Spectrometry to Determine Mitochondrial Purity

This approach requires ESI-QqQ MS with an online cap/nano HPLC.

2.3.1 Selection and Optimization of SRM Transitions

1. Set of previously published SRM assay with all necessary machine and peptide specific parameters or historical proteomics data/predicted SRM transitions [from a source such as the Arabidopsis Proteotypic Predictor (APP), http://www.plantenergy.uwa.edu.au/APP/] and the software package Skyline [93].

2. Crude plant protein extract, or subcellular protein extracts of the subcellular locations of interest for SRM assay optimization.
3. Acetone precipitated extracts as outlined in Subheading 3.1.1.
4. Resuspension solution: 8 M urea, 50 mM NH_4HCO_3, 5 mM DTT, pH 8.0.
5. Vortex.
6. IAA stock solution: 100 mM IAA.
7. Dilution buffer: 50 mM NH_4HCO_3, pH 8.0.
8. Digestion solution: 1 μg/μL trypsin in 1 mM $CaCl_2$.
9. FA.
10. C18 spin columns (such as Pierce C18 spin columns, Thermo Scientific) or C18 embedded tips (such as ZipTips, Merck Millipore).
11. Charging and elution solution: 70 % (v/v) ACN, 0.1 % (v/v) FA (LCMS grade).
12. Equilibration and washing solution: 2 % (v/v) ACN, 0.1 % (v/v) FA (LCMS grade).
13. Vacuum centrifuge.
14. ESI-QqQ MS such as an Agilent Technologies 6490 or equivalent.
15. LCMS grade ACN, water and FA.
16. C18 column (*see* **Note 5**).

2.3.2 Determining the Abundance of Target Proteins

1. Optimized SRM assay list.
2. Acetone precipitated isolated mitochondrial protein extracts as outlined in Subheading 3.1.1.
3. Resuspension solution: 8 M urea, 50 mM NH_4HCO_3, 5 mM DTT, pH 8.0.
4. Vortex.
5. IAA stock solution: 100 mM IAA.
6. Dilution buffer: 50 mM NH_4HCO_3, pH 8.0.
7. Digestion solution: 1 μg/μL trypsin in 1 mM $CaCl_2$.
8. FA.
9. C18 spin columns (such as Pierce C18 spin columns, Thermo Scientific) or C18 embedded tips (such as ZipTips, Merck Millipore).
10. Charging and elution solution: 70 % (v/v) ACN, 0.1 % (v/v) FA (LCMS grade).
11. Equilibration and washing solution: 2 % (v/v) ACN, 0.1 % (v/v) FA (LCMS grade).
12. Vacuum centrifuge.

13. ESI-QqQ MS such as an Agilent Technologies 6490 or equivalent.
14. LCMS grade ACN, water and FA.
15. C18 column (*see* **Note 5**).

3 Methods

3.1 Differential In-Gel Electrophoresis (DIGE) of Purified Mitochondrial Proteins

2D-IEF-SDS-PAGE-DIGE can be used to compare the purity of mitochondrial fractions by identifying the proteins that differ in abundance between two samples that were prepared using different isolation procedures such as a highly enriched and less highly enriched sample. We have previously used 2D-IEF-SDS-PAGE-DIGE to show that free flow electrophoresis (FFE) purification of mitochondria results in lower abundance of proteins from contaminating organelles (Fig. 1) [19, 43]. Compared to other methods of assessing mitochondrial purity such as Western blot, the main advantage of 2D-SDS-PAGE-DIGE is that a far higher number of proteins can be quantified in a single experiment (Fig. 1).

3.1.1 Mitochondrial Precipitation and Resuspension

1. Purified mitochondria (50 μg) are acetone precipitated by adding 9× the sample volume of cold acetone and placing them at −20 °C overnight or at −80 °C for 2 h. This step removes salts, lipids, chlorophyll and cellular components that could potentially interfere with CyDye labeling, the IEF step and downstream mass spectrometry.
2. The precipitated sample is spun at 20,000 × *g* for 15 min at 4 °C. The resulting supernatant is discarded and the pellets dried at room temperature for 15 min. The pellets (mitochondria proteins) are then resuspended in 10 μL of lysis-buffer 1 at a protein concentration ~5 μg/μL (*see* **Note 6**).
3. The resuspended samples are spun at 20,000 × *g* for 10 min at 4 °C to remove any insoluble material. Transfer the supernatant to a new tube.

3.1.2 CyDye Labeling

When running a DIGE gel, it is recommended to prepare three samples: the two samples undergoing direct comparison are labeled with either Cy3 or Cy5, while a pooled mixture of all the samples in the experiment (internal standard) is labeled with Cy2. When running multiple biological replicates of the same sample, it is important that dye allocation is swapped between replicates. Routinely we use minimal labeling, where CyDyes bind to ~1–2 % of all arginine or lysine residues in sample. Samples are incubated with the appropriate label on ice for 30 min, and the excess dye is then quenched by the addition of 1 mM lysine chloride (*see* **Note 7**).

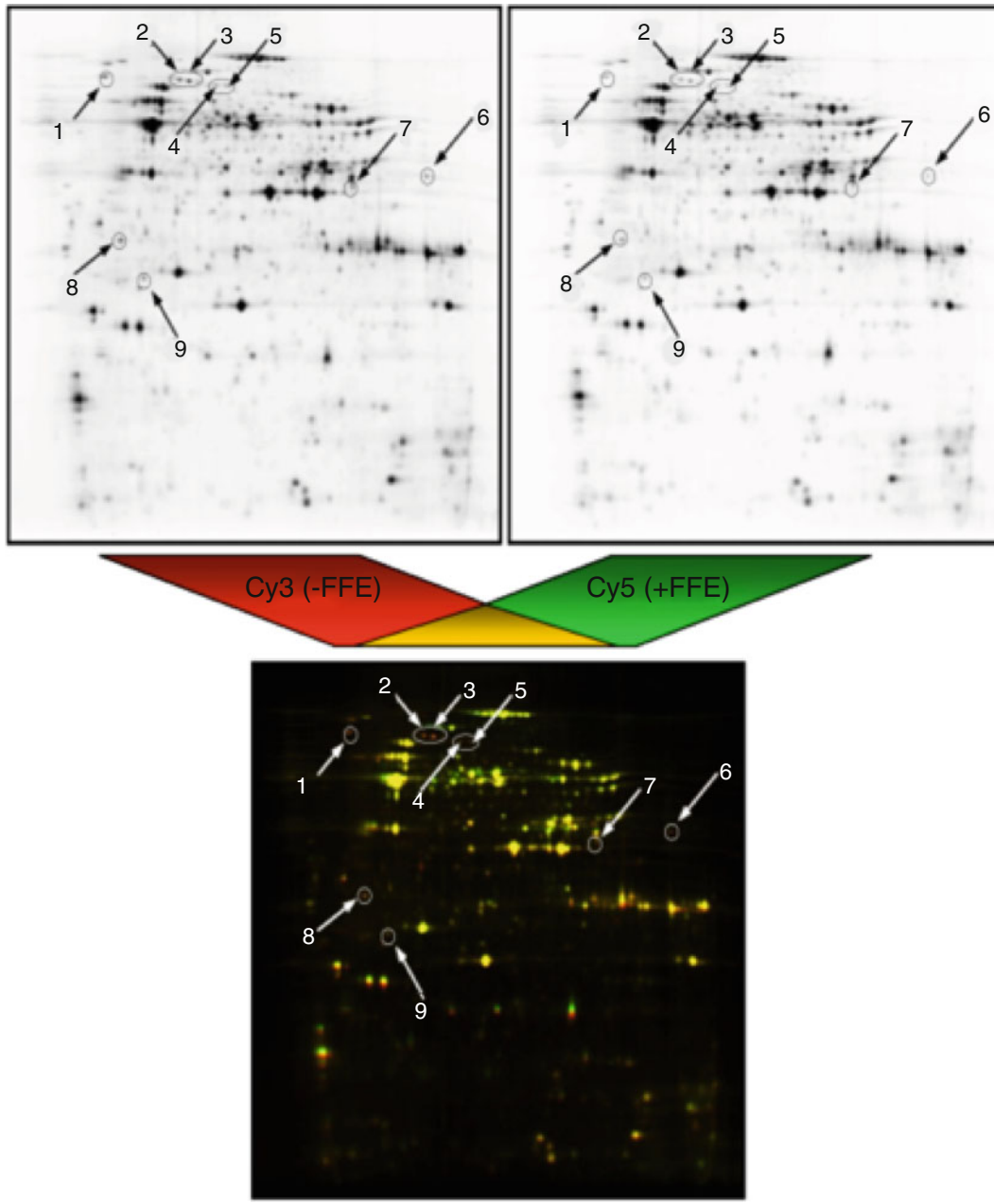

Fig. 1 Example of 2D-IEF-SDS-PAGE-DIGE of isolated rice mitochondria before and after free flow electrophoresis (FFE) purification to determine degree of contamination [43] Copyright American Society of Plant Biologists (www.plantphysiol.org). Samples before FFE treatment (–FFE; labeled with Cy3, shown in *red*) and after FFE treatment (+FFE; labeled with Cy5, shown in *green*) were compared. The *top panels* are gel images of each fluorescence signal, and the *bottom panel* is a combined fluorescence image electronically overlaid using ImageQuant TL software (GE Healthcare Life Sciences). *Yellow spots* represent proteins of equal abundance before and after FFE purification. Spots that are more abundant in samples before FFE purification are red, and those more abundant in samples after FFE purification are green. The *numbered arrows* indicate proteins with statistically significantly decreased abundance after FFE purification ($n=3$, $p>0.05$), which were chloroplastic or peroxisomal proteins when identified by mass spectrometry

1. Dilute CyDyes to 400 pM in water free DMF.
2. Add 1 μL of the diluted CyDye solution to each of the three samples and vortex and spin down. Incubate on ice and in the dark for 30 min.
3. Add 1 μL of a freshly prepared 10 mM lysine solution to each sample to stop the labeling reaction. Vortex and spin down. Incubate on ice for 10 min.
4. Add 12 μL of lysis-buffer. Vortex and spin down.

3.1.3 Isoelectric Focusing (IEF)

Samples are pooled and diluted in rehydration buffer, which contains ampholytes to enable IEF (*see* **Note 8**). The IEF parameters are based on the use of an Ettan IPGphor 3 electrophoresis unit and Immobiline DryStrips 3-10NL 240 mm (GE Heathcare Life Sciences).

1. Pool the different samples you want to compare. Add rehydration buffer to yield a final volume suitable for the IPG strips you intend to use (450 μL for 240-mm strips). Vortex and spin at 20,000 × *g* for 20 min. Transfer the supernatant to a new tube, discarding insoluble pellet.
2. Distribute the sample evenly with the well of the ceramic strip holder and cover with an IPG strip with "gel-side" facing downwards. Completely cover the strip with 1 mL of IPG cover fluid, and place the lid onto the ceramic strip holder.
3. Place the ceramic strip holder on the IPGphor system aligned in the direction indicated by anode and cathode regions. Run the IEF parameters for 24 h run as the following: 30 V for 12 h (step), 500 V for 1 h (step), 1,000 V for 2 h (gradient), 8,000 V for 2 h (gradient), 8,000 V for 6 h (step).

3.1.4 Transferring and Setting IEF Strips onto SDS-PAGE

This step involves reducing and alkylating the strip-bound proteins, and transferring the IPG strip onto a preprepared 12 % (w/v) acrylamide gel without a stacking gel encased in low-fluorescent glass plates (*see* **Note 9**).

1. Incubate the IPG strip in equilibration buffer containing 65 mM DTT for 15 min in the dark with gentle rocking (*see* **Note 10**).
2. Incubate the IPG strip in equilibration buffer containing 135 mM IAA for 15 min in the dark with gentle rocking (*see* **Note 10**).
3. Rinse the strip for 5–10 s in 1.5 M Tris–HCl pH 8.8 containing 1 % (w/v) SDS.
4. Place the strip on the top of a 12 % (w/v) acrylamide gel, then add about 5 mL of warm IEF fixing solution to secure the strip (*see* **Note 11**).
5. Once the IPG fixing solution has solidified, assemble the gel apparatus and run the gels (*see* **Notes 12** and **13**).

3.1.5 Gel Scanning and Software Analysis

Once the SDS-PAGE step is completed, the different proteomes under comparison are visualized by scanning the gel at three wavelengths (633, 532, and 488 nm) with a fluorescent scanner according to the manufacturer's instructions. The generated files are analyzed by commercial software packages such as DeCyder 2D Software (GE Healthcare Life Sciences) or Delta 2D Software (DECODON). Generally the literature [22, 43, 66, 94] considers a protein spot to differ significantly between the two samples if the abundance differs by greater than 1.5-fold with a p-value of less than 0.05 following the Student's *t*-test.

3.1.6 Determination of Proteins Abundance on 2D-IEF-SDS-PAGE-DIGE

The DIGE analysis reveals which protein spots display differing abundance, but peptide mass spectrometry is required to identify these proteins. As CyDye-labeled proteins cannot be seen with the naked eye and DIGE gels are relatively low abundance, it is advantageous to use preparative gels for mass spectrometry identification (*see* **Note 14**).

1. Match the spots of interest carefully from the DIGE gel with its corresponding spot on the preparative gel, excise the spots, and place them into the wells of the 96-well plate.
2. To each well add 50 µL of destain solution to each excised gel plug and cover the 96-well plate and shake on orbital rocker at 700 rpm for 30–45 min.
3. Remove destain solution and discard, add another 50 µL of destaining solution. Cover the 96-well plate and shake on orbital rocker at 700 rpm for 30–45 min.
4. Remove destain solution and discard. Dry gel pieces at 50 °C for 20 min with the lid open (*see* **Note 15**).
5. Add 15 µL of digestion solution to each dried gel spot (visually check to ensure each gel spot is immersed in solution). Cover and incubate at 37 °C for 12–16 h for digestion.
6. Add 10–15 µL 100 % (v/v) ACN to each well and cover and shake on orbital rocker at 750 rpm for 15 min.
7. Take supernatant from each sample and place into a new 96-well plate.
8. Add 10–15 µL of extraction solution to gel pieces. Cover and shake on orbital rocker at 750 rpm for 15 min.
9. Take supernatant from each sample and place into the same well of the 96-well plate from step 7 above.
10. Repeat **steps 4–5**.
11. Dry down samples in new plates in a vacuum centrifuge.

3.1.7 Determination of Proteins Abundance on 2D-SDS-PAGE-DIGE

The identification of proteins that differ in abundance following the isolation of mitochondria by two differing isolation techniques allows us to determine the degree of contamination from a number

of likely sources including other organelles or cellular compartments. Recently, we showed that the top six sources of contaminating protein of mitochondria following two-density gradient isolation were the chloroplast (45 % of contaminating proteins), the plasma membrane (35 % of contaminating proteins), the cytoplasm (12 % of contaminating proteins), the vacuole (5 % of contaminating proteins), extracellular proteins (2 % of contaminating proteins), and the peroxisome (1 % of contaminating proteins) [33]. Although protein tandem mass spectrometry is a highly variable process depending on both the type of ionization and configuration of mass spectrometry used, we have outlined a general procedure for both MALDI-MS/MS and ESI-MS/MS to the point of sample ionization following which machine specific parameters/knowledge is required for each hardware setup.

3.1.8 Protein Identification on 2D-IEF-SDS-PAGE-DIGE by MALDI-MS/MS

Peptide samples derived from trypsin digestion of excised gel spots to be analyzed by MALDI-MS/MS are "spotted" onto a MALDI plate with an appropriate matrix using a dried droplet method.

1. Appropriate machine specific calibration standards should always be spotted close to the samples being analyzed.
2. The extracted peptides are resuspended in 1–2 μL 5 % (v/v) ACN, 0.1 % (v/v) TFA.
3. Pipette 1–2 μL of resuspended peptides on the MALDI plate and let dry until the volume has reduced by ~50 %.
4. To this add 1–2 μL of matrix solution on the sample and mix (*see* **Note 16**).
5. Let the spot dry.
6. The sample plate is then placed in the mass spectrometer and MS and MS/MS spectra obtained.
7. The resulting MS and MS/MS spectra can then be interpreted by standard proteomics approaches using software packages such as Mascot (Matrix Sciences), Seaquest (Thermo Scientific), or X!tandem (www.thegpm.org/tandem/).

3.1.9 Protein Identification on 2D-IEF-SDS-PAGE-DIGE by ESI-MS/MS

Peptide samples derived from trypsin digestion of excised gel spots to be analyzed by ESI-MS/MS require fractionation to allow separation of the various peptides in time to allow identification. This is crucial to allow the assessment of peptide abundance (MS mode), selection of a precursor peptide (MS mode), its fragmentation and detection of fragment ions (MS/MS mode). If peptides are not fractionated then the duty cycle of the mass spectrometry would not allow the identification of sufficient peptides to confirm identification. This fractionation is typically achieved by capillary- or nano-flow reverse phase (RP)-HPLC using a C18 column (*see* **Note 5**).

1. The extracted peptides are resuspended in 10 μL 5 % (v/v) ACN, 0.1 % (v/v) FA.

2. The resuspended sample is loaded into the HPLC flow (5 % (v/v) ACN, 0.1 % (v/v) FA) prior to the in line C18 column by direct injection by use of a HPLC sampler (*see* **Note 17**).
3. Once the sample has bound the C18 column a gradient of 5 % (v/v) ACN, 0.1 % (v/v) FA to 60 % (v/v) ACN, 0.1 % (v/v) FA is run to sequentially elute bound peptides directly into the mass spectrometer and MS and MS/MS spectra collected.
4. The resulting MS and MS/MS spectra can then be interpreted by standard proteomics approaches using software packages such as Mascot (Matrix Sciences), Seaquest (Thermo Scientific), or X!tandem (www.thegpm.org/tandem/).
5. The column is then washed briefly at 80 % (v/v) ACN, 0.1 % (v/v) FA and re-equilibrated with 5 % (v/v) ACN, 0.1 % (v/v) FA prior to the next sample.

3.2 Gel Free Peptide Fractionation to Determine Mitochondrial Purity

Increasingly peptide level separations of digested protein extracts are becoming the preferred means of sample fractionation in proteomics. These approaches are higher throughput, overcome many of the physiochemical biases inherent in gel based approaches, and typically identify many more proteins including lower abundance proteins that are not stained on gels. However, they lack visual representation of the sample achieved by gel separation and the knowledge gained of a protein's molecular mass (Mr) and isoelectric point (pl), which can add an additional level of confidence to the protein identifications obtained. Gel free techniques can also be used to determine the mitochondrial or non-mitochondrial origin of a protein, by harnessing the high throughput capability of direct RP-HPLC-ESI-MS/MS. To do this, we produce triplicate samples of low quality, mid quality and high quality mitochondrial isolations. Typically, these have been collected pre gradients (for low quality), post gradients and washes (for medium quality) and following FFE (for high quality) [19, 29, 35]. These samples are then quantitatively analyzed to determine quantitative enrichment (QE) of mitochondrial proteins and quantitative depletion (QD) of non-mitochondrial proteins in the increasingly purified mitochondrial samples (low → medium → high). Using this approach, proteins seen to increase in abundance when analyzing our increasingly pure mitochondria sample are more likely of mitochondrial origin and proteins seen to decrease in abundance are more likely to be contaminants. Here we outline methods for determining the mitochondrial origin of proteins using a quantitative enrichment/depletion (QED) approach.

3.2.1 Sample Preparation

Tryptic digestion and peptide mass spectrometry can be impaired by the presence of salts, lipids, cellular components, and particularly charged species. To remove these mitochondrial proteins are acetone precipitated as outlined in Subheading 3.1.1.

1. Following precipitation, add resuspension buffer to the dried pellets (1 μL per 10 μg of mitochondrial protein) and incubate at room temperature for 45–60 min with occasional vortexing.
2. Once the sample is in solution, add IAA to 10 mM and incubate in the dark for 30 min.
3. Dilute the sample to 1 M urea with dilution buffer.
4. Add digestion solution, incubate at 37 °C for 12–16 h.
5. The high concentrations of urea, DTT, IAA and NH_4HCO_3 in the sample are incompatible with ionization/mass spectrometry. These are removed by a reverse phase-solid phase extraction (RP-SPE) step using C18 spin columns or C18 embedded pipette tips.
6. To the sample add 2.5 μL of FA to the sample.
7. Charge the C18 column (or tip) by loading with 750 μL (10 μL, pipette once) of 70 % (v/v) ACN, 0.1 % (v/v) FA and spinning at 150 × *g* for 2 min, discard the flow-through.
8. Equilibrate the C18 column by loading with 750 μL (10 μL, pipette twice) of 2 % ACN (v/v), 0.1 % (v/v) FA and spinning at 150 × *g* for 3 min, discard the flow-through.
9. Load the C18 column (or tip, pipette ten times from well) with sample, and spin at for 3 min, discard the flow-through.
10. Wash the sample by loading the C18 column with 400 μL (10 μL, pipette once) of 2 % (v/v) ACN, 0.1 % (v/v) FA and spinning at 150 × *g* for 3 min, discard the flow-through.
11. Repeat previous step.
12. Elute your sample by loading the C18 column with 750 μL (2–10 μL, pipette ten times into well) of 70 % (v/v) ACN, 0.1 % (v/v) FA and spinning at 150 × *g* for 2 min, retain the flow-through.
13. Repeat previous step, and pool the two flow-throughs together.
14. Dry down sample in vacuum centrifuge.

3.2.2 Sample Fractionation and Mass Spectrometry

Complex peptide mixtures such as those derived from trypsin digestion of whole mitochondria can simply be fractionated and analyzed by RP-HPLC-ESI-MS/MS; however, to increase the number of proteins identified from the sample other fractionation techniques can be implemented prior to the RP. Common approaches are Strong Cation Exchange (SCX) where peptides are fractionated by their net surface charge, High pH Reverse Phase (HpHRP) where peptides are fractionated differently than in normal low pH reverse phase and Off Gel Electrophoresis (OGE) where peptides are fractionated by their total net charge. Protocols for these approaches will not be covered in this review, but these techniques generate many fractions for, and are directly amenable to, subsequent RP-HPLC-ESI-MS/MS.

1. The extracted peptides are resuspended in 2 μL 5 % (v/v) ACN, 0.1 % (v/v) FA.
2. The resuspended sample is loaded into the HPLC flow (5 % (v/v) ACN, 0.1 % (v/v) FA) prior to the in line C18 column by direct injection by use of a HPLC sampler (*see* **Note 18**).
3. Once the sample has bound the C18 column a gradient of 5 % (v/v) ACN, 0.1 % (v/v) FA to 60 % (v/v) ACN, 0.1 % (v/v) FA is run to sequentially elute bound peptides directly into the mass spectrometer and MS and MS/MS spectra collected.
4. The resulting MS and MS/MS spectra can then be interpreted by standard proteomics approaches using software packages such as Mascot (Matrix Sciences), Seaquest (Thermo Scientific), or X!tandem (www.thegpm.org/tandem/).
5. The column is then washed briefly at 80 % (v/v) ACN, 0.1 % (v/v) FA and re-equilibrated with 5 % (v/v) ACN, 0.1 % (v/v) FA prior to the next sample.

3.2.3 Data Analysis

To determine the mitochondrial or non-mitochondrial origin of a protein we use a quantitative measure of protein abundance across the differentially enriched mitochondria isolations. In its simplest form this involves spectral counting, in which the number of peptides identified for a given protein is used as a measure of its abundance. For example, if for a particular protein 6 peptides were matched in the low purity sample, 9 in the medium purity sample and 12 in the high purity sample, then this protein would be confirmed as a mitochondrial protein. As the number of peptides identified for this protein increases in abundance with increasing mitochondrial purity we can confirm its mitochondrial origin. A further extension of this method is a statistical analysis of the changes observed for a particular protein. To do this using standard statistical tests such as the Student's *t*-test, a number of statistical assumptions must be met. To meet these Zybailov et al. [95] developed the Normalized Spectral Abundance Factor (NSAF), which includes a parameter that also compensates for variations in different proteins lengths. They showed that the natural log of each NSAF results in a Gaussian distribution of a dataset, permitting analysis using the Student's *t*-tests. However, it becomes essential to avoid ln(0), and thus, zero spectral counts need to be replaced by a fractional value empirically derived for each data set analyzed. The aim is to find the smallest value that maintains a normal distribution of the ln(NSAF) data [95] and replace all zero values with this fractional value. Once these statistical parameters are implemented it becomes possible to determine the statistical significance of a particular protein enrichment/depletion, confirming or refuting its mitochondrial origin. However, in some cases, difficulties with abundant mitochondrial can occur where all possible peptides for a protein are found in all three samples and thus no enrichment is

observed; fortunately in most cases we have encountered proteins that are generally well known mitochondrial proteins that have had their subcellular localization previously confirmed by other techniques.

3.3 SRM Mass Spectrometry to Determine Mitochondrial Purity

The most recently emerged technique in plant mitochondrial proteomics is the development of targeted SRM mass spectrometry. As with the quantitative techniques discussed above, this approach can be used to quantify proteins in control versus treatment studies and it can also be used to determine the quality of subcellular isolations. This approach was first used by Ito et al. [89] to assess the level of contamination in a cytosolic extract to determine the cytosolic proteome and was justified by comparison to traditional Western blotting of marker proteins from various subcellular compartments. With the increasing acceptance of protein SRM mass spectrometry as a sensitive and reliable approach of protein quantitation and suggestions it will eventually replace Western blotting [96], it seems likely it will be increasingly used to determine mitochondrial purity in proteomics experiments.

3.3.1 Selection and Optimization of SRM Transitions

The first step of any targeted SRM mass spectrometry experiment is to determine the proteins you wish to target, in some respects this is similar in concept to selecting marker enzymes or marker proteins to be probed with antibodies. We have previously shown that mitochondria isolated using a two-density gradient isolation are contaminated with chloroplast (45 % of contaminating proteins), plasma membrane (35 % of contaminating proteins), cytoplasmic (12 % of contaminating proteins), vacuolar (5 % of contaminating proteins), extracellular proteins (2 % of contaminating proteins), and peroxisome (1 % of contaminating proteins) proteins [33]. So it seems sensible to include highly abundant proteins from all these compartments when attempting to assess the level of contamination of a mitochondrial preparation. An overview of the workflow for an SRM experiment to determine the level of contamination is presented in Fig. 2.

1. The starting point for developing SRM assays is the selection of proteins to be quantified and determining what previous mass spectrometry information is available. The simplest approach (labeled A, Fig. 2) is to use previously optimized SRM assays from published work such as those assembled in Table 1. In this table, SRM assays developed in Arabidopsis from four studies are collated that represent proteins from the cytoplasm, mitochondria, nucleus, peroxisome, plasmid membrane, and plastid (*see* **Note 19**). Further information required for the implementation of these assays on a QqQ-MS, including collision energy, qualifiers ions or retention times can be found in the individual references. If previously published SRM assay are unavailable for the protein(s) of interest then previously collected historical mass spectral information from discovery proteomics studies

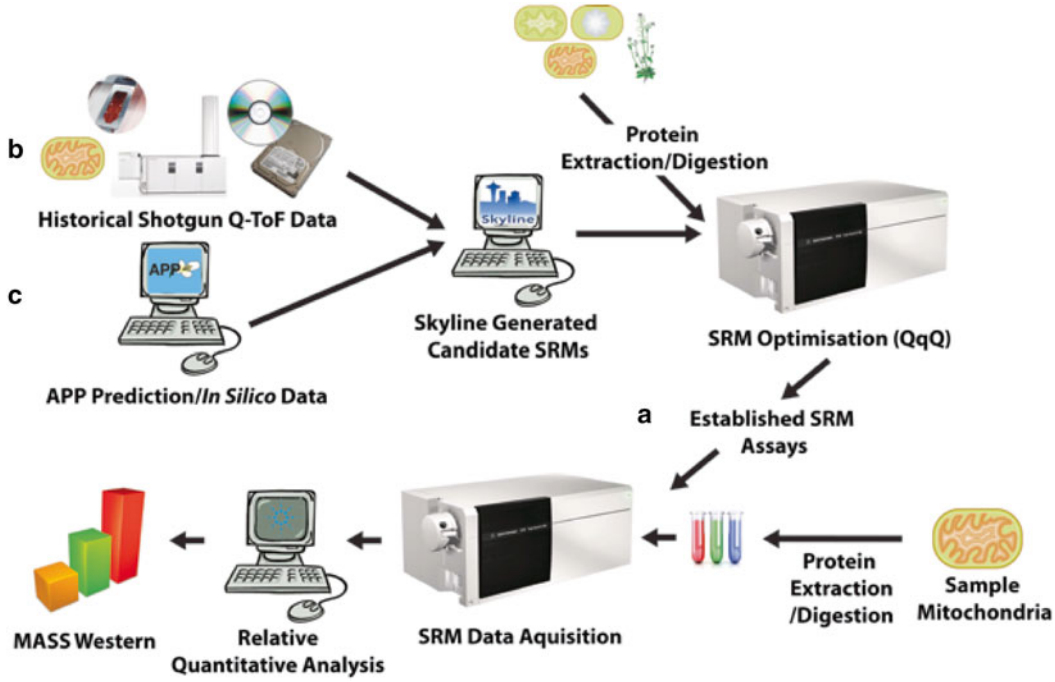

Fig. 2 SRM mass spectrometry workflow. Three potential start points are highlighted in *red* (A, B, and C) depending on the amount of previously available information about the proteins of interest

can be used to generate candidate SRM assays using the Skyline software package (labeled B, Fig. 2) [93]. These candidate SRM assays are then tested and optimized using a QqQ-MS, the Skyline predicted peptide specific parameters and a crude plant protein extract, or subcellular protein extracts of the subcellular locations of interest. Similarly, if no previously available mass spectrometry data exists for the protein(s) of interest then Arabidopsis candidate SRM peptides can be predicted from using the Arabidopsis Proteotypic Predictor, http://www.plantenergy.uwa.edu.au/APP/ (labeled C, Fig. 2). As with historical mass spectral information, these candidates are then tested and optimized using a QqQ-MS, the Skyline predicted values and crude protein extracts.

2. Proteins extracts should be prepared as in Subheading 3.2.1.
3. The extracted peptides are resuspended in 2 μL 5 % (v/v) ACN, 0.1 % (v/v) FA.
4. The resuspended sample is loaded into the HPLC flow (5 % (v/v) ACN, 0.1 % (v/v) FA) prior to the in line C18 column by direct injection by use of a HPLC sampler (*see* **Note 18**).
5. Once the sample has bound the C18 column a gradient of 5 % (v/v) ACN, 0.1 % (v/v) FA to 60 % (v/v) ACN, 0.1 % (v/v) FA is run to sequentially elute bound peptides directly into the

Table 1
Quantifier ions used for SRM assays of Arabidopsis proteins from a range of subcellular locations

Location	AGI	Protein	Peptide sequence	Precursor charge (*z*)	Precursor ion (*m/z*)	Product ion (*m/z*)	Ref.
Cytoplasm	AT1G56070.1	LOS1	IMGPNYIPGEK	2	609.8	430.2	[89]
Cytoplasm	AT3G04120.1 AT1G13440.1	GAPC	GILGYTEDDVVSTDFVGDNR	2	1,086.5	461.2	[89]
Mitochondria	AT5G08670.1 AT5G08680.1 AT5G08689.1	ATP-B	DAPALVDLATGQEILATGIK	2	998.6	1,029.5	[89]
Mitochondria	AT5G08670.1 AT5G08680.1 AT5G08689.1	ATP-B	VLNTGAPITVPVGR	2	697.3	838.7	[89]
Mitochondria	At1g53240.1	MDH1	SEVVGYMGDDNLAK	2	749.4	749.4	[90]
Mitochondria	At1g53240.1	MDH1	EGLEALKPELK	2	409.6	409.6	[90]
Mitochondria	At1g53240.1	MDH1	VAILGAAGGIGQPLALLMK	2	897	897	[90]
Mitochondria	At2g05710.1	ACO1	VVNFSFDGQPAELK	2	775.9	557.3	[90]
Mitochondria	At2g05710.1	ACO1	SSGEDTIILAGAEYGSGSSR	2	979	970.4	[90]
Mitochondria	At2g05710.1	ACO1	LSVFDAAMR	3	505.3	710.3	[90]
Mitochondria	AT5G66760.1	SDH1-1	TIAWLDR	2	437.7	660.3	[88]
Mitochondria	AT5G66760.1	SDH1-1	SSQTILATGGYGR	2	655.8	794.4	[88]
Mitochondria	AT5G23250.1	SCoAL	GGTEHLGLPVFNTVAEAK	2	614	879.5	[88]
Nucleus	AT1G07660.1 AT1G07820.1 AT2G28740.1 AT3G45930.1 AT3G46320.1 AT3G53730.1 AT5G59690.1 AT5G59970.1	HIS H4	ISGLIYEETR	2	590.8	697.5	[89]
Peroxisome	AT1G20630.1	CAT	EGNFDLVGNNFPVFFVR	2	986	764.5	[89]
Peroxisome	AT1G20630.1	CAT	GPILLEDYHLLEK	3	514	1,046.5	[89]
Plasma membrane	AT2G45960.1	PIP1;2	SLGAAIIFNK	2	517.3	634.4	[97]
Plasma membrane	AT3G53420.1	PIP2;1	DVEAVPGEGFQTR	2	702.8	891.4	[97]
Plastid	AT3G26650.1	GAPA	DSPLDIIAINDTGGVK	2	814.4	987.5	[89]

Location, subcellular location; AGI, Arabidopsis Gene Initiative identifier; Protein, protein abbreviation; Peptide sequence, amino acid sequence of selected peptide; Precursor charge (*z*), the charge of the peptide when detected by mass spectrometry; Precursor ion (*m/z*); the mass-to-charge ratio of the peptide when detected by mass spectrometry; Product ion (*m/z*); the mass-to-charge ratio of the product ion when detected by mass spectrometry following precursor fragmentation; Ref, publication of each peptide SRM assay

mass spectrometer and the various predicted settings methods for the selected peptides are run.

6. The resulting spectra are then interpreted to determine the optimal values for each individual SRM assay by using either Agilent Technologies Mass Hunter or Skyline software packages (*see* **Note 20**) to generate a list of optimized SRM assays.
7. The column is then washed briefly at 80 % (v/v) ACN, 0.1 % (v/v) FA and re-equilibrated with 5 % (v/v) ACN, 0.1 % (v/v) FA prior to the next sample.

3.3.2 Determining the Abundance of Target Proteins

Having tested and optimized each MRM assay for each protein of interest or using previously tested and optimized MRM assay from publications these values are then used to determine the abundance of a protein in a mitochondrial sample.

1. Mitochondrial extracts should be prepared as in Subheading 3.2.1.
2. The extracted peptides are resuspended in 2 μL 5 % (v/v) ACN, 0.1 % (v/v) FA.
3. The resuspended sample is loaded into the HPLC flow (5 % (v/v) ACN, 0.1 % (v/v) FA) prior to the in line C18 column by direct injection by use of a HPLC sampler (*see* **Note 18**).
4. Once the sample has bound the C18 column a gradient of 5 % (v/v) ACN, 0.1 % (v/v) FA to 60 % (v/v) ACN, 0.1 % (v/v) FA is run to sequentially elute bound peptides directly into the mass spectrometer and whilst the mass spectrometer detects the optimized SRM assays.
5. The column is then washed briefly at 80 % (v/v) ACN, 0.1 % (v/v) FA and re-equilibrated with 5 % (v/v) ACN, 0.1 % (v/v) FA prior to the next sample.
6. The resulting data is uploaded into either vendor specific analysis software or into the Skyline software package (http://proteome.gs.washington.edu/software/skyline/) and the abundance of each protein on interest can be quantified.
7. This can then be used to create a mass western of proteins from various organellar compartments as in Ito et al. [89].

4 Notes

1. Aliquots of lysis and rehydration buffers are stored indefinitely at −20 °C.
2. TFA should be prepared at the concentration of 10 % (v/v) and diluted to the required concentration before use.
3. Trypsin typically comes in aliquots of 25 μg that is resuspended in 250 μL of 0.01 % (v/v) TFA (100 μg/mL trypsin) and made up to final concentration 12.5 μg/mL and 10 mM NH_4HCO_3 using 200 mM NH_4HCO_3 and water.

4. Saturated CHCA matrix solution can be used for 7 days, all other solutions should be made immediately prior to use.
5. Many varieties of commercial columns with many variations in column architecture and stationary phases exist for proteomic analysis, we typically use homemade Microsorb C18 0.5 mm × 100 mm, 5 μm, 100 Å columns for short gradients and Agilent Technologies HPLC chips for longer gradients.
6. Full solubilization should occur in around 20 min using a pipette and vortex mixer to disrupt pellet. When using whole tissue extracts, the resuspension step can be notoriously problematic, but typically mitochondria proteins resuspend relative easily.
7. The time the CyDyes are exposed to light should be minimized, as the dyes are libel to bleaching.
8. Some proteins are insoluble in this buffer, so we have found that a centrifugation step prior to IEF removes insoluble proteins that cause vertical streaking on the final image.
9. Low-fluorescent glass plates are available from GE Healthcare Life Sciences or The Gel Company.
10. We use an orbital rocker set to ~150 rpm, ensuring that the "gel side" of the strip is facing upwards, to prevent bound proteins from rubbing against the base of the container.
11. We use a 0.75-mm thick spacer to press the strip against the top of the gel, and take care to minimize the number of air bubbles between the strip and the gel. It is important to heat the overlay solution to around 50 °C to melt the agarose, but do not overheat, as this might strip the proteins off the IEF strip.
12. We use the Ettan Dalt 6 system, and in our hands, a typical gel requires 270 mAh of electrophoresis. For convenience, we usually run this step overnight (i.e., 15 mA per gel for 18 h).
13. It is important to cover the entire gel apparatus with aluminum foil to minimize the exposure of CyDyes to light.
14. Preparative gels typically contain 500–1,000 μg of protein and are otherwise run identically to the DIGE gels. The resulting gels are stained with colloidal Coomassie blue for visualization.
15. Dried gel pieces are lightweight and can acquire static charge, take care to ensure that gel pieces do not "jump" out of wells.
16. Care must be taken to avoid introducing air bubbles and touching the MALDI plate with the pipette tip.
17. We typically run a 15-min gradient at 10 μL/min.
18. We typically run a 60-min gradient at 300 nL/min.
19. It should be noted that unless the peptide sequences chosen are conserved across species these SRM are Arabidopsis specific.
20. The exact parameters that need to be optimized vary between mass spectrometers, but an experienced user will be able to determine which are important.

Acknowledgements

This work is supported by the Australian Research Council Centre of Excellence in Plant Energy Biology and NLT and AHM as Australian Research Council Future Fellows.

References

1. Wilkins MR, Sanchez JC, Gooley AA et al (1996) Progress with proteome projects: why all proteins expressed by a genome should be identified and how to do it. Biotechnology Genet Eng Rev 13:19–50
2. Boutry M, Briquet M, Goffeau A (1983) The alpha subunit of a plant mitochondrial F1-ATPase is translated in mitochondria. J Biol Chem 258:8524–8526
3. AGI (2000) Analysis of the genome sequence of the flowering plant Arabidopsis thaliana. Nature 408:796–815
4. Kruft V, Eubel H, Jansch L et al (2001) Proteomic approach to identify novel mitochondrial proteins in Arabidopsis. Plant Physiol 127:1694–1710
5. Millar AH, Sweetlove LJ, Giege P et al (2001) Analysis of the Arabidopsis mitochondrial proteome. Plant Physiol 127:1711–1727
6. Bardel J, Louwagie M, Jaquinod M et al (2002) A survey of the plant mitochondrial proteome in relation to development. Proteomics 2:880–898
7. Sweetlove LJ, Heazlewood JL, Herald V et al (2002) The impact of oxidative stress on Arabidopsis mitochondria. Plant J 32:891–904
8. Werhahn W, Braun HP (2002) Biochemical dissection of the mitochondrial proteome from Arabidopsis thaliana by three-dimensional gel electrophoresis. Electrophoresis 23:640–646
9. Herald VL, Heazlewood JL, Day DA et al (2003) Proteomic identification of divalent metal cation binding proteins in plant mitochondria. FEBS Lett 537:96–100
10. Millar AH, Heazlewood JL (2003) Genomic and proteomic analysis of mitochondrial carrier proteins in Arabidopsis. Plant Physiol 131:443–453
11. Millar AH, Eubel H, Jansch L et al (2004) Mitochondrial cytochrome c oxidase and succinate dehydrogenase complexes contain plant specific subunits. Plant Mol Biol 56:77–90
12. Dunkley TP, Dupree P, Watson RB et al (2004) The use of isotope-coded affinity tags (ICAT) to study organelle proteomes in Arabidopsis thaliana. Biochem Soc Trans 32:520–523
13. Heazlewood JL, Tonti-Filippini JS, Gout AM et al (2004) Experimental analysis of the Arabidopsis mitochondrial proteome highlights signaling and regulatory components, provides assessment of targeting prediction programs, and indicates plant-specific mitochondrial proteins. Plant Cell 16:241–256
14. Brugiere S, Kowalski S, Ferro M et al (2004) The hydrophobic proteome of mitochondrial membranes from Arabidopsis cell suspensions. Phytochemistry 65:1693–1707
15. Peltier JB, Ripoll DR, Friso G et al (2004) Clp protease complexes from photosynthetic and non-photosynthetic plastids and mitochondria of plants, their predicted three-dimensional structures, and functional implications. J Biol Chem 279:4768–4781
16. Perales M, Eubel H, Heinemeyer J et al (2005) Disruption of a nuclear gene encoding a mitochondrial gamma carbonic anhydrase reduces complex I and supercomplex I+III2 levels and alters mitochondrial physiology in Arabidopsis. J Mol Biol 350:263–277
17. Koh S, Andre A, Edwards H et al (2005) Arabidopsis thaliana subcellular responses to compatible Erysiphe cichoracearum infections. Plant J 44:516–529
18. Ito J, Heazlewood JL, Millar AH (2006) Analysis of the soluble ATP-binding proteome of plant mitochondria identifies new proteins and nucleotide triphosphate interactions within the matrix. J Proteome Res 5:3459–3469
19. Eubel H, Lee CP, Kuo J et al (2007) Free-flow electrophoresis for purification of plant mitochondria by surface charge. Plant J 52:583–594
20. Winger AM, Taylor NL, Heazlewood JL et al (2007) Identification of intra- and intermolecular disulphide bonding in the plant mitochondrial proteome by diagonal gel electrophoresis. Proteomics 7:4158–4170
21. Livaja M, Palmieri MC, von Rad U et al (2008) The effect of the bacterial effector protein harpin on transcriptional profile and mitochondrial proteins of Arabidopsis thaliana. J Proteomics 71:148–159
22. Lee CP, Eubel H, O'Toole N et al (2008) Heterogeneity of the mitochondrial proteome for photosynthetic and non-photosynthetic Arabidopsis metabolism. Mol Cell Proteomics 7:1297–1316

23. Ito J, Taylor NL, Castleden I et al (2009) A survey of the Arabidopsis thaliana mitochondrial phosphoproteome. Proteomics 9:4229–4240
24. Taylor NL, Tan YF, Jacoby RP et al (2009) Abiotic environmental stress induced changes in the Arabidopsis thaliana chloroplast, mitochondria and peroxisome proteomes. J Proteomics 72:367–378
25. Klodmann J, Sunderhaus S, Nimtz M et al (2010) Internal architecture of mitochondrial complex I from Arabidopsis thaliana. Plant Cell 22:797–810
26. Lee CP, Eubel H, Millar AH (2010) Diurnal changes in mitochondrial function reveal daily optimisation of light and dark respiratory metabolism in Arabidopsis. Mol Cell Proteomics 9:2125–39
27. Tan YF, O'Toole N, Taylor NL et al (2010) Divalent metal ions in plant mitochondria and their role in interactions with proteins and oxidative stress-induced damage to respiratory function. Plant Physiol 152:747–761
28. Cui J, Liu J, Li Y et al (2011) Integrative identification of Arabidopsis mitochondrial proteome and its function exploitation through protein interaction network. PLoS One 6:e16022
29. Duncan O, Taylor NL, Carrie C et al (2011) Multiple lines of evidence localize signaling, morphology, and lipid biosynthesis machinery to the mitochondrial outer membrane of Arabidopsis. Plant Physiol 157:1093–1113
30. Klodmann J, Senkler M, Rode C et al (2011) Defining the protein complex proteome of plant mitochondria. Plant Physiol 157: 587–598
31. Lee CP, Eubel H, O'Toole N et al (2011) Combining proteomics of root and shoot mitochondria and transcript analysis to define constitutive and variable components in plant mitochondria. Phytochemistry 72:1092–1108
32. Skirycz A, Memmi S, De Bodt S et al (2011) A reciprocal 15N-labeling proteomic analysis of expanding Arabidopsis leaves subjected to osmotic stress indicates importance of mitochondria in preserving plastid functions. J Proteome Res 10:1018–1029
33. Taylor NL, Heazlewood JL, Millar AH (2011) The Arabidopsis thaliana 2-D gel mitochondrial proteome: refining the value of reference maps for assessing protein abundance, contaminants and post-translational modifications. Proteomics 11:1720–1733
34. Lee CP, Eubel H, Solheim C et al (2012) Mitochondrial proteome heterogeneity between tissues from the vegetative and reproductive stages of Arabidopsis thaliana development. J Proteome Res 11:3326–3343
35. Tan YF, Millar AH, Taylor NL (2012) Components of mitochondrial oxidative phosphorylation vary in abundance following exposure to cold and chemical stresses. J Proteome Res 11:3860–3879
36. Wang Y, Slabas AR, Chivasa S (2012) Proteomic analysis of dark response in Arabidopsis cell suspension cultures. J Plant Physiol 169:1690–1697
37. Lee CP, Taylor NL, Millar AH (2013) Recent advances in the composition and heterogeneity of the Arabidopsis mitochondrial proteome. Front Plant Sci 4:4
38. Heazlewood JL, Howell KA, Millar AH (2003) Mitochondrial complex I from Arabidopsis and rice: orthologs of mammalian and fungal components coupled with plant-specific subunits. Biochim Biophys Acta 1604:159–169
39. Millar AH, Trend AE, Heazlewood JL (2004) Changes in the mitochondrial proteome during the anoxia to air transition in rice focus around cytochrome-containing respiratory complexes. J Biol Chem 279:39471–39478
40. Tanaka N, Fujita M, Handa H et al (2004) Proteomics of the rice cell: systematic identification of the protein populations in subcellular compartments. Mol Genet Genomics 271:566–576
41. Kristensen BK, Askerlund P, Bykova NV et al (2004) Identification of oxidised proteins in the matrix of rice leaf mitochondria by immunoprecipitation and two-dimensional liquid chromatography-tandem mass spectrometry. Phytochemistry 65:1839–1851
42. Chen X, Wang Y, Li JY et al (2009) Mitochondrial proteome during salt stress-induced programmed cell death in rice. Plant Physiol Biochem 47:407–415
43. Huang S, Taylor NL, Narsai R et al (2009) Experimental analysis of the rice mitochondrial proteome, its biogenesis, and heterogeneity. Plant Physiol 149:719–734
44. Taylor NL, Howell KA, Heazlewood JL et al (2010) Analysis of the rice mitochondrial carrier family reveals anaerobic accumulation of a basic amino acid carrier involved in arginine metabolism during seed germination. Plant Physiol 154:691–704
45. Huang S, Shingaki-Wells RN, Taylor NL et al (2013) The rice mitochondria proteome and its response during development and to the environment. Front Plant Sci 4:16
46. Li CZ, Huang HQ, Yin FY et al (2008) The effect of Haynaldia villosa v chromosome on the mitochondrial proteome of wheat-H. villosa chromosome substitution line and translocation line. Fen Zi Xi Bao Sheng Wu Xue Bao 41:150–154

47. Jacoby RP, Millar AH, Taylor NL (2010) Wheat mitochondrial proteomes provide new links between antioxidant defense and plant salinity tolerance. J Proteome Res 9:6595–6604
48. Jacoby RP, Millar AH, Taylor NL (2013) Investigating the role of respiration in plant salinity tolerance by analyzing mitochondrial proteomes from wheat and a salinity-tolerant Amphiploid (wheat x Lophopyrum elongatum). J Proteome Res 12:4807–4829
49. Hochholdinger F, Guo L, Schnable PS (2004) Cytoplasmic regulation of the accumulation of nuclear-encoded proteins in the mitochondrial proteome of maize. Plant J 37:199–208
50. Dahal D, Mooney BP, Newton KJ (2012) Specific changes in total and mitochondrial proteomes are associated with higher levels of heterosis in maize hybrids. Plant J 72:70–83
51. Shahpiri A, Svensson B, Finnie C (2009) From proteomics to structural studies of cytosolic/mitochondrial-type thioredoxin systems in barley seeds. Mol Plant 2:378–389
52. Taylor NL, Heazlewood JL, Day DA et al (2005) Differential impact of environmental stresses on the pea mitochondrial proteome. Mol Cell Proteomics 4:1122–1133
53. Hoa L T-P, Nomura M, Kajiwara H et al (2004) Proteomic analysis on symbiotic differentiation of mitochondria in soybean nodules. Plant Cell Physiol 45:300–308
54. Yin G, Sun H, Xin X et al (2009) Mitochondrial damage in the soybean seed axis during imbibition at chilling temperatures. Plant Cell Physiol 50:1305–1318
55. Komatsu S, Yamamoto A, Nakamura T et al (2011) Comprehensive analysis of mitochondria in roots and hypocotyls of soybean under flooding stress using proteomics and metabolomics techniques. J Proteome Res 10:3993–4004
56. Dubinin J, Braun HP, Schmitz U et al (2011) The mitochondrial proteome of the model legume Medicago truncatula. Biochim Biophys Acta 1814:1658–1668
57. Matamoros MA, Fernandez-Garcia N, Wienkoop S et al (2013) Mitochondria are an early target of oxidative modifications in senescing legume nodules. New Phytol 197: 873–885
58. Salvato F, Havelund JF, Chen M et al (2013) The potato tuber mitochondrial proteome. Plant Physiol 164:637–653
59. Atteia A, Adrait A, Brugiere S et al (2009) A proteomic survey of Chlamydomonas reinhardtii mitochondria sheds new light on the metabolic plasticity of the organelle and on the nature of the alpha-proteobacterial mitochondrial ancestor. Mol Biol Evol 26:1533–1548
60. Kim DW, Rakwal R, Agrawal GK et al (2005) A hydroponic rice seedling culture model system for investigating proteome of salt stress in rice leaf. Electrophoresis 26:4521–4539
61. Ndimba BK, Chivasa S, Simon WJ et al (2005) Identification of Arabidopsis salt and osmotic stress responsive proteins using two-dimensional difference gel electrophoresis and mass spectrometry. Proteomics 5:4185–4196
62. Yan S, Tang Z, Su W et al (2005) Proteomic analysis of salt stress-responsive proteins in rice root. Proteomics 5:235–244
63. Dooki AD, Mayer-Posner FJ, Askari H et al (2006) Proteomic responses of rice young panicles to salinity. Proteomics 6:6498–6507
64. Chitteti BR, Peng Z (2007) Proteome and phosphoproteome differential expression under salinity stress in rice (Oryza sativa) roots. J Proteome Res 6:1718–1727
65. Jiang Y, Yang B, Harris NS et al (2007) Comparative proteomic analysis of NaCl stress-responsive proteins in Arabidopsis roots. J Exp Bot 58:3591–3607
66. Shingaki-Wells RN, Huang S, Taylor NL et al (2011) Differential molecular responses of rice and wheat coleoptiles to anoxia reveal novel metabolic adaptations in amino acid metabolism for tissue tolerance. Plant Physiol 156:1706–1724
67. Bae MS, Cho EJ, Choi EY et al (2003) Analysis of the Arabidopsis nuclear proteome and its response to cold stress. Plant J 36:652–663
68. Cui S, Huang F, Wang J et al (2005) A proteomic analysis of cold stress responses in rice seedlings. Proteomics 5:3162–3172
69. Goulas E, Schubert M, Kieselbach T et al (2006) The chloroplast lumen and stromal proteomes of Arabidopsis thaliana show differential sensitivity to short- and long-term exposure to low temperature. Plant J 47:720–734
70. Hashimoto M, Komatsu S (2007) Proteomic analysis of rice seedlings during cold stress. Proteomics 7:1293–1302
71. Yan SP, Zhang QY, Tang ZC et al (2006) Comparative proteomic analysis provides new insights into chilling stress responses in rice. Mol Cell Proteomics 5:484–496
72. Komatsu S, Yamada E, Furukawa K (2009) Cold stress changes the concanavalin A-positive glycosylation pattern of proteins expressed in the basal parts of rice leaf sheaths. Amino Acids 36:115–123
73. Lee DG, Ahsan N, Lee SH et al (2009) Chilling stress-induced proteomic changes in rice roots. J Plant Physiol 166:1–11
74. Heidarvand L, Maali-Amiri R (2013) Physio-biochemical and proteome analysis of chickpea

in early phases of cold stress. J Plant Physiol 170:459–469

75. Lee DG, Ahsan N, Lee SH et al (2007) A proteomic approach in analyzing heat-responsive proteins in rice leaves. Proteomics 7: 3369–3383
76. Palmblad M, Mills DJ, Bindschedler LV (2008) Heat-shock response in Arabidopsis thaliana explored by multiplexed quantitative proteomics using differential metabolic labeling. J Proteome Res 7:780–785
77. Ahsan N, Lee SH, Lee DG et al (2007) Physiological and protein profiles alternation of germinating rice seedlings exposed to acute cadmium toxicity. C R Biol 330:735–746
78. Sarry JE, Kuhn L, Ducruix C et al (2006) The early responses of Arabidopsis thaliana cells to cadmium exposure explored by protein and metabolite profiling analyses. Proteomics 6: 2180–2198
79. Lanquar V, Kuhn L, Lelievre F et al (2007) 15N-metabolic labeling for comparative plasma membrane proteomics in Arabidopsis cells. Proteomics 7:750–754
80. Adam Z, Rudella A, van Wijk KJ (2006) Recent advances in the study of Clp. FtsH and other proteases located in chloroplasts. Curr Opin Plant Biol 9:234–240
81. Huang S, Millar AH, Taylor NL (2011) In: Kempken F (ed) Advances in plant biology. vol 1. Springer, New York, NY, p 533
82. Hossain Z, Nouri MZ, Komatsu S (2012) Plant cell organelle proteomics in response to abiotic stress. J Proteome Res 11:37–48
83. Qin G, Wang Q, Liu J et al (2009) Proteomic analysis of changes in mitochondrial protein expression during fruit senescence. Proteomics 9:4241–4253
84. Jones AM, Thomas V, Bennett MH et al (2006) Modifications to the Arabidopsis defense proteome occur prior to significant transcriptional change in response to inoculation with Pseudomonas syringae. Plant Physiol 142:1603–1620
85. Havelund JF, Thelen JJ, Moller IM (2013) Biochemistry, proteomics, and phosphoproteomics of plant mitochondria from non-photosynthetic cells. Front Plant Sci 4:51
86. Lehmann U, Wienkoop S, Tschoep H et al (2008) If the antibody fails–a mass western approach. Plant J 55:1039–1046
87. Picotti P, Aebersold R (2012) Selected reaction monitoring-based proteomics: workflows, potential, pitfalls and future directions. Nat Methods 9:555–566
88. Huang S, Taylor NL, Stroher E et al (2013) Succinate dehydrogenase assembly factor 2 is needed for assembly and activity of mitochondrial complex II and for normal root elongation in Arabidopsis. Plant J 73:429–441
89. Ito J, Batth TS, Petzold CJ et al (2011) Analysis of the Arabidopsis cytosolic proteome highlights subcellular partitioning of central plant metabolism. J Proteome Res 10:1571–1582
90. Taylor NL, Fenske R, Castleden I et al (2014) Selected reaction monitoring (SRM) to determine protein abundance in Arabidopsis using the Arabidopsis proteotypic predictor (APP). Plant Physiol 164:525–536
91. Eubel H, Braun HP, Millar AH (2005) Blue-native PAGE in plants: a tool in analysis of protein-protein interactions. Plant Methods 1:11
92. Heinemeyer J, Scheibe B, Schmitz UK et al (2009) Blue native DIGE as a tool for comparative analyses of protein complexes. J Proteomics 72:539–544
93. MacLean B, Tomazela DM, Shulman N et al (2010) Skyline: an open source document editor for creating and analyzing targeted proteomics experiments. Bioinformatics 26: 966–968
94. Jacoby RP, Taylor NL, Millar AH (2011) The role of mitochondrial respiration in salinity tolerance. Trends Plant Sci 16:614–623
95. Zybailov B, Mosley AL, Sardiu ME et al (2006) Statistical analysis of membrane proteome expression changes in Saccharomyces cerevisiae. J Proteome Res 5:2339–2347
96. Aebersold R, Burlingame AL, Bradshaw RA (2013) Western blots versus selected reaction monitoring assays: time to turn the tables? Mol Cell Proteomics 12:2381–2382
97. Monneuse JM, Sugano M, Becue T et al (2011) Towards the profiling of the Arabidopsis thaliana plasma membrane transportome by targeted proteomics. Proteomics 11:1789–1797

Chapter 7

Identification of Lysine-Acetylated Mitochondrial Proteins and Their Acetylation Sites

Markus Hartl, Ann-Christine König, and Iris Finkemeier

Abstract

The $^{\varepsilon}$N-acetylation of lysine side chains is a highly conserved posttranslational modification of both prokaryotic and eukaryotic proteins. Lysine acetylation not only occurs on histones in the nucleus but also on many mitochondrial proteins in plants and animals. As the transfer of the acetyl group to lysine eliminates its positive charge, lysine acetylation can affect the biological function of proteins. This chapter describes two methods for the identification of lysine-acetylated proteins in plant mitochondria using an anti-acetyllysine antibody. We describe the Western blot analysis of a two-dimensional blue native-polyacrylamide gel electrophoresis with an anti-acetyllysine antibody as well as the immuno-enrichment of lysine-acetylated peptides followed by liquid chromatography-tandem mass spectrometry data acquisition and analysis.

Key words Lysine acetylation, Mitochondria, Arabidopsis, Protein complexes, Blue native-polyacrylamide gel electrophoresis (BN-PAGE)

1 Introduction

Plant mitochondria function in the fundamental energy metabolism and have additional unique properties when compared to their mammalian relatives. Besides oxidative phosphorylation that produces energy in the form of ATP, plant mitochondria also host enzymes for photorespiration as well as alternative electron complexes to limit oxidative stress in the cell. These metabolic pathways have to be tightly regulated and adjusted to the always changing environmental conditions plants are experiencing. Posttranslational modifications (PTMs) have the capability to regulate central metabolic pathways as well as to maintain the flexibility of the organellar metabolism [1]. One recently emerging PTM in prokaryotes and eukaryotes with predicted key regulatory function in metabolic pathways is the lysine acetylation of proteins [2–6]. Lysine acetylation was first investigated on histones where it affects chromatin structure and gene expression [7], but

James Whelan and Monika W. Murcha (eds.), *Plant Mitochondria: Methods and Protocols*, Methods in Molecular Biology, vol. 1305, DOI 10.1007/978-1-4939-2639-8_7,

lately it was also identified to occur on nonhistone proteins. However, lysine acetylation depends on the availability of acetyl-CoA, a central metabolite of several metabolic pathways, which indicates that information on the metabolic state of the cell could directly be sensed and transduced via lysine acetylation [8, 6]. Also in plants there is mounting evidence that lysine acetylation affects protein functions as well as enzyme activities [9–11]. Especially plant mitochondrial proteins show a high abundance of lysine-acetylated proteins [12] but due to the overall low abundance of mitochondria in the cell it is challenging to detect lysine-acetylated mitochondrial proteins in whole-cell extracts. Here, we present two methods to detect and analyze mitochondrial lysine-acetylated proteins with the help of an anti-acetyllysine antibody: (1) the detection of lysine-acetylated proteins in native mitochondrial protein complexes and (2) the identification of lysine-acetylated peptides and sites via immuno-enrichment of lysine-acetylated peptides followed by liquid chromatography-tandem mass spectrometry (LC-MS/MS) data acquisition and analysis.

The two-dimensional blue native-polyacrylamide gel electrophoresis (BN-PAGE) is a relevant method to determine protein complex compositions of supercomplexes and is especially useful for membrane-bound complexes lacking an internal charge [13]. To explore the extent of lysine acetylation in plant mitochondria, intact protein complexes from mitochondria are isolated and solubilization of membranes occurs with digitonin. Separation of protein complexes is carried out by BN-PAGE as explained in Klodmann et al. [14] and followed by Western blot analysis using the anti-acetyllysine antibody as well as Ponceau S stain after immunotransfer for quality control. The Ponceau S stain visualizes mitochondrial protein abundance (Fig. 1).

The BN-PAGE approach yields valuable information on the lysine acetylation state of proteins and protein complexes. However, it falls short of identifying the actual acetylation sites of particular proteins of interest, which is most relevant for understanding the functional or structural implications of a particular modification. Generating site-specific antibodies is costly, time consuming, and technically not always feasible. Thus, the identification of lysine acetylation sites using LC-MS/MS became a valuable alternative. The identification of lysine-acetylated protein peptides by LC-MS/MS is based on the detection of a 42.01 Da increase in peptide mass using high-resolution accurate mass LC-MS/MS [15–17]. In principle this technique allows the identification and to some extent also quantification of peptides at a proteome-wide scale. However, LC-MS/MS also has technical limitations, which mainly depend on the properties of a protein and the peptides generated from it. Thus, it is possible that certain lysine acetylation sites escape detection, for example due to inadequate peptide length or

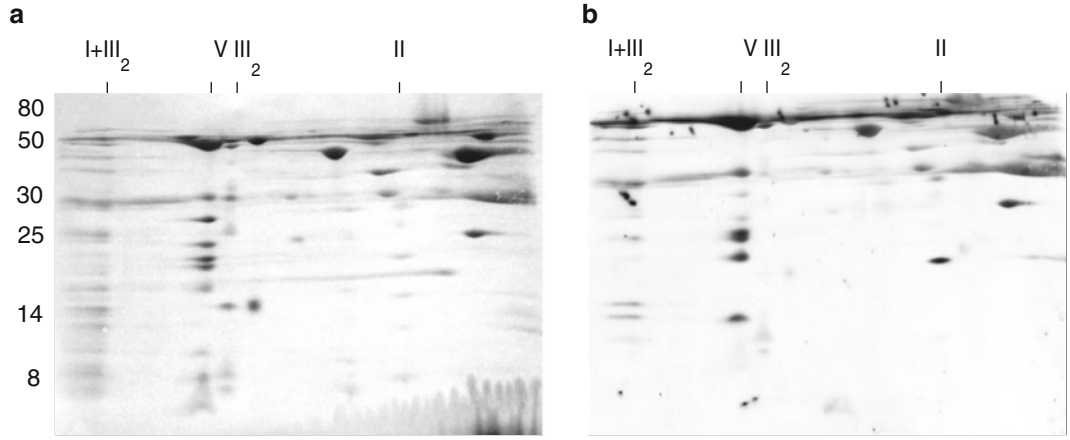

Fig. 1 Detection of lysine acetylation in mitochondrial protein complexes of Arabidopsis analyzed by 2D BN SDS-PAGE and Western blot. (**a**) Ponceau S stain of 2D BN/SDS-PAGE of mitochondrial protein complexes. The identity of oxidative phosphorylation (OXPHOS) complexes is indicated above the gels. $I + III_2$, supercomplex composed of Complex I and dimeric Complex III; I, Complex I; V, Complex V (ATP synthase); III_2, dimeric Complex III. The molecular mass scale (in kDa) is indicated on the left. (**b**) Lysine-acetylated proteins from Arabidopsis mitochondria detected by Western blot analysis using the anti-acetyllysine antibody

unfavorable physicochemical properties that prevent it from reaching the detector of the MS. Despite these limitations LC-MS/MS is currently the most powerful technique available to identify and quantify lysine-acetylated peptides.

Here we provide a procedure for sample preparation and enrichment for lysine-acetylated peptides from plant mitochondria (Fig. 2), which we previously applied successfully to identify 243 acetylated lysine sites on 120 mitochondrial proteins from Arabidopsis (*Arabidopsis thaliana*) [12]. We deliberately chose not to include a detailed protocol for LC-MS/MS, as this would require referring to a particular instrumental setup that would be of limited use to a wider community. However, as very similar results can be obtained with a range of LC-MS/MS setups from different vendors, we will provide basic measurement parameters that should enable users to develop a suitable protocol for the instruments at hand. For the same reason, we also do not include procedures for data analysis because these are in many cases platform dependent.

Our sample preparation procedure for the identification of lysine-acetylated peptides comprises two major steps: (1) Extensive solubilization and digestion of proteins: These are absolute prerequisites for deep proteome coverage. Given that many membrane proteins are essential for mitochondrial function and metabolism, their solubilization should be facilitated by the method applied. In this protocol we use a filter-assisted sample preparation (FASP),

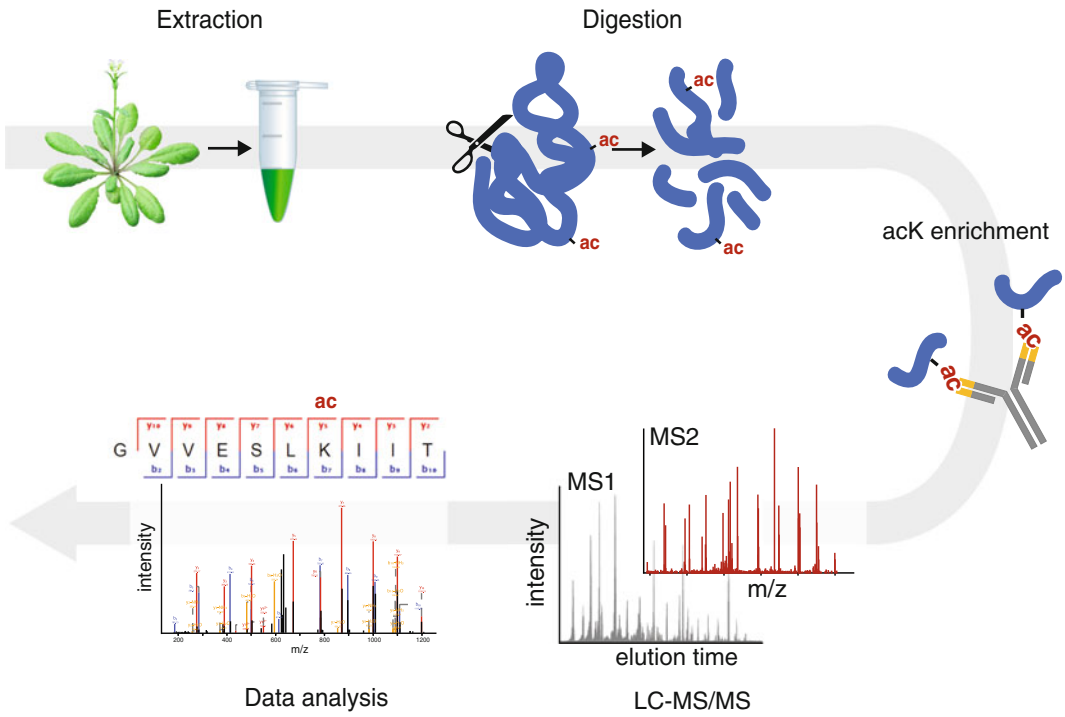

Fig. 2 Workflow for the identification of lysine-acetylated peptides using LC-MS/MS. After cell lysis, proteins are digested enzymatically and lysine-acetylated peptides are enriched using an anti-acetyllysine antibody. Enriched peptides are separated and measured using nano-LC-MS/MS; raw data are computationally processed to identify the peptides and acetylated lysines

which was originally described by Wisniewksi et al. [18], and which we slightly adapted for our purpose. It has the advantage of solubilizing proteins very well and of removing compounds interfering with LC-MS/MS, without the need of precipitating the protein. Nevertheless, other approaches might be similarly successful. (2) Enrichment of lysine-acetylated peptides: This step is absolutely necessary because the abundance of acetylated peptides can be rather low and thus their detection would be hampered by the bulk of non-acetylated peptides. So far, the only method available for enrichment of lysine-acetylated peptides uses an anti-acetyllysine antibody [2, 19, 15] and the protocol presented here largely follows this method.

We highly recommend desalting samples after the enrichment. We prefer using custom-made C18 StageTips, as described in detail by Rappsilber et al. [20], but other approaches are possible. As each mass spectrometry laboratory usually has its own preferred standard procedure for sample cleanup, we do not provide a protocol for this step.

2 Materials

2.1 Materials for BN-PAGE and Anti-acetyllysine Immunoblotting

For the first dimension of the BN-PAGE and for material for sample preparation *see* Chapter 8.

2.1.1 First-Dimension BN-PAGE

2.1.2 Components for Preparing the Gel Strip for Second Dimension

Denaturing solution: 1 % (w/v) sodium dodecyl sulfate (SDS), 1 % (v/v) β-mercaptoethanol.

2.1.3 Second-Dimension (Tricine-SDS-PAGE) Components

1. Tricine gel buffer: 3 M Tris–HCl pH 8.45, 0.3 % (w/v) SDS.
2. Acrylamide 40 % (w/v): Rotiphorese® Gel 40 (37.5:1) (Carl ROTH).
3. Anode buffer: 0.2 M Tris–HCl pH 8.9.
4. Cathode buffer: 0.1 M Tris–HCl, 0.1 M tricine, 0.1 % (w/v) SDS, pH 8.25.
5. Overlay solution: 1 M Tris–HCl pH 8.45, 0.1 % (w/v) SDS.
6. 87 % (v/v) and 100 % glycerol.
7. 6× Gel buffer BN: 1.5 M amino caproic acid, 150 mM BisTris, pH 7 (store at 4 °C).
8. SDS solution: 10 % (w/v) SDS.
9. *N*,*N*,*N*′,*N*′-tetramethylethylenediamine (TEMED).
10. Ammonium persulfate (APS): 10 % (w/v) solution in water.
11. 70 % (v/v) ethanol.
12. Hoefer SE600 Standard Dual Cooled Vertical Unit.

2.1.4 Western Blot Components

1. Nitrocellulose membrane.
2. Grade 3MM Chr Cellulose Chromatography Papers (GE Healthcare Life Science Whatman™).
3. Western blot transfer buffer: 0.048 M Tris–HCl, pH 8.3, 0.039 M glycine, 20 % (v/v) methanol.
4. Tris-buffered saline (TBS): 0.05 M Tris–HCl pH 7.5, 0.15 M NaCl.
5. TBS containing 0.05 % (v/v) Tween-20 (TBST).
6. Blocking solution: 2 % (w/v) gelatin from cold water fish skin (SIGMA) in TBS.
7. Plastic container.
8. Bag sealer (Severin, Folio FS 3602).
9. Plastic bags (Sekuroka®-disposal bags, ROTH).

10. Ponceau S staining solution: 0.1 % (w/v) Ponceau S in 5 % (v/v) acetic acid.
11. Orbital Shaker (ELMI Large Sky Line Digital DOS-10L/20L).
12. Scissors.
13. Anti-acetyllysine antibody (ImmuneChem Pharmaceuticals).
14. Anti-horseradish peroxidase antibody (Thermo Fisher Scientific).
15. SuperSignal West Dura enhanced chemiluminescent substrate (Thermo Fisher Scientific).
16. Fastblot Semi-Dry Electrophoretic Transfer Apparatus B44 (Biometra).
17. Fusion Imaging System (PEQLAB).

2.2 Materials for Digestion of Mitochondrial Proteins and Immuno-Enrichment of Lysine-Acetylated Peptides

2.2.1 Filter-Assisted Sample Preparation (FASP)

1. SDS-lysis buffer: 4 % (w/v) SDS, 0.1 M dithiothreitol (DTT) in 100 mM Tris–HCl pH 7.6.
2. Urea buffer: 8 M urea in 0.1 M Tris–HCl pH 8.5. Prepare 25 mL per sample (*see* **Note 1**).
3. Iodoacetamide (IAA) solution: 0.05 M IAA in urea buffer. Prepare 1 mL per sample (*see* **Note 1**).
4. Proteomics-grade trypsin (for example Trypsin Gold, Promega).
5. ABC buffer: 0.05 M NH_4HCO_3 in water. Prepare 20 mL per sample.
6. Buffer A: 0.05 % (v/v) formic acid in ultrapure water.
7. Buffer B: 80 % (v/v) acetonitrile (ACN) (HPLC grade), 0.05 % (v/v) formic acid (FA) in ultrapure water.
8. Methanol.
9. 10 % (v/v) Trifluoroacetic acid (TFA) in ultrapure water.
10. 660 nm protein assay with compatibility reagent (Pierce—Thermo Scientific).
11. Centrifugal filter device (CFD): Amicon Ultra-4 30k MWCO (Millipore) or similar.
12. Benchtop centrifuge for microfuge tubes.
13. Benchtop centrifuge, accommodating 15-mL conical bottomed tubes, ideally in a swinging-bucket rotor at a speed of 4,000 × *g*.
14. Heat block.
15. Microvolume UV–VIS photometer (for example NanoDrop 2000, Thermo Scientific).
16. Vacuum concentrator (for example Concentrator 5301, Eppendorf).
17. Sep-Pak C18 1 cm^3 cartridge, 100 mg sorbent per cartridge, 55–105 μm particle size (Waters).

2.2.2 Immuno-Enrichment of Lysine-Acetylated Peptides

1. 20 % (v/v) ACN (MS grade) in ultrapure water.
2. TBS: 50 mM Tris–HCl, 150 mM NaCl, pH 7.6, stored at 4 °C.
3. 1.5-mL Protein LoBind tubes (Eppendorf), and 1.5-mL microcentrifuge tubes.
4. Ultrapure water.
5. Acetyllysine antibody, immobilized to beaded agarose (ImmuneChem, ICP0388).
6. GELoader® tips (Eppendorf) or similar gel-loading pipette tips.
7. Rolling wheel at 4 °C.
8. Ice for cooling samples.
9. Universal pH indicator paper, pH 1–11.
10. Ultrasonic bath.

3 Methods

3.1 BN-PAGE and Anti-acetyllysine Immunoblotting

Run the first dimension of a BN-PAGE according to published procedures, such as that outlined in Chapter 8.

3.1.1 Transfer of Gel Strip of First Dimension onto Second Dimension

1. Cut out lane of interest from first dimension with a razor blade.
2. Incubate in denaturing solution for 30-min shaking (100 rpm) at room temperature (20–25 °C).
3. Wash gel strip in distilled water two times to avoid β-mercaptoethanol contamination.

3.1.2 Second Dimension (Tricine-SDS-PAGE)

Second dimension is carried out in a Hoefer SE600 Standard Dual Cooled Vertical Unit chamber or a comparable gel electrophoresis system. All procedures are performed at room temperature.

1. Wash glass plates of running chamber three times with 70 % (v/v) ethanol and then three times with distilled water.
2. Place strip of first dimension at the upper part of one glass plate where usually the comb is situated.
3. Place second glass plate exactly on top of the first plate using 0.7-mm spacers and assemble plates (*see* **Note 2**).
4. For the 16.5 % (w/v) tricine-SDS-PAGE, prepare resolving gel as well as spacer gel in parallel (Table 1). Shortly before pouring the gel add APS and TEMED.
5. For pouring the second dimension, first add resolving gel and then the spacer gel solution into the assembled glass plates and overlay it with overlay solution (*see* **Note 3**).

Table 1
Preparation of resolving gel and spacer gel for second dimension

	Resolving gel (30 mL)	Spacer gel (10 mL)
Acrylamide 40 % (w/v)	12.4 mL	2.5 mL
Tricine gel buffer	10 mL	3.4 mL
Glycerol 87 % (v/v)	4 mL	–
Distilled water	3.6 mL	4.1 mL
APS 10 % (w/v)	100 µL	34 µL
TEMED	10 µL	3.4 µL

Amount of solutions is calculated for two 16.5 % (w/v) tricine-SDS-PAGE gels

Table 2
Preparation of sample gel for second dimension

	Sample gel (10 mL)
Acrylamide 40 % (w/v)	2.5 mL
Gel buffer BN (6×)	3.4 mL
Glycerol 100 %	1 mL
SDS 10 % (w/v)	100 µL
Distilled water	2.9 mL
APS 10 % (w/v)	83 µL
TEMED	8.3 µL

Amount of solutions is calculated for two sample gels

6. The sample gel (Table 2) is prepared after polymerization of resolving and spacer gel. Shortly before pouring the gel add APS and TEMED.
7. Remove overlay solution; add sample gel until the upper edge of the gel strip and let the sample gel polymerize before transferring the glass plates into the running chamber (*see* **Note 4**).
8. Add the anode buffer and the cathode buffer to the lower and upper chamber of the gel unit.
9. Run the second dimension for 13 h with limit set to 30 mA and 500 V per 1-mm spacer width.

3.1.3 Western Blot

For Western blotting, the Fastblot Semi-Dry Electrophoretic Transfer Apparatus B44 (Biometra) has been used. All procedures were carried out at room temperature. For detection of the chemiluminescent substrate the Fusion Imaging System from PEQLAB was used.

1. Cut eight pieces of cellulose chromatography paper in the size of the gel of the second dimension as well as one piece of nitrocellulose membrane.
2. Soak four pieces of cellulose chromatography paper in Western blot transfer buffer and then transfer them onto the Fastblot.
3. Shortly incubate the nitrocellulose membrane in Western blot transfer buffer and place it on top of the cellulose chromatography papers.
4. Remove the gel from the second dimension carefully from the glass plates and discard the sample gel. Quickly incubate the gel in Western blot transfer buffer and place it on top of the nitrocellulose membrane.
5. Add another four layers of cellulose chromatography papers soaked in Western blot transfer buffer on top of the gel (*see* **Note 5**).
6. Assemble the blotting system. Transfer of proteins onto the nitrocellulose membrane is carried out at 320 mA for 90 min (*see* **Note 6**).
7. After transfer disassemble the blotting system and remove the nitrocellulose membrane carefully.
8. To assess the success of the transfer the nitrocellulose membrane is placed in a plastic container and incubated in Ponceau S staining solution for 1 min. The membrane should be completely covered with staining solution (*see* **Note 7**).
9. For destaining, wash nitrocellulose membrane three times for 5 min with TBS, slightly shaking.
10. Add blocking solution until the nitrocellulose membrane is completely covered and incubate for 60 min, slightly shaking.
11. After blocking, wash the nitrocellulose membrane three times for 10 min with TBST, slightly shaking.
12. Seal the nitrocellulose membrane in a plastic bag with one side left open (*see* **Note 8**).
13. Dilute anti-acetyllysine antibody 1:2,000 in 12 mL TBST and pour the solution into the open side of the plastic bag containing the nitrocellulose membrane. Seal the open side of the plastic sheets and incubate for 16 h shaking at 150 rpm.
14. Remove nitrocellulose membrane from the plastic sheets and wash as in **step 11**.
15. Dilute the anti-horseradish peroxidase antibody 1:1,000 in 12 mL TBST and proceed as in **steps 12** and **13** but incubate just for 1 h.
16. Repeat **step 14**.
17. For visualization of lysine-acetylated proteins, SuperSignal West Dura enhanced chemiluminescent substrate is used and for detection a chemiluminescent imager (*see* **Note 9**).

3.2 Identification of Lysine-Acetylated Peptides

All steps are carried out at room temperature unless indicated else. Placing SDS or urea-containing buffers on ice or at 4 °C can lead to precipitation.

3.2.1 Protein Digestion Using FASP

1. Purified mitochondria (*see* Chapter 2) (corresponding to at least 0.5–1 mg mitochondrial protein) are pelleted at 15,000 × *g* for 10 min at 4 °C in a microcentrifuge tube (*see* **Note 10**). For better coverage, we recommend processing at least three independent biological replicates. Pellets can be snap-frozen in liquid nitrogen and stored at −80 °C until further processing.
2. Resuspend the pellet in 400 µL SDS-lysis buffer, vortex until the pellet is resuspended, and place for 5 min in a heat block at 95 °C, vortexing two times for 20 s in between.
3. Sonicate sample in an ultrasonic bath for 1 min.
4. Centrifuge for 20 min in a benchtop centrifuge at top speed (15,000–21,000 × *g*) at room temperature.
5. Transfer the supernatant to a new tube without disturbing any sedimented material.
6. Repeat **steps 4** and **5** once.
7. Determine the amount of protein using the 660 nm protein assay with compatibility reagent according to the manufacturer's instructions.
8. Add 2 mL urea buffer to the CFD and centrifuge for 5 min to condition the membrane. Stop the centrifuge after approximately 1 min and check the buffer retention. In rare cases, unusually fast flow-through occurs, which indicates a leak in the membrane. Such damaged units cannot be used and must be replaced.
9. Dilute the sample with urea buffer to a total volume of 4 mL and transfer to the CFD (*see* **Note 11**)—final SDS concentration must not exceed 0.5 % (w/v).
10. Centrifuge at 4,000 × *g* for 15 min (or until at least tenfold concentration).
11. Discard flow-through, add another 4 mL urea buffer, and repeat centrifugation.
12. Discard flow-through, add 1 mL IAA solution, mix gently for 1 min with a pipette without touching the membrane, and incubate for 30 min at room temperature in darkness.
13. Centrifuge the CFD at 4,000 × *g* for 10 min, and discard flow-through.
14. Add 4 mL of urea buffer to the CFD and centrifuge at 4,000 × *g* for 15 min or until at least tenfold concentration. Discard the flow-through and repeat this step twice.

15. Add 4 mL ABC buffer to the CFD and centrifuge at 4,000 × *g* for 15 min or until at least tenfold concentration. Discard the flow-through and repeat this step twice.
16. Transfer the CFD to new 15-mL collection tubes.
17. Add 1 mL ABC buffer containing trypsin at an enzyme-to-protein ratio of 1:100 (e.g., 10 µg trypsin for 1 mg protein) and gently mix with a pipette (do not touch the membrane while pipetting) (*see* **Note 12**).
18. Tighten the lid of the tube well and incubate the CFD at 37 °C overnight.
19. Centrifuge the CFD at 4,000 × *g* for 10 min. The eluate now contains the peptides.
20. Add 1 mL ABC buffer to the CFD (rinsing the filters when adding the buffer) and repeat the centrifugation.
21. Repeat **step 20**.
22. Assess the peptide yield on a microvolume UV–VIS photometer at 280 nm, assuming absorption of 1 for a peptide concentration of 1 mg/mL. Typical yields are approximately 50–60 % of the starting amount.
23. Acidify the eluate to a final concentration of 1 % (v/v) TFA.
24. Condition a C18 SepPak cartridge by flushing it with 3 mL methanol, 3 mL buffer B, and then 3 mL buffer A.
25. Slowly load peptide sample on the cartridge.
26. Wash with 3× 1 mL of buffer A.
27. Elute two times with 0.6 mL buffer B into a 1.5-mL Protein LoBind tube.
28. Evaporate the sample to complete dryness on a vacuum concentrator, if necessary overnight. After drying, peptides can be stored for short term at –20 °C or for long term at –80 °C.

3.2.2 Enrichment of Lysine-Acetylated Peptides

Sample preparation can be carried out at room temperature to facilitate dissolution of peptides. All steps involving the anti-acetyllysine antibody should be carried out on ice or at 4 °C.

1. Redissolve dried peptides in 50 µL 20 % ACN, vortex vigorously, and let rest for 10 min. Then add 450 µL TBS and vortex (*see* **Note 13**).
2. Check the pH of the solution by pipetting 1 µL of sample on pH indicator paper (*see* **Note 14**).
3. Assess the peptide yield on a microvolume UV–VIS photometer at 280 nm, assuming absorption of 1 for a peptide concentration of 1 mg/mL.
4. Take an aliquot of 10 µg and store it for measuring the background proteome (*see* **Note 15**).

5. Transfer 50 µL antibody bead slurry to a 1.5-mL Protein LoBind tube with a cut 200 µL pipette tip (*see* **Note 16**).
6. Wash beads three times for 5 min with 1 mL TBS on a rolling wheel. Centrifuge at 1,000 × *g* in between washes and carefully remove the supernatant (*see* **Note 17**).
7. Add the redissolved peptides to the beads and incubate overnight at 4 °C on a rolling wheel.
8. Wash beads four times for 5 min with 1 mL TBS on a rolling wheel at 4 °C.
9. Wash beads two times shortly with ultrapure water to reduce the salt concentration, centrifuging in between at 1,000 × *g* for 1 min.
10. Elute three times for 5 min with 50 µL 0.1 % (v/v) TFA, mixing the beads gently with the pipette and letting them rest for the remaining time period. Centrifuge in between at 2,000 × *g* and try to recover as much liquid as possible without transferring beads using gel-loading tips.
11. Assess the peptide concentration of the combined eluates on a microvolume UV–VIS photometer at 280 nm as in **step 3**. Usually the concentration is very low (only a few µg yield in total). Higher concentrations might indicate massive background contamination.
12. Clean up combined eluates on StageTips and run the samples on an LC-MS/MS system.

3.2.3 Guidelines for Measuring the Samples on LC-MS/MS

In general every high-resolution accurate mass nano-UHPLC-MS/MS setup used for shotgun proteomics can be used for measuring these samples. Typically, we run them on self-pulled capillary columns with 75-µm diameter, packed with 20–50 cm C18 reversed-phase material (for example: 1.9 µm ReproSil-Pur C18-AQ, Dr. Maisch GmbH). The column is kept at 50 °C in a column oven throughout the run. We inject maximum 1–2 µg peptides and separate them at a flow rate of 250 nL/min with a 90-min linear gradient from 2 to 30 % buffer B in buffer A (buffer A: 0.1 % (v/v) FA; buffer B: 80 % (v/v) ACN, 0.1 % (v/v) FA), followed by a 5-min linear gradient to 60 % buffer B, and then a 5-min linear gradient to 95 % buffer B. If sample complexity is high, the gradient time should be prolonged accordingly (for example to a total of 4-h runtime) or fractionation should be considered. We typically detect the peptides on a Q-Exactive MS (Thermo Scientific) in positive mode with a scanned mass range of 300–1,650 m/z, at a resolution of 70,000 and an AGC target value of 3e6. The ten most intense ions are selected for MS2 at a resolution of 35,000 with an isolation window of 1.6 m/z and an AGC target of 1e6. Peptides with a charge of +1 or with unassigned charge state are excluded from fragmentation for MS2; dynamic exclusion prevents repeated

selection of selected masses for 20 s. We process raw data using MaxQuant software (http://www.maxquant.org/) [21] and search against The Arabidopsis Information Resource (TAIR, http://www.arabidopsis.org) protein database, with trypsin specificity and a maximum of four missed cleavages at a protein and peptide false discovery rate of 1 %. Carbamidomethylation of cysteine residues was set as fixed, and oxidation of methionine, N-terminal acetylation, and lysine acetylation as variable modifications.

4 Notes

1. Urea and IAA solutions must be freshly prepared. Prepare the urea buffer early in advance. It needs time to dissolve but should not be heated above room temperature to prevent formation of isocyanate and carbamylation of proteins. The IAA solution should be stored in the dark until use.
2. Place the edges of the plates exactly on top of each other before touching the gel strip. Do not adjust the second glass plate when it already touches the gel strip because this could damage it.
3. For pouring the tricine-SDS-PAGE, start with the resolving gel, trying not to touch the gel strip with the solution. Directly after pouring, take the assembled glass plates with the resolving gel parallel to the surface and slowly add the spacer gel. Add half of the spacer gel solution on the left side and the other half on the right side of the gel strip. The spacer gel should not touch the gel strip in order to have space for the sample gel. Add overlay solution on top of the spacer gel in the same way like the spacer gel was added. Slowly put the gel back in a vertical position and let the gel polymerize for 1 h.
4. Pour the sample gel from one side into the glass plates avoiding air bubbles in between sample gel and gel strip. This is achieved by holding the glass plates tilted while pouring.
5. Try to avoid air bubbles between the different layers of paper.
6. The current to be applied depends on the gel size. For the Fastblot Semi-Dry Electrophoretic Transfer Apparatus B44 (Biometra) 2 mA/cm^2 is recommended.
7. We recommend documenting the result of the Ponceau S stain with a scanner or a camera. The membrane should be washed with distilled water until proteins become clearly visible.
8. Cut a plastic bag with a scissor into two separate sheets. Place the nitrocellulose membrane carefully on one sheet and put the second sheet on top of the nitrocellulose membrane. Seal three sides of the plastic sheets close to the borders of the nitrocellulose membrane with one side remaining open.

9. The SuperSignal West Dura enhanced chemiluminescent substrate contains two components (Luminol/Enhancer Solution and Stable Peroxide Buffer), which have to be mixed together in a volume proportion of 1:1. The mixture is then added immediately on top of the membrane making sure that it is covered completely.
10. The amount of mitochondrial protein will mainly be dictated by the quality and number of isolations. We consider 0.5 mg total protein as the absolute minimum. Ideally, 0.8 mg or more should be used to obtain a high number of identified acetylation sites. In general, the number of identified sites correlates with the amount of peptides used in the enrichment step [15].
11. We recommend using 4-mL centrifugation devices (for example Amicon Ultra-4, Millipore) for digesting samples in the range of 0.3–3 mg total protein. For larger amounts the protocol can also be scaled up to devices such as Amicon Ultra-15 (Millipore).
12. To reach more complete digestion, it is possible to additionally digest the sample with LysC. For example, LysC is added at an enzyme-to-protein ratio of 1:100 and the sample is incubated for 2 h at room temperature, before adding trypsin and incubating overnight as specified.
13. If the peptides do not dissolve well, the sample can also be placed in an ultrasonic bath for 5 min. Higher amounts of 20 % ACN can also help to redissolve the pellet; however bear in mind that the antibody tolerates only low amounts of ACN.
14. FA remaining after desalting and evaporation on the vacuum concentrator can lower the pH substantially. After adding the TBS buffer check whether the pH is in the desired range and, if necessary, correct by adding small amounts of 1 M Tris–HCl pH 7.6.
15. We recommend desalting this aliquot directly on C18 Stage Tips [21] and keeping the sample until measurement at –20 °C.
16. 50 µL slurry corresponds to 100 µg antibody. A ratio of 100 µg antibody per 1 mg of peptides results in a reasonable compromise between the number of sites identified and the costs for the antibody. The antibody is quite sensitive to temperature changes and cannot be reused in our experience.
17. Take care not to lose beads while washing. Gel-loading tips are useful for taking off the remaining buffer close to the beads.

References

1. Deribe YL, Pawson T, Dikic I (2010) Post-translational modifications in signal integration. Nat Struct Mol Biol 17:666–672
2. Choudhary C, Kumar C, Gnad F et al (2009) Lysine acetylation targets protein complexes and co-regulates major cellular functions. Science 325:834–840
3. Close P, Creppe C, Gillard M et al (2010) The emerging role of lysine acetylation of non-nuclear proteins. Cell Mol Life Sci 67: 1255–1264
4. Norvell A, Mcmahon SB (2010) Rise of the rival. Science 327:964–965
5. Weinert BT, Wagner SA, Horn H et al (2011) Proteome-wide mapping of the Drosophila acetylome demonstrates a high degree of conservation of lysine acetylation. Sci Signal 4:ra48
6. Xing S, Poirier Y (2012) The protein acetylome and the regulation of metabolism. Trends Plant Sci 17:423–430
7. Gershey EL, Vidali G, Allfrey VG (1968) Chemical studies of histone acetylation. The occurrence of epsilon-N-acetyllysine in the f2a1 histone. J Biol Chem 243:5018–5022
8. Hartl M, Finkemeier I (2012) Plant mitochondrial retrograde signaling: post-translational modifications enter the stage. Front Plant Sci 3:253
9. Finkemeier I, Laxa M, Miguet L et al (2011) Proteins of diverse function and subcellular location are lysine acetylated in Arabidopsis. Plant Physiol 155:1779–1790
10. Koenig AC, Hartl M, Pham PA et al (2014) The Arabidopsis class II sirtuin is a lysine deacetylase and interacts with mitochondrial energy metabolism. Plant Physiol 164:1401
11. Wu X, Oh MH, Schwarz EM et al (2011) Lysine acetylation is a widespread protein modification for diverse proteins in Arabidopsis. Plant Physiol 155:1769–1778
12. König AC, Hartl M, Boersema P et al (2014) The mitochondrial lysine acetylome of Arabidopsis. Mitochondrion 19:252
13. Heinemeyer J, Lewejohann D, Braun HP (2007) Blue-native gel electrophoresis for the characterization of protein complexes in plants. Methods Mol Biol 355:343–352
14. Klodmann J, Senkler M, Rode C et al (2011) Defining the protein complex proteome of plant mitochondria. Plant Physiol 157:587–598
15. Mertins P, Qiao JW, Patel J et al (2013) Integrated proteomic analysis of post-translational modifications by serial enrichment. Nat Methods 10:634–637
16. Dormeyer W, Ott M, Schnolzer M (2005) Probing lysine acetylation in proteins: strategies, limitations, and pitfalls of in vitro acetyltransferase assays. Mol Cell Prot 4:1226–1239
17. Kim JY, Kim KW, Kwon HJ et al (2002) Probing lysine acetylation with a modification-specific marker ion using high-performance liquid chromatography/electrospray-mass spectrometry with collision-induced dissociation. Anal Chem 74:5443–5449
18. Wisniewski JR, Zougman A, Nagaraj N et al (2009) Universal sample preparation method for proteome analysis. Nat Methods 6:359–362
19. Guan KL, Yu W, Lin Y et al (2010) Generation of acetyllysine antibodies and affinity enrichment of acetylated peptides. Nat Protoc 5: 1583–1595
20. Rappsilber J, Mann M, Ishihama Y (2007) Protocol for micro-purification, enrichment, pre-fractionation and storage of peptides for proteomics using StageTips. Nat Protoc 2: 1896–1906
21. Cox J, Mann M (2008) MaxQuant enables high peptide identification rates, individualized p.p.b.-range mass accuracies and proteome-wide protein quantification. Nat Biotechnol 26:1367–1372

Chapter 8

A Flowchart to Analyze Protease Activity in Plant Mitochondria

Pedro F. Teixeira, Rui M. Branca, Beata Kmiec, and Elzbieta Glaser

Abstract

Proteases are one of the most abundant classes of enzymes and are involved in a plethora of biological processes in many cellular compartments, including the mitochondria. To understand the role of proteases is essential to determine their substrate repertoire, preferably in an in vivo setting. In this chapter we describe general guidelines to analyze protease activity using several strategies, from in-gel analysis to mass spectrometry mapping of the cleavage site(s) and fluorogenic probes that can easily be used in vivo. To exemplify this flowchart, we used the recently characterized organellar oligopeptidase of Arabidopsis (*Arabidopsis thaliana*), an enzyme that takes part in degradation of short peptides within mitochondria and chloroplasts.

Key words Peptide, Protease, Mitochondria, Electrophoresis, Mass spectrometry, Fluorogenic probe

1 Introduction

The endosymbiotic organelles mitochondria and chloroplasts are sites of intensive proteolytic activity [1]. The proteases resident in these two compartments are responsible not only for the removal of damaged or unassembled proteins but also for the maturation of newly imported proteins and the degradation of short peptide products averting their toxic effects [2]. In protease research, one of the fundamental aspects is the ability to measure protease activity. This aspect is dependent on the identification of relevant substrates and their optimization for usage not only in vitro with a purified protein but also in complex biological samples such as cell extracts. To facilitate this process we propose an organized flowchart highlighting some of the available strategies to analyze protease activity (Fig. 1). We exemplify it by analyzing the activity of the mitochondrial and chloroplastic organellar oligopeptidase (OOP) [3]. This protease was recently characterized as one of the components of the targeting peptide degradation pathway in

James Whelan and Monika W. Murcha (eds.), *Plant Mitochondria: Methods and Protocols*, Methods in Molecular Biology, vol. 1305, DOI 10.1007/978-1-4939-2639-8_8,

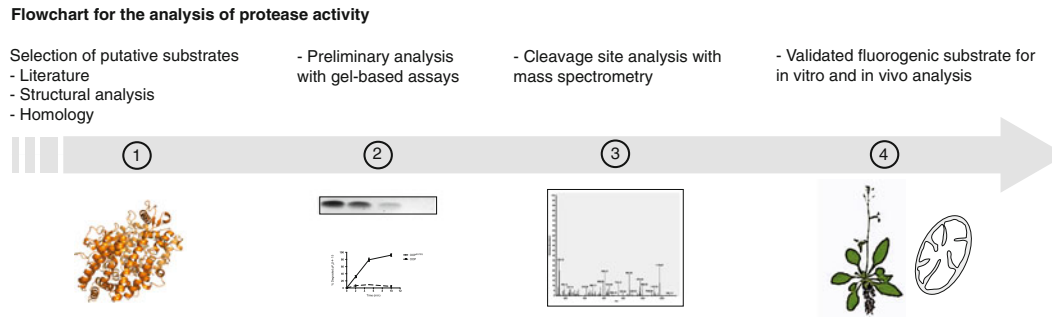

Fig. 1 Outline of the proposed four-step flowchart to analyze the activity of proteases. The process is exemplified for the OOP protease and consists of in-gel degradation assays, mass spectrometry mapping of the cleavage sites, and design of specific fluorogenic probes that can be used in complex biological samples

mitochondria and chloroplasts together with the previously described presequence protease (PreP) [2, 4, 5]. The analysis starts with putative substrate selection (Fig. 1, step 1; based on literature, structural information, sequence analysis, etc.) and confirmation with a simple in-gel assay (Fig. 1, step 2). The result can be further validated with mass spectrometry analysis (Fig. 1, step 3) that allows also the precise identification of the cleavage site(s). Based on the substrate validation by mass spectrometry analysis one can design a fluorogenic probe (Fig. 1, step 4) that allows a quick activity assay in complex samples. In this example we used a probe with an N-terminal methoxycoumarin (MCA) moiety and C-terminal lysine derivatized with dinitrophenol (Dnp), previously characterized in the context of protease activity measurements [6]. In such a system, when the peptide is cleaved the fluorescence of the MCA moiety is no longer quenched by Dnp and an increase in fluorescence proportional to the amount of peptide cleaved is observed. We exemplify the utility of such probes with the analysis of peptide degradation in mitochondrial extracts obtained from both Arabidopsis wild-type [*Arabidopsis thaliana* ecotype Colombia-0 (Col-0)] and *oop* knockout line [3]. The flowchart described in this chapter is illustrated for OOP but the principle is readily applicable to other proteases.

2 Materials

2.1 Components for Activity Assays

1. Reaction buffer: 50 mM HEPES-KOH pH 8.2 (stock solution 0.5 M HEPES-KOH pH 8.2).
2. Purified OOP, according to [3].
3. Peptides, $pF_1\beta(43–53)$ (sequence KGFLLNRAVQY) and MCA-$pF_1\beta(43–53)$-Dnp(methoxycoumarin-KGFLLNRAVQYK-2,4-dinitrophenyl), custom synthesis (GenicBio).

4. Mitochondria isolated from 10-day-old seedlings of both Arabidopsis wild-type Col-0 and *oop* knockout line (following the procedure described in Chapter 2).
5. Mitochondrial extracts prepared according to [7].

2.2 Components for Liquid Chromatography-Mass Spectrometry Analysis

1. Formic acid (FA) 10 % (v/v) solution as liquid chromatography-mass spectrometry (LC-MS) sample solvent.
2. LC-MS mobile phase A: MilliQ water 97 % (v/v), acetonitrile (ACN) 3 % (v/v), FA 0.1 % (v/v).
3. LC-MS mobile phase B: MilliQ water (5 %), ACN 95 % (v/v), FA (0.1 % v/v).
4. C18 guard desalting column Zorbax 300SB-C18, 5× 0.3 mm, 5 μm bead size (Agilent).
5. C18 picofrit column, 15 cm in length, 100 μm internal diameter, 5 μm bead size (Nikkyo Technos Co., Tokyo, Japan).
6. Nano flow High Performance Liquid Chromatography (HPLC) system (Agilent, 1200 series).
7. Q exactive Mass Spectrometer (Thermo) equipped with a nano electrospray ionization source.

2.3 Tricine-SDS-Polyacrylamide Gel Components

1. 4× Peptide sample buffer: 150 mM Tris–HCl pH 7, 4 % (w/v) SDS, 6 % (v/v) β-mercaptoethanol, 30 % (v/v) glycerol, 0.05 % (w/v) Coomassie brilliant blue G-250.
2. 16 % Acrylamide-tricine-sodium dodecyl sulfate (SDS) gel, prepared according to [8].
3. Formaldehyde fixation solution: 25 % (v/v) ethanol, 15 % (v/v) formalin solution [35 % (v/v) formaldehyde, Sigma], 60 % (v/v) water.
4. Staining solution, colloidal Coomassie "Blue Silver," according to [9].

3 Methods

The procedures are performed at room temperature (23 °C) unless otherwise indicated.

3.1 In-Gel Analysis of Peptide Degradation

1. For a typical protease activity reaction mix OOP (25 ng/μL final concentration) with the substrate $pF_1\beta(43–53)$ (0.2 μg/μL) in reaction buffer (50 mM HEPES-KOH pH 8.2), in a total volume of 100 μL. Prepare the reactions in triplicate and use an appropriate negative control (peptide only, inactive variant of the enzyme or an inhibitor).
2. Incubate the reactions at 30 °C and remove 20 μL aliquots at time points 0, 2, 5, and 10 min after the reaction was initiated.

3. Stop the reaction by mixing the 20 μL aliquot with the appropriate volume of peptide sample buffer (*see* **Note 1**). Alternatively, if mass spectrometry analysis follows, stop the reaction by adding 100 μL of 10 % (v/v) FA solution to the sample aliquot (continue to Subheading 3.2, **step 4**).
4. Heat the samples at 56 °C for 15 min.
5. Load half volume of the reaction samples in a 16 % acrylamide-tricine-SDS gel (*see* **Note 2**). Run the electrophoresis for 4–5 h at 30 V (mini-gels).
6. Fix the peptides in the gel by incubating with formaldehyde fixation solution (*see* **Note 3**) for 45 min. Rinse twice with water.
7. Stain the gel with Coomassie blue (blue silver solution) for at least 4 h. Destain with water until the bands are clearly visible.
8. Perform densitometric analysis of the gels for quantification (Fig. 2).

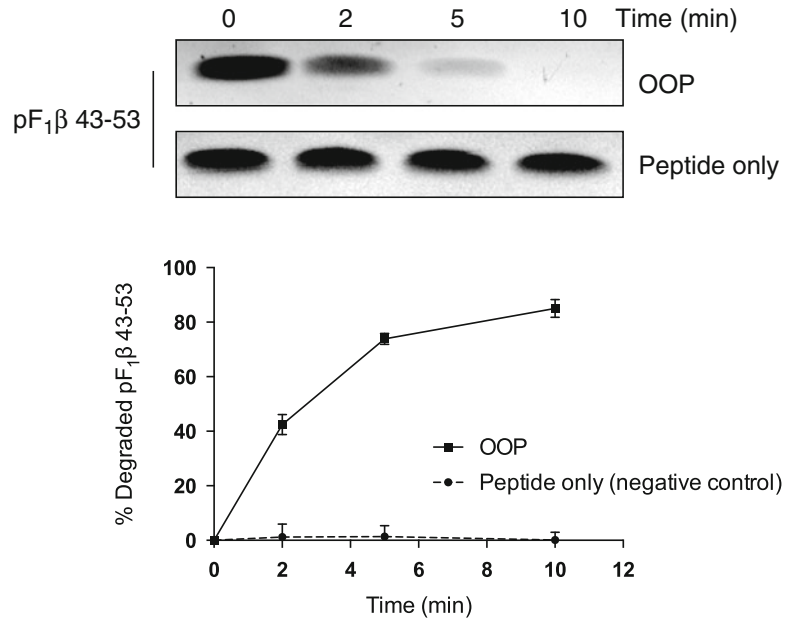

Fig. 2 Degradation of $pF_1\beta(43–53)$ by OOP analyzed by tricine-SDS-electrophoresis followed by Coomassie staining. An enzyme-free reaction was used as a negative control (peptide only). The gels corresponding to three replicate experiments were analyzed and the intensity of the bands quantified and plotted as indicated

3.2 Liquid Chromatography-Mass Spectrometry Analysis of Peptide Cleavage Sites

1. Run each peptide degradation reaction replicate sample in analytical LC-MS triplicates for robust quantification of the cleavage products. In addition, always include an enzyme-free negative control for each substrate (*see* **Note 4**).
2. If the peptide substrate contains at least one cysteine residue *see* **Note 5**.
3. To the 20 μL of sample from the peptide degradation assay add 100 μL of 10 % (v/v) FA solution.
4. For each LC-MS run, inject 3 μL of this acidified solution into the guard column using the autosampler of the HPLC system. After an initial wash with mobile phase A for 3 min using the sample loading capillary pump at a flow rate of 6 μL/min, switch the valve to direct the flow from the gradient nano pump into the guard column (using back flush configuration and a nano flow rate of 0.4 μL/min). The gradient then immediately starts from 2 % B up to 40 % B in 15 min, and is followed by a steep increase to 100 % B in 5 min, plateau at 100 % B for 3 min, steep decrease down to 2 % B in 3 min, and re-equilibration at 2 % B for 10 min.
5. Mass spectrometry acquisition proceeds in scan cycles which comprise an initial MS1 survey scan (300–1,700 m/z range, 70,000 resolution), which is followed by five data-dependent MS/MS (MS2) scans (17,500 resolution, 30 % HCD collision energy) on the five most abundant ions from the survey scan. Precursor ion isolation window should be 2 m/z. Automatic gain control (AGC) targets should be set to 1E6 for MS1 and 1E5 for MS2, with maximum injection times of 100 ms. Dynamic exclusion should be used with 30–60-s duration. Precursors with unassigned charge state should be excluded, whereas precursors with charge state 1 may be included. An underfill ratio of 1–10 % should be used.
6. All MS/MS spectra should be searched (with a search engine algorithm such as Mascot, Sequest, or MSGF+) against a FASTA database containing the sequence of the peptide used as substrate. Set precursor mass tolerance to 10 ppm and product mass tolerance to 0.02 Da. Consider oxidation of methionine and other possible artifactual modifications (such as amidation of C-terminus) as dynamic modifications. Use the precursor peak area as the quantifier parameter (*see* **Note 6**) (Fig. 3).

3.3 Analysis of protease Activity with a Fluorogenic Probe

1. Mix OOP (1 ng/μL) with the substrate MCA-pF1β(43–53)-Dnp (40 ng/μL) in reaction buffer, in a volume of 100 μL. Perform reactions in triplicate and use appropriate negative control (peptide-only control is used in Fig. 4a).
2. Incubate the reactions at 30 °C and follow the fluorescence increase in a spectrofluorometer ($\lambda^{\text{excitation}} = 327$ nm; $\lambda^{\text{emission}} = 395$ nm) (*see* **Note 7**).

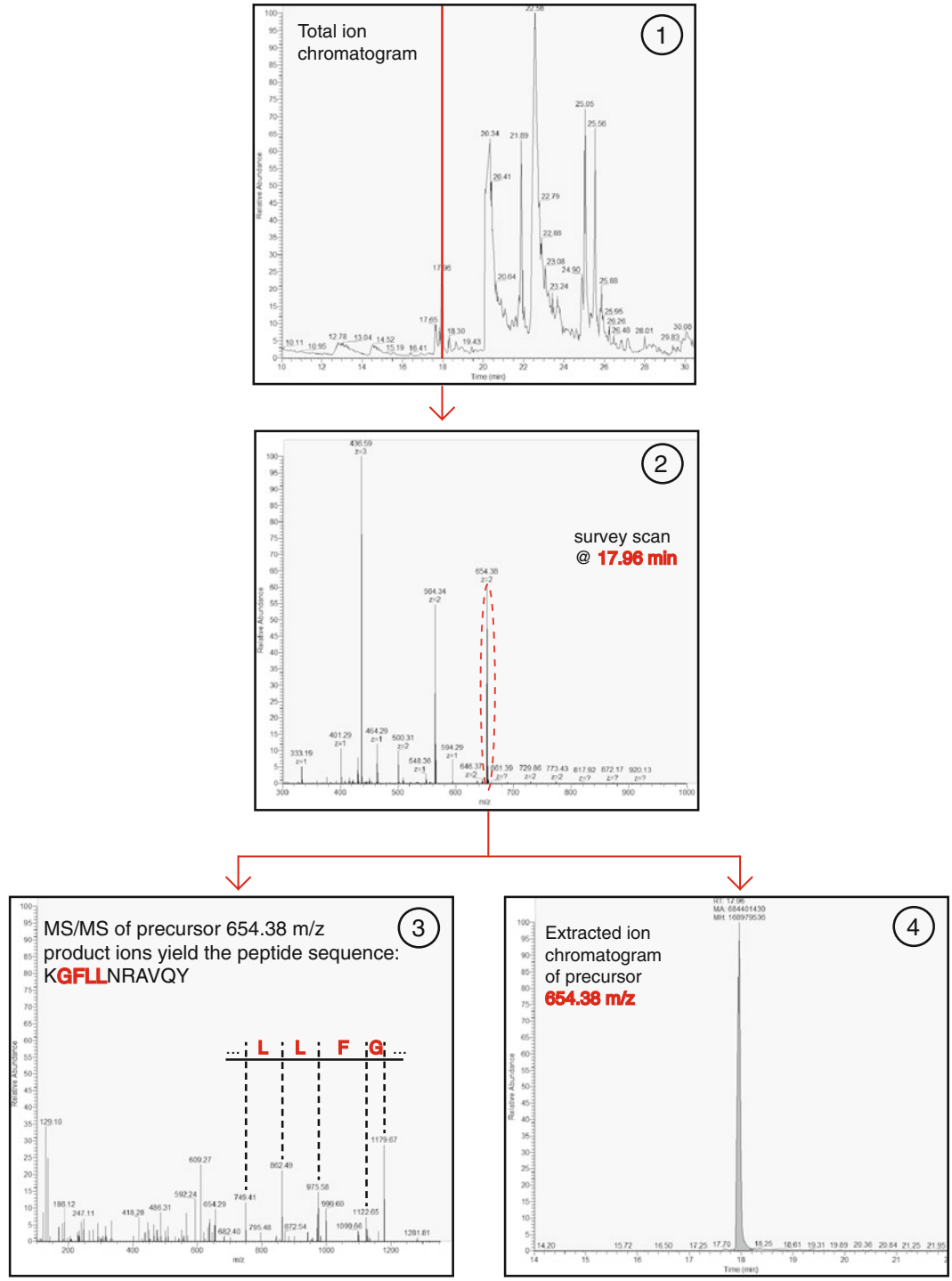

Fig. 3 LC-MS identification and quantification of peptides. The total ion chromatogram (*panel 1*) of each LC-MS run is the result of accumulated MS1 survey scans over time. The survey scan taken at retention time 17.96 min (*panel 2*) reveals a number of different precursor ions eluting at that time point. MS/MS was performed, for example on the precursor 654.38 *m*/*z* yielding a series of fragment ions, which can be used to identify the peptide sequence (*panel 3*). The intensity of the 654.38 *m*/*z* precursor peak in the consecutive MS1 survey scans over time yields the extracted ion chromatogram (*panel 4*), and the area under the curve is used to quantify the peptide in the sample

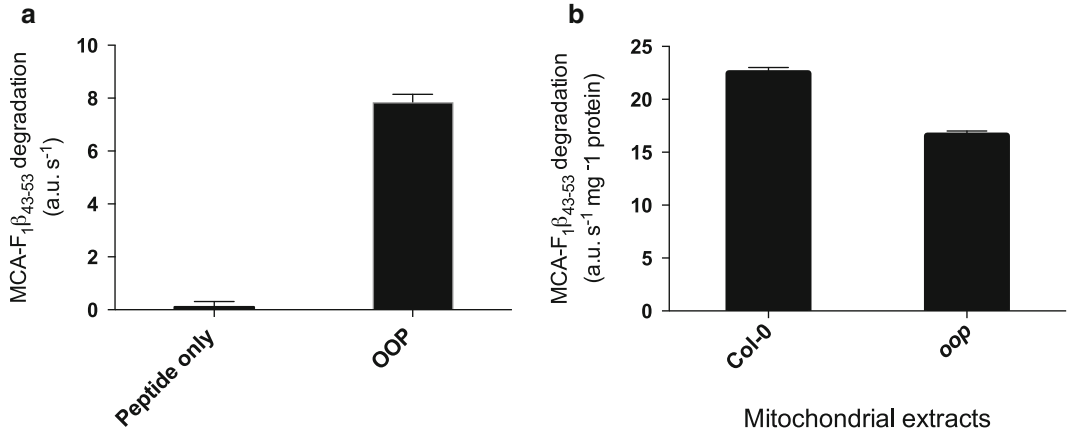

Fig. 4 Degradation of MCA-pF$_1$β(43–53)-Dnp by purified OOP (**a**) and mitochondrial extracts from Arabidopsis Col-0 or *oop* knockout line (**b**). Results show the peptide degradation rate and are the average of three replicate experiments

3. Calculate and plot the peptide degradation rate (Fig. 4a).
4. For the analysis in mitochondrial extracts incubate the sample volume corresponding to 100 µg of mitochondrial protein from either wild-type Col-0 or *oop* knockout line with the substrate MCA-pF$_1$β(43–53)-Dnp in a reaction volume of 100 µL.
5. Run the reactions at 30 °C and follow the fluorescence increase.
6. Calculate and plot the peptide degradation rate in wild-type Col-0 and *oop* knockout line extracts to analyze the contribution of OOP for MCA-pF$_1$β(43–53)-Dnp degradation (Fig. 4b).

4 Notes

1. For optimal resolution of the peptide bands a lower concentration of SDS in the sample buffer is recommended [4 % (w/v) SDS in the 4× sample buffer].
2. Uniform acrylamide-tricine-SDS gels offer higher resolution for peptides than the glycine-SDS system. A comparison of the resolution of both systems has been published elsewhere [8].
3. Small peptides may be resistant to the common acid fixation procedures (acetic acid/ethanol), resulting in diffusion out of the gel, smeared bands, and general decrease in staining sensitivity. A recommended alternative to such methods is the covalent cross-linking with formaldehyde.
4. This negative control will serve as the reference quantity of undigested peptide substrate, to which the enzymatic assay samples should be compared.

5. Peptide substrates that contain cysteines should have their cysteinyl sites reduced and alkylated to facilitate the mass spectrometry analysis. Because reduction is usually done with dithiothreitol (DTT), and this requires pH ≥7, the enzymatic degradation assay should not be stopped by acidification in this case. Instead, enzymatic activity in the collected aliquot should be stopped by addition of DTT (to 0.5 mM final concentration) and placement of the sample in a block heater at 60 °C (preheated) for 15 min. Then, bring the sample to room temperature, add iodoacetamide (IAA, 2.5 mM final concentration), and incubate the sample in the dark for 10 min. After this continue the procedure from Subheading 3.2, **step 3**, with the acidification by addition of 10 % (v/v) FA.
6. There are several software packages that can integrate the peak area automatically, such as the "precursor ion area detector" module from the Proteome Discoverer 1.3 software, which is usually provided with Thermo Mass Spectrometers.
7. For higher throughput of analysis a 96-well plate reader format is recommended.

Acknowledgement

This work was supported by grants from the Swedish Research Council to EG.

References

1. Vierstra RD (1996) Proteolysis in plants: mechanisms and functions. Plant Mol Biol 32:275–302
2. Teixeira PF, Glaser E (2013) Processing peptidases in mitochondria and chloroplasts. Biochim Biophys Acta 1833:360–370
3. Kmiec B, Teixeira PF, Berntsson RP, Murcha MW, Branca RM, Radomiljac JD, Regberg J, Svensson LM, Bakali A, Langel U, Lehtio J, Whelan J, Stenmark P, Glaser E (2013) Organellar oligopeptidase (OOP) provides a complementary pathway for targeting peptide degradation in mitochondria and chloroplasts. Proc Natl Acad Sci U S A 110:E3761–E3769
4. Stahl A, Moberg P, Ytterberg J, Panfilov O, Brockenhuus Von Lowenhielm H, Nilsson F, Glaser E (2002) Isolation and identification of a novel mitochondrial metalloprotease (PreP) that degrades targeting presequences in plants. J Biol Chem 277:41931–41939
5. Kmiec B, Glaser E (2012) A novel mitochondrial and chloroplast peptidasome, PreP. Physiol Plant 145:180–186
6. Troeberg L, Nagase H (2004) Monitoring metalloproteinase activity using synthetic fluorogenic substrates. Curr Protoc Protein Sci Chapter 21: Unit 21.16
7. Kmiec B, Teixeira PF, Glaser E (2013) Phenotypical consequences of expressing the dually targeted Presequence Protease, AtPreP, exclusively in mitochondria. Biochimie 100: 167–170
8. Schagger H (2006) Tricine-SDS-PAGE. Nat Protoc 1:16–22
9. Candiano G, Bruschi M, Musante L, Santucci L, Ghiggeri GM, Carnemolla B, Orecchia P, Zardi L, Righetti PG (2004) Blue silver: a very sensitive colloidal Coomassie G-250 staining for proteome analysis. Electrophoresis 25:1327–1333

Chapter 9

Activity Measurements of Mitochondrial Enzymes in Native Gels

Peter Schertl and Hans-Peter Braun

Abstract

In-gel activity assays are useful tools to identify and characterize enzymes within gels. Prerequisite are electrophoretic protein separations that are carried out under conditions compatible with enzyme activity. While blue native-polyacrylamide gel electrophoresis (BN-PAGE) is widely used for activity assays of the five enzyme complexes of the oxidative phosphorylation system, the blue background of this electrophoretic system is not compatible with activity assays for some other mitochondrial enzymes. As an alternative system, clear native (CN)-PAGE can be used for visualizing activities of mitochondrial enzymes. Here, we describe enzyme activity assays for mitochondrial enzymes in BN and CN gels.

Key words In-gel assay, BN-PAGE, CN-PAGE, Activity assays

1 Introduction

Blue native-polyacrylamide gel electrophoresis (BN-PAGE), in contrast to SDS-PAGE, allows protein separations under native conditions [1]. BN-PAGE is based on the usage of the dye Coomassie blue. Originally, Coomassie blue was used *after* completion of electrophoretic runs to stain and thereby visualize proteins within gels [2]. In contrast, during BN-PAGE, Coomassie blue is added to protein fractions *before* gel electrophoresis. Due to its anionic properties it introduces negative charge into proteins, thereby allowing their separation according to molecular mass. In contrast to the anionic detergent sodium dodecyl sulfate (SDS), Coomassie does not denature proteins and therefore is perfectly compatible for characterizing enzyme activities. In-gel enzyme assays offer the direct identification of enzymes in gels based on their activity. In contrast to immunoblotting procedures for protein identification, in-gel enzyme assays do not require the availability of antibodies. Furthermore, in-gel activity assays offer characterizing enzymes within gels, e.g., by usage of specific inhibitors. Protocols to visualize enzyme activities within BN gels

James Whelan and Monika W. Murcha (eds.), *Plant Mitochondria: Methods and Protocols*, Methods in Molecular Biology, vol. 1305, DOI 10.1007/978-1-4939-2639-8_9,

first were established for the enzyme complexes of the oxidative phosphorylation (OXPHOS) system [[3] and references within]. Later, in-gel activity assays were successfully used to characterize dysfunctions of OXPHOS complexes caused by mutations [4–6]. Numerous further enzyme activity assays meanwhile were established for BN gels, e.g., [7]. However, some enzyme assays are not compatible with BN-PAGE because the blue background of the gels interferes with the activity signals. As an alternative system, clear native (CN)-PAGE [8] can be used under these circumstances. During CN-PAGE Coomassie blue is omitted. As a result, protein separation is exclusively based on the intrinsic charge of proteins. Separation capacity of CN gels is slightly reduced and molecular mass determinations cannot be carried out. However, CN-PAGE is an especially mild procedure and not associated with blue background formation. It ideally can be used for visualization of the enzymatic activities that only result in faint color changes or for assays that are based on usage of blue redox dyes.

Here we present protocols for activity assays of the five OXPHOS complexes and for L-galactono-1,4-Lactone dehydrogenase (GLDH) within BN gels (Fig. 1). GLDH catalyzes the

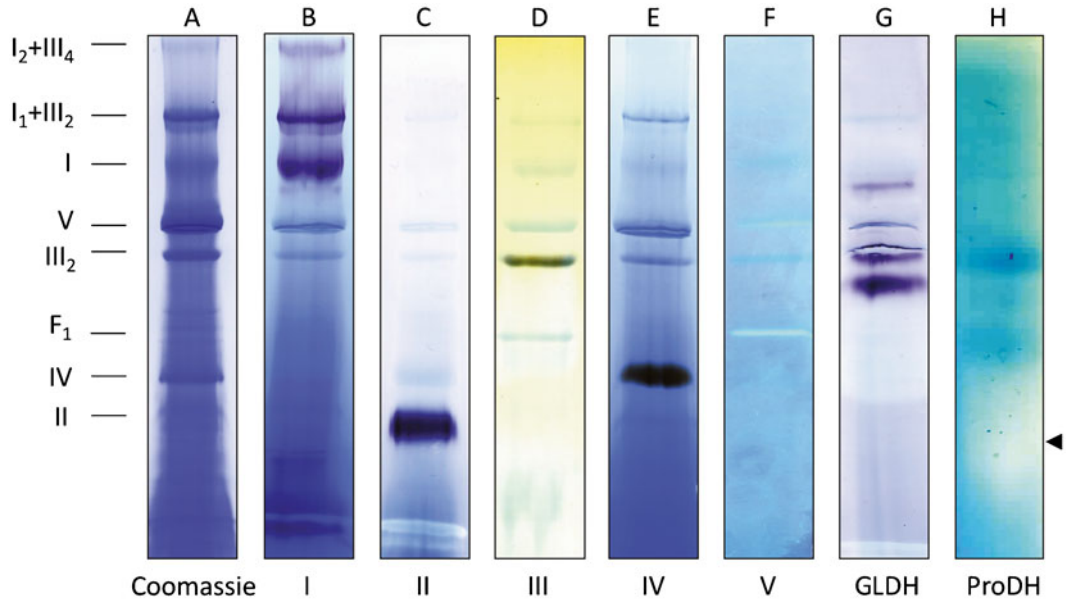

Fig. 1 In-gel activity assays of mitochondrial enzymes in native gels. Arabidopsis mitochondrial proteins (500 μg) were solubilized by digitonin and subsequently separated by 1D BN-PAGE (**a**–**g**) or by 1D CN-PAGE (**h**). Designations to the bottom: Coomassie, Coomassie-stained gel strip. I, II, III, IV, and V: Gel strips after in-gel activity stainings for Complexes I, II, III, IV, and V. GLDH, gel strip after GLDH activity staining. ProDH, gel strip after ProDH activity staining. For ProDH activity staining, mitochondria from proline-treated Arabidopsis cells were isolated and separated on a 1D CN-PAGE. Identities of the separated protein complexes and supercomplexes are given to the left: I_2+III_4, supercomplex consisting of two copies of Complex I and two copies of dimeric Complex III; I_1+III_2, supercomplex consisting of one copy of Complex I and one copy of dimeric Complex III; I, Complex I; V, ATP synthase; III_2, dimeric Complex III; IV, Complex IV; II, Complex II, F_1, F_1 subcomplex of Complex V

terminal step of the ascorbate biosynthesis pathway, which in plants takes place in mitochondria. Furthermore, a proline dehydrogenase assay, which is carried out within a CN gel, is presented (Fig. 1).

2 Materials

All buffers are prepared with analytical grade chemicals and with pure deionized water. It is not necessary to prepare stock solutions fresh. All other solutions are prepared freshly.

2.1 Components for Casting and Running a BN Gel

1. Acrylamide solution: 40 % (w/v) acrylamide/bisacrylamide (32:1).
2. 6× BN gel buffer: 1.5 M aminocaproic acid, 150 mM bis-Tris (Bis(2-hydroxyethyl)-amino-tris(hydroxymethyl)-methane), pH 7.0 (adjust at 4 °C).
3. 100 % Glycerol.
4. 99 % (w/v) *N*,*N*,*N*′,*N*′-Tetramethylethylenediamine (TEMED).
5. 10 % (w/v) ammonium persulfate (APS).
6. 5× BN cathode buffer: 250 mM tricine, 75 mM bis-Tris (Bis(2-hydroxyethyl)-amino-tris(hydroxymethyl)-methane), 0.1 % (w/v) Coomassie G-250, pH 7.0 (adjust at 4 °C).
7. 6× BN anode buffer: 300 mM bis-Tris (Bis(2-hydroxyethyl)-amino-tris(hydroxymethyl)-methane), pH 7.0 (adjust at 4 °C).
8. Gradient former (for example: Model 485 Gradient Former #165-4120; Bio-Rad, USA).
9. Gel electrophoresis unit (e.g., PROTEAN® II gel unit, Bio-Rad, USA).

2.2 Components for CN Gel Run

1. Precasted mini gels: NativePAGE™ Novex® 4–16 % bis-Tris (Bis(2-hydroxyethyl)-amino-tris(hydroxymethyl)-methane) Protein Gels, 1.0-mm, 10-wells (Life Technologies GmbH, Germany).
2. 10× Anode and cathode running buffer: 250 mM Tris (tris(hydroxymethyl)aminomethane) and 192 mM glycine.
3. XCell SureLock® Mini-Cell (Life Technologies GmbH, Germany).

2.3 Components for Sample Preparation

1. Solubilization buffer with 5 % (w/v) digitonin, pH 7.4: 30 mM HEPES, 150 mM K-acetate, 10 % (v/v) glycerol, 5 % (w/v) digitonin (*see* **Note 1**). Buffer is stored at –20 °C.
2. 20× Blue loading buffer for BN-PAGE: 750 mM aminocaproic acid, 5 % (w/v) Coomassie G-250, stored at 4 °C.

3. Solubilization buffer for proline dehydrogenase: 2.5 % (w/v) digitonin in 50 mM Tris-HCl pH 7.2.
4. 5× Native loading buffer for CN-PAGE: 62.5 mM Tris-HCl pH 6.8, 10 % (w/v) glycerol, 0.00125 % (w/v) bromophenol blue.

2.4 Components for In-Gel Activity Assays

1. 2 M Tris-HCl, pH 7.4.
2. 2 M Tris-HCl, pH 8.8.
3. Phosphate buffer stock solution: 0.5 M KH_2PO_4, 0.5 M K_2HPO_4, pH 7.4.

Staining solutions:

4. NADH dehydrogenase staining solution (Complex I): 0.1 M Tris-HCl pH 7.4, 0.14 mM NADH, 0.1 % (w/v) nitroblue tetrazolium [9].
5. Succinate dehydrogenase staining solution (Complex II): 50 mM phosphate buffer pH 7.4, 84 mM succinic acid, 0.2 mM phenazine methosulfate, 0.2 % (w/v) nitroblue tetrazolium, [10].
6. Cytochrome c reductase staining solution (Complex III): Pierce 1-Step TMB-Blotting Substrate (Pierce, Rockford, IL, USA) [11].
7. Cytochrome c oxidase staining solution (Complex IV): 10 mM phosphate buffer pH 7.4, 0.1 % (w/v) 3,3′-diaminobenzidine (DAB), and 16 mM cytochrome c (Sigma-Aldrich, USA) [12].
8. ATPase staining solution (Complex V): 35 mM Tris-HCl pH 7.4, 270 mM glycine, 14 mM, $MgSO_4$, 0.2 % $Pb(NO_3)_2$, and 8 mM ATP [13].
9. GLDH staining solution: 40 mM Tris-HCl pH 8.8, 2 mM L-galactono-1,4-lactone, 0.1 % (w/v) nitroblue tetrazolium, 0.2 mM phenazine methosulfate [7].
10. Preincubation solution for proline dehydrogenase (ProDH) activity: 1.2 mM 2,6-dichlorophenolindophenol (DCPIP), 50 mM Tris-HCl pH 7.2 [14].
11. ProDH staining solution: 50 mM Tris-HCl pH 7.2, 5 mM $MgCl_2$, 0.25 mM flavin adenine dinucleotide (FAD), 0.5 mM phenazine methosulfate (PMS), 100 mM L-proline [14].
12. Fixing solution: 40 % (v/v) methanol, 10 % (w/v) acetic acid.

3 Methods

3.1 Preparation of a BN Gel

The following instructions refer to a gel dimension of 0.15× 16×20 cm. However, units from a variety of manufacturers are of comparable suitability for BN-PAGE.

1. 4.5 % separation gel solution is prepared by mixing 2.4 mL of acrylamide solution with 3.5 mL of BN gel buffer and 15.1 mL of deionized water.
2. 16 % separation gel solution is prepared by mixing 7.4 mL of acrylamide solution with 3 mL of BN gel buffer, 4.6 mL deionized water, and 3.5 mL glycerol.
3. Use a gradient former and connect it with a tube and a needle with the space in between two glass plates which are preassembled in a gel-casting stand. Transfer the two gel solutions into the two chambers of the gradient former. Gradient gels can either be cast from the top (16 % gel solution has to enter the gel sandwich first) or from the bottom (4.5 % gel solution has to enter the glass plates first). For casting the gel from the bottom, an adjustable pump is required.
4. 95 μL APS and 9.5 μL TEMED are added to the 4.5 % gel solution. To the 16 % gel solution 61 μL APS and 6.1 μL TEMED have to be added.
5. Cast the gradient gel and overlay it with deionized water to get a sharp line at the top after polymerization. The gel is polymerized within 60 min.
6. Discard the deionized water.
7. For the stacking gel, mix 1.5 mL of acrylamide solution with 2.5 mL of BN gel buffer and 11 mL of deionized water.
8. For polymerization, add 65 μL APS and 6.5 μL TEMED and cast the stacking gel on top of the separation gel. Use a comb according to the number of samples you want to analyze. The gel is polymerized within 30 min.
9. Prepare 1× BN anode buffer and 1× BN cathode buffer by diluting the corresponding stock solutions (*see* **Note 2**).
10. After removing the comb add the BN cathode and anode buffers to the upper and lower chambers of the gel unit, respectively. Cool the unit down to 4 °C.

3.2 Sample Preparation for BN Gel and CN Gel

The samples should be treated carefully in order to keep proteins in their native conformation (avoid high salt, ionic detergents, high temperatures, urea, etc). All steps of the sample preparation should be carried out on ice. The BN and CN gel should be prepared and cooled down before the sample preparation is started. Here we describe sample preparation for isolated mitochondria from Arabidopsis (*Arabidopsis thaliana*) cell culture but mitochondria from any other source can be used accordingly.

Sample preparation for BN gel:

1. Mitochondria (corresponding to about 500 μg mitochondrial protein) are centrifuged at 15,000 × *g* for 10 min at 4 °C using a microcentrifuge tube.

2. The mitochondrial pellet is resuspended in 100 µL of 5 % (w/v) digitonin solubilization buffer pH 7.4, and incubated for 15 min on ice.
3. Afterwards, samples are centrifuged for 10 min, 4 °C, at 20,000 × *g* using a microcentrifuge tube to remove insoluble material.
4. The supernatant contains solubilized proteins and protein complexes. Mix the supernatant with 5 µL blue loading buffer.

Sample preparation for CN gel:

5. Mitochondria including 45 µg protein are centrifuged at 15,000 × *g* for 10 min at 4 °C using a microcentrifuge tube.
6. The mitochondrial pellet is resuspended in 30 µL of 2.5 % digitonin solubilization buffer (solubilization buffer for ProDH; Subheading 2.3) and incubated for 15 min on ice.
7. Afterwards, samples are centrifuged for 10 min, 4 °C, at 20,000 × *g* using a microcentrifuge tube to remove insoluble material.
8. Mix the supernatant with 7.5 µL native loading buffer.

3.3 BN-PAGE Run

1. Load samples mixed with blue loading buffer into the gel pockets.
2. Connect the gel unit to a power supply. Start electrophoresis at constant voltage (100 V for 45 min) and continue at constant current (15 mA for about 11 h). Electrophoresis should be carried out at 4 °C. Bands of the OXPHOS complexes are already visible during the gel run.

3.4 CN-PAGE Run

1. Load the samples mixed with native loading buffer into the gel pockets.
2. Run the gel at 375 V, 4 °C, for ~3.5 h using a mini electrophoresis system available from a variety of suppliers.

3.5 In-Gel Activity Assays for BN-PAGE

1. Incubate the gel with 50 mL freshly prepared staining solution at room temperature (NADH dehydrogenase staining solution, succinate dehydrogenase staining solution, cytochrome c reductase staining solution (*see* **Note 3**), cytochrome c oxidase staining solution, ATPase staining solution (*see* **Note 4**), or GLDH staining solution (*see* **Note 5**)).
2. Staining takes 10–30 min for NADH dehydrogenase, up to several hours for succinate dehydrogenase, minimum of 6 h for cytochrome c reductase, 2 h for cytochrome c oxidase, 3 h to overnight incubation for ATPase, and ~30 min for GLDH.
3. The reactions are stopped by transferring the gel into fixing solution (*see* **Note 6**).

3.6 In-Gel Activity Assay for CN-PAGE

1. Incubate the gel for 10 min with 50 mL preincubation solution for ProDH activity while gently shaking. Subsequently discard the solution and incubate the gel with ProDH activity staining solution without shaking (*see* **Note 7**) for 1.5 h in the dark.
2. Scan the gel immediately after activity staining. The staining solution can be washed out with water. Subsequently the gel can be Coomassie stained.

4 Notes

1. Digitonin is necessary for the solubilization of membrane-bound protein complexes of cellular or organellar fractions. Solubilization buffer with digitonin should be heated to dissolve digitonin.
2. It is recommended to use cold water for dilution of the anode and cathode buffer; otherwise you have to wait to start the gel run until the buffers are cold.
3. After completion of the staining reaction visibility of precipitated TMB can be optimized using an image processing software (e.g., Adobe® Photoshop) by decreasing the blue channel of the RGB image file. The Coomassie blue background is not altered [for details *see* ref. 11].
4. After Complex V staining, do not transfer the gel to fixing solution. Acidic solutions can dissolve lead phosphate precipitates. Instead use 50 % (v/v) methanol for stopping the activity assay [15].
5. Incubate in the dark because PMS is light sensitive.
6. For some activity assays it is advisable to scan gels after incubation with fixing solution again. Coomassie blue background should be decreased after this step.
7. Do not shake the gel in the staining solution. Otherwise DCPIP will be washed out and activity bands are not visible anymore.

Acknowledgment

We thank Dagmar Lewejohann for expert technical assistance.

References

1. Schägger H, von Jagow G (1991) Blue native electrophoresis for isolation of membrane protein complexes in enzymatically active form. Anal Biochem 199:223–231
2. de St F, Groth S, Webster RG, Datyner A (1963) Two new staining procedures for quantitative estimation of proteins on electrophoretic strips. Biochim Biophys Acta 71:377–391
3. Zerbetto E, Vergani L, Dabbeni-Sala F (1997) Quantification of muscle mitochondrial oxidative phosphorylation enzymes via histochemical staining of blue native polyacrylamide gels. Electrophoresis 18:2059–2064
4. Jung C, Higgins CM, Xu Z (2000) Measuring the quantity and activity of mitochondrial electron transport chain complexes in tissues of central nervous system using blue native polyacrylamide gel electrophoresis. Anal Biochem 286:214–223
5. van Coster R, Smet J, George E et al (2001) Blue native polyacrylamide gel electrophoresis: a powerful tool in diagnosis of oxidative phosphorylation defects. Pediatr Res 50:658–665
6. Sabar M, Gagliardi D, Balk J, Leaver CJ (2003) ORFB is a subunit of F1F(O)-ATP synthase: insight into the basis of cytoplasmic male sterility in sunflower. EMBO Rep 4:381–386
7. Schertl P, Sunderhaus S, Klodmann J et al (2012) L-galactono-1,4-lactone dehydrogenase (GLDH) forms part of three subcomplexes of mitochondrial complex I in Arabidopsis thaliana. J Biol Chem 287:14412–14419
8. Schägger H, Cramer WA, von Jagow G (1994) Analysis of molecular masses and oligomeric states of protein complexes by blue native electrophoresis and isolation of membrane protein complexes by two-dimensional native electrophoresis. Anal Biochem 217:220–230
9. Lojda Z, Gossrau R, Schiebler T (1979) Enzyme histochemistry: a laboratory manual. Springer, Berlin, pp 1–270
10. Dubowitz V (1985) Muscle biopsy, a practical approach. Bailliere Tindall, London
11. Smet J, de Paepe B, Seneca S et al (2011) Complex III staining in blue native polyacrylamide gels. J Inherit Metab Dis 34: 741–747
12. Seligman AM, Karnovsky MJ, Wasserkrug HL et al (1968) Nondroplet ultrastructural demonstration of cytochrome oxidase activity with a polymerizing osmiophilic reagent, diaminobenzidine (DAB). J Cell Biol 38: 1–14
13. Cox GB, Downie JA, Fayle DR et al (1978) Inhibition, by a protease inhibitor, of the solubilization of the F1-portion of the Mg_2+-stimulated adenosine triphosphatase of Escherichia coli. J Bacteriol 133:287–292
14. Schertl P, Cabassa C, Saadallah K et al (2014) Biochemical characterization of ProDH activity in Arabidopsis mitochondria. FEBS J 281: 2794–2804
15. Wittig I, Karas M, Schägger H (2007) High resolution clear native electrophoresis for in-gel functional assays and fluorescence studies of membrane protein complexes. Mol Cell Proteomics 6:1215–1225

Chapter 10

Activity Assay for Plant Mitochondrial Enzymes

Shaobai Huang, Chun Pong Lee, and A. Harvey Millar

Abstract

Mitochondria are sites for respiration to produce chemical energy via oxidative phosphorylation. Their primary role has been viewed as the oxidation of organic acids via the tricarboxylic acid (TCA) cycle and the synthesis of ATP coupled to the transfer of electrons to O_2. TCA cycle enzymes are essential for plant carbon metabolism and provide the reductant for the electron transport chain (ETC) enzymes that in turn drives ATP synthesis. The activity of individual enzymes will determine the flux of metabolism and thus the downstream consequences for respiration rate. Measurements of activities of mitochondrial enzymes, such as components of TCA cycle and the ETC, can provide insight into regulation of mitochondrial function. The activities of these enzymes vary between developmental stages, in different tissues, and in response to environmental conditions. In this chapter, methods for enzymatic assay of TCA cycle enzymes and a number of the ETC complex enzymes are described in detail.

Key words Plant mitochondria, Mitochondrial metabolism, Mitochondrial enzymes, Tricarboxylic acid (TCA) cycle, Electron transport chain (ETC), Enzyme assay

1 Introduction

Mitochondria are the heart of chemical energy conversion processes in cells. The primary role of mitochondria has been viewed as the oxidation of organic acids via the tricarboxylic acid (TCA) cycle in conjunction with the synthesis of ATP that is coupled to the transfer of electrons to O_2. This pathway starts with the transport of pyruvate, the product of glycolysis in the cytosol, across the two mitochondrial membranes. Pyruvate is then decarboxylated and bonded to coenzyme A (CoA) to form acetyl-CoA with the production of NADH and the release of CO_2 by pyruvate dehydrogenase complex (PDC). Acetyl-CoA is subsequently oxidized in a sequence of reactions which are catalyzed by the enzymes of the TCA cycle. As shown in Fig. 1, these enzymes are citrate synthase, aconitase, isocitrate dehydrogenase, α-ketoglutarate dehydrogenase, succinyl-CoA synthetase, succinate dehydrogenase, fumarase, and malate dehydrogenase. In the TCA cycle, electrons are sequentially removed from acetyl-CoA and used to reduce NAD^+ to NADH or FAD to $FADH_2$.

James Whelan and Monika W. Murcha (eds.), *Plant Mitochondria: Methods and Protocols*, Methods in Molecular Biology, vol. 1305, DOI 10.1007/978-1-4939-2639-8_10,

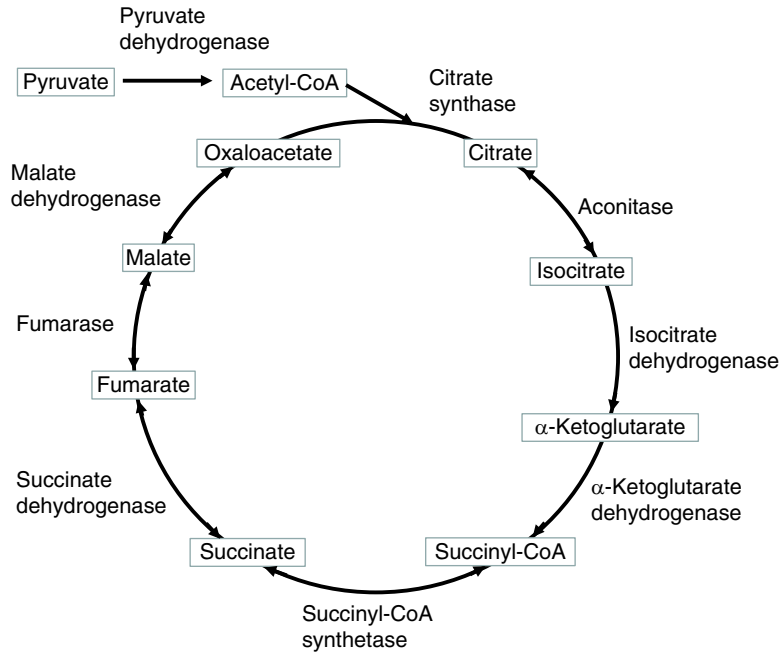

Fig. 1 Enzymes for the TCA cycle. The detailed reaction equation of individual enzyme is given in the enzyme assay

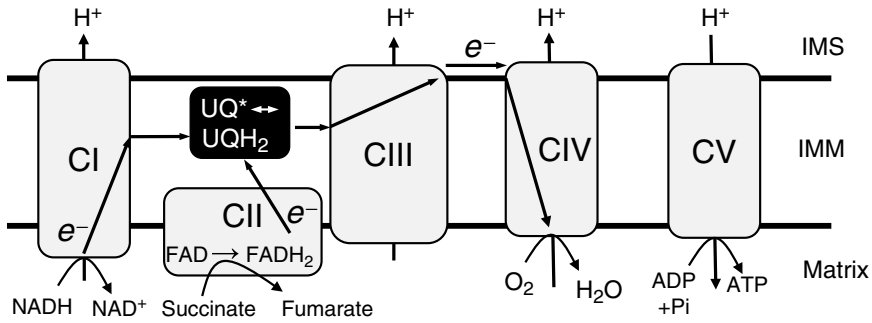

Fig. 2 Diagram of electron transport chain in the inner mitochondrial membrane. CI, CIII, and CIV pump protons from the matrix to the intermembrane space which builds a membrane potential that can be harnessed for ATP generation by CV. *CI* complex I, NADH dehydrogenase, *CII* complex II, succinate dehydrogenase, *CIII* complex III, cytochrome bc1, *CIV* complex IV, cytochrome c oxidase, *CV* complex V, ATP synthase, *UQ** ubisemiquinone, *UQH_2* reduced ubiquinone, *IMM* inner membrane, *IMS* intermembrane space

ATP is also generated within the TCA cycle in the reaction catalyzed by succinyl-CoA synthetase.

The mitochondrial inner membrane-located electron transport chain (ETC) consists of Complex I (NADH dehydrogenase), Complex II (succinate dehydrogenase), Complex III (cytochrome b/c_1 reductase), and Complex IV (cytochrome c oxidase) (Fig. 2). Electrons are transferred from NADH by Complex I and $FADH_2$

by Complex II to a lipid-soluble carrier, ubiquinone (UQ). The reduced product ubiquinol (UQH_2) then passes electrons through Complex III to Complex IV which reduces O_2 to form H_2O. Energy released through the transfer of electrons to O_2 is used to pump proton (H^+) from the matrix into the intermembrane space, creating an electrochemical proton gradient across the inner membrane. This H^+ gradient allows ATP synthase (Complex V) to generate ATP by harnessing the flow of H^+ back to the matrix (Fig. 2).

Activity measurements of mitochondrial enzymes, such as components of TCA cycle and the ETC, can provide insight into regulation of mitochondrial function. The activity of these enzymes varies between developmental stages, in different tissues, and in response to environmental conditions. The methods and procedures of isolation of plant mitochondria used for enzymatic assay are described in Chapter 2 of this book (*see* **Notes 1** and **2**). In this chapter, enzymatic assays for TCA cycle enzymes in Fig. 1 and a number of the ETC complex enzymes in Fig. 2 are described in detail.

2 Materials

2.1 Equipment

1. UV–VIS spectrophotometer (wavelength from 190 to 700 nm).
2. Cuvettes: Glass (reusable) or plastic (disposable) cuvette for wavelengths from 380 to 780 nm (visible spectrum).
3. Fused quartz cuvettes for wavelengths below 380 nm (ultraviolet spectrum).
4. Plate reader spectrophotometer.
5. Clear-bottom 96-well plates.
6. Micropipettes capable of dispensing 1–1,000 μL of solution.

2.2 Stock Solutions

1. PDC assay: 100 mM *N*,*N*,*N*′,*N*′-tetraethylsulfamide (TES)-NaOH pH 7.6, 10 % (v/v) Triton X-100, 100 mM $MgCl_2$, 100 mM β-NAD^+, 10 mM thiamine pyrophosphate (TPP), 10 mM lithium CoA (in 0.1 M cysteine), 100 mM L-cysteine, 100 mM sodium pyruvate.
2. Citrate synthase assay: 100 mM triethanolamine-KOH pH 7.9, 8.5 mM acetyl-CoA, 10 mM 3-acetylpyridine adenine dinucleotide (APAD), 300 mM malate, 10 % (v/v) Triton X-100, 200 U/mL commercial malate dehydrogenase.
3. Aconitase assay: 160 mM KH_2PO_4-NaOH pH 7.5, 100 mM β-nicotinamide adenine dinucleotide phosphate (β-$NADP^+$), 100 mM $MnCl_2$, 2 U of commercial NADP-isocitrate dehydrogenase, 10 % (v/v) Triton X-100, 400 mM aconitate.

4. Isocitrate dehydrogenase assay: 250 mM 4-(2-hydroxyethyl)-1-piperazineethanesulfonic acid (HEPES) buffer pH 7.6, 20 mM DL-isocitric acid, 6.6 mM β-$NADP^+$, 20 mM $MgSO_4$.
5. α-Ketoglutarate dehydrogenase assay: 1,000 mM 2-{[2-hydroxy-1,1-bis (hydroxymethyl)ethyl]amino} ethanesulfonic acid (TES)-KOH pH 7.0, 100 mM $MgCl_2$, 10 mM TPP, 100 mM NAD^+, 10 mM CoA (in 0.1 M cysteine), 100 mM cysteine, 10 mM adenine monophosphate, 10 mM α-ketoglutarate, 40–100 U/mg protein commercial lipoamide dehydrogenase.
6. Succinyl-CoA synthetase assay: *Reaction 1*—1 M tricine/KOH pH 8.0, 0.1 M $MgCl_2$, 1 mM ethylenedinitrilo tetraacetic acid (EDTA), 300–600 U/mL commercial glycerokinase, 1 M KH_2PO_4, 100 mM ADP, 1 mM 5′,5′-diadenosinpentaphosphate, 1 M glycerol, 0.05 M succinyl-CoA, 1 M HCl, 1 M NaOH. *Reaction 2*—1 M tricine–KOH pH 8.0, 50 mM $MgCl_2$, 50 mM β-NADH, ≥10 U/mg commercial glycerol-3-phosphate oxidase, 100–300 U/mg protein commercial α-glycerophosphate dehydrogenase.
7. Succinate dehydrogenase assay: 1 M potassium phosphate buffer pH 7.4, 1 M KCN, 10 mM EDTA-Na_2, 500 mM succinate Na_2, 90 mM 2,6-dichloroindolephenol (DCPIP), 160 mM phenazine methosulfate (PMS) (*see* **Note 3**), 10 % (w/v) BSA.
8. Fumarase assay: 1 M KH_2PO_4/NaOH pH 7.7, 1 M sodium malate.
9. Malate dehydrogenase assay: 1 M potassium phosphate buffer pH 7.4, 10 % (v/v) Triton X-100, 100 mM $MgCl_2$, 10 mM NADH, 50 mM oxaloacetic acid.
10. NADH:Q reductase (Complex I) assay: 100 mM Tris–HCl buffer pH 7.2, 100 mM NaCl, 10 mM NADH or deamino-NADH, 100 mM ferricyanide (FeCN).
11. Cytochrome c oxidase (Complex IV) assay: 100 mM KH_2PO_4/NaOH buffer pH 7.4, 1 mM cytochrome c (reduced) from bovine heart.

3 Methods

The concept of enzyme assays relies on measuring the loss of a substrate or the accumulation of a product. There are two main approaches to detect an enzyme reaction, termed direct or coupled approaches. If the substrate or product has a specific absorbance, the concentration of a substrate or a product can be directly measured. This is the case for some mitochondrial dehydrogenases, such as pyruvate dehydrogenase, malate dehydrogenase, and isocitrate dehydrogenase, because NADH formed during these enzy-

matic assays has a much higher absorbance at 340 nm than NAD^+. In contrast, coupled reaction uses one of the products as a reactant for an additional enzyme or another chemical reaction, such as in the case of citrate synthase, aconitase, and succinate dehydrogenase measurements. The second enzyme or chemical reaction is typically easier to measure as an absorbance change of this by-product. It is important to ensure that this coupled reaction is not rate limiting.

3.1 General Assay Methods Used in Enzyme Measurements

1. Assay methods: There are two main methods for quantifying the activity of an enzyme, a stop-time assay and a real-time assay. While the stop-time method is the easiest way to perform high-throughput assays, two criteria need to be fulfilled before it can be considered to be used: (a) the reaction rate must be linear, and (b) the substrate or product to be measured spectrophotometrically must be stable during the incubation. The stop-time method is used for assay of succinyl-CoA synthatase. Assays of most of the mitochondrial enzymes are determined in real-time assays. This method provides continual measurement of absorbance changes over time. From the graph (commonly from the software linked to the spectrophotometer), a region that is approximately linear is selected for calculating OD/min. This rate is then converted into a more descriptive value of enzymatic activities using the absorption coefficient (extinction coefficient) of the compound being measured. Enzymatic activity is usually expressed in moles per minute per milligram of total mitochondrial protein (mol/min/mg protein).
2. Temperature: Plant mitochondria enzyme assays are normally conducted at 25 °C unless otherwise stated below.
3. Absorbance: Most spectrophotometers can only read between 0.01 and 3.0 absorbance units and the assays have been configured to work within this range.
4. Control assays: A control assay has all the substrates needed for initiating reactions but does not contain any mitochondrial extract. Performing control assays is important to account for any drift in the baseline absorbance.
5. Reaction volume and loading amount of mitochondria: Usually the final volume of reaction solution is one mL or three mL and depends on cuvettes, the expense on chemicals, or the amount of enzymes available. Each assay uses 10–50 μg of mitochondrial protein in a 1 mL reaction solution but this can vary with the activity of each enzyme.

3.2 Pyruvate Dehydrogenase Complex

Pyruvate dehydrogenase complex (PDC) is the entry enzyme for TCA cycle and catalyzes the following reaction:

$$\text{Pyruvate} + \text{NAD}^+ + \text{CoA} \rightarrow \text{Acetyl} - \text{CoA} + \text{CO}_2 + \text{NADH}$$

PDC activity is assayed spectrophotometrically by measuring NADH formation at 340 nm. The extinction coefficient of NADH at 340 nm (ε340) is 6,220 M^{-1} cm^{-1} [1–3].

1. Mix the stock solutions listed in Subheading 2.2 to the final reaction concentrations: 50 mM TES-NaOH (pH 7.6), 0.2 % (v/v) Triton X-100, 1 mM $MgCl_2$, 2 mM β-NAD^+, 0.2 mM thiamine pyrophosphate, 0.12 mM lithium-CoA, 2 mM L-cysteine, 1 mM sodium pyruvate.
2. Add the isolated mitochondrial sample to initiate the reaction.
3. Record the change of absorbance at 340 nm against time.

3.3 Citrate Synthase

Citrate synthase catalyzes the following reaction:

$$\text{Oxaloacetate} + \text{Acetyl} - \text{CoA} + \text{H}_2\text{O} \rightarrow \text{Citrate} + \text{CoA} - \text{SH}$$

Citrate synthase activity is measured by following the reduction of APAD at 365 nm. Malate oxidation to oxaloacetate (OAA) by commercial malate dehydrogenase is coupled to APAD reduction. This reaction only proceeds if OAA is being used by citrate synthase because the malate dehydrogenase reaction is strongly inhibited by OAA. The overall combined reaction is therefore:

$$\text{Malate} + \text{acetyl} - \text{CoA} + \text{APAD}^+ \rightarrow \text{citrate} + \text{APADH} + \text{CoA} - \text{SH}$$

The rate of APAD reduction is followed spectrophotometrically by measuring absorbance changes at 365 nm. The extinction coefficient of APADH at 365 nm (ε365) is 9,100 M^{-1} cm^{-1} [4, 5].

1. Mix the stock solutions listed in Subheading 2.2 to the final reaction concentrations: 90 mM triethanolamine-KOH (pH 7.9), 0.05 % (v/v) Triton X-100, 3 mM malate, 0.2 mM APAD, 12 U/mL malate dehydrogenase, and 0.2 mM acetyl-CoA.
2. The mitochondrial sample is initially incubated in reaction medium without acetyl-CoA at 25 °C for 10–15 min. Assays are initiated by the addition of acetyl-CoA.
3. The absorbance at 365 nm over time is measured.

3.4 Aconitase

Aconitase catalyzes the following reaction:

$$\text{Citrate} \Leftrightarrow \text{cis} - \text{aconitate} + \text{H}_2\text{O} \Leftrightarrow \text{isocitrate}$$

The coupled reaction involves measuring the rate of $NADP^+$-isocitrate dehydrogenase with the following equation:

$$\text{Isocitrate} + \text{NADP}^+ \rightarrow \alpha - \text{ketoglutarate} + \text{CO}_2 + \text{NADPH} + \text{H}^+$$

The rate of NADPH synthesis is measured by change of absorbance at 340 nm. The extinction coefficient of NADPH at 340 nm (ε340) is 6,220 M^{-1} cm^{-1} [6, 7].

1. Mix the stock solutions listed in Subheading 2.2 to the final reaction concentrations: 80 mM KH_2PO_4-NaOH (pH 7.8), 0.5 mM $NADP^+$, 0.5 mM $MnCl_2$, 2 U/mL of NADP-isocitrate dehydrogenase, 0.05 % (v/v) Triton X-100, 8 mM aconitate.
2. The reaction is initiated by adding the mitochondrial sample.
3. The absorbance at 340 nm is measured over time.

3.5 Isocitrate Dehydrogenase

Isocitrate dehydrogenase catalyzes the following reaction:

$$\text{Isocitrate} + \text{NAD}^+ \rightarrow \alpha - \text{ketoglutarate} + \text{CO}_2 + \text{NADH} + \text{H}^+$$

The rate of NADH synthesis can be directly measured as increased absorbance at 340 nm. The extinction coefficient of NADH at 340 nm (ε340) is 6,220 M^{-1} cm^{-1} [8].

1. Mix the stock solutions listed in Subheading 2.2 to the final reaction concentrations: 50 mM HEPES (pH 7.6), 1 mM $MnSO_4$, 2 mM DL-isocitrate acid, 0.66 mM β-NAD^+.
2. The reaction is initiated by adding mitochondrial sample.
3. The absorbance at 340 nm is measured over time.

3.6 α-Ketoglutarate Dehydrogenase

α-Ketoglutarate dehydrogenase catalyzes the following reaction:

$$\alpha - \text{Ketoglutarate} + \text{NAD}^+ + \text{CoA} - \text{SH} \rightarrow \text{succinyl} - \text{CoA} + \text{NADH} + \text{H}^+ + \text{CO}_2$$

NADH synthesis can be directly measured as increased absorbance at 340 nm. The extinction coefficient of NADH at 340 nm (ε340) is 6,220 M^{-1} cm^{-1} [9, 10].

1. Mix the stock solutions listed in Subheading 2.2 to the final reaction concentrations: 70 mM TES-KOH (pH 7.0), 2 mM $MgCl_2$, 0.2 mM TPP, 2 mM NAD^+, 0.12 mM CoA, 20 mM cysteine, 0.5 mM AMP, 1 mM α-ketoglutarate, 2 U/mL commercial porcine lipoamide dehydrogenase.
2. The reaction is initiated by adding mitochondrial sample.
3. The absorbance at 340 nm is measured over time.

3.7 Succinyl-CoA Synthetase

Succinyl-CoA synthetase catalyzes the following reaction:

$$\text{Succinyl} - \text{CoA} + \text{ADP} + \text{Pi} \Leftrightarrow \text{succinate} + \text{CoA} - \text{SH} + \text{ATP}$$

In this coupled assay, ATP produced by succinyl-CoA drives the oxidation of NADH in the enzymatic cycle between glycerol-3-phosphate oxidase and glycerol-3-phosphate dehydrogenase. The complete reactions of this enzymatic assay are

1. $\text{Succinyl} - \text{CoA} + \text{ADP} + \text{Pi} \Leftrightarrow \text{succinate} + \text{CoA} - \text{SH} + \text{ATP}$ (succinyl-CoA synthetase)
2. $\text{ATP} + \text{glycerol} \rightarrow \text{ADP} + \text{glycerol 3} - \text{phosphate}$ (Glycerokinase)
3. $O_2 + \text{NADH} + H^+ \rightarrow H_2O_2 + NAD^+$ (glycerol-3-phosphate oxidase/glycerol-3-phosphate dehydrogenase cycle)

The rate of NADH oxidation is measured as a decreased absorbance at 340 nm. The extinction coefficient of NAD^+ at 340 nm (ε340) is 6,220 M^{-1} cm^{-1} [11].

Reaction 1

1. Mix the stock solutions listed in Subheading 2.2 to the final reaction concentrations in the final volume of 100 μL: 100 mM tricine/KOH (pH 8.0), 10 mM $MgCl_2$, 0.1 mM EDTA, 1 U/mL glycerokinase, 10 mM KH_2PO_4, 2.5 mM ADP, 100 μM 5′,5′-diadenosinpentaphosphate, 120 mM glycerol, and 100 μM succinyl-CoA.
2. The reaction is initiated by adding mitochondrial sample and terminated by the addition of 50 μL 1 M HCl and 50 μL 1 M NaOH.
3. The reaction mixture is heated at 95 °C for 20 min to destroy un-reacted 5′,5′-diadenosinpentaphosphate and is then allowed to cool on ice.

Reaction 2

1. Prepare reaction solution by mixing the stock solutions listed in Subheading 2.2 for this step to the final reaction concentrations: 100 mM tricine-KOH (pH 8.0), 2.25 mM $MgCl_2$, 1.5 mM NADH, ~2.7 U/mL glycerol-3-phosphate oxidase, ~1.1 U/mL glycerol-3-phosphate dehydrogenase.
2. Mix 200 μL solution from of reaction 1 to the 100 μL of reaction solution.
3. Immediately after a brief mixing of the media, the absorbance is measured at 340 nm at 30 °C for 30 min (or until the rates are stabilized) using a plate reader.

3.8 Succinate Dehydrogenase

Succinate dehydrogenase (Complex II) is both an enzyme of the TCA cycle and a complex of the ETC complex. Succinate dehydrogenase catalyzes the following reaction equation:

$$\text{Succinate} + \text{UQ} \Leftrightarrow \text{fumarate} + \text{UQH}_2$$

In this reaction, UQ is the receptor of electrons from succinate. For enzymatic activity assays, PMS is used as an intermediate electron carrier and coupled with DCPIP as an electron acceptor. Succinate dehydrogenase activity is assayed spectrophotometrically by measuring the change of the absorbance of DCPIP at 600 nm. The extinction coefficient of DCPIP at 600 nm is 0.021 M^{-1} cm^{-1} [12, 13].

1. Mix the stock solutions listed in Subheading 2.2 to the final reaction concentrations: 50 mM potassium phosphate buffer (pH 7.4), 50 mM KCN, 0.1 mM EDTA-Na_2, 10 mM succinate Na_2, 0.09 mM DCPIP, 1.6 mM PMS, 0.1 % BSA.
2. Assay is initiated by adding the mitochondrial sample.
3. The absorbance at 600 nm is measured over time.

3.9 Fumarase

Fumarase (fumarate hydratase) catalyzes the following reaction:

$$\text{Fumarate} + H_2O \Leftrightarrow \text{L} - \text{malate}$$

The absorbance of fumarate at 240 nm can be recorded directly by spectrophotometry. The extinction coefficient of fumarate at 240 nm (ε240) is 2,530 M^{-1} cm^{-1} [6, 7, 14].

1. Mix the stock solutions listed in Subheading 2.2 to the final reaction concentrations: 70 mM KH_2PO_4/NaOH (pH 7.7), and 40 mM sodium malate.
2. The reaction is initiated by adding the mitochondrial sample.
3. The absorbance at 240 nm is measured over time.

3.10 Malate Dehydrogenase

Malate dehydrogenase catalyzes the following reaction:

$$\text{L} - \text{Malate} + NAD^+ \Leftrightarrow \text{oxaloacetate} + NADH + H^+$$

The reaction rate is determined directly by measuring the decrease in absorbance at 340 nm due to the oxidation of NADH. The extinction coefficient of NADH at 340 nm (ε340) is 6,220 M^{-1} cm^{-1} [6].

1. Mix the stock solutions listed in Subheading 2.2 to the final reaction concentrations: 100 mM potassium phosphate buffer (pH 7.4), 0.05 % (v/v) Triton X-100, 5 mM $MgCl_2$, 0.25 mM NADH, and 0.2 mM oxaloacetic acid.
2. The reaction is initiated by adding the mitochondrial sample.
3. The absorbance at 340 nm is measured over time.

3.11 NADH:UQ Oxidoreductase (Complex I)

NADH:UQ Oxidoreductase or Complex I is a large transmembrane protein complex in the inner mitochondrial membrane and catalyzes the following reaction:

$$NADH + H^+ + CoQ + 4H^+_{in} \rightarrow NAD^+ + CoQH_2 + 4H^+_{out}$$

The rate of NADH:UQ oxidoreductase activity is typically measured using FeCN rather than UQ as an electron acceptor. The reduction of FeCN by NADH can be spectrophotometrically monitored at an absorbance of 420 nm. For calculation of specific NADH:FeCN reductase activity, an extinction coefficient at 420 nm of 0.00103 M^{-1} cm^{-1} is used [15, 16].

1. Mix the stock solutions listed in Subheading 2.2 to the final reaction concentrations: 50 mM Tris–HCl, pH 7.2, 50 mM NaCl, 0.2 mM NADH or deamino-NADH (*see* **Note 4**), and 1 mM FeCN.
2. The reaction is initiated by adding mitochondrial sample.
3. The absorbance at 420 nm is measured over time.

3.12 Cytochrome c Oxidase (Complex IV)

The enzyme cytochrome c oxidase or Complex IV is a large transmembrane protein complex in the inner mitochondrial membrane. Cytochrome c oxidase catalyzes the following reaction:

$$4\ Fe^{2+} - \text{cytochrome c} + 8\ H^{+}_{in} + O_2 \rightarrow 4\ Fe^{3+} - \text{cytochrome c} + 2H_2O + 4\ H^{+}_{out}$$

The absorbance of reduced cytochrome c at 550 nm can be recorded directly by spectrophotometry. The extinction coefficient of reduced cytochrome c from bovine heart at 550 nm is 28 M^{-1} cm^{-1} [7].

1. Mix the stock solutions listed in Subheading 2.2 to the final reaction concentrations: 21 mM KH_2PO_4/NaOH (pH 7.4), and 0.05 mM cytochrome c (reduced).
2. The reaction is initiated by adding the mitochondrial sample.
3. The absorbance at 550 nm is measured over time.

4 Notes

1. Some loss of mitochondrial enzyme activity occurs following multiple freeze/thaw cycles.
2. Once thawed, mitochondrial samples must be kept on ice to prevent proteolysis.
3. The stock solutions of DCPIP and PMS should be stored in the dark.
4. Only Complex I and not the rotenone-insensitive NAD(P)H dehydrogenase can use deamino-NADH as electron donor [17], so selective use of deamino-NADH makes this assay specific for Complex I.

Acknowledgements

AHM is funded by the Australian Research Council (ARC) through the ARC Centre of Excellence in Plant Energy Biology (CE140100008). SH and AHM are supported by ARC Future Fellowship (FT130101338 and FT110100242). CPL is funded by a long-term EMBO Fellowship (ALTF1140-2011).

References

1. Budde RJ, Randall DD (1990) Pea leaf mitochondrial pyruvate dehydrogenase complex is inactivated in vivo in a light-dependent manner. Proc Natl Acad Sci 87:673–676
2. Moore AL, Gemel J, Randall DD (1993) The regulation of pyruvate dehydrogenase activity in pea leaf mitochondria (the effect of respiration and oxidative phosphorylation). Plant Physiol 103:1431–1435
3. Millar AH, Knorpp C, Leaver CJ, Hill SA (1998) Plant mitochondrial pyruvate dehydrogenase complex: purification and identification of catalytic components in potato. Biochem J 334:571–576
4. Stitt M, Lilley R, Gerhardt R et al (1989) Metabolite levels in specific cells and subcellular compartments of plant leaves. Methods Enzymol 174:518–552
5. Jenner HL, Winning BM, Millar AH et al (2001) NAD malic enzyme and the control of carbohydrate metabolism in potato tubers. Plant Physiol 126:1139–1149
6. Cooper TG, Beevers H (1969) Mitochondria and glyoxysomes from castor bean endosperm. J Biol Chem 244:3507–3513
7. MacDougall AJ, ap Rees T (1991) Control of the Krebs cycle in Arum spadix. J Plant Physiol 137:683–690
8. Cox GF, Davies DD (1967) Nicotinamide-adenine dinucleotide-specific isocitrate dehydrogenase from pea mitochondria, purification and properties. Biochem J 105:729–734
9. Millar AH, Hill SA, Leaver CJ (1999) Plant mitochondrial 2-oxoglutarate dehydrogenase complex: purification and characterization in potato. Biochem J 343:327–334
10. Taylor NL, Heazlewood JL, Day DA et al (2004) Lipoic acid-dependent oxidative catabolism of α-keto acids in mitochondria provides evidence for branched-chain amino acid catabolism in Arabidopsis. Plant Physiol 134:838–848
11. Studart-Guimaraes C, Gibon Y, Frankel N et al (2005) Identification and characterisation of the alpha and beta subunits of succinyl CoA ligase of tomato. Plant Mol Biol 59:781–791
12. Oestreicher G, Hogue P, Singer TP (1973) Regulation of succinate dehydrogenase in higher plants: II. Activation by substrates, reduced coenzyme Q, nucleotides, and anions. Plant Physiol 52:622–626
13. Huang S, Taylor NL, Narsai R et al (2010) Functional and composition differences between mitochondrial complex II in Arabidopsis and rice are correlated with the complex genetic history of the enzyme. Plant Mol Biol 72:331–342
14. Hatch MD (1978) A simple spectrophotometric assay for fumarate hydratase in crude tissue extracts. Anal Biochem 85:271–275
15. Friedrich T, Hofhaus G, Ise W et al (1989) A small isoform of NADH: ubiquinone oxidoreductase (complex I) without mitochondrially encoded subunits is made in chloramphenicol-treated Neurospora crassa. Eur J Biochem 180:173–180
16. Herz U, Schröder W, Liddell A et al (1994) Purification of the NADH:ubiquinone oxidoreductase (complex I) of the respiratory chain from the inner mitochondrial membrane of Solanum tuberosum. J Biol Chem 269:2263–2269
17. Rasmusson AG, Møller IM (1991) NAD(P)H dehydrogenases on the inner surface of the inner mitochondrial membrane studied using inside-out submitochondrial particles. Physiol Plant 83:357–365

Chapter 11

Analysis of Type II NAD(P)H Dehydrogenases

Kathleen L. Soole and Chevaun A. Smith

Abstract

Plant mitochondria contain at least four type II NAD(P)H dehydrogenases that link NAD(P)H oxidation to the inner membrane electron transport chain and bypass proton pumping at Complex I, hence ATP synthesis. These activities have been found in mitochondria isolated from all plant species analyzed to date. In this chapter, methods are presented to analyze the expression of genes encoding these dehydrogenases and to detect protein levels in mitochondria isolated from Arabidopsis (*Arabidopsis thaliana*). In addition, methods and assay conditions are presented to detect the activity of each of these four type II NAD(P)H dehydrogenases in isolated plant mitochondria.

Key words Type II NAD(P)H dehydrogenase, Plant mitochondria, Alamethicin, qPCR, Immunoblotting

1 Introduction

Plant mitochondria are characterized by the presence of a non-phosphorylating electron transport chain (ETC) that comprises separate proteins, distinct from the protein complexes (I–V) that are known as the phosphorylating, or cytochrome pathway (CP). The presence of this alternative pathway (AP) of electron transport allows the flow of electrons from cytosolic and matrix NAD(P)H or FADH to oxygen without pumping protons and producing ATP, and includes a number of type II NAD(P)H dehydrogenases and the alternative oxidase (AOX). While these proteins are distinct from those of the CP, they do interact with the phosphorylating pathway through the ubiquinone pool, thus providing plant mitochondria with a level of flexibility with respect to the number of proton-pumping sites electron pass through. Consequently, ATP production can range from potentially 0 to 2.5 ATP per pair of electrons. This gives the plant metabolic flexibility by uncoupling respiration from the cellular energy charge, which may be important at times of high respiration, as seen in thermogenic plants, and during stress responses. This is evident from the well-documented

James Whelan and Monika W. Murcha (eds.), *Plant Mitochondria: Methods and Protocols*, Methods in Molecular Biology, vol. 1305, DOI 10.1007/978-1-4939-2639-8_11,

increase in AOX under various cellular stresses [1]. While there are extensive studies assessing the role of AOX, there is less known about the biological role of the non-phosphorylating, alternative NAD(P)H dehydrogenases. However, evidence is building that they respond in a similar way during stress and may play a role in reactive oxygen species (ROS) minimization and enhancing plant growth under environmental stress [2]. Additionally, it has been observed that these NAD(P)H dehydrogenases can influence the cellular redox state, as transgenic tobacco plants with altered levels of these enzymes can alter the NADPH:NADP ratio and impact the timing of flower development and internode length [3, 4].

Plant mitochondria generally show five different activities associated with NAD(P)H oxidation, four associated with the inner membrane and one with the outer membrane (Fig. 1) [5, 6]. The outer membrane activity is often overlooked but an NADH:cytochrome b5 reductase has been shown to be linked to lipid metabolism in Arabidopsis using a T-DNA mutation in the corresponding gene [7, 8]. However, under particular in vitro assay conditions, this activity can donate electrons to cytochrome c in the inner membrane space, and thereby has the capacity to donate electron to Complex IV. If this occurs in vivo, it may provide another pathway for cytosolic NAD(P)H to contribute to ATP production. This has been demonstrated in isolated mitochondria, but it is not clear whether this occurs *in planta* [9].

Two of the inner membrane type II dehydrogenases face the cytosolic side of the inner membrane and can oxidise extramitochondrial NADH and NADPH. Inhibitor and biochemical analyses in the 1980s and 1990s led to the conclusion that two separate dehydrogenases are responsible for these activities (*see* [6] for review). Within the mitochondria, NADH can be oxidized by Complex I of the CP, but also by a type II dehydrogenase that is insensitive to Complex I inhibitors such as rotenone. NADPH generated in the matrix can also be oxidized in a rotenone-insensitive manner and inhibitor studies have shown that two separate, matrix-facing, or internal dehydrogenases are responsible for matrix NADH and NADPH oxidation, rather than interconversion of matrix NADPH to NADH via a transhydrogenase as found in mammalian mitochondria [10]. The four alternative NAD(P)H dehydrogenases show differential sensitivity to the calcium chelator, EGTA, suggesting the need for different calcium levels for full activity. NADPH oxidation often shows a complete dependence on the presence of calcium while there appears to be a level of calcium-independent, as well as calcium-dependent, NADH oxidation. This is the case for both external and matrix-facing NAD(P)H oxidation and provides further evidence to suggest that these two activities are mediated by separate dehydrogenases.

During the 1980s and 1990s, several protein purification studies showed that the plant type II dehydrogenases were simple,

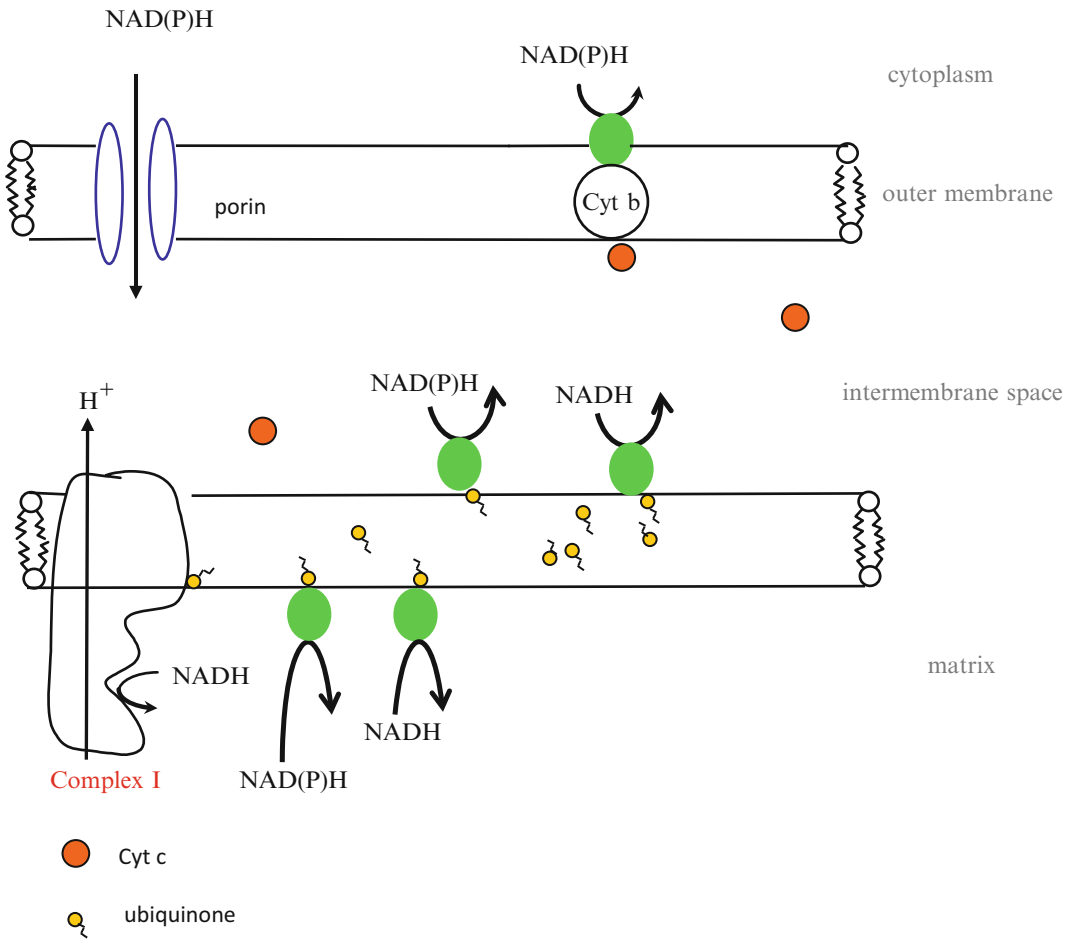

Fig. 1 Type II NAD(P)H dehydrogenases associated with plant mitochondria. This diagram shows an abridged form of the inner membrane electron transport chain (ETC) with only the NAD(P)H dehydrogenases. These enzymes accept electrons from NAD(P) and donate them to the ubiquinone pool. This diagram includes an NADH(P)H dehydrogenase shown to be associated with the outer membrane; under certain conditions in vitro, such as in the presence of added cytochrome c, it is possible to link this enzyme to the inner membrane ETC via an association with cytochrome c in the intermembrane space. It is not clear whether this occurs in vivo

single, or dimeric polypeptides of size ranging from 43 kDa in red beet to 58 kDa in maize [11–13]. The release of the Arabidopsis genome sequence has allowed the link between gene and enzyme activity in this species to be explored using a recombinant protein expression approach [14, 15] as well as a reverse genetic approach *in planta* [2, 16]. From the Arabidopsis genome, seven genes encoding type II NAD(P)H dehydrogenases have been identified (Table 1). In vitro translation, protein import, recombinant protein expression, and a transgenic plant approach have linked these genes to the various activities found in isolated mitochondria, as summarized (Table 1), although some uncertainties about substrate specificity for each gene product in Arabidopsis continue to exist.

Table 1
Summary of type II NAD(P)H dehydrogenases associated with the Arabidopsis inner mitochondrial membrane

	Accession number	Intramitochondrial location	Intracellular location	Protein length (amino acids)	Substrate specificity	Calcium dependence
NDA1	At1g07180	Matrix facing/internal	M/P	510	Unknown	Calcium binding unknown
NDA2	At2g29990	Matrix facing/internal	M/P	508	Unknown	Calcium binding unknown
NDB1	At4g28220	External	M/P	571	NADPH [1,2]	EF-hand motif; shown to bind calcium
NDB2	At4g05020	External	M	582	NADH [1]	EF-hand motif; shown to bind calcium
NDB3	At4g21490	External	Not expressed	581	Unknown	EF-hand motif; calcium binding unknown
NDB4	At2g20800	External	M	582	NADH/NADPH [1,2]	EF-hand motif; sensitivity to calcium unclear
NDC1	At5g08740	Matrix facing/internal	M/Chl	519	Unknown	Calcium binding unknown

The intramitochondrial location determined from both bioinformatics and in vitro import experiments [15]. Dual-cellular location as determined by sequence analysis and in vivo targeting data [17, 18] and defined as M for mitochondria, P for peroxisome, and Chl for plastid location. As indicated these proteins have an EF-hand motif determined from sequence alignment and indicative of a potential calcium binding capacity [19]. Some enzyme activities have been determined for recombinant expression in bacterial system[1], where calcium binding was also demonstrated [14]. For NDB1 and NDB4 enzyme assays of isolated mitochondria from transgenic plants[2] have linked this protein with specific activities [2, 3]

For example, NAD(P)H dehydrogenase C1 (NDC1) has been shown to span the inner membrane [15] and it is unclear whether the active site for NAD(P)H is on the intermembrane space side or the matrix side of the membrane. The substrate for this enzyme also has not been determined. To further complicate our view of the role of these alternative NAD(P)H dehydrogenases, it has been shown that some of the Arabidopsis genes encoding them contain dual targeting sequences within their coding sequences, resulting in potentially multiple cellular locations for these gene products [17, 18]. This has also been shown for the rice homologues of the Arabidopsis genes and is summarized in Table 1. Some substrate specificities have been determined but only for NDB1 [3], NDB2, and NDB4, using both recombinant expression in bacteria and plants [2, 3, 14]. It is evident that NDB1 is an NADPH-specific external dehydrogenase and NDB2 is an NADH-specific external

dehydrogenase. However, for NDB4 it is unclear whether it shows specificity and may use both NADH and NADPH [2, 14].

In this chapter, we present a method to quantitate the expression level of the genes encoding this family in Arabidopsis, using quantitative real-time PCR, and immunoblot methods for the determination at protein levels. The antibodies that we have developed detect these proteins in both Arabidopsis and rice. We also present assays to measure the activity of each of the dehydrogenases found associated with the inner membrane.

1.1 Conditions for Measuring NAD(P)H Oxidation

Unlike AOX, which can be assayed in whole-tissue samples using the oxygen isotope discrimination method [20], the alternative dehydrogenases cannot be measured in whole tissues, so purified mitochondria must be the starting material when determining specific dehydrogenase activities. Routine methods for purification of mitochondria from most plant tissues exist but each tissue needs the protocol to be optimized for extraction and gradient choice (Chapter 2). However, for isolation of Arabidopsis leaf and root mitochondria, we use the method of Day et al. [21] based on a continuous Percoll (28 %) gradient with a 0–10 % PVP gradient. This focuses the mitochondria towards the bottom of the gradient, with peroxisomes as a pellet.

The features that distinguish the multiple NAD(P)H dehydrogenases found on the inner membrane from each other are their sidedness on the membrane, their substrate specificity, and their sensitivity to calcium. These enzymes can have their activity determined by either measuring electron flow to oxygen or to artificial electron acceptors such as ubiquinone-50 analogues or ferricyanide/DCPIP. However, the calcium sensitivity is only preserved when activity is determined using oxygen uptake or ubiquinone analogues such as decyl-ubiquinone. Thus the use of ferricyanide/ or 2,6-dichlorophenolindophenol (DCPIP) as electron acceptors cannot distinguish between the Ca-sensitive or -insensitive activities. Further, if mitochondria are disrupted and the dehydrogenases released either by sonication or detergent treatment, the properties that distinguish these dehydrogenases from each other may be lost. Consequently, as previously mentioned these activities can only be determined in intact mitochondria, using isotonic reaction media with either oxygen [22] or decylubiquinone as the electron acceptor [14].

Because the active site of the dehydrogenases faces the inner side of the inner membrane and NAD(P)H cannot cross this membrane, the assay for the internal matrix-facing NAD(P)H dehydrogenases requires a set of conditions where access of NAD(P)H is provided. This can be achieved in at least three ways:

1. By generating NAD(P)H in the matrix: This can be done by providing a substrate to the isolated mitochondria that will generate NAD(P)H in the matrix and then using rotenone to inhibit any electron flow through Complex I. For example,

malate can be oxidized by malate dehydrogenase and/or malic enzyme [2, 22].

2. By creating submitochondrial particles, using conditions where there is a higher concentration of inside-out particles [23], and then supplying NAD(P)H directly in the presence of the Complex I inhibitor, rotenone.
3. By allowing NAD(P)H to cross the inner membrane by use of an ionophore to permeabilize the membrane, which has proven to give equivalent rates: It has been shown that the ionophore, alamethicin (AlaM), which is a 20-residue channel-forming peptide from the fungus *Trichoderma viride* used to permeabilize the inner membrane of mammalian mitochondria [24], can also do this in potato root and leaf mitochondria [25] and in mitochondria isolated from *Hoya carnosa* leaves [26].

The first of the above strategies may lead to underestimations of the maximal capacity of these dehydrogenases as it relies on an additional step to generate NADH. Further, this method cannot distinguish between NADH-specific or NADPH-specific enzymes as there are NAD and NADP isoforms of the malate-oxidizing enzymes present in plant mitochondria. The second approach also has limitations as it has been shown that the type II dehydrogenases can be released from the membrane using sonication [13], which again will result in an underestimation of capacity. Additionally, even though a higher ionic strength sonication media can result in a high proportion of inside-out particles, right-side-out particles are still present, allowing the external-facing NAD(P)H dehydrogenases to contribute to the NAD(P)H oxidation rates. Consequently, the use of AlaM to allow entry of NAD(P)H into the matrix directly remains the most favorable method currently and is the recommended method here.

The following sections present the methods for the quantitative assessment of the level of transcript and protein of the type II NAD(P)H dehydrogenases as well as specific assays for each of these enzymes found in plant mitochondria.

2 Materials

2.1 Growth of Plants

Plants (*Arabidopsis thaliana* ecotype. Columbia-0) are grown under controlled conditions: 14-h light, 10-h dark, light intensity 100–120 μE/m/s, 23 °C in soil.

Hydroponic plant growth: 0.5× Hoagland's solution: 2.5 mM KNO_3, 2.5 mM $Ca(NO_3)_2$, 1 mM $MgSO_4$, 0.5 mM KH_2PO_4, 0.05 % (v/v) micronutrient stock solution (46.2 mM H_3BO_3, 9.14 mM $MnCl_2{\cdot}4H_2O$, 0.765 mM $ZnSO_4{\cdot}7H_2O$, 0.32 mM $CuSO_4{\cdot}5H_2O$, 1.03 mM $Na_2MoO_4{\cdot}2H_2O$), 0.447 mM $FeCl_3{\cdot}6H_2O$, 1.02 mM Na EDTA. Add $FeCl_3$ and EDTA together and mix before adding to final solution pH 5.8 (*see* **Note 1**).

2.2 Determination of Transcript Abundance of the NAD(P)H Dehydrogenase

Performed using commercial kits, such as Plant mini RNA kit (Bioline, USA), iScript (Bio-Rad), and the SsoFast™ EvaGreen® Supermix in a CFX96™ Real-Time PCR Detection System (Bio-Rad, USA).

2.2.1 RNA Isolation and cDNA Synthesis

1. Nuclease-free water.
2. Spectrometer.
3. Commercial RNase-free DNase (1 U/μL).
4. PCR machine.
5. 0.2-mL PCR tubes.
6. 0.2 mM $MgCl_2$.
7. 0.2 mM dNTPs.
8. NanoDrop™1000 Spectrophotometer (Thermo-Scientific, USA).

2.3 Analysis of Type-II NAD(P)H Dehydrogenase Proteins

1. SDS-PAGE loading buffer: 250 mM Tris-HCl pH 6.8, 8 % (w/v), sodium dodecyl sulfate (SDS), 40 % (w/v) glycerol 0.01 % (v/v), bromophenol blue. Add 400 mM dithiothreitol (DTT) to a small aliquot prior to use.
2. TBST solution: 50 mM Tris, 150 mM NaCl, and 0.05 % (v/v) Tween-20 pH 7.4 with 5 % (w/v) skim milk powder were used where indicated and for membrane washing steps.
3. Protein molecular mass marker.
4. Secondary antibody: Anti-rabbit-horseradish peroxidase (HRP)-goat IgG.
5. Clarity Luminol Substrate and Clarity Peroxide Solution of the Clarity™ Western ECL substrate mix (Bio-Rad).
6. Chemiluminescence imagining system.

2.4 Determination of the Enzyme Activity of the Type II NAD(P)H Dehydrogenase

1. Clark oxygen electrode; Rank Brothers, Cambridge, UK or Hansatech, Norwich, UK.
2. Spectrophotometer suitable to detect NAD(P)H oxidation.
3. Reaction medium (external NAD(P)H dehydrogenase measurement): 50 mM MOPS/KOH, pH 7.2, 50 mM KCl, 150 mM mannitol, 2.5 mM $MgCl_2$, 0.2 mg/L antimycin A, 50 μM *n*-propyl gallate, 0.4 μM FCCP, 0.5 mM EGTA.
4. Reaction medium (internal NAD(P)H dehydrogenase measurement): 0.3 M sucrose, 10 mM TES (N-tris [hydroxymethyl] methyl-2-aminoethanesulfonic acid), 10 mM KH_2PO_4, 10 mM $MgCl_2$, pH 7.2.
5. Substrates and other compounds were purchased from Sigma-Aldrich, St Louis, USA. Stock solutions NADH (100 mM), NADPH (100 mM), and EGTA (250 mM) were made up in 10 mM TES pH 7.2. FCCP (0.3 mM), rotenone (10 μM), antimycin A (50 mg/mL), and *n*-propyl gallate (50 μM) were

dissolved in molecular biology-grade ethanol. AlaM was dissolved in ethanol to a concentration of 10 mg/mL in the stock solution. All reagents can be stored at –20 °C.

3 Methods

3.1 Determination of Transcript Abundance of the NAD(P)H Dehydrogenase Gene Family from Arabidopsis

3.1.1 Preparation of RNA

1. RNA is isolated using a commercial RNA isolation kit. The RNA extracts are eluted in 50 μL of nuclease-free water.
2. Check the RNA integrity by resolving and visualizing the RNA samples on 1 % (w/v) agarose gel following standard protocols.
3. Determine the RNA concentration and purity spectrophotometrically by measuring the absorbance at 260 and 280 nm. A ratio of approximately 2 for 260/280 is a good guide for quality RNA. DNase treatment is added to each RNA sample using a commercial RNase-free DNase as per the manufacturer's protocols.

3.1.2 cDNA Synthesis

1. Following RNA extraction, 1 μg of the purified RNA is reverse-transcribed into cDNA using a commercial kit, such as the iScript™ cDNA Synthesis Kit (Bio-Rad, USA) following the manufacturer's protocols. Using a PCR machine the reaction is incubated for 5 min at 25 °C, 30 min at 42 °C, and 5 min at 85 °C and held at 4 °C until required.
2. The cDNA is then diluted 1:10 with autoclaved molecular biology-grade water and stored at –80 °C (*see* **Note 2**).

3.1.3 Generation of Standards for Quantitative Reverse Transcriptase-PCR

This method requires the preparation of a standard curve for the quantification of the target transcript. The standard curve is derived from known amounts of the target sequences prepared by PCR. Thus, primers were designed to amplify the target sequences of approximately 100–200 bp near the 3′ end specific for each of the NAD(P)H dehydrogenase genes. *Ubiquitin* and protein phosphatase 2A subunit (*pdf2*) are used to normalize transcript abundance (*see* Table 2 for the primer sequences, amplification conditions, and product size).

1. Generate PCR products for samples of each gene of interest and the reference genes by setting up a PCR reaction in 0.2-mL PCR tubes in a 20 μL final volume.
2. Add the following PCR reagents from Promega (USA): autoclaved molecular biology-grade water, 1× Green GoTaq® Flexi PCR buffer, 0.2 mM $MgCl_2$, 0.2 mM dNTPs, 0.4 mM primers, 1.25 U Taq DNA polymerase, and 0.5 μg template DNA.

Table 2
Primer list and conditions for quantitative reverse transcriptase-PCR

Primer	Target (gene)	Sequence (5′–3′)	Tm (°C)	Product size (bp)	
				gDNA	cDNA
Atnda1Fw	*Atnda1*	AGAGCAAGGAAGGGAAAG	48	None	180
Atnda1Rv	At1g07180.1	GAAGTGGAGGGGATATGG	50		
Atnda2Fw	*Atnda2*	CTTGGAAGCATGGCTACTAT	50	264	190
Atnda2Rv	At2g29990.1	CAAAAACGAAAGTGGTGAA	44		
Atndb1Fw	*Atndb1*	GAAAAATCTTGGGGGATATT	46	None	146
Atndb1Rv	At4g28220.1	ATGCTTGCTTTTCAGGTAGA	48		
Atndb2Fw	*Atndb2*	GTCTACGCCAGTAAGCAAGT	52	None	151
Atndb2Rv	At4g05020.1	TGTAACTCGTGAGAGAGAGAGA	53		
Atndb3Fw	*Atndb3*	TTTACGCTAGTAAGCAAGTGAG	51	None	140
Atndb3Rv	At4g21490.1	CCATGATAATTCAAACGAGAG	48		
Atndb4Fw	*Atndb4*	TGAGGACACACAAGTGAATATC	51	231	157
Atndb4Rv	At2g20800.1	TGGCTTCTTCTCACATTTCT	48		
Atndc1Fw	*Atndc1*	CCTTTATTACCATTCAGGTTTC	49	None	141
Atndc1Rv	At5g08740.1	TCAAATACGCCAGTTTTCTC	48		
UbiqFw	*Ubiquitin*	GACAGAGCAGAGAACATAAGG	52	292	184
UbiqRv	At2g17190	TGGGGATTGGGTAAAGAGG	51		
pdf2Fw	*pdf2*	ATTCCGATAGTCGACCAAGC	52	None	84
pdf2Rv	At1g13320.1	AACATCAACATCTGGGTCTTCA	51		

Primers were designed against the cDNA sequence near the 3′ end and spanning an intron where possible. Primer sequences were checked in primerBLAST (http://www.ncbi.nlm.nih.gov/tools/primer-blast/). Primers were designed to avoid products in genomic DNA contamination; however this was not always possible and genomic DNA product sizes are indicated

3. The standard PCR cycles are run using the following conditions: 95 °C for 2 min; 30 cycles of 95 °C for 30 s, 54 °C for 30 s, and 72 °C for 30 s; 72 °C for 5 min; and 4 °C on hold for completion.
4. Purify the PCR products using a PCR Clean up Kit (e.g., Promega) as per the manufacturer's guidelines.
5. Determine the concentrations and purity of the PCR products using a NanoDrop™1000 Spectrophotometer (Thermo-Scientific, USA).
6. Dilute the QRT-PCR standards to the following dilutions (10^{-2}, 10^{-4}, 10^{-6}, and 10^{-8} fmol/μL) with autoclaved molecular biology-grade water.

7. The standards of known concentrations are used to determine the concentration of the unknown samples.
8. Use the purified products as target template standards at different concentrations of 10^{-2} fmol/μL, 10^{-4} fmol/μL, and 10^{-6} fmol/μL for the QRT-PCR reactions.
9. Add cDNA prepared from at least three individual plants (i.e., three biological replicates), and each biological replicate is used in duplicate reaction on the QRT-PCR plate.
10. Always include a no-template control (water) and a no-reverse-transcription control (RNA) on each qPCR reaction plate.

3.1.4 Execution of the QRT-PCR Reaction and Quantitation

1. Use SoFast™ EvaGreen® Supermix PCR reagents for quantitative PCR in a CFX96™ Real-Time PCR Detection System (Bio-Rad, USA).
2. Set up the reactions as they have been optimized. Add the following to a master mix: 1× SoFast™ EvaGreen® Supermix PCR mix, 2 μL cDNA from a 1/10 dilution stock template, and forward and reverse primers to a final concentration of 500 nM each, made up to 10 μL with autoclaved molecular grade water.
3. Set up the PCR reaction plate in a laminar flow cabinet using sterile filter tips. Use the following PCR cycle conditions: 1 cycle of 95 °C for 3 min; 40 cycles of 95 °C for 10 s and 54 °C for 30 s, followed by the melt curve step from 65 to 98 °C.
4. The threshold fluorescence is set as the default of the program (CFX Manager, Bio-Rad, USA).
5. Calculate the cDNA concentration of the target gene from each sample; the $C(t)$ value of the sample is plotted against a standard curve of the respective genes.
6. Analyze each gene to the reference gene. Use *pdf2* as the reference gene to normalize the expression of the targeted genes. Calculate the average $C(t)$ value for each gene of interest by dividing by the average $C(t)$ for *pdf2*. This will give the relative gene expression. Repeat this using an additional reference gene, such as *ubiquitin*, to confirm results.

3.2 Determination of Protein Abundance of the NAD(P)H Dehydrogenase Gene Family from Arabidopsis

This method has been optimized for using purified mitochondria as the protein source, but can be adapted for total protein extracts from whole tissue. This requires optimization of the primary antibody dilution. Denaturing 10 % (w/v) SDS gels are made and run according to the Laemmli [27] protocol.

3.2.1 SDS-PAGE and Transfer Procedure

1. Prepare the previously purified mitochondria (40 μg) by incubation in SDS-PAGE running buffer with fresh DTT at 95 °C for 5 min (*see* **Note 3**).

Table 3
Summary of antisera generation and apparent molecular mass of proteins detected

Antibody	Sequence	Dilution	Detected band mass (kDa)
NDB1	AYADANEEANKKE	1:2,000–1:2,500	60
NDB2	ETDDVSKNNIELKIE	1:10,000	63
NDB3	KSVELDIEELKS	1:10,000–1:30,000	65
NDB4	ANGEDTQVNIEKFKQA	1:10,000	65
NDA1	SEVPGIGEDEKKR	1:10,000	60/56
NDA2	SDTPGISKEEKRR	1:10,000	59/55
NDC1	KRASNLEEDEGYFLE	1:10,000	70/60

Antibodies were raised against synthetic peptides in rabbits. The peptides were designed from alignments of all members of the type II dehydrogenase family selecting regions of least homology of the Arabidopsis proteins. Similar size polypeptides have also been detected in rice leaf and root mitochondria

2. Run this protein sample on the SDS-PAGE gel immersed in SDS-PAGE running buffer following Laemmli protocol [27]. Add a molecular weight ladder in a separate lane together with the samples. We suggest Kaleidoscope ladder (Bio-Rad, USA).
3. Transfer the separated proteins onto nitrocellulose membrane, using either a semidry blot method or wet transfer system.

3.2.2 Detection of the NAD(P)H Dehydrogenase Protein

1. After transfer, block the membrane in blocking buffer (TBST with skim milk powder) for 1 h at room temperature with shaking.
2. Incubate the membrane with primary antibody at appropriate dilution (*see* Table 3) at 4 °C in 10 mL of TBST (with skim milk powder), shaking overnight.
3. Wash the membrane for 15 min in TBST with skim milk powder, followed by 2× 5-min washes.
4. Add the secondary antibody, anti-rabbit-HRP-goat IgG conjugated with HRP, at a dilution of 1:1,000 to 10 mL of TBST with skim milk powder and add to the membrane, which is then incubated for 1 h at room temperature with shaking.
5. Wash the membrane with a 15-min wash in TBST buffer, followed by a further 2× 5-min washes.

3.2.3 Development of the Membrane

1. Place the washed membrane in a small snap-lock bag and a total of 1 mL (0.5 mL of each Clarity Luminol Substrate and Clarity Peroxide Solution) of the Clarity™ Western ECL substrate mix (Bio-Rad, USA).
2. Use any chemiluminescence imagining system to detect the HRP reaction. We recommend the ChemiDoc™ MP imaging system (Bio-Rad, USA) with a 5-min exposure.

3.3 Determination of the Enzyme Activity of the Type II NAD(P)H Dehydrogenase

3.3.1 Cytosolic-Facing External NAD(P)H Dehydrogenase Assay

1. Place the required volume of reaction medium in a spectrophotometer cuvette.
2. Add ~80 μg of mitochondrial protein, wait for 2 min to allow chelation of any residual calcium by the EGTA (*see* **Note 4**), then add either 200 μM NADH or NADPH, and determine if there is any background rate of NADH oxidation in the spectrophotometer set at 340 nm.
3. Initiate the reaction with 40 μM decylubiquinone (solubilized in molecular biology-grade ethanol) and monitor NADH(P)H oxidation.
4. For calcium-dependent NAD(P)H dehydrogenase activities, repeat with 1 mM $CaCl_2$ present in the initial reaction medium and no EGTA. The rate of calcium-dependent NAD(P)H oxidation is the difference between this rate and the rate in the presence of EGTA (**step 3** above).

3.3.2 Matrix-Facing Internal NAD(P)H Dehydrogenase Assay

This method measures NADH oxidation through to oxygen, so the use of a sealed temperature-regulated oxygen electrode is recommended.

1. Add the required volume of reaction medium to the oxygen electrode vessel set at 25 °C. Add FCCP and rotenone to 0.4 μM and 25 μM, respectively. The oxygen electrode vessel is closed.
2. Add ~80 μg of mitochondrial protein (when using Arabidopsis leaf mitochondria—this may vary depending on the source tissue). If the calcium-independent activities are being determined then 0.5 mM EGTA should be added to the reaction media at this point and the mitochondria incubated in this mix for 2 min. The NAD(P)H oxidation rate is initiated by the addition of 1 mM NAD(P)H. This will give an estimate of the external NAD(P)H oxidation rate through to oxygen as the electron acceptor.
3. When a steady rate is reached or before if this rate is not required, add AlaM to the electrode system (between 30 and 40 μg/mL); the oxidation rate should increase as now the NAD(P)H has access to the matrix space (*see* **Note 5**). Complex I will not contribute, as the inhibitor rotenone is present. Once a steady rate is achieved, then the addition of 0.2 mg/L antimycin A, followed by 50 nM *n*-propyl gallate, should completely inhibit the oxidation rate. If not, then this residual rate of NAD(P)H oxidation should be subtracted from all other rates.
4. Again as for the external NAD(P)H dehydrogenase activities, to determine the calcium-dependent activities, repeat with 1 mM $CaCl_2$ present in the initial reaction medium and no EGTA. The rate of calcium-dependent NAD(P)H oxidation is the difference between this rate and the rate in the presence of EGTA.

4 Notes

1. Adjust the pH of the Hoagland's solution with KOH; this avoids adding Na^+ into the solution.
2. Store the aliquots of the 1:10 cDNA dilutions in PCR tubes in 20 μL volumes. This avoids exposing the samples to numerous freeze/thaw cycles.
3. Make up the SDS-PAGE loading buffer at 4× concentrated mix to allow capacity for the addition of protein samples and DTT or β-mercaptoethanol on the day.
4. The inhibitory effect of the calcium chelator, EGTA, is sensitive to the pH of the reaction media. The degree of inhibition decreases in acidic media [28].
5. The required concentration of AlaM may require optimization when using mitochondria from other plants and tissues and can be affected by the protein concentration of the mitochondrial suspension. The method for optimization is detailed in [25] and once optimized, future experiments should use mitochondria at similar protein concentration for these assays.

References

1. Clifton R, Lister R, Parker KL, Sappl PG, Elhafez D, Millar AH et al (2005) Stress-induced co-expression of alternative respiratory chain components in Arabidopsis thaliana. Plant Mol Biol 58:193–212
2. Smith C, Barthet M, Melino V, Smith P, Day D, Soole K (2011) Alterations in the mitochondrial alternative NAD(P)H Dehydrogenase NDB4 lead to changes in mitochondrial electron transport chain composition, plant growth and response to oxidative stress. Plant Cell Physiol 52:1222–1237
3. Liu Y-J, Norberg FEB, Szilagyi A, De Paepe R, Akerlund H-E, Allan G, Rasmusson AG (2008) The mitochondrial external NADPH dehydrogenase modulates the leaf NADPH/NADP+ ratio in transgenic *Nicotiana sylvestris*. Plant Cell Physiol 49(2):251–263
4. Liu Y-J, Nunes-Nesi A, Wallstrom SV, Lager I, Michalecka AM, Norberg FEB, Widell S, Fredlund KM, Fernie AR, Rasmusson AG (2009) A redox-mediated modulation of stem bolting in transgenic Nicotiana sylvestris differentially expressing the external mitochondrial NADPH dehydrogenase. Plant Physiol 150:1248–1259
5. Finnegan P, Soole KL, Umbach AL (2004) Alternative mitochondrial electron transport proteins in higher plants. In: Day DA, Millar AH, Whelan J (eds) Plant mitochondria: from genome to function - advances in photosynthesis and respiration. Springer, New York, NY, pp 163–230
6. Rasmusson AG, Soole KL, Elthon TE (2004) Alternative NAD(P)H dehydrogenases of plant mitochondria. Annu Rev Plant Biol 55:23–39
7. Kumar R, Wallis JG, Skidmore C, Browse J (2006) A mutation in Arabidopsis cytochrome b5 reductase identified by high-throughput screening differentially affects hydroxylation and desaturation. Plant J 48:920–932
8. Duncan O, Taylor NL, Carrie C, Eubel H, Kubiszewski-Jakubiak S, Zhang B, Narsai N, Millar AH, Whelan J (2011) Multiple lines of evidence localize signaling, morphology, and lipid biosynthesis machinery to the mitochondrial outer membrane of Arabidopsis. Plant Physiol 157:1093–1113
9. Soole KL, Turpin D, Wiskich JT (1997) Inducement of external (DA)-NAD(P)H oxidation in beet mitochondria. Plant Physiol 114(3S):1017
10. Melo AMP, Roberts TH, Møller IM (1996) Evidence for the presence of two rotenone-insensitive NAD(P)H dehydrogenases on the inner surface of the inner membrane of potato tuber mitochondria. Biochim Biophys Acta 1276:133–139

11. Menz RI, Day DA (1996) Identification and characterization of an inducible NAD(P)H dehydrogenase from red beetroot mitochondria. Plant Physiol 112(2):607–613
12. Menz RI, Day DA (1996) Purification and characterization of a 43-kDa rotenone-insensitive NADH dehydrogenase from plant mitochondria. J Biol Chem 271:23117–23120
13. Luethy MH, Thelen JJ, Knudten AF, Elthon TE (1995) Purification, characterization, and submitochondrial localization of a 58-kilodalton NAD(P)H dehydrogenase. Plant Physiol 107:443–450
14. Geisler DA, Broselid C, Hederstedt L, Rasmusson AG (2007) Ca2+-binding and Ca2+-independent respiratory NADH and NADPH dehydrogenases of Arabidopsis thaliana. J Biol Chem 282:28455–28464
15. Elhafez D, Murcha MW, Clifton R, Soole KL, Day DA, Whelan J (2006) Characterization of mitochondrial alternative NAD(P)H dehydrogenases in Arabidopsis: intraorganelle location and expression. Plant Cell Physiol 47:43–54
16. Moore CS, Cook-Johnson RJ, Rudhe C, Whelan J, Day DA, Wiskich JT et al (2003) Identification of AtNDI1, an internal non-phosphorylating NAD(P)H dehydrogenase in Arabidopsis mitochondria. Plant Physiol 133: 1968–1978
17. Carrie C, Murcha MW, Kuehn K, Duncan O, Barthet M, Smith PM et al (2008) Type II NAD(P)H dehydrogenases are targeted to mitochondria and chloroplasts or peroxisomes in Arabidopsis thaliana. FEBS Lett 582:3 073–3079
18. Xu L, Law SR, Murcha MW, Whelan J, Carrie C (2013) The dual targeting ability of type II NAD(P)H dehydrogenases arose early in land plant evolution. BMC Plant Biol 13:100
19. Michalecka AM, Svensson AS, Johansson FI, Agius SC, Johanson U, Brennicke A, Binder S, Rasmusson AG (2003) Arabidopsis genes encoding mitochondrial type II NAD(P)H dehydrogenases have different evolutionary origin and show distinct responses to light. Plant Physiol 133:642–652
20. Robinson SA, Yakir D, Ribas-Carbo M, Giles L, Osmond CB, Siedow JN, Berry JA (1992) Measurements of the engagement of cyanide-resistant respiration in the crassulacean acid metabolism plant *Kalanchoe daigremontiana* with the use of on-line oxygen isotope discrimination. Plant Physiol 100:1087–1091
21. Day DA, Neuberger M, Douce R (1985) Biochemical characterisation of chlorophyll-free mitochondria form pea leaves. Aust J Plant Physiol 12(2):219–228
22. Smith CA, Melino VJ, Sweetman C, Soole KL (2009) Manipulation of alternative oxidase can influence salt tolerance in Arabidopsis thaliana. Physiol Plant 137:459–472
23. Rasmusson AG, Møller IM (1991) NAD(P)H dehydrogenases on the inner surface of the inner mitochondrial membrane studied using inside-out submitochondrial particles. Physiol Plant 83:357–365
24. Gostimskaya IS, Grivennikova VG, Zharova TV, Bakeeva LE, Vinogradov AD (2003) In situ assay of the intramitochondrial enzymes: use of alamethicin for permeabilization of mitochondria. Anal Biochem 313:46–52
25. Johansson FI, Michalecka AM, Moller IM, Rasmusson AG (2004) Oxidation and reduction of pyridine nucleotides in alamethicin permeabilized plant mitochondria. Biochem J 380:193–202
26. Hong H, Nose A (2012) Characteristics of external and internal NAD(P)H dehydrogenases in *Hoya carnosa* mitochondria. J Bioenerg Biomembr 44:655–664
27. Laemmli UK (1970) Cleavage of structural proteins during the assembly of the head of bacteriophage T4. Nature 227:680–685
28. Møller IM, Palmer JM (1981) Charge screening by cations affects the conformation of the mitochondrial inner membrane. A study of exogenous MAD(P)H oxidation in plant mitochondria. Biochem J 195:583–588

Chapter 12

Assessment of Respiration in Isolated Plant Mitochondria Using Clark-Type Electrodes

Richard P. Jacoby, A. Harvey Millar, and Nicolas L. Taylor

Abstract

Mitochondrial respiration involves two key gas exchanges, the consumption of oxygen and the release of carbon dioxide. The ability to measure the consumption of oxygen via Clark-type electrodes has been one of the key techniques for advancing our knowledge of mitochondrial function in whole organisms, tissue samples, cells, and isolated subcellular fractions. In plants, oxygen electrode analyses provided the first evidence for some of the unique respiratory properties of plant mitochondria. This chapter briefs the principles of respiration and oxidative phosphorylation, how oxygen consumption measurements can be used to assess the quality of isolated mitochondrial preparations, and how these measurements can answer important questions in plant biochemistry and physiology. Finally, it presents instructions on assembling the oxygen electrode apparatus and how to conduct various assays.

Key words Mitochondria, Clark-type electrode, Respiration, ADP/O ratio, Respiratory control ratio, Cytochrome pathway, Alternative pathway

1 Introduction

1.1 Theory Behind Oxygen Consumption Measurements of Isolated Mitochondria

1.1.1 Oxygen Consumption Measurements to Assess Mitochondrial Function

Respiration fuels the energetic demands of the cell by extracting chemical energy from sugars, fats, and amino acids, and converting this energy into ATP. Phosphorylation of ADP is conducted by the ATP synthase complex, which is driven by a proton gradient formed across the inner membrane by electron flow through the mitochondrial electron transport chain (ETC). The ETC oxidizes respiratory substrates, and then passes the liberated electrons through a series of donors and acceptors until they reach the terminal oxidase enzymes that reduce oxygen to water (Fig. 1). This arrangement means that the processes of oxygen consumption and ADP phosphorylation are coupled; together they are known as oxidative phosphorylation (OXPHOS). Therefore, measuring oxygen consumption is a powerful method to assess the biochemical properties of isolated mitochondria, including the speed of substrate oxidation, the efficiency of ATP generation, and the dominant routes of electron transport.

James Whelan and Monika W. Murcha (eds.), *Plant Mitochondria: Methods and Protocols*, Methods in Molecular Biology, vol. 1305, DOI 10.1007/978-1-4939-2639-8_12,

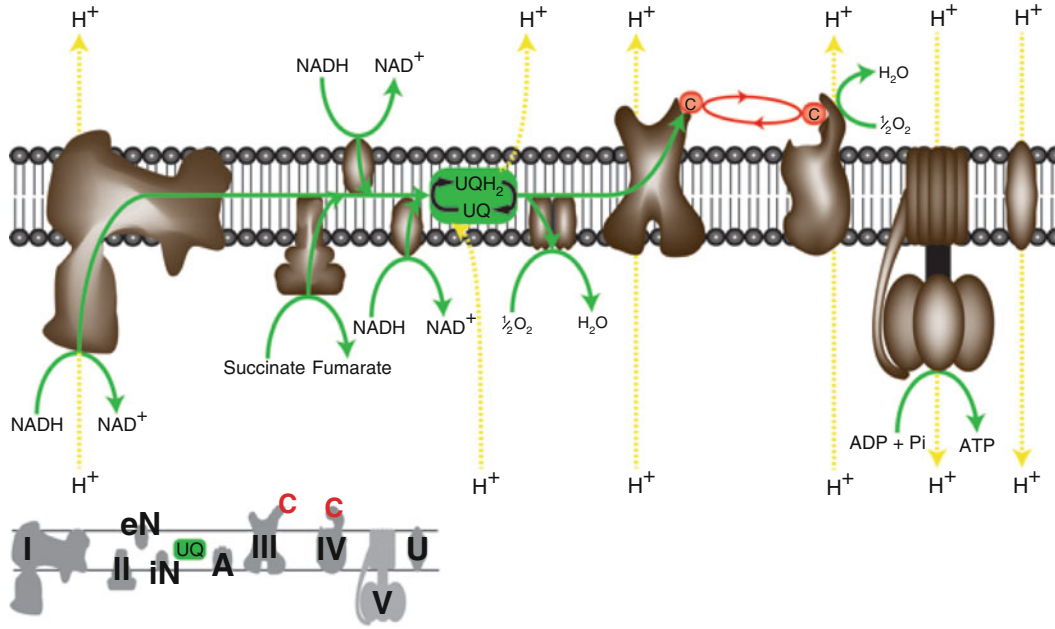

Fig. 1 The electron transport chain of plant mitochondria. Numbers (*I–V*) identify the large respiratory complexes located on the inner mitochondrial membrane. Complex I, NADH:ubiquinone oxidoreductase; Complex II, succinate dehydrogenase; Complex III, ubiquinone-cytochrome c oxidoreductase; Complex IV, cytochrome c oxidase; Complex V, ATP synthase. Letters identify alternative pathway enzymes, *eN* external NAD(P)H dehydrogenase, *iN* internal NAD(P)H dehydrogenase, *A* alternative oxidase, *UQ* ubiquinone/ubiquinole pool, *c* cytochrome c, *U* uncoupling protein, *NADH* nicotinamide adenine dinucleotide (reduced), *NAD+* nicotinamide adenine dinucleotide (oxidized), *ATP* adenosine triphosphate, *ADP* adenosine diphosphate, *Pi* inorganic phosphate. *Unbroken arrows* indicate pathways of electron flow; *broken arrows* indicate proton translocation sites

1.1.2 Electrochemistry of Oxygen Measurement

The history of oxygen consumption measurements via Clark-type electrodes is well detailed in Severinghaus' 1986 publication [1]. Briefly, oxygen can be electrochemically reduced at a platinum or gold cathode, which is connected via a salt bridge to a silver anode. Applying a constant voltage between the cathode and the anode forms an electrical circuit. The magnitude of the current through this circuit is proportional to the rate of oxygen being reduced at the cathode, which is linearly dependent on the oxygen concentration in the solution surrounding the cathode. To convert this electrical signal to an actual oxygen concentration, a two-point calibration is applied. First, the magnitude of the electrical current is measured in air-saturated water, and second, the current is measured in water that has been chemically deoxygenated. The electrical current measured in air-saturated water is converted to an oxygen concentration with reference to a literature value based on temperature, pressure, and solution contents [2], and the current measured in deoxygenated water is converted to an oxygen concentration of zero.

1.1.3 Oxygen-Permeable Membranes

A simple oxygen electrode configuration (platinum cathode—salt bridge—argentum (a.k.a. silver) anode) is capable of measuring oxygen concentrations in chemically simple solutions. However, most solutions used for biology research will contain a mixture of redox-active molecules, which can accept electrons at the platinum cathode and thus confound oxygen concentration measurements [1]. To overcome this limitation, Clark [3] demonstrated the effectiveness of gas-permeable membranes for excluding larger molecules from interacting with the platinum cathode. This was the key advance that facilitated the application of oxygen electrodes to the study of isolated mitochondria.

1.2 Applications of Clark-Type Oxygen Electrodes in Plant Science Research

High-quality preparations of isolated mitochondria have been crucial for furthering our knowledge of how metabolism is compartmentalized between different organelles within plant cells [4]. Ascertaining the purity and activity of isolated mitochondria has been one of the major uses for oxygen electrodes in plant science [5]. Oxygen electrode measurements can demonstrate that the mitochondria have been isolated in a physiologically active state, with inner and outer membranes both intact. This assessment of function is the main advantage of oxygen electrode measurements over marker-based techniques such as Western blots or enzyme assays. For assessments of mitochondrial quality, oxygen electrode measurements are typically expected to fulfil three requirements:

1.2.1 Assessing the Quality of Mitochondrial Preparations

1. That the isolated mitochondria are able to consume oxygen consumption at reasonable rates (100–500 nmol/min/mg mitochondrial protein) in the presence of conventional substrates (e.g., malate, pyruvate, glutamate, succinate, NADH, or appropriate combinations thereof) and added ADP.
2. That oxygen consumption is coupled to ADP phosphorylation: This is assessed by the respiratory control ratio (RCR) >2.5 (i.e., the ratio of respiratory rate in the presence versus the absence of added ADP) and the ADP/O ratio (i.e., the ratio of mole ADP used per mole oxygen consumed in process) approaching literature values between 2 and 3, when assayed in the presence of alternative oxidase inhibitors like *n*-propyl gallate (nPG).
3. That oxygen consumption ceases (<5 % of maximum) when both respiratory oxidases are chemically inhibited.

These measurements are rarely the key results of a contemporary publication, but they are important for showing that a quality mitochondrial sample has been isolated.

1.2.2 Comparing Mitochondrial Activity Across Genotype and Environmental Treatment

Comparative measurements using Clark-type oxygen electrodes have informed our knowledge of how ETC biochemistry varies between plant mitochondria isolated from different contexts. For instance, mitochondria isolated from a range of different species display divergent ETC kinetics when assayed at low temperature,

with cold-tolerant species exhibiting different responses compared to cold-sensitive species [6]. Also, mitochondria isolated from plant species adapted to different light intensities exhibit differing rates of oxygen uptake, depending on light intensity during growth [7]. Oxygen electrode results have informed our understanding of how the plant mitochondrial ETC responds to environmental stress treatments [8, 9]. Furthermore, oxygen electrode results have featured in several recent publications using reverse genetics tools in the model plant Arabidopsis (*Arabidopsis thaliana*), to assess the biochemical consequences of transgenically manipulating genes encoding mitochondrial proteins [10–12].

1.2.3 Using Oxygen Electrodes to Characterize Plant-Specific Mitochondrial Properties

When isolated plant mitochondria were first analyzed with Clark-type oxygen electrodes, it was revealed that plant mitochondria consume oxygen in a different manner to isolated animal mitochondria. At first, this inability to match the "rat liver standard" was wrongly attributed to the isolation of poor-quality, contaminated mitochondrial preparations [13]. However, decades of research overturned this opinion, by unraveling the unique characteristics of plant mitochondria that were responsible for these effects. Specifically, Clark-type oxygen electrodes have contributed to the discovery of plant-specific mitochondrial ETC components [14, 15] and plant-specific substrate preferences of isolated mitochondria [16, 17] and that the optimal media composition for supporting isolated plant mitochondria is quite different to the usual medium used for respiratory studies of isolated animal mitochondria [18]. Of particular note is the role of oxygen electrodes in furthering our knowledge of the ALTERNATIVE OXIDASE (AOX) and rotenone-insensitive NADH dehydrogenases. The function of both eluded plant scientists for decades but measurements of oxygen consumption rates using Clark-type electrodes have been very useful in characterizing their expression [19–21], activation [22–24], inhibition [25], and efficiency [14, 26, 27].

2 Materials

2.1 Oxygen Electrode

1. Oxygen electrode and polarographic systems: The configuration of a standard Clark-type electrode setup is shown in Fig. 2. A platinum cathode is facing upwards at the base of the reaction chamber. The cathode is covered first by an electrolyte-moistened paper wick that forms a salt bridge to the silver anode, and second by an oxygen-permeable membrane. The chamber is surrounded by a water jacket, which regulates temperature. A plunger is placed on top of the chamber to form a seal. This apparatus sits atop a magnetic stirring platform. There are

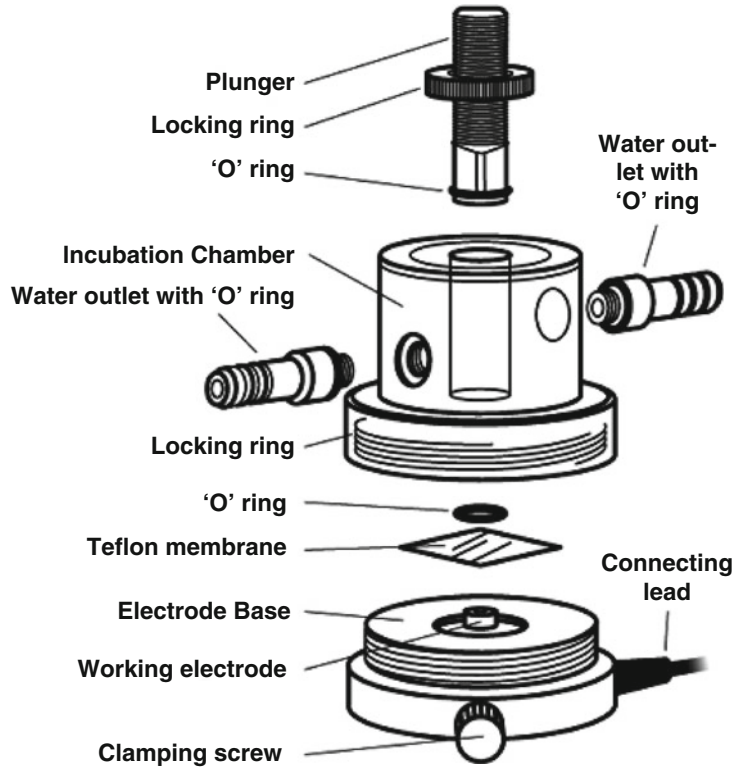

Fig. 2 General representation of the Clark-type electrode and experimental setup. Image reproduced with permission from Rank Brothers Limited, Cambridge, UK (www.rankbrothers.co.uk)

several companies manufacturing off-the-shelf oxygen electrode systems, such as Hansatech Instruments (http://hansatech-instruments.com), Rank Brothers Ltd (www.rankbrothers.co.uk), Stathkelvin Instruments (www.strathkelvin.com), and Oroboros Instruments (www.oroboros.at). Each will have its own instructions regarding assembly and setup.

2. Oxygen-permeable membranes: The oxygen-permeable membranes that are typically used for Clark electrode analyses are polytetrafluoroethylene (PTFE), which is commercially known as Teflon.
3. Electrolyte solution: A 2.5–3 M KCl solution can be stored at room temperature for years. Oroboros membranes are bought pre-fitted with electrolyte solution.
4. Syringes and pipette tips: Use standard laboratory pipettes and tips to load assay buffer and isolated mitochondria into the reaction chamber before the plunger is sealed (*see* **Note 1**).

For adding effector molecules once the plunger is in place, use either disposable polypropylene gel loading pipette tips or non-disposable microliter syringes (e.g., Hamilton syringes). Disposable gel loading tips are preferred for use of inhibitors, while Hamilton syringes impart the smallest amount of air into the reaction chamber when the fluid is ejected to minimize electrode voltage disturbance. If using Hamilton syringes, ensure to thoroughly rinse the syringe head between additions, to avoid contaminating stock solutions.

2.2 Oxygen Consumption Assays

1. Respiration medium: 300 mM sucrose, 10 mM NaCl, 5 mM KH_2PO_4, 2 mM $MgSO_4$, 0.1 % (w/v) bovine serum albumin (BSA), 10 mM TES, pH 7.2.

   Principle: It is crucial to include an osmoticum at isotonic concentrations, to prevent mitochondrial swelling or shrinkage. For most plant mitochondrial preparations, an osmotium of mannitol or sucrose at concentrations between 300 and 400 mM is used. The solution should be buffered to a physiological pH; 10 mM TES pH 7.2 works well (*see* **Note 2**). Publications propose that addition of BSA is necessary for obtaining good coupling of OXPHOS [28, 29], and include 0.1 % (w/v) BSA in assay media. Mitochondrial assay medium often contains three ionic salts, 10 mM NaCl, 5 mM KH_2PO_4, and 2 mM $MgSO_4$. The phosphate salt is essential to provide a pool of PO_4^{3-} that can drive ADP phosphorylation during assays. Regarding salts more generally, there is a body of literature that investigates the biophysical effects of ionic salts on plant mitochondrial respiration [30–32]. Generally, low concentrations of salts are stimulatory whereas higher concentrations are inhibitory.

2. Suspension medium: 300 mM sucrose, 10 mM TES, pH 7.5.

   Principle: The buffers used for the last few steps of mitochondrial isolation dictate the composition of the medium that suspends the mitochondria prior to oxygen electrode analyses. Although complex buffers are used during the initial stages of mitochondrial isolation, the buffers used during the last few steps of the procedure can be greatly simplified. Suspending mitochondria in a very simple buffer that is compatible with oxygen electrode analyses also aids other downstream assays of mitochondria in laboratories.

3. Solutions

   A list of substrates, uncouplers, inhibitors, and effector molecules with stock and final concentrations can be found in Table 1.

Table 1
List of substrates, uncouplers, inhibitors, and effector molecules for use in oxygen electrode for measuring mitochondrial respiration

	Abbreviation	Site of action	Stock concentration (solvent)	Store	Final Conc.	Volume added (µL), assuming 1 mL reaction volume
Substrates						
Succinate	Succ	CII	500 mM (H_2O)	−20 °C	5 mM	10
Glutamate	Glu	GDH → TCA cycle	1 M (H_2O)	−20 °C	10 mM	10
Malate	Mal	MDH → TCA cycle	1 M (H_2O)	−20 °C	10 mM	10
Pyruvate	Pyr	PDC → TCA cycle	1 M in (H_2O)	−20 °C	10 mM	10
Nicotinamide adenine dinucleotide (reduced)	NADH	NDex	0.1 M in (H_2O)	−20 °C	1 mM	10
Nicotinamide hypoxanthine dinucleotide (reduced)	Deamino-NADH	CI	0.1 M in (H_2O)	−20 °C	1 mM	10
Cytochrome c	Cyt C	CIV	2.5 mM (H_2O)	−20 °C	25 µM	10
Tetramethylphenyldiamine	TMPD	CIV	150 mM (H_2O)	−20 °C	300 µM	2
Uncouplers						
Carbonyl cyanide-p-trifluoromethoxyphenylhydrazone	FCCP	Membranes	20 mM (EtOH), diluted to 2 mM (EtOH) on day of assay	−20 °C	4 µM	2 (from 2 mM stock)
Inhibitors						
Rotenone	Rot	CI	1 mM (EtOH) dissolve by warming to ~60 °C	−20 °C	5 µM	5
Antimycin A	AA	CIII	1 mM (EtOH)	−20 °C	1–5 µM	1–5
Myxothiazol	Myxo	CIII	500 µM (EtOH)	−20 °C	2.5 µM	5
n-Propyl Gallate	nPG	AOX	100 mM (EtOH)	−20 °C	500 µM	5

(continued)

Table 1
(continued)

	Abbreviation	Site of action	Stock concentration (solvent)	Store	Final Conc.	Volume added (µL), assuming 1 mL reaction volume
Cyanide	KCN	CIV	100 mM (H_2O)	4 °C	1 mM	10
Oligomycin	Oligo	ATP synthase	1 mg/mL (EtOH)	–20 °C	2 µg/mL	2
Effectors						
Ascorbate	Asc	Cyt C	500 mM (H_2O)	Make fresh	10 mM	20
Thiamine pyrophosphate	TPP	PDC, 2-OGDH	50 mM (H_2O)	–20 °C	200 µM	4
Coenzyme A	CoA	PDC, 2-OGDH	1.2 mM (0.1 % cysteine in H_2O)	–20 °C	12 µM	10
Dithiothreitol	DTT	AOX	1 M (H_2O)	Make fresh	5 mM	5
Nicotinamide adenine dinucleotide (oxidized)	NAD^+	Dehydrogenase enzymes of TCA cycle	100 mM (H_2O)	–20 °C	2 mM	20
ATP	ATP	CII	100 mM (H_2O)	–20 °C	500 µM	5
ADP	ADP	CV	100 mM (H_2O)	–20 °C	200–300 µM	2–3
Triton-X 100	Triton	Membranes	10 % (v/v) (H_2O)	4 °C	0.05 % (v/v)	5
Pyruvate	Pyr	AOX	1 M (H_2O)	–20 °C	10 mM	1

2-OGDH 2-oxoglutarate dehydrogenase, *AOX* alternative oxidase, *CI* complex I (NADH:ubiquinone oxidoreductase), *CII* complex II (succinate dehydrogenase), *CIII* complex III (ubiquinone-cytochrome c oxidoreductase), *CIV* complex IV (cytochrome c oxidase), *GDH* glutamate dehydrogenase, *MDH* malate dehydrogenase, *NDex* external NADH dehydrogenase, *PDC* pyruvate dehydrogenase complex, *TCA* tricarboxylic acid

3 Methods

3.1 Oxygen Electrode Preparation and Maintenance

Calibration using sodium dithionite

1. Assemble the electrode following the manufacturer's instructions, and allow the membrane equilibrate in water for ~30 min.
2. Place 1 mL of air-saturated water (*see* **Note 3**) in the measurement chamber, ensuring that the water and the chamber are both equilibrated to the measurement temperature.
3. Wait for the electrical current to stabilize (*see* **Note 4**), and then add ~5 mg of sodium dithionite (sodium hydrosulfite) (*see* **Note 5**). At this point, the electrode signal should dramatically decrease.
4. Wait for the electrode signal to reach its minimum value.
5. Activate this two-point calibration on the instrument. Most commercial software packages enable "click button" execution of this procedure.

Cleaning with water and solvents between runs

Most reagents used in Clark electrode assays are water soluble and can easily be removed by rinsing five times with water between runs. However, some chemicals used for assays are only soluble in organic solvents, such as nPG, SHAM, antimycin A, FCCP, and rotenone. Therefore, rinsing with an organic solvent between assays is necessary to remove residual traces of these molecules. This is complicated by the fact that some oxygen electrodes are constructed from Perspex, which is damaged by most organic solvents. When using organic-soluble molecules, only work with ~10× K_i for the inhibitor, briefly rinse the chamber with 50 % (v/v) ethanol, and then rinse five times with water to deplete residues.

Respiration medium

Prior to the assay, respiration medium should be warmed to the same temperature as the assay chamber. Most studies are conducted at 25 °C, although insights into temperature responses can be gathered by measuring respiratory rates at higher and lower temperatures [33]. Prior to each measurement, the buffer should be air saturated (*see* **Note 4**).

Storage of mitochondria and effector molecules during assays

Mitochondria should be stored on ice and only the aliquots being assayed should be warmed to room temperature during the assay to limit proteolysis (mitochondria contain an array of endogenous proteases). Most effector molecules should be stored at −20 °C, some at 4 °C, and others should be made fresh (Table 1). On the day of the assay, aliquots of the relevant effector molecules should be thawed completely, thoroughly mixed, and stored on ice while assays are taking place.

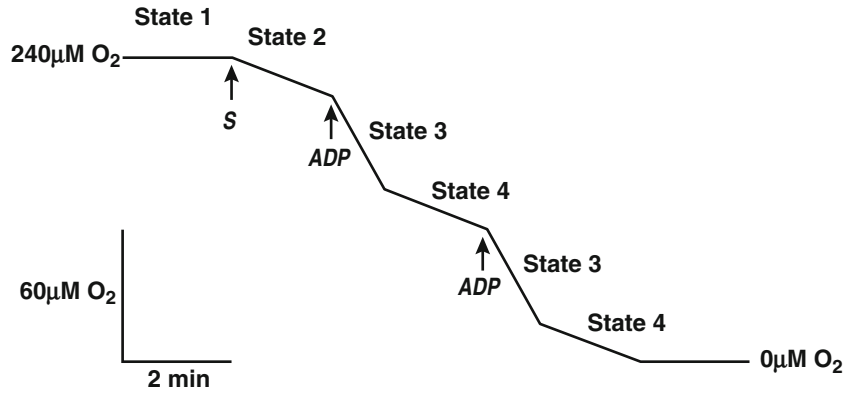

Fig. 3 Representative oxygen electrode trace. Oxygen electrode trace showing states 1–4 and the points of addition of substrates (*S*) and ADP (*ADP*)

Respiratory states

Isolated mitochondrial respiratory assays are typically conducted in a certain order. First mitochondria are added, then substrate, and then ADP. The respiratory rates elicited by these additions are described as four different "states," using the method of Estabrook [34], refined from Chance and Williams [35] (Fig. 3). Mitochondria added to respiration buffer exhibit "state 1" respiration prior to substrate addition. In state 1, there should be very slow oxygen consumption—faster rates may reflect technical problems with the Clark electrode, or otherwise the presence of endogenous substrates in the mitochondrial suspension. Upon addition of substrate(s), the mitochondria enter state 2 respiration, where oxygen consumption rate should increase significantly. It is important to wait until state 2 respiratory rate is stable, to ensure that electrical potential has formed across the inner mitochondrial membrane. Then, ADP is added and the mitochondria enter state 3, where respiration rate increases dramatically. In state 3, ADP is phosphorylated by ATP synthase, driven by proton translocation from the intermembrane space to the matrix. This diminishes the membrane potential across the inner membrane, promoting faster ETC flow. Without any further intervention from the experimenter, the added ADP will be fully converted to ATP, and an electrical potential will be reformed. The mitochondria have now entered state 4, where respiratory rate is slower than state 3, but similar to state 2. When reporting results, the key rate is usually state 3 (sometimes referred to as the "substrate + ADP" rate). However, researchers should note respiratory rates across all states, as these values can be used to calculate RCR (defined as state 3/state 4), and also to assess anomalous assays.

3.2 Calculations

Selecting the appropriate portion of the assay

The control software for most commercially available oxygen electrodes enable "click button" calculations of oxygen consumption rate in units of nmol O_2/min. Care should be taken when selecting the portion of the assay that is used to calculate this rate. As a general principle, the experimenter should select the longest possible portion of the assay where oxygen consumption rate is consistent and linear and beware the impact of transient electrical noise in the reading at specific times.

Normalization

Rates of isolated mitochondrial oxygen consumption are usually expressed in units of nmol O_2/min/mg mitochondrial protein. The fact that respiratory rates are normalized to mass of mitochondrial protein means that the researcher should ideally measure the protein concentration of the isolated mitochondrial preparation before commencing assays. If a protein concentration is known, then the researcher can load a known mass of mitochondrial protein into each assay, simplifying calculations (*see* **Note 6**).

Respiratory control ratio (*RCR*)

RCR is the ratio between ADP-stimulated respiratory rate versus ADP-exhausted respiratory rate. It is calculated by dividing the oxygen consumption rate during state 3 by the oxygen consumption rate during state 4 (Subheading 3.1). High RCRs (>2.5) are one indication of good-quality mitochondrial preparations. However, the activity of AOX lowers RCR values, so if experimenters plan to use RCRs to assess the quality of their mitochondrial preparation, then it is advisable to inhibit AOX with nPG before RCR measurements (Subheading 3.3.3).

ADP/O ratio

ADP/O expresses the ratio between the amount of ADP phosphorylated versus the amount of oxygen consumed during state 3 respiration (Subheading 3.1). It measures the efficiency of OXPHOS, with higher values indicating that ADP phosphorylation is efficient per unit of oxygen reduced (*see* **Note 7**). It is calculated by dividing the amount of ADP that was phosphorylated by the amount of oxygen that was reduced to water. The moles of oxygen atoms (O) are twice the moles of oxygen molecules, so if 50 nmol of oxygen was consumed, this would equate to 100 nmol of O consumed. Sometimes the transitions into and out of state 3 are not "sharp," and it is difficult to precisely measure oxygen concentrations at which state 3 began and ended. In these cases, it is best to use "lines of best fit" over the top state 2, state 3, and state 4 rates. Then, calculate where these lines intersect to estimate where state 3

began and ended (this can be done electronically or with paper and ruler). The activity of AOX and the use of NADH and succinate as substrates all lower ADP/O values, so if the experimenter plans to use ADP/Os to assess the quality of their mitochondrial preparation, then it is advisable to inhibit AOX with nPG and use TCA-linked substrates to maximize ADP/O (Subheading 3.3.3).

3.3 Oxygen Consumption Assays

3.3.1 Total ETC-Linked Respiration

Reagents: ATP, succinate, NADH, and ADP (Table 1).

Principle: A basic assay of respiratory rate is to provide isolated mitochondria with NADH and succinate. This substrate combination delivers reductant directly to the ETC at Complex II and external NAD(P) dehydrogenases and bypasses soluble enzymes of the TCA cycle. This measurement assesses maximal activity of the ETC. ATP is included to activate succinate dehydrogenase and ADP is added to relieve any limitation from a proton motive force across the inner membrane.

1. With plunger open, add ~950 μL of freshly oxygenated respiration media to the reaction chamber (*see* **Note 3**).
2. Add isolated mitochondria [~100 μg of protein (*see* **Note 6**)], close plunger, and wait for oxygen consumption rate to stabilize (1–2 min). This rate is state 1 (Fig. 3).
3. Add 500 μM ATP, 1 mM NADH, and 5 mM succinate. Wait for 3–5 min. This is state 2 respiration (Fig. 3).
4. Add 200 nM ADP. Wait for 4–8 min. First the mitochondria will enter state 3 respiration, and then subsequently state 4 (Fig. 3).

3.3.2 Total Tricarboxylic Acid-Linked Respiration

Reagents: NAD^+, coenzyme A (CoA), thiamine pyrophosphate (TPP), malate, pyruvate, glutamate, and ADP (Table 1).

Principle: Another common assay is to provide isolated mitochondria with tricarboxylic acid (TCA) cycle substrates, usually both malate and pyruvate. The combination of malate and glutamate can also be chosen. Malate and pyruvate ensures that OAA is produced from malate and acetyl-CoA from pyruvate so that citrate synthase has substrates to initiate its condensation to form citrate and begin the TCA cycle. Addition of glutamate with malate allows excess OAA to be transaminated to aspartate by aspartate aminotransferase to prevent OAA inhibition of respiration, and also generation of NADH from glutamate dehydrogenase that delivers 2-oxoglutarate to the lower half of the TCA cycle. Several cofactors are needed for decarboxylating dehydrogenases such as pyruvate and 2-oxoglutarate dehydrogenase complexes (CoA and TPP) and many TCA cycle enzymes require NAD^+ [17]. It is recommended to provide two or more substrates, to promote flux through the TCA cycle. This measurement can assess the

combined activity of the three key steps in mitochondrial metabolism: substrate transport, TCA cycle oxidation, and the ETC.

1. With plunger open, add ~900 µL of freshly oxygenated respiration medium to the reaction chamber (*see* **Note 3**).
2. Add isolated mitochondria [~100 µg of protein (*see* **Note 6**)], close plunger, and wait for oxygen consumption rate to stabilize (1–2 min). This rate is state 1 (Fig. 3).
3. Add cofactors: 2 mM NAD^+, 200 µM CoA, and 12 µM TPP (*see* **Note 8**).
4. Add respiratory substrates: 10 mM malate and 10 mM pyruvate. Wait for 5–7 min. This is state 2 respiration (Fig. 3).
5. Add 200 nm ADP. Wait for 4–8 min. First this will be state 3 respiration, and then subsequently state 4 (Fig. 3).

3.3.3 Cytochrome Pathway Respiration (Complex I and Complex II to Oxygen$^{(Cyt)}$)

Reagents: NADH, succinate, ATP, ADP, and nPG (Table 1, *see* **Note 9**).

Principle: AOX activity can be chemically inhibited by nPG. Once this inhibitor has been applied, the rate of oxygen consumption reflects the capacity of electron flow through the cytochrome pathway alone. This assay provides information about the capacity of energy-conserving electron flow through the cytochrome pathway. However, this measurement of capacity does not necessarily reflect the in vivo activity of the cytochrome pathway. This is because Complex III and AOX both use electrons donated from ubiquinol, so when AOX is chemically inhibited the ubiquinol pool is more reduced and Complex III can operate faster than it could in vivo. When reporting the results of this assay, it is normal to use the term "capacity" to describe the measurement rather than "activity," to indicate this distinction.

1. With plunger open, add ~950 µL of freshly oxygenated respiration media to the reaction chamber (*see* **Note 3**).
2. Add 500 µM of nPG to inhibit AOX.
3. Add isolated mitochondria [~100 µg of protein (*see* **Note 6**)], close plunger, and wait for oxygen consumption rate to stabilize (1–2 min). This rate is state 1 (Fig. 3).
4. Add 500 µM ATP, 1 mM NADH, and 5 mM succinate. Wait for 3–5 min. This is state 2 respiration (Fig. 3).
5. Add 200 nM ADP. Wait for 4–8 min. First this will be state 3 respiration, and then subsequently state 4 (Fig. 3).
6. Optional: Add 1 mM KCN, and wait for 2 min. This assesses residual oxygen consumption rate that cannot be inhibited by KCN or nPG.

3.3.4 Alternative Pathway Respiration (Complex I and Complex II to Oxygen $^{(Alt)}$)

Reagents: NADH, succinate, ATP, ADP, KCN, dithiothreitol (DTT), and pyruvate (*see* **Note 9**).

Principle: Cytochrome oxidase activity can be chemically inhibited with KCN. Once KCN has been applied, the rate of oxygen consumption reflects the capacity of electron flow through the alternative pathway. This assay provides information about the capacity of energy-dissipating electron flow through the alternative pathway. Again, this is not fully reflective of in vivo partitioning, due to competition between Complex III and AOX. When reporting the results of this assay, it is normal to use the term "capacity" to describe the measurement. There are some considerations to remember when assaying AOX. First, AOX is chemically activated by reductant and organic acids [22, 23], so these chemicals should be applied to assess capacity of the alternative pathway. Second, if KCN is added at the start of the trace, it can prevent AOX from reaching its maximal capacity, because no membrane potential is built and substrate loading is restricted. To avoid this, ETC flux should be "primed" by adding substrate and then ADP to uninhibited mitochondria, before KCN is applied later in the assay.

1. With plunger open, add ~900 μL of freshly oxygenated respiration media to the reaction chamber (*see* **Note 3**).
2. Add isolated mitochondria [~100 μg of protein (*see* **Note 6**)], close plunger, and wait for oxygen consumption rate to stabilize (1–2 min). This rate is state 1 (Fig. 3).
3. Add 500 μM ATP, 1 mM NADH, and 5 mM succinate. Wait for 3–5 min. This is state 2 respiration (Fig. 3).
4. Add 200 nM ADP. Wait for 4–8 min. First the mitochondria will enter state 3 respiration, and then subsequently state 4. Wait for state 4 rate to fully stabilize (3–5 min after the state 3–state 4 transition, Fig. 3).
5. Add 1 mM KCN, 5 mM DTT, and 10 mM pyruvate. Wait for 5–7 min. This rate is the capacity of AOX.
6. Optional: Add 500 μM nPG, and wait for 2 min. This assesses residual oxygen consumption rate that cannot be chemically inhibited.

3.3.5 External NADH-Stimulated Respiration (Alternative NADH Dehydrogenase to Oxygen$^{(Cyt)}$ and Oxygen $^{(Alt)}$)

Reagents: NADH and ADP.

Principle: NADH cannot cross the mitochondrial inner membrane, but plant mitochondria contain NADH and NADPH dehydrogenases on the outer surface of the mitochondrial inner membrane (NDex) and donate to ubiquinone. When NADH is provided to isolated plant mitochondria, the NDex enzymes can drive ETC flow and oxygen consumption. For more detailed methods dissecting the activities of the different alternative NAD(P)H dehydrogenases operating in the plant mitochondrial ETC, there are a variety

of detailed oxygen electrode assays involving NADH, NADPH, and Ca^{2+} [12].

1. With plunger open, add ~950 μL of freshly oxygenated respiration media to the reaction chamber (*see* **Note 3**).
2. Add isolated mitochondria [~100 μg of protein (*see* **Note 6**)], close plunger, and wait for oxygen consumption rate to stabilize (1–2 min). This rate is state 1 (Fig. 3).
3. Add 1 mM NADH. Wait for 3–5 min. This is state 2 respiration (Fig. 3).
4. Add 200 nM ADP. Wait for 4–8 min. First the mitochondria will enter state 3 respiration, and then subsequently state 4. Wait for state 4 rate to fully stabilize (3–5 min after the state 3–state 4 transition (Fig. 3)).

3.3.6 Artificial Electron Donors and Acceptors

Artificial electron acceptors and donors interact with the ETC at unconventional points and are often more soluble molecules than ubiquinone. These assays can be used to dissect the function of individual respiratory chain complexes or groups of complexes in intact or ruptured mitochondrial samples.

Ascorbate-TMPD assay of Complex IV

Reagents: Ascorbate and *N*,*N*,*N*′,*N*′-tetramethyl-p-phenylenediamine (TMPD or Wurster's blue) (Table 1).

Principle: TMPD can donate electrons directly to cytochrome c, which passes them to Complex IV. Ascorbate is added to ensure that TMPD is reduced and continues to donate electrons to build a linear rate of Complex IV activity.

1. With plunger open, add ~950 μL of freshly oxygenated respiration media to the reaction chamber (*see* **Note 3**).
2. Add isolated mitochondria [~50 μg of protein (*see* **Note 6**)], close plunger, and wait for oxygen consumption rate to stabilize (1–2 min).
3. Add 10 mM ascorbate, and then 300 μM TMPD. It is important to add ascorbate first, and TMPD second. Wait for 5 min. This is the Complex IV rate.

Deamino-NADH assay of Complex I

Reagents: Deamino-NADH (reduced nicotinamide hypoxanthinedinucleotide) (Table 1).

Principle: Deamino-NADH can be oxidized by Complex I, but not by the other components that oxidize NAD(P)H such as NDex and NDin. Rates of oxygen consumption elicited by deamino-NADH therefore reflect Complex I activity, without contributions from NDin or NDex [36]. Deamino-NADH is not

readily transported across the mitochondrial inner membrane, so mitochondria should be freeze-thawed three times for this assay to be optimal (*see* **Note 10**).

1. With plunger open, add ~950 μL of freshly oxygenated respiration media to the reaction chamber (*see* **Note 3**).
2. Add isolated mitochondria that have been freeze-thawed three times (*see* **Note 10**) [~100 μg of protein (*see* **Note 6**)], close plunger, and wait for oxygen consumption rate to stabilize (1–2 min).
3. Add 1 mM deamino-NADH and 0.05 % (v/v) Triton X-100. Wait for 10 min. This is the Complex I rate.
4. Optional: Add 5 μM rotenone, and wait for 2 min. This assesses residual oxygen consumption from rotenone-insensitive deamino-NADH oxidation.

3.3.7 Determination of Mitochondrial Integrity and Complex IV Activity

Reagents: Cytochrome c, ascorbate, and Triton X-100 (Table 1).

Principle: Complex IV accepts electrons from reduced cytochrome c in the intermembrane space, and passes these electrons onto oxygen to produce water. Exogenous cytochrome c cannot cross the outer mitochondrial membrane. So when reduced cytochrome c is provided as a substrate to intact, isolated mitochondria, oxygen consumption rates are slow, because the electron donor cannot cross the outer membrane. However, all mitochondrial preparations contain a proportion of mitochondria that lack or have damaged outer membranes (referred to as mitoplasts). In contrast to intact mitochondria, mitoplasts will consume oxygen in the presence of reduced cytochrome c, because reduced cytochrome c is free to donate electrons directly to cytochrome oxidase. Mitochondrial quality can be calculated as the proportion of mitoplasts, which is represented by the ratio between Complex IV activity in the initial preparation and total Complex IV activity following the chemical dissociation of membranes with the detergent Triton X-100. The post-Triton X-100 rate of oxygen consumption measures the total cytochrome oxidase activity of the mitochondrial preparation.

1. With plunger open, add ~950 μL of freshly oxygenated respiration media to the reaction chamber (*see* **Note 3**).
2. Add isolated mitochondria [~50 μg of protein (*see* **Note 6**)], close plunger, and wait for oxygen consumption rate to stabilize (1–2 min).
3. Add 10 mM ascorbate and 25 μM cytochrome c. It is important to add ascorbate first, and cytochrome c second. Wait for 5 min. When calculating integrity, this is the "before detergent" rate.
4. Add 0.05 % (v/v) Triton X-100. Wait for 3 min. When calculating integrity, this is the "after detergent" rate. This rate is also the maximum activity of Complex IV.

5. To calculate mitochondrial integrity, divide the "before detergent" rate by the "after detergent" rate, express it as a percentage, and subtract it from 100.

3.3.8 Glycine-Dependent Respiration

Reagents: Glycine and ADP

Principle: Plant mitochondria engage in the photorespiratory cycle by oxidizing glycine to produce serine which is exported to the plastid. In mitochondria isolated from photosynthetic tissues, a reasonable rate of glycine oxidation can be detected. In non-photosynthetic tissues, the rate is very low. In some plant species the measurement of glycine-dependent mitochondrial oxygen consumption rate requires special steps to be taken during mitochondrial isolation, such as glycine in isolation buffers [37].

1. Mitochondria for glycine oxidation should be incubated on ice for 1 h with 5 mM glycine and 0.5 mM ATP to maximize glycine decarboxylase activity.
2. With plunger open, add ~950 μL of freshly oxygenated respiration media to the reaction chamber (*see* **Note 3**).
3. Add isolated mitochondria [~100 μg of protein (*see* **Note 6**)], close plunger, and wait for oxygen consumption rate to stabilize (1–2 min).
4. Add 0.5 mM NAD^+ and 0.25 mM ADP. First the mitochondria will enter state 3 respiration, and then subsequently state 4 (Fig. 3).

3.3.9 Uncoupled Respiratory Capacity

Reagents: NADH, succinate, ATP, ADP, and FCCP (*see* **Note 9**).

Principle: During OXPHOS, the rate of electron transport-driven oxygen consumption is restricted by the formation of a proton gradient across the inner membrane. Once formed, this gradient thermodynamically slows ETC enzymes from operating at maximum capacity. Addition of the ionophore carbonyl cyanide-p-trifluoromethoxyphenylhydrazone (FCCP) permeabilizes the inner membrane to protons, which dissipates the proton gradient. After FCCP addition, mitochondria are said to be "uncoupled," because oxygen consumption is no longer coupled to ATP synthesis or limited in rate by the absence of ADP. In a similar manner to the assessment of AOX capacity in the presence of KCN, this assay works best when the mitochondria have been "primed" with ADP, before FCCP is added.

1. With plunger open, add ~950 μL of freshly oxygenated respiration media to the reaction chamber (*see* **Note 3**).
2. Add isolated mitochondria [~100 μg of protein (*see* **Note 6**)], close plunger, and wait for oxygen consumption rate to stabilize (1–2 min).

3. Add 500 μM ATP, 1 mM NADH, and 5 mM succinate. Wait for 3–5 min.
4. Add 50 nM ADP. Wait for 1–3 min. First this will be state 3 respiration, and then subsequently state 4.
5. Add 2 μM FCCP. Wait for 3–5 min. This is the uncoupled respiratory capacity.

4 Notes

1. Mitochondria from certain tissue types, such as fruits, might be damaged when pipetted through the aperture of regular pipette tips. In these cases, it is recommended to use a wide-aperture pipette or cut tips.
2. There are reports that media should be acidified to pH 6.8 to obtain optimal results when malate and glutamate are provided as substrates. This is because of the different pH optima of malic enzyme (NAD-ME) that converts malate to pyruvate compared to malate dehydrogenase (NAD-MDH) that converts malate to OAA. Lowering the pH below 7.0 inhibits MDH, enhances ME activity, and prevents OAA inhibition of respiration [38]. However, this effect does not always manifest depending on the MDH/ME ratio in the samples.
3. Air saturation is accomplished by opening the lid of the water (or buffer) to introduce atmospheric air, closing the lid, and then shaking vigorously a number of times, or otherwise by bubbling air through water.
4. Check to see that the electrode records a good signal in air-saturated water. For our Hansatech Oxygraph system, we find that an initial signal between 1,600 and 2,100 mV is indicative of good electrode preparation. The performance of oxygen electrodes deteriorates over time due to electrochemical deposition of chloride and oxide salts on the silver anode. This can be detected by low signal during the first step of calibration. To restore the signal, it is necessary to periodically clean the anode using aluminum oxide polishing paste.
5. Once exposed to air, dithionite oxidizes over time. Therefore, the laboratory stock should be renewed once per year, or sooner if calibrations are taking a long time to reach zero.
6. It is important not to add too much mitochondrial suspension; otherwise the rate of oxygen consumption will exceed the response time of the oxygen electrode. It is therefore advisable to test several different concentrations of mitochondrial suspension and choose one that is appropriate for the experiment.

7. Despite decades of research, the precise value of maximum attainable ADP/O ratios for different substrates is still not conclusively defined. There are a number of uncertainties, such as the stoichiometry of ATP synthase activity, rates of proton leak, and uncoupling protein activity. Based on a wide collection of results, consensus ratios are approximately 1 at Complex I, 0.5 at Complex III, and 1 at Complex IV [39]. In the presence of nPG, this would mean that the maximum theoretical ADP/O ratios are ~2.5 for Complex I-linked substrates, and ~1.5 for NADH/succinate.
8. Including this many chemicals to begin the assay can be laborious and error prone, so some researchers combine the different reagents into a "master mix" that is added in a single injection.
9. These assays could be conducted with any respiratory substrate (e.g., malate, pyruvate, glutamate, NADH, succinate). For the purposes of this chapter, we have chosen NADH and succinate as the substrates for these assays.
10. Mitochondria can be ruptured via repeated freeze-thaw cycles, or membranes can be dissolved by the addition of 0.05 % (v/v) Triton X-100. Ruptured mitochondria can conduct full ETC reactions; dissolved mitochondria can only be used for single-enzyme assays.

Acknowledgements

We thank Peter Rank (Rank Brothers Limited) for granting permission to use Fig. 2. This work is supported by the Australian Research Council Centre of Excellence in Plant Energy Biology and NLT and AHM as Australian Research Council Future Fellows.

References

1. Severinghaus JW, Astrup PB (1986) History of blood gas analysis. IV. Leland Clark's oxygen electrode. J Clin Monit 2:125–139
2. Truesdale GA, Downing AL (1954) Solubility of oxygen in water. Nature 173:1236
3. Clark LC, Wolf R, Granger D et al (1953) Continuous recording of blood oxygen tensions by polarography. J Appl Physiol 6: 189–193
4. Sweetlove LJ, Fernie AR (2013) The spatial organization of metabolism within the plant cell. Annu Rev Plant Biol 64:723–746
5. Day DA, Neuburger M, Douce R (1985) Biochemical-characterization of chlorophyll-free mitochondria from pea leaves. Aust J Plant Physiol 12:219–228
6. Lyons JM, Raison JK (1970) Oxidative activity of mitochondria isolated from plant tissues sensitive and resistant to chilling injury. Plant Physiol 45:386–389
7. Noguchi K, Taylor NL, Millar AH et al (2005) Response of mitochondria to light intensity in the leaves of sun and shade species. Plant Cell Environ 28:760–771
8. Vassileva V, Simova-Stoilova L, Demirevska K et al (2009) Variety-specific response of wheat (*Triticum aestivum* L.) leaf mitochondria to drought stress. J Plant Res 122:445–454
9. Jacoby RP, Millar AH, Taylor NL (2013) Investigating the role of respiration in plant salinity tolerance by analyzing mitochondrial proteomes from wheat and a salinity-tolerant

Amphiploid (wheat x *Lophopyrum elongatum*). J Proteome Res 12:4807–4829

10. Meyer EH, Tomaz T, Carroll AJ et al (2009) Remodeled respiration in ndufs4 with low phosphorylation efficiency suppresses Arabidopsis germination and growth and alters control of metabolism at night. Plant Physiol 151:603–619
11. Gehl B, Lee CP, Bota P et al (2014) An Arabidopsis stomatin-like protein affects mitochondrial respiratory supercomplex organization. Plant Physiol 164:1389–1400
12. Smith C, Barthet M, Melino V et al (2011) Alterations in the mitochondrial alternative NAD(P)H dehydrogenase NDB4 lead to changes in mitochondrial electron transport chain composition, plant growth and response to oxidative stress. Plant Cell Physiol 52: 1222–1237
13. Douce R, Neuburger M (1989) The uniqueness of plant mitochondria. Annu Rev Plant Physiol Plant Mol Biol 40:371–414
14. Bendall DS, Bonner WD (1971) Cyanide-insensitive respiration in plant mitochondria. Plant Physiol 47:236–245
15. Moller IM, Palmer JM (1982) Direct evidence for the presence of a rotenone-resistant NADH dehydrogenase on the inner surface of the inner membrane of plant-mitochondria. Physiol Plant 54:267–274
16. Dry IB, Day DA, Wiskich JT (1983) Preferential oxidation of glycine by the respiratory-chain of pea leaf mitochondria. FEBS Lett 158:154–158
17. Taylor NL, Heazlewood JL, Day DA et al (2004) Lipoic acid-dependent oxidative catabolism of alpha-keto acids in mitochondria provides evidence for branched-chain amino acid catabolism in Arabidopsis. Plant Physiol 134:838–848
18. Shugaev AG, Shugaeva N, Vyskrebentseva EI (2005) Effect of KCl medium on malate oxidation in mitochondria of sugar beet taproot. Russ J Plant Physiol 52:616–622
19. Kearns A, Whelan J, Young S et al (1992) Tissue-specific expression of the alternative oxidase in soybean and siratro. Plant Physiol 99:712–717
20. Vanlerberghe GC, McIntosh L (1992) Lower growth temperature increases alternative pathway capacity and alternative oxidase protein in tobacco. Plant Physiol 100:115–119
21. Svensson AS, Johansson FI, Moller IM et al (2002) Cold stress decreases the capacity for respiratory NADH oxidation in potato leaves. FEBS Lett 517:79–82
22. Millar AH, Wiskich JT, Whelan J et al (1993) Organic-acid activation of the alternative oxidase of plant-mitochondria. FEBS Lett 329:259–262
23. Umbach AL, Siedow JN (1993) Covalent and noncovalent dimmers of the cyanide-resistant alternative oxidase protein in higher-plant mitochondria and their relationship to enzyme-activity. Plant Physiol 103:845–854
24. Moller IM, Palmer JM (1981) Charge screening by cations affects the conformation of the mitochondrial inner membrane. A study of exogenous MAD(P)H oxidation in plant mitochondria. Biochem J 195:583–588
25. Schonbaum GR, Bonner WD, Storey BT et al (1971) Specific inhibition of cyanide-insensitive respiratory pathway in plant mitochondria by hydroxamic acids. Plant Physiol 47:124–128
26. Tomlinson PF, Moreland DE (1975) Cyanide-resistant respiration of sweet potato mitochondria. Plant Physiol 55:365–369
27. Brunton CJ, Palmer JM (1973) Pathways for the oxidation of malate and reduced pyridine nucleotide by wheat mitochondria. Eur J Biochem 39:283–291
28. Diolez P, Moreau F (1983) Effect of Bovine Serum Albumin on membrane potential in plant mitochondria. Physiol Plant 59:177–182
29. Ducet G (1979) Influence of Bovine Serum Albumin on the proton conductance of potato mitochondria membranes. Planta 147:122–126
30. Flowers TJ (1974) Salt tolerance in Suaeda-maritima (L) Dum - comparison of mitochondria isolated from green tissues of Suaeda and Pisum. J Exp Bot 25:101–110
31. Campbell LC, Raison JK, Brady CJ (1976) Response of plant mitochondria to media of high solute content. J Bioenerg Biomembr 8:121–129
32. Krab K, Wagner MJ, Wagner AM et al (2000) Identification of the site where the electron transfer chain of plant mitochondria is stimulated by electrostatic charge screening. Eur J Biochem 267:869–876
33. Atkin OK, Zhang QS, Wiskich JT (2002) Effect of temperature on rates of alternative and cytochrome pathway respiration and their relationship with the redox poise of the quinone pool. Plant Physiol 128:212–222
34. Estabrook RW (1967) Mitochondrial respiratory control and the polarographic measurement of ADP:O ratios. In: Estabrook RW, Pullman ME (eds) Methods in enzymology, vol 10. Academic, New York, NY, pp 41–47
35. Chance B, Williams GR (1955) Respiratory enzymes in oxidative phosphorylation 3. The steady state. J Bio Chem 217:409–427

36. Menz RI, Griffith M, Day DA et al (1992) Matrix NADH dehydrogenases of plant mitochondria and sites of quinone reduction by complex I. Eur J Biochem 208:481–485
37. Zhang Q, Wiskich JT (1995) Activation of glycine decarboxylase in pea leaf mitochondria by ATP. Arch Biochem Biophys 320:250–256
38. Wiskich JT, Bryce JH, Day DA et al (1990) Evidence for metabolic domains within the matrix compartment of pea leaf mitochondria: implications for photorespiratory metabolism. Plant Physiol 93:611–616
39. Hinkle PC (2005) P/O ratios of mitochondrial oxidative phosphorylation. Biochim Biophys Acta 1706:1–11

Chapter 13

Micro-Respiratory Measurements in Plants

Yun Shin Sew, A. Harvey Millar, and Elke Stroeher

Abstract

Respiratory measurement in plants is one of the commonly used techniques to assess metabolic activity and in vivo redox state of plant mitochondria. However, respiration rate monitoring of Arabidopsis (*Arabidopsis thaliana*) remains a challenge for researchers due to the small size of its organs. In this chapter we introduce adaptations to micro-respiratory technologies to study three tissues of special interest to plant biologists: leaf sections, root tips, and seeds in this model plant species. This assay opens up new possibilities to screen and study mutants and to identify differences in ecotypes or populations of plants.

Key words Respiration, Arabidopsis, Mitochondria, Seeds, Root tips, Leaves

1 Introduction

Respiration is an essential metabolic process in plants that provides energy to sustain growth via respiratory pathways of glycolysis, tricarboxylic acid (TCA) cycle, and mitochondrial electron transport chain. There are strong correlations between plant cellular respiration, carbon balance, and biomass accumulation of plants [1], with nitrogen assimilation [2], optimizing photosynthetic carbon dioxide fixation [3, 4], facilitating plant biotic and abiotic stress acclimation [5, 6], reactive oxygen species (ROS) production, programed cell death, and even fruit ripening. Respiration rate can be measured from plant tissues by many means as described previously [7]. The two most common assays are the Clark-type oxygen electrode to measure oxygen consumption and infrared gas analyzer (IRGA) to measure carbon dioxide production. Both techniques deliver very reliable results but usually suffer from lack of high-throughput options and normally require a substantial amount of plant material. A minimum of 20–50 mg of plant tissue is needed for a single assay in most cases [8–10].

With the advancement of fluorescence assays, oxygen consumption measurements in living cells and tissues can be undertaken by combining micro-respiratory technologies with multiplex assays,

James Whelan and Monika W. Murcha (eds.), *Plant Mitochondria: Methods and Protocols*, Methods in Molecular Biology, vol. 1305, DOI 10.1007/978-1-4939-2639-8_13,

e.g., in the multi-well microplate format of the commercial Seahorse XF96 Extracellular Flux Analyzer. This technology was originally designed for use with intact animal cell specimens such as cell cultures [11], tissue slices [12, 13], and synaptosomes [14] and for use with isolated mitochondria [15, 16]. Its application for plant respiratory studies has not been widely exploited.

Here we describe in detail a range of optimized methods that adapt the Seahorse XF96 Analyzer for the microplate-based measurement of oxygen consumption from Arabidopsis leaf, root, and seed. Following this adapted method, this commercial system would also suit a wider range of plant species, particularly where small, flat tissue specimens can be easily obtained.

1.1 Principle of the Seahorse XF96 Instrument

Seahorse XF96 Extracellular Flux Analyzer is one of the recently developed commercial platforms for metabolic assays using cell culture and tissue samples. This instrument allows fast, sensitive, and noninvasive cellular bioenergetics measurements, enabling real-time fluorimetric detection of oxygen levels via fluorophores in a commercial sensor cartridge in a microliter-scale chamber. A single-analyte sensor spot is embedded on the bottom of each probe and measures oxygen consumption via detecting oxygen concentration changes over time. Oxygen quenches the fluorescence of a fluorescein complex; the fluorescence is detected by a fiber-optic wave guide and converted into the oxygen consumption rate (OCR) using the values from different time points. There are three main steps in a complete cycle referred to as "mixing," "waiting," and "measurement." Oxygen levels in the sample are measured continuously during the "measurement" phase until the rate of change is linear and then the slope is used to calculate the OCR. The analyzer uses an open system method in which oxygen is reintroduced into the solution by the steps of "mixing" during which the probe is repeatedly lifted and lowered to mix with air. The "waiting" phase allows redissolved oxygen to distribute evenly within the solution in the transient micro-chamber, thus restoring the oxygen concentration values to baseline and allowing a new cycle of "measurement." The recorded OCR can be visualized and analyzed in both XF96 Analyzer software and an Excel-based data viewer. The details of Seahorse XF designs and calculation of oxygen concentration from the fluorescence response of the oxygen probe are published [17].

2 Materials

2.1 Calibration of Probes of Sensor Cartridge

The following materials are needed for all methods described below:

1. Seahorse Bioscience XF96 Extracellular Flux Analyzer.
2. Seahorse Bioscience XF96 green sensor cartridge.

3. Seahorse Bioscience XF96 utility plate.
4. Seahorse Bioscience XF96 calibrant solution.
5. 37 °C incubator.
6. Cling wrap.
7. Repeater pipettor with suitable tip or multichannel pipette with suitable tips. Alternatively, a robotic liquid-handling station (e.g., we have used Bravo, Agilent Technologies with a suitable program) ensures equal loading of the wells with respiration buffer and greatly speeds assay assembly.

2.2 Preparation of Adhesive Mixture

1. Leukosan® Adhesive (*see* **Note 1**).
2. 0.25 % (w/v) agarose in water.
3. 1.5-mL microcentrifuge tube.
4. Thermo block or water bath at 70 °C.
5. Pipette and suitable tips.

2.3 Leaf Respiration Measurement by Seahorse XF96 Assay

1. Arabidopsis leaves.
2. Seahorse Bioscience XF96 cell plate.
3. Adhesive mixture (Subheadings 2.2 and 3.2).
4. Cotton bud.
5. Respiration buffer (10 mM HEPES, 10 mM MES, and 2 mM $CaCl_2$, pH 7.2) (*see* **Note 2**).
6. Razor blade or scissors.
7. 2.5-mm-diameter cork borer.
8. Piece of cardboard.
9. Pipette and tips.
10. Tweezers.

2.4 Root Respiration Measurement by Seahorse XF96 Assay

1. Arabidopsis root samples (*see* **Note 3**).
2. Seahorse Bioscience XF96 cell plate.
3. Respiration buffer (10 mM HEPES, 10 mM MES, and 2 mM $CaCl_2$, pH 7.2).
4. Adhesive mixture (Subheadings 2.2 and 3.2).
5. Tweezers.
6. Scissors.
7. Piece of colored paper cut to the length the roots should be cut to or a ruler used for consistency.
8. Black cloth.
9. 100-mL beaker with water.

2.5 Seed Respiration Measurements by Seahorse XF96 Assay

1. Arabidopsis seeds.
2. Seahorse Bioscience XF96 cell plate.
3. Adhesive mixture (Subheadings 2.2 and 3.2).
4. Toothpicks.
5. Seed respiration medium (5 mM KH_2PO_4, 10 mM TES, 10 mM NaCl, 2 mM $MgSO_4$, pH 7.2).
6. Optional: Material for seed sterilization: Seed fumigation solution (100 mL 12 % NaOCl and 3 mL 37 % HClO) in a beaker, desiccator.

3 Methods

3.1 Calibration of Probes of Sensor Cartridges and Preparation of the Seahorse XF96 Analyzer

A 24-well version and a 96-well version of the Seahorse Analyzer are available. Described here are the methods for the 96-well plate version.

Prior to all respiration measurements using the Seahorse XF96 Analyzer described here, the sensor cartridge has to be calibrated.

It is important to note that only one plate can be measured at a time. A sensor cartridge should be calibrated when needed. Even if all 96 wells are not used, they have to be filled with buffer.

1. Add 100 μL of XF96 calibrant solution to each well of the XF96 utility plate using a pipettor or robot if available. Place the sensor cartridge back on top of the utility plate and wrap the plates with cling wrap to prevent evaporation prior to incubation at 37 °C overnight.
2. The next day, discard the calibrant solution thoroughly and refill with 200 μL fresh calibrant solution in the XF96 utility plate using a pipettor or robot if available.
3. Turn on the Seahorse XF96 Analyzer instrument and launch the Seahorse XF96 software. For plant samples, the assay temperature should be maintained at room temperature. Therefore the instrument heater needs to be turned off immediately after starting the software.
4. Select the assay wizard to generate a new assay template or load saved/existing templates for assay design.
5. For easier analysis later, define the content of each well in the microplate by labeling the cell type, cell media, compounds for injection port, specimen tested, etc. shown in the tabs of "assay wizards" accordingly.
6. Assign wells for background corrections (e.g., blank) and turn on the background corrections options in the "Back. Corrections" tab.

7. Create a run protocol for the assay by inserting the steps, e.g., repeating cycles (loop) of mix, waiting, and measure according to one's preference or type of specimen [see below in the corresponding sections (*see* **Note 4**)]. Save the protocol and assay template before ending the "assay wizard."
8. Start the calibration step and load the sensor cartridge with the utility plate filled with fresh calibrant.
9. Once the calibration is completed, only the utility plate will be released by the machine and can be replaced by the cell plate containing the samples; see steps below.

3.2 Preparation of Adhesive Mixture

Measuring oxygen consumption rate in microtiter plates requires the tissue to remain at the bottom of the well and not to move during the different steps of the run protocol. This is especially important when working with plant tissues that are often buoyant structures. We have developed a low-cost adhesive mixture, which enables effective fixation of the material but does not interfere with the oxygen consumption rate measurement [18].

1. Prepare 2.5 % (v/v) Leukosan® Adhesive in 0.25 % (w/v) agarose in a microcentrifuge tube (*see* **Note 5**).
2. Keep the adhesive mixture at 70 °C in a thermo block to avoid solidification.
3. Vortex before using the mixture (*see* **Note 6**).

3.3 Leaf Respiration Measurement by Seahorse XF96 Assay

1. The day before the respiration measurement should be performed, start incubation of the sensor cartridge (Subheading 3.1).
2. On the day, while the sensor cartridge is calibrating which takes approximately 30 min, proceed with the following steps.
3. Cut the leaf from the plant using a razor blade or scissors and place on top of a piece of cardboard (*see* **Note 7**).
4. Pipet 1 µL of the adhesive mixture (Subheading 3.2) onto the center of the well bottom.
5. Quickly excise a single 2.5-mm-diameter leaf disc using the cork borer (*see* **Notes 8–10**).
6. Position the leaf disc on top of the mixture and then gently press with a cotton bud to ensure proper adhesion.
7. Allow the adhesive mixture to set for 2–5 min.
8. Carefully add 200 µL of respiration buffer on top of the leaf discs to avoid dehydration (*see* **Note 11**).
9. Prepare wells for the background measurement by pipetting 1µL of adhesive mixture onto the center of a well, let it set for 2-5 min and add 200 µL of respiration buffer.
10. Once the plate is prepared, check that all leaf discs are at the bottom of the well.

11. Replace the utility plate of the calibrated sensor cartridge (Subheading 3.1) with the cell plate.
12. Start the run.
13. For routine basal leaf respiration measurement, the run protocol is set as mixing (3 min) and measuring (5 min) and the cycle is repeated ten times (*see* **Note 12**).
14. The OCRs of single-leaf disc are recorded and analyzed using Seahorse XF96 Acquisition and Analysis Software.

3.4 Root Respiration Measurement by Seahorse XF96 Assay

1. The day before, start incubation of the sensor cartridge (Subheading 3.1).
2. On the day, while the sensor cartridge is calibrating, proceed with the following steps.
3. Place the plate containing the plants on a black cloth for better visibility of the roots.
4. Lay the colored piece of paper under the plate and use as an indicator for the length of the root section which has to be cut.
5. Using very sharp scissors cut ~5 mm of the root (*see* **Note 13**).
6. Add 1 μL of the adhesive mixture (Subheading 3.2) onto the center of the bottom of the well (*see* **Note 14**).
7. Place the root section in the center using tweezers (*see* **Notes 10** and **15**).
8. Allow the adhesive mixture to set for 2–5 min.
9. Carefully fill the 96-well Seahorse Bioscience XF96 cell plate with 200 μL of respiration buffer (*see* **Note 16**).
10. Prepare wells for the background measurement by pipetting 1 μL of adhesive mixture onto the center of a well, let it set for 2-5 min and add 200 μL of respiration buffer.
11. Once the plate is prepared, check that all root sections are at the bottom of the well.
12. Replace the utility plate of a calibrated sensor cartridge with the cell plate containing the root sections and load into the Seahorse Bioscience XF96 Analyzer.
13. Start the run.
14. For routine basal root respiration measurement, the run protocol is set as mixing (3 min) and measuring (5 min) and the cycle is repeated ten times (*see* **Note 12**).
15. The OCRs of roots are recorded and analyzed using Seahorse XF Acquisition and Analysis Software.

3.5 Seed Respiration Measurements by Seahorse XF96 Assay

1. Optional: If the Seahorse assay is running over a long period (>12 h), we recommend using sterile seeds and toothpicks.
2. The day before, start incubation of the sensor cartridge (Subheading 3.1).

3. On the day, while the sensor cartridge is calibrating, proceed with the following steps.
4. Pipette 1 μL of the adhesive mixture (Subheading 3.2) onto the bottom center of every well of the Seahorse Bioscience XF96 cell plate.
5. Place ten Arabidopsis seeds with a toothpick onto the adhesive mixture (*see* **Note 17**).
6. Complete this for all seeds to be measured.
7. If you only have used a few wells, wait for 2–5 min until seed adhesion is achieved.
8. Carefully fill the wells with 200 μL of seed respiration buffer using a pipette. Make sure that you do not flush the seeds away from the adhesive mixture.
9. Prepare wells for the background measurement by pipetting 1 μL of adhesive mixture onto the center of a well, let it set for 2-5 min and add 200 μL of respiration buffer.
10. Replace the utility plate of the calibrated sensor cartridge with the cell plate containing the seeds and load into the Seahorse Bioscience XF96 Analyzer.
11. Start the run.
12. For routine basal seed respiration measurement, the run protocol is set as mixing (3 min) and measuring (5 min) and the cycle is repeated ten times (*see* **Note 12**).
13. The OCRs of seeds are recorded and analyzed using Seahorse XF Acquisition and Analysis Software.
14. Optional: For seed growth induction and inhibition studies, hormones or inhibitors (e.g., 2.4 μM abscisic acid or 1.2 mM gibberellic acid, respectively) can be added into injection ports of XF96 sensor cartridge prior to calibration steps. Additional injection steps have then to be added to the run protocol [18].

4 Notes

1. There is commercial available skin adhesive, e.g., from BSN Medical.
2. The buffer has been successfully used in other respiratory studies before [19, 20].
3. For easy sampling of the roots, the plants should be grown in vertical agar plates containing appropriate media, e.g., Murashige and Skoog.
4. For more information about run protocols the reader is referred to XF96 Extracellular Flux Analyzer and Prep Station: Installation and Operation Manual (Seahorse Biosciences) [16]. For the plant tissues analyzed here the “wait” step has

been completely omitted. This decision was made as no effectors are used which would need a certain incubation time to show full affect on the tissue.

5. Prepare at least 100 μL of the mixture.
6. Discard and make new adhesive mixture when it turns to a whitish and highly viscous mixture.
7. The cardboard aids in the cutting of the leaf disc using the cork borer.
8. The maximal size of the leaf disc is limited by the diameter of the well and only one leaf disc can be used per well. A 2.5-mm-diameter leaf disc corresponds to ~0.7 mg fresh weight. Additional measurements have shown that the OCR measured using the Seahorse XF96 Analyzer increases linearly with increasing tissue amount [18]. The leaf disc size used here is within the linear range. However, measurements of different leaf ages have also shown that the OCR gradually increases from mature to immature leaves [18]. It is not recommended to measure OCRs above 500 pmol oxygen/min/disc (please refer to XF96 Extracellular Flux Analyzer and Prep Station—Installation and Operation Manual, page 87).
9. To ensure consistency of the measurement, we recommend avoiding the midribs of the leaves. For more details see [18].
10. We recommend measuring at least six replicates.
11. If large numbers of leaf discs are used, sequential handling is required. In our hands, it worked very well to perform **steps 3–6** for 6 wells, then add the buffer, and continue with the next 6 wells. A full 96-well plate can be manually adhered in ~45 min.
12. The "waiting" step has been omitted in experiments where no inhibitors/effectors are used. The minimum number of cycles is 6, but can be increased if needed. Some tissues might not have a stable respiration over time; therefore the datasets have to be analyzed carefully.
13. Decide first which part of the root should be analyzed and use roughly the same section for all plants to be analyzed, as there are OCR differences, e.g., between root tip and expanded section; see [18]. This can be difficult when analyzing mutants with short roots. In that case shorter sections can be analyzed if multiple sections are used per well.
14. It is important to form a drop-like shape, as this is much easier to fix the root section.
15. Keep the tweezers in a beaker with water between the steps; this aids in removing adhesive mixture. Otherwise the root section can stick to the tweezers after preparation of multiple wells. We recommend marking the wells that already have been filled as the root sections can be hard to see once submerged in the buffer.

16. If large numbers of root sections are measured, sequential handling is required. In our hands it worked very well to perform **steps 5**–7 for 8 wells, then add the buffer, and continue with the next 8 wells. A full 96-well plate can be manually adhered in ~60 min.
17. Single Arabidopsis seeds can be measured when increasing the cycle number. We recommend at least 6 replicates for 10 seeds and at least 14 replicates when measuring single-seed respiration.

Acknowledgments

Development of these protocols was funded by the Australian Research Council through the ARC Centre of Excellence in Plant Energy Biology (CE140100008). Y.S.S. is supported by a PhD scholarship from Malaysian Agricultural Research and Development Institute (MARDI). A.H.M. is supported by an ARC Future Fellowship (FT110100242) and E.S. by an ARC Postdoctoral Fellowship (DP110104865).

References

1. Amthor JS (1989) Respiration and crop productivity. Springer, New York, NY
2. Lancien M, Gadal P, Hodges M (2000) Enzyme redundancy and the importance of 2-oxoglutarate in higher plant ammonium assimilation. Plant Physiol 123:817–824
3. Raghavendra AS, Padmasree K (2003) Beneficial interactions of mitochondrial metabolism with photosynthetic carbon assimilation. Trends Plant Sci 8:546–553
4. Krömer S (1995) Respiration during photosynthesis. Annu Rev Plant Physiol Plant Mol Biol 46:45–70
5. Plaxton WC (1996) The organization and regulation of plant glycolysis. Annu Rev Plant Physiol Plant Mol Biol 47:185–214
6. Plaxton WC (2004) Plant response to stress: biochemical adaptations of to phosphate deficiency. In: Goodman R (ed) Encyclopedia of plant and crop science. CRC Press, New York, NY, pp 976–980
7. Roberto Millan-Almaraz J, Gerardo Guevara-Gonzalez R, de Jesus Romero-Troncoso R, Alfredo Osornio-Rios R, Torres-Pacheco I (2009) Advantages and disadvantages on photosynthesis measurement techniques: a review. Afr J Biotechnol 8:7340–7349
8. Hunt S (2003) Measurements of photosynthesis and respiration in plants. Physiol Plant 117: 314–325
9. Meyer EH, Tomaz T, Carroll AJ, Estavillo G, Delannoy E, Tanz SK, Small ID, Pogson BJ, Millar AH (2009) Remodeled respiration in ndufs4 with low phosphorylation efficiency suppresses Arabidopsis germination and growth and alters control of metabolism at night. Plant Physiol 151:603–609
10. Tomaz T, Bagard M, Pracharoenwattana I, Linden P, Lee CP, Carroll AJ, Stroeher E, Smith SM, Gardestrom P, Millar AH (2010) Mitochondrial malate dehydrogenase lowers leaf respiration and alters photorespiration and plant growth in Arabidopsis. Plant Physiol 154:1143–1157
11. Wu M, Neilson A, Swift AL, Moran R, Tamagnine J, Parslow D, Armistead S, Lemire K, Orrell J, Teich J, Chomicz S, Ferrick DA (2007) Multiparameter metabolic analysis reveals a close link between attenuated mitochondrial bioenergetic function and enhanced glycolysis dependency in human tumor cells. Am J Physiol Cell Physiol 292:C125–C136
12. O'Riordan TC, Zhdanov AV, Ponomarev GV, Papkovsky DB (2007) Analysis of intracellular oxygen and metabolic responses of mammalian

cells by time-resolved fluorometry. Anal Chem 79:9414–9419

13. Schuh RA, Clerc P, Hwang H, Mehrabian Z, Bittman K, Chen H, Polster BM (2011) Adaptation of microplate-based respirometry for hippocampal slices and analysis of respiratory capacity. J Neurosci Res 89:1979–1988
14. Choi SW, Gerencser AA, Nicholls DG (2009) Bioenergetic analysis of isolated cerebrocortical nerve terminals on a microgram scale: spare respiratory capacity and stochastic mitochondrial failure. J Neurochem 109:1179–1191
15. Dykens JA, Jamieson JD, Marroquin LD, Nadanaciva S, Xu JJ, Dunn MC, Smith AR, Will Y (2008) In vitro assessment of mitochondrial dysfunction and cytotoxicity of nefazodone, trazodone, and buspirone. Toxicol Sci 103: 335–345
16. Rogers GW, Brand MD, Petrosyan S, Ashok D, Elorza AA, Ferrick DA, Murphy AN (2011) High throughput microplate respiratory measurements using minimal quantities of isolated mitochondria. PLoS One 6:e21746
17. Gerencser AA, Neilson A, Choi SW, Edman U, Yadava N, Oh RJ, Ferrick DA, Nicholls DG, Brand MD (2009) Quantitative microplate-based respirometry with correction for oxygen diffusion. Anal Chem 81:6868–6878
18. Sew YS, Stroeher E, Holzmann C, Huang S, Taylor N, Jordana X, Millar AH (2013) Multiplex micro-respiratory measurements of Arabidopsis tissues. New Phytol 200: 922–932
19. Atkin OK, Cummins WR, Collier DE (1993) Light Induction of alternative pathway capacity in leaf slices of Belgium endive. Plant Cell Environ 16:231–235
20. Armstrong AF, Logan DC, Atkin OK (2006) On the developmental dependence of leaf respiration: responses to short- and long-term changes in growth temperature. Am J Bot 93: 1633–1639

Chapter 14

Improvements to Define Mitochondrial Metabolomics Using Nonaqueous Fractionation

Richard Fly, James Lloyd, Stephan Krueger, Alisdair Fernie, and Margaretha J. van der Merwe

Abstract

Defining metabolite abundance and resulting fractional isotope enrichments, within and between cellular compartments, still remain a major challenge in modern plant biochemistry. Optimized protocols for rapid isolation of mitochondria (e.g., silicone oil centrifugation or membrane filters) or visualization of metabolites/metabolic states (e.g., fluorescence resonance energy transfer (FRET) or redox-sensitive fluorescent markers (*ro*GFP)) have significantly improved and expanded our knowledge regarding mitochondrial metabolism. However, the application of nonaqueous fractionation (NAQF) to separate and quantify metabolites across subcellular compartments remains popular as a nontargeted, validated approach towards studying metabolism, and provides a top-down overview of metabolite distribution across the majority of the subcellular compartments in a single preparation. Unfortunately, of all the organelles resolved using this method, the mitochondrion still remains the most poorly defined. Here, the development and suggested improvements to resolve the mitochondrial metabolome are described.

Key words Enzymatic activities, Mass spectrometry, Metabolomics, Nonaqueous fractionation, Proteomics

1 Introduction

Novel biological insights can be obtained from studying subcellular biochemistry; yet the development of techniques to elucidate the subcellular distribution of small molecules in a high-throughput manner still remains a significant technical challenge. In plant mitochondria, metabolites play important roles, serving as valuable cofactors and intermediates that drive fundamental processes such as growth, N assimilation, and photorespiration, impacting whole-plant performance and yield. The accelerated advances in genomic, transcriptomic, and proteomic resources have further illustrated that mitochondria play many other important metabolic roles, including serving as one of the major sites for the biosynthesis of ascorbate [1, 2], folate, and thymidylate [3, 4]. Ligands that alter

James Whelan and Monika W. Murcha (eds.), *Plant Mitochondria: Methods and Protocols*, Methods in Molecular Biology, vol. 1305, DOI 10.1007/978-1-4939-2639-8_14,

the catalytic binding capacities of proteins or bind to specific signaling effectors [5] could transiently be transported to, or transduced from, the mitochondrion, suggesting that mitochondria potentially serve as central integration points during metabolism. The need to define mitochondrial metabolite content (and associated fluxes) within and across compartments is thus an essential component to understand metabolic regulation.

Nonaqueous fractionation (NAQF) is a powerful technique to enrich for subcellular compartments, characterized by the critical requirement of minimizing metabolite turnover and loss during the lengthy fractionation process. The principle of NAQF relies on an equilibrium distribution of small particles that aggregate to each other (based on their subcellular lipid, ionic, and protein composition) during sonication, and resulting separation along a nonaqueous gradient. Following fractionation, protein marker abundances, subcellular enrichment, and compartmental separation can be assessed. Critical towards enrichment analyses are the proper optimization and implementation of a gradient that will facilitate the separation of fractions (or compartments) of interest. Factors that can influence the efficiency of enrichment include high-molecular-weight compounds, including starch and glycogen. Also, the selection of marker enzymes or protein abundances for compartmental assignment is crucial; two or more markers per fraction should be chosen and validated. Currently, a targeted enzymatic approach for determining maximal catalytic activity (*see also* Chapter 10) is employed. The degree of enrichment can be significantly improved by the use of high-resolution proteomic techniques (*see also* Chapter 6) providing that protein abundance is sufficient for detection and that the protein identity can be confirmed to be exclusively localized to a particular compartment.

In order to determine metabolite identities or levels (absolute or relative), an array of standard protocols could be applied to the obtained fractionated material. Examples of technologies, and the range of metabolites that can be measured include (but are not limited to) enzymatic coupled spectrophotometric assays (e.g., sugars, starch, redox metabolites) to high-throughput technologies. These high-throughput technologies include hyphenated chromatography mass spectrometry to determine abundant primary metabolites (e.g., sugars, organic acids, and amino acids (via gas chromatography mass spectrometry (GC MS); [6]). The nature of GC-MS analysis, however, often hampers the reliable detection and quantification of charged compounds, like phosphorylated and nucleotide sugars. Profiling by GC MS relies on the compound of interest being vaporized in order for separation of compounds within complex extracts to occur in a capillary column. While this is applicable to a range of volatile compounds, chemical modification of nonvolatile compounds (in a process called derivatization) can also be employed to increase the volatility of the analyte of

interest for gas chromatographic separation. More polar metabolites, however, such as ionic species containing phosphate groups, are not readily amenable to standard derivatization techniques and often result in artifact formation. For this reason, phosphorylated metabolites, nucleotides, and nucleotide sugars can be assessed via liquid chromatography mass spectrometry (LC MS) [7]. Moreover, secondary or more specialized metabolites can also be assessed via LC MS technologies [8]. Using MS-based technologies, isotope fractional enrichment analyses could also be employed to study the time-resolved dynamics of metabolite levels [9]. The principle of chromatography (gas or liquid) is the separation of chemical complexity on a silica-fused column that elutes metabolites on the basis of their inherent chemical properties (and the specificity of the column used). The eluted compounds are then directly injected into a mass spectrometer, allowing the fragmentation of individual chemicals to be obtained, and a confidence level assigned to the identification of metabolite(s) of interest. In this chapter, both GC MS and LC MS protocols (for detection and quantification of primary metabolites) are described to confidently assign 100–150 metabolites between the majority of the subcellular compartments, including mitochondrial, plastidial, vacuolar, and cytosolic fractions.

2 Materials

2.1 Nonaqueous Fractionation Components

1. Sonicator with single probe (Bandelin Sonopuls HD2070 sonicator fitted with a Bandelin UW 2070 probe).
2. Sonicator bath.
3. Heptane.
4. Tetrachloroethylene.
5. Ethanol.
6. 50-mL sterile Corning® centrifuge tubes.
7. Nylon mesh filters.
8. Programmable gradient pourer.
9. Hydrometer.
10. Ultracentrifuge.
11. Eppendorf tubes (2 mL).
12. Evaporator and trap for organic solvents.
13. Silica gel beads.

2.2 Protein Distribution Components

1. Protein extraction buffer (PEB):

   50 mM 4-(2-Hydroxyethyl)-1-piperazine ethane sulfonic acid (Hepes)-KOH (pH 7.4).

   5 mM $MgCl_2$.

1 mM Ethylene diaminetetraacetic acid (EDTA).
5 mM Dithiothreitol (DTT).
0.1 % (v/v) Triton.
10 % (v/v) glycerol.

2. Ultrasonic bath.
3. Benchtop centrifuge.
4. Bradford reagent (or other protein determination assay).
5. Spectrophotometer.
6. Microtiter plates.
7. Hepes-HCl (pH 7.5).
8. 5 mM $MgCl_2$.
9. 1 U/mL glycerokinase.
10. 1 mM ADP-glucose.
11. 5 mM 3-phosphoglycerate.
12. 1.5 mM sodium fluoride.
13. 120 mM glycerol.
14. 2 mM PPi.
15. 0.5 M HCl.
16. 1.87 U/mL glycerol 3-phosphate oxidase.
17. 0.7 U/mL glycerol 3-phosphate dehydrogenase.
18. 1 mM NADH.
19. 1.5 mM $MgCl_2$.
20. 100 mM Tricine-KOH (pH 8.0).
21. 2 mM $MgCl_2$.
22. 100 mM citrate-KOH (pH 4.5).
23. 5 mM *p*-nitrophenyl-D-α-mannoside.
24. 1 M Na_2CO_3.
25. Glucose standards (ranging from 0 to 1 nmol).
26. 50 mM acetate-KOH (pH 4.5).
27. 20 mM sucrose.
28. 0.5 M NaOH.
29. 0.5 M HCl.
30. 100 mM Hepes-KOH (pH 7.0).
31. 50 mM Hepes-KOH (pH 7.0).
32. 1 U/mL glucose oxidase.
33. 0.0015 U/mL horseradish peroxidase.
34. 200 μM dihydroxyphenoxasine.

35. 10 µmol sodium acetate buffer (pH 6.5).
36. 2.48 µmol maltotriose.
37. 1 mM NADP.
38. 1 U/mL hexokinase.
39. 1 U/mL glucose 6-phosphate dehydrogenase.
40. ATP standards (ranging between 0 and 1 nmol).
41. 1 mM UDP-glucose.
42. Fructose 1,6-bisphosphate standards (ranging from 0 to 80 µM).
43. 50 mM Hepes-HCl (pH 7.5).
44. 2 mM $MgCl_2$.
45. 0.25 mM NADH.
46. 5 mM ATP.
47. 7.5 mM fructose 6-phosphate.
48. 10 µM fructose 2,6-bisphosphate.
49. 1 U/mL aldolase.
50. 1 U/mL triose-phosphate isomerase.
51. 1 U/mL glycerol 3-phosphate dehydrogenase.
52. 0.25 mM PPi.
53. 50 mM potassium phosphate (pH 7.4).
54. 10 mM sodium succinate.
55. 100 µM EDTA.
56. 10 mM potassium cyanide.
57. 150 µM dichlorophenolindophenol (DCPIP).
58. 2 mM phenazine methosulfate.
59. 100 mM Tricine-KOH (pH 8.0).
60. 10 mM $MgCl_2$.
61. 100 µM EDTA.
62. 1 U/mL glycerokinase.
63. 10 mM phosphate.
64. 2.5 mM ADP.
65. 100 µM 5′,5′ diadenosinpentaphosphate.
66. 120 mM glycerol.
67. 100 µM succinyl CoA.
68. 1.8 U/mL glycerol 3-phosphate oxidase.
69. 0.7 U/mL glycerol 3-phosphate dehydrogenase.
70. 1 mM NADH.
71. 1.5 mM $MgCl_2$.
72. 100 mM Tricine-KOH (pH 8.0).

2.3 Metabolite Analysis Components

1. Ribitol (or eq. internal standard of your choice).
2. Vortex.
3. Sonicator bath.
4. Methoxyamine-HCl (15 mg/mL) dissolved in pyridine.
5. Heating block.
6. *N*-methyl trimethylsilylfluoroacetamide (MSTFA).
7. Trichloromethylchlorosilane (TMCS).
8. 3 kDa Low-binding regenerated cellulose membrane filter (Amicon).

3 Methods

Carry out all procedures in a cold room (4 °C) unless otherwise specified.

3.1 NAQF: Centrifugation and Fractionation

1. Homogenize 2–4 g harvested tissue in a tissue-lyzer by shaking at ~30 Hz for 30-s, or use a clean, prechilled mortar and pestle while maintaining a frozen temperature. Freeze-dry the tissue for 48–96 h in a manifold freeze dryer (negative pressure of ~0.325 mbar) until aqueous-free.
2. Resuspend the sample in 20 mL heptane:tetrachloroethylene (43:57 v/v, density 1.23 g/cm) solution (*see* **Note 1**) in a sterile 50-mL Corning® centrifuge tube and sonicate in an ethanol ice bath in three successive 30-s bursts with 20-s intervals in between at ~40 % power in an ultrasonic cleaner.
3. Filter the material through a nylon mesh filter with a mesh width between 20 and 82 μm to remove large debris.
4. Centrifuge at 4,000 × *g* for 10 min in a swing-out rotor and discard the supernatant.
5. Resuspend pellet in 3 mL heptane:tetrachloroethylene solution.

   Take aliquots of the extracts at this stage for a representation of total protein and metabolite pools. Set the remainder of the homogenate aside in a closed tube to prevent condensation of water vapor in the solvents, and prepare the exponential density gradient (*see below*).
6. For mitochondrial enrichment, the gradient should consist of a 4 mL cushion of 100 % tetrachloroethylene (density of 1.64 g/cm) poured by using an automated gradient pourer, followed by an exponential gradient of (1) 80 % (v/v) heptane (poured for 2 min), (2) 50 % (v/v) heptane (poured for 4 min), and (3) 5 % (v/v) heptane (poured for 1 min) at a constant flow rate of 1.8 mL/min, and the density of the gradient ranging from 1.29 to 1.4 g/cm. Check the density gradient with a calibrated hydrometer at 4 °C.

7. Load the remainder of the extract on top of the gradient for ultracentrifugal cell fractionation (*see* **Note 2**).
8. Centrifuge samples for 150 min at 12,000 × *g* using a rotor and ultracentrifuge (Beckman Coulter) at 4 °C.
9. Obtain 12 blind fractions of 1.2 mL each from each sample by carefully pipetting from the top layer in each case. Divide each of these resulting fractions in separate aliquots for protein and metabolite determinations, respectively. Depending on the determinations of interest (*see below*), this should range between three and seven aliquots per fraction.
10. Evaporate the fractions under vacuum in an airtight desiccator filled with silica gel beads and, upon dryness, store in sealed plastic bags containing silica gel beads at −20 °C.

3.2 Protein Extraction and Protein Enrichment Determinations

1. Extract proteins from the evaporated samples with a protocol modified from [10].
2. Add 200 μL protein extraction buffer (PEB) to the dried aliquot for protein determination and sonicate at ~40 % power in an ultrasonic cleaner.
3. Centrifuge at 4,000 × *g* for 15 min and discard the pellet.
4. Determine total soluble protein concentrations by Bradford protein determination method [11] or an equivalent method of choice for each fraction taken from each sample.

3.2.1 Marker Enzyme Determinations

If possible use a pipetting robot equipped with a cooling block, an incubator block, shaker, and gripper (e.g., Perkin-Elmer).

α-Mannosidase Maximal Catalytic Activity Determination

α-Mannosidase activity (for vacuolar enrichment) is measured as the hydrolysis of *p*-nitrophenyl D-α-mannoside to *p*-nitrophenol [12].

1. Incubate extracts with 100 μL 100 mM citrate-KOH (pH 4.5).
2. Start the reaction by adding 25 μL 5 mM *p*-nitrophenyl-D-α-mannoside.
3. Incubate for 30 min at 37 °C, and stop the reaction by adding 150 μL Na_2CO_3.
4. Measure the change in absorbance at 405 nm wavelength using a spectrophotometer.

Acid Invertase Maximal Catalytic Activity Determination

Acid invertase activity (for vacuolar enrichment) is assayed fluorimetrically from glucose liberated from sucrose hydrolysis [13].

1. Incubate glucose standards (ranging from 0 to 1 nmol) and total and fractionated extracts in 50 mM acetate-KOH (pH 4.5).
2. Add 20 mM sucrose to start reaction.
3. Incubate for 10 and 20 min.

4. Stop the reaction by adding 20 μL of 0.5 M NaOH.
5. Neutralize the extract with 20 μL of 0.5 M HCl (in 100 mM Hepes-KOH (pH 7.0)).
6. Perform fluorimetry (excitation 530 nm, emission 590 nm) after addition of 50 mM Hepes-KOH (pH 7.0), 1 U/mL glucose oxidase, 0.0015 U/mL horseradish peroxidase, and 200 μM dihydroxyphenoxasine final concentration.

D-Enzyme Maximal Catalytic Activity Determination

D-enzyme activity (for plastidial enrichment) is measured as the increase in glucose from the hydrolysis of maltotriose [14].

1. Incubate extracts in 250 μL 10 μmol sodium acetate buffer (pH 6.5) and 2.48 μmol maltotriose for 30 min at 37 °C.
2. Stop the reaction by heating at 95 °C for 30-s.
3. Measure the release of glucose by the reduction of 1 mM NADP in the presence of 1 U/mL hexokinase and 1 U/mL glucose 6-phosphate dehydrogenase at 340 nm using a spectrophotometer.

ADP-Glucose Pyrophosphorylase Maximal Catalytic Activity Determination

ADP-glucose pyrophosphorylase (AGPase) activity (for plastidial enrichment) is assayed in the reverse reaction by measuring PPi-dependent production of ATP from ADP-glucose [15].

1. Incubate ATP standards (ranging from 0 to 1 nmol) and total and fractionated extracts in a buffer containing 50 mM Hepes-HCl (pH 7.5), 5 mM $MgCl_2$, 1 U/mL glycerokinase, 0 (blank) or 1 mM (maximal activity) ADP-glucose, 5 mM 3-phosphoglycerate, 1.5 mM sodium fluoride, and 120 mM glycerol.
2. Start the reaction by adding 2 mM PPi.
3. Incubate for 5 min.
4. Stop the reaction by adding 20 μL of 0.5 M HCl.
5. Neutralize the extract with 20 μL of 0.5 M NaOH.
6. Proceed to glycerol 3-phosphate cycling determination assay.

UDP-Glucose Pyrophosphorylase Maximal Catalytic Activity Determination

UDP-glucose pyrophosphorylase (UGPase) activity (for cytosolic enrichment) is assayed in the forward reaction by measuring the production of ATP from ADP.

1. Incubate ATP standards (ranging from 0 to 1 nmol) and total and fractionated extracts in a buffer containing 50 mM Hepes-HCl (pH 7.5), 5 mM $MgCl_2$, 1 U/mL glycerokinase, 0 (blank) or 1 mM (maximal activity) UDP-glucose, 5 mM 3-phosphoglycerate, 1.5 mM sodium fluoride, and 120 mM glycerol.

2. Start the reaction by adding 2 mM PPi.
3. Incubate for 5 min.
4. Stop the reaction by adding 20 μL of 0.5 M HCl.
5. Neutralize the extract with 20 μL of 0.5 M NaOH.
6. Proceed to glycerol 3-phosphate cycling determination assay.

Pyrophosphate-Dependent Phosphofructokinase Maximal Catalytic Activity Determination

Phosphofructokinase (PFP) activity (for cytosolic enrichment) is assayed in the forward reaction by measuring PPi-dependent production of fructose 1,6-bisphosphate ($F1,6P_2$) from fructose 6-phosphate [15].

1. Incubate $F1,6P_2$ standards (ranging from 0 to 80 μM) and total and fractionated extracts in a buffer containing 50 mM Hepes-HCl (pH 7.5), 2 mM $MgCl_2$, 0.25 mM NADH, 5 mM ATP, 7.5 mM fructose 6-phosphate, 10 μM fructose 2,6-bisphosphate, 1 U/mL aldolase, 1 U/mL triose-phosphate isomerase, and 1 U/mL glycerol 3-phosphate dehydrogenase.
2. Start the reaction by adding PPi to a final concentration of 0 (blank) or 0.25 mM (maximal activity).
3. Incubate for 5 min.
4. Stop the reaction by adding 20 μL of 0.5 M HCl.
5. Neutralize the extract with 20 μL of 0.5 M NaOH.
6. Proceed to glycerol 3-phosphate cycling determination assay.

Succinate Dehydrogenase Maximal Catalytic Activity Determination

Succinate dehydrogenase (SDH) activity (for mitochondrial enrichment) is measured as the colorimetric determination of oxidized:reduced dichlorophenolindophenol (DCPIP) [16].

1. Incubate extracts in a reaction medium containing 50 mM potassium phosphate (pH 7.4), 10 mM sodium succinate, 100 μM EDTA, 10 mM potassium cyanide, 150 μM DCPIP, and 2 mM phenazine methosulfate.
2. Assay the activity spectrophotometrically at 600 nm and 25 °C.

Succinyl CoA Ligase Maximal Catalytic Activity Determination

Succinyl CoA ligase (SCoAl) activity (for mitochondrial enrichment) is assayed in the forward reaction by measuring the production of ATP from ADP [17].

1. Incubate ATP standards (ranging from 0 to 1 nmol) and total and fractionated extracts in a buffer containing 100 mM tricine-KOH (pH 8.0), 10 mM $MgCl_2$, 100 μM EDTA, 1 U/mL glycerokinase, 10 mM phosphate, 2.5 mM ADP, 100 μM 5′,5′ diadenosinpentaphosphate, 120 mM glycerol, and 0 (blank) or 100 μM (maximal activity) succinyl CoA.

2. Incubate for 5 min.
3. Stop the reaction by adding 20 μL of 0.5 M HCl.
4. Neutralize the extract with 20 μL of 0.5 M NaOH.
5. Proceed to glycerol 3-phosphate cycling determination assay.

Glycerol 3-Phosphate Cycling Determination Assay

1. Determine glycerol 3-phosphate content by adding 1.8 U/mL glycerol 3-phosphate oxidase, 0.7 U/mL glycerol 3-phosphate dehydrogenase, 1 mM NADH, 1.5 mM $MgCl_2$, and 100 mM tricine-KOH (pH 8.0). For PFP determination, also add 1 U/mL triose phosphate isomerase to the reaction mix.
2. Read the absorbance at a wavelength of 340 nm and at 30 °C until the rate is stabilized, and calculate the difference in absorbance over time for the standard calibration curve and, subsequently, the enzyme activities of the total and fractionated samples.

3.3 Metabolite Extraction and Determinations

3.3.1 Primary Metabolite Profiling (via Gas Chromatography Mass Spectrometry Technology)

1. Extract primary metabolites by resuspending the dried homogenate (of total and fractionated samples) in 7.5 nM aqueous ribitol solution.
2. Vortex the samples for 30-s and sonicate in a sonication bath until complete resuspension of the pellet is achieved.
3. Evaporate the homogenate to dryness in a vacuum dryer. Proceed to derivatization step (**step 4**) or store samples upon inert argon gas at −80 °C until ready for GC MS analyses.
4. For derivatization, add 60 μL of methoxyamine-HCl in pyridine.
5. Vortex samples for 30-s, and incubate at 50 °C for 1 h.
6. Add 60 μL *N*-methyl trimethylsilylfluoroacetamide (MSTFA) containing 1 % (v/v) trichloromethylchlorosilane (TMCS).
7. Incubate sample for a further 1 h at 50 °C.
8. Transfer the samples to glass inserts for analyses by GC-(TOF)/(QUAD) MS technology.
9. For GC QUAD-MS analyses:

   The system is composed of an Agilent technologies 6890N network GC system coupled to an Agilent 5975 MS (www.agilent.com). Chromatographic separation is performed on a 10 m guard column and 30 m Restek column (www.restek.com) with a 2.5 μm film thickness. Running conditions are as follows. Helium, as a carrier gas, is at a flow rate of 1 mL/min. Injection temperature is set at 230 °C, the interface at 250 °C, and the ion source at 200 °C. The oven temperature is set at 70 °C for 5 min followed by a 5 °C/min increase to 310 °C with 1 min of heating at 310 °C. The system is equilibrated for 6 min at 70 °C prior to the injection.

Instrument control and data acquisition are performed by the MSD Chemstation software (v 02.00.237, www.agilent.com).

Data preprocessing for baseline correction, scaling, and alignment was conducted with in-house scripts and TagFinder 4.0 software [18] (*see* **Note 3**).

3.3.2 Phosphorylated and Nucleotide Profiling (via Liquid Chromatography Mass Spectrometry Technology)

1. Metabolites are extracted by a chloroform/methanol method [19] with modifications specified by [7].
2. Add 250 µL ice-cold $CHCl_3$:CH_3OH (3:7 v/v) to the dried homogenate (of total and fractionated samples).
3. Let the frozen mixture warm to −20 °C while shaking vigorously and incubate for 2 h at −20 °C.
4. Extract the soluble metabolites from the $CHCl_3$ phase by the addition of 200 µL dH_2O.
5. Let the mixture warm to 4 °C and centrifuge at 200 × *g* for 4 min.
6. Remove the upper aqueous phase and store at 4 °C while re-extracting the lower chloroform phase through **steps 4** and **5**.
7. Combine the two upper phase extracts (**step 6**) and evaporate to dryness in a vacuum dryer.
8. Resuspend in 150 µL dH_2O.
9. Remove high-molecular-weight molecules from the extract by passing through a 3 kDa low-binding regenerated cellulose membrane filter.
10. Analyze total extracts and fractions by reverse-phase liquid chromatography.
11. For LC-Q-TOF MS analyses:

    The system composes of a Waters Aquity Ultra Performance LC coupled to a Micromass Q-TOF Ultima MS (www.waters.com), and a Waters Atlantis 10 × 150 mm C18 3 µm column (www.waters.com) coupled to an Agilent 10 × 30 mm 3.5 µm bonus reverse-phase guard column (www.agilent.com) is used. Chromatographic separations vary greatly between makers and models, and need to be thoroughly optimized. In our experience, nucleotide sugars were best separated on an octylammonium acetate/acetonitrile (OAAN) gradient and phosphorylated sugars on a tributylamine/methanol (TBAM) gradient.

    For this, the running conditions were run in negative ion mode with a cone voltage of 35.0 V and a capillary voltage of 3.70 V. The source temperature is operated at 100 °C and the desolvation temperature and gas at 350 °C.

    The octylammonium acetate/acetonitrile (OAAN) buffer composition and elution conditions consist of 10 mM aqueous

octylammonium acetate (pH 3.0, buffer A) and 95 % acetonitrile (pH 3.0, buffer B) with a linear gradient ranging from 0–1 min 100–95 % buffer A, 3 min 90 % buffer A, 3.30 min 85 % buffer A, 4 min 85 % buffer A, 5 min 80 % buffer A, 5.30 min 80 % buffer A, 6 min 70 % buffer A, 7 min 65 % buffer A, 8 min 60 % buffer A, 9 min 50 % buffer A, 14 min 50 % buffer A, 20 min 21 % A, 22 min 10 % buffer A, and 22.10–30 min 95 % buffer A. The flow rate was maintained at 0.06 mL/min.

The TBAM buffer composition and elution condition consists of 10 mM aqueous tributylamine (pH 4.95, adjusted with acetic acid, buffer A) and 100 % methanol (buffer B) with a linear gradient ranging from 0–5 min 95 % buffer A, 15 min 90 % buffer A, 22 min 85 % buffer A, 37 min 80 % buffer A, 40 min 65 % buffer A, 43 min 65 % buffer A, 47 min 40 % buffer A, 50 min 40 % buffer A, 50.01 min 10 % buffer A, 54 min 10 % buffer A, 54.01 min 95 % buffer A, and 65 min 95 % buffer A. The flow rate was maintained at 0.06 mL/min.

Chromatographic separation of nucleotides and nucleotide sugars were achieved by injecting 5 μL extract or 1 μL standard.

Data acquisition and analyses are done by MassLynx V4.0 SP4 (www.micromass.co.uk) for instrument control and data acquisition, while data preprocessing is performed with MetAlign v 200410 (www.metalign.wur.nl/UK/) for baseline correction, scaling, and alignment.

3.4 Statistical Analyses

For assignment of compartmental distributions, statistical software (e.g., Bestfit or customized in-house command tools) can be applied to the results obtained from the protein distribution analyses to assess the robustness and quality of the fractionation procedures, and determine the resulting metabolite distributions in either 2- or 3-compartmental models.

3.5 Perspectives

NAQF provides a powerful technique to study mitochondrial metabolism, particularly when trying to resolve the subcellular dynamics with whole-cell function (*see* **Note 4**). The separation of the mitochondrial metabolome, however, still remains poorly resolved. Using the protocol described here, a significant enrichment in the last remaining fractions can be obtained for mitochondria (Fly et al., *manuscript in preparation*). Critical towards this improvement in separation is the optimization of a gradient to allow for mitochondrial compartmental enrichment. However, a further improvement that needs to be addressed in future is the choice and selection of a suitable marker system to validate the compartmental enrichments. For this purpose, the expanded view of different

protein constituents across compartments is vital. Proteomics (shot-gun MS-based profiling, as well as subcellular localization studies) have provided a useful roadmap of protein distribution across all the compartments in the majority of the model species. The technology is freely applicable to non-model species, and will also aid in NAQF-assisted marker selection. Setting up multiple reaction monitoring (MRM) strategies to assess multiple proteins that are exclusively localized to a particular compartment will significantly improve the quality of the enrichment analyses. However, this technology will probably not replace the enzymatic activity assays, since contamination of other sources as well as protein functionality are ideally assayed using spectrophotometry.

4 Notes

1. Note that the organic solvent composition (heptane: tetrachloroethylene 43:57 v/v) for mitochondrial enrichment analyses differs from most other protocols currently being used to enrich for, particularly, plastidial (and sub-plastidial) fractions (i.e., heptane:tetrachloroethylene 66:44 v/v) [20–24].
2. For gradient optimization it is important to consider the source material (species, tissue, organ, etc.) as different constituents will influence the separation efficiency. Tissues with higher starch (or glycogen) content generally tend to disrupt the membrane separation, and hence the purity of the fractions obtained. In order to obtain the most reproducible gradients, an automatic gradient loader is recommended. A modified protein gradient former with a Tris pump cassette controlled by a fraction collector (e.g., Foxy Jr) was used here.
3. Due to variation in machine models and makes, running conditions need to be optimized for the particular instrument of choice with authentic standards of metabolites of interest, and data deconvolution parameters need to be carefully considered depending on the operating system.
4. Organellar isolation is not suitable for metabolite determinations due to the fast diffusion kinetics and turnover of metabolites in aqueous solutions.

Acknowledgements

This work was financially supported by the National Research Foundation (South Africa).

References

1. Conklin PL, Williams EH, Last RL (1996) Environmental stress sensitivity of an ascorbic acid-deficient Arabidopsis mutant. Proc Natl Acad Sci U S A 93:9970–9974
2. Wheeler GL, Jones MA, Smirnoff N (1998) The biosynthetic pathway of vitamin C in higher plants. Nature 393:365–369. doi:10.1038/30728
3. Duncan O, Taylor NL, Carrie C et al (2011) Multiple lines of evidence localize signaling, morphology, and lipid biosynthesis machinery to the mitochondrial outer membrane of Arabidopsis. Plant Physiol 157:1093–1113
4. Scott I, Tobin AK, Logan DC (2006) BIGYIN, an orthologue of human and yeast FIS1 genes functions in the control of mitochondrial size and number in Arabidopsis thaliana. J Exp Bot 57:1275–1280
5. Radomiljac JD, Whelan J, Van Der Merwe M (2013) Coordinating metabolite changes with our perception of plant abiotic stress responses: emerging views revealed by integrative—omic analyses. Metabolites 3:761–786
6. Roessner U, Luedemann A, Brust D et al (2001) Metabolic profiling allows comprehensive phenotyping of genetically or environmentally modified plant systems. Plant Cell 13:11–29
7. Arrivault S, Guenther M, Ivakov A et al (2009) Use of reverse-phase liquid chromatography, linked to tandem mass spectrometry, to profile the Calvin cycle and other metabolic intermediates in Arabidopsis rosettes at different carbon dioxide concentrations. Plant J 59:826–839
8. Fukushima A, Kusano M, Meijia RF et al (2014) Metabolomic characterization of knock-out mutants in Arabidopsis-development of a metabolite profiling database for knock-out mutants in Arabidopsis (MeKO). Plant Physiol 165:948–961
9. Szecowka M, Heise R, Tohge T et al (2013) Metabolic fluxes in an illuminated Arabidopsis rosette. Plant Cell 25:694–714
10. Geigenberger P, Stitt M (1993) Sucrose synthase catalyses a readily reversible reaction in vivo in developing potato tubers and other plant tissues. Planta 189:329–339
11. Bradford MM (1976) A rapid and sensitive method for the quantitation of microgram quantities of protein utilizing the principle of protein-dye binding. Anal Biochem 72:248–254
12. Stitt M, Lilley RM, Gerhardt R et al (1989) Metabolite levels in specific cells and subcellular compartments of plant leaves. Methods Enzymol 174:518–552
13. Huber SC (1984) Biochemical basis for effects of K-deficiency on assimilate export rate and accumulation of soluble sugars in soybean leaves. Plant Physiol 76:424–430
14. Lin TP, Preiss J (1988) Characterization of D-enzyme (4-α-glucanotransferase) in Arabidopsis leaf. Plant Physiol 86:260–265
15. Gibon Y, Blaesing OE, Hannemann J et al (2004) A robot-based platform to measure multiple enzyme activities in Arabidopsis using a set of cycling assays: comparison of changes of enzyme activities and transcript levels during diurnal cycles and in prolonged darkness. Plant Cell 16:3304–3325
16. Araújo WL, Nunes-Nesi A, Osorio S et al (2011) Antisense inhibition of the iron-sulphur subunit of succinate dehydrogenase enhances photosynthesis and growth in tomato via an organic acid-mediated effect on stomatal aperture. Plant Cell 23:600–627
17. Studart-Guimaraes C, Gibon Y, Frankel N et al (2005) Identification and characterisation of the α and β subunits of succinyl CoA ligase of tomato. Plant Mol Biol 59:781–791
18. Lisec J, Schauer N, Kopka J et al (2006) Gas chromatography mass spectrometry-based metabolite profiling in plants. Nat Protoc 1:387–396
19. Lunn J, Feil R, Hendriks JH et al (2006) Sugar-induced increases in trehalose 6-phosphate are correlated with redox activation of ADP-glucose pyrophosphorylase and higher rates of starch synthesis in Arabidopsis thaliana. Biochem J 397:139–148
20. Kuzma MM, Winter H, Storer P et al (1999) The site of oxygen limitation in soybean nodules. Plant Physiol 119:399–408
21. Farre EM, Tiessen A, Roessner U et al (2001) Analysis of the compartmentation of glycolytic intermediates, nucleotides, sugars, organic acids, amino acids, and sugar alcohols in potato tubers using a nonaqueous fractionation method. Plant Physiol 127:685–700
22. Krueger S, Steinhauser D, Lisec J et al (2014) Analysis of subcellular metabolite distributions within Arabidopsis thaliana leaf tissue: a primer for subcellular metabolomics. In: Arabidopsis protocols. Humana Press, Totowa, NJ, pp 575–596
23. Krueger S, Giavalisco P, Krall L et al (2011) A topological map of the compartmentalized Arabidopsis thaliana leaf metabolome. PLoS One 6(3):e17806
24. Arrivault S, Guenther M, Florian A et al (2014) Dissecting the subcellular compartmentation of proteins and metabolites in Arabidopsis leaves using non-aqueous fractionation. Mol Cell Proteomics 13:2246

Chapter 15

Mitochondrial Markers of Programmed Cell Death in *Arabidopsis thaliana*

Theresa J. Reape, Joanna Kacprzyk, Niall Brogan, Lee Sweetlove, and Paul F. McCabe

Abstract

In plants, apoptosis-like programmed cell death (AL-PCD) is readily distinguished from other forms of programmed cell death (PCD) through a distinct morphology. Detection of cytochrome c release from mitochondria and changes in mitochondrial morphology are the earliest markers for detection of this form of PCD in plants. In this chapter we provide detailed technical methods for the visualization of both of these mitochondrial markers of AL-PCD in Arabidopsis.

Key words Programmed cell death (PCD), Apoptosis-like programed cell death (AL-PCD), Mitochondria, Cytochrome c, Western blot, Mitochondrial swelling

1 Introduction

Programed cell death (PCD), the process of controlled and organized destruction of cells, is crucial for development, defence responses to restrict the spread of pathogens (the hypersensitive response), and response to stress [1]. Our laboratories study apoptosis-like PCD (AL-PCD) which is morphologically characterized by retraction of the protoplast away from the cell wall [2, 3]. We routinely employ two models to study AL-PCD in Arabidopsis (*Arabidopsis thaliana*)—an in vitro cell suspension model [4–6] and an in vivo root hair model [7, 8]. In these models AL-PCD can be induced via biotic or moderate abiotic stresses such as salicylic acid (SA) treatment, pathogen infection, or heat stress, respectively [5–8]. Higher levels of stress induce cells or root hairs to undergo necrotic cell death and this type of death can be readily distinguished from AL-PCD due to lack of protoplast retraction [2–8]. Release of cytochrome c from the mitochondria and mitochondrial swelling remain the earliest markers for AL-PCD [6, 9–11]. Cytochrome c release from the mitochondria can be detected as early as 10 min after a moderate heat shock in Arabidopsis suspension cells with no

James Whelan and Monika W. Murcha (eds.), *Plant Mitochondria: Methods and Protocols*, Methods in Molecular Biology, vol. 1305, DOI 10.1007/978-1-4939-2639-8_15,

loss of voltage-dependent anion channel (VDAC)/porin [6, 11]. Mitochondrial swelling can be detected 5 min after a moderate 10-min heat treatment in Arabidopsis protoplasts [9].

In this chapter we describe how to induce and quantify AL-PCD in Arabidopsis suspension cells and root hairs, isolate mitochondria and detect cytochrome c release in Arabidopsis suspension cells by Western blotting, and visualize mitochondrial swelling in Arabidopsis root hairs which have been induced to undergo AL-PCD.

2 Materials

2.1 Growth of Plant Material and AL-PCD Scoring

2.1.1 Arabidopsis Suspension Cell Culture

1. Stock solutions of naphthaleneacetic acid (NAA) and kinetin are made up by dissolving hormones in a small quantity of 1 M NaOH and bringing up to 100 mL with distilled water. Stock solutions are stored at 4 °C.
2. Murashige and Skoog (MS) medium: 0.5 mg/L NAA, 0.05 mg/L kinetin, and 3 % (w/v) sucrose [12]. Dissolve in double-deionized water (DDI) and the pH adjusted to 5.8 with NaOH. 90 mL of media is dispensed into 250-mL flasks which are then covered with foil caps and autoclaved. If not being used immediately, store at 4 °C and warm to room temperature prior to use.

2.1.2 Arabidopsis Seedlings

1. Arabidopsis seedling medium: 0.5× MS basal salt medium, 1 % (w/v) sucrose, pH is adjusted to 5.8 with KOH. 1.5 % (w/v) agar is added. Medium is autoclaved and poured into 12 × 12 cm square sterile Petri dishes.
2. Sterilizing solution: 20 % (v/v) commercial bleach. The final concentration of sodium hypochlorite is approximately 1 % (v/v).
3. Other materials: Sterile distilled water, 1,000-μL pipettes and pipette tips, 200-μL pipettes and pipette tips with ends cut off, 1.5-mL microcentrifuge tubes.

2.1.3 AL-PCD Scoring

1. Microscope slides and coverslips.
2. Fluorescein diacetate (FDA) is made up as 0.1 % (w/v) stock solution in acetone and stored at −20 °C.
3. Phase-contrast microscope with a fluorescein isothiocyanate (FITC) filter and an attached fluorescence lamp.

2.2 Isolation of Mitochondria from Arabidopsis Suspension Cultures

All buffers should be made up the day before use and stored at 4 °C.

1. Homogenization buffer: 0.3 M mannitol, 50 mM sodium pyrophosphate, 0.2 % (w/v) bovine serum albumin (BSA), 0.5 % (w/v) PVP-40, 2 mM EGTA, 20 mM cysteine, pH 8.0 (with phosphoric acid). The cysteine is added just prior to use.

2. Wash buffer: 0.3 M mannitol, 10 mM TES-KOH, pH 7.5.
3. Percoll gradient buffer: 0.3 M mannitol, 10 mM TES, pH 7.5, and 0.1 % (w/v) BSA.
4. 2× Sodium dodecyl sulfate (SDS) loading buffer: 100 mM Tris–HCl, pH 6.8, 4 % SDS (w/v), 40 % (v/v) glycerol, and 200 mM dithiothreitol (DTT). DTT is added just prior to use.

2.3 Western Blot Analysis

All buffers used in SDS-PAGE, electrophoretic transfer, and Western blotting are made up exactly as per the manufacturer's instructions for the BIORAD Mini-PROTEAN® 3 Cell, BIORAD Mini Trans-Blot® Electrophoretic Transfer Cell, and the Amersham Biosciences ECL Western blotting detection system, respectively.

1. Antibody to cytochrome c 7H8.2C12 (BD Pharmingen, Oxford, UK).
2. Antibody to VDAC/porin (Sigma/Aldrich)—used as marker for mitochondrial integrity.
3. Horseradish peroxidase (HRP)-conjugated anti-mouse or rabbit IgG (Sigma Aldrich).

2.4 AL-PCD Induction in Arabidopsis Seedlings

1. Forceps, 24-well culture plates, DDI water.
2. Heat treatment: Water bath (no shaking), Leucopore tape.
3. SA treatment: 0.1 M SA stock solution in ethanol is prepared directly prior to use.

2.5 Monitoring of Mitochondrial Swelling In Vivo in Arabidopsis Root Hairs

1. Microscope slides and coverslips, electrical tape, forceps.
2. Fluorescent dye Mito Tracker Green (MTG) FM (Molecular Probes, The Netherlands) made up in DDI water (70 nM) directly prior to use.
3. Confocal microscope, for example Olympus Fluoview FV1000 microscope, with argon laser (488 nm excitation wavelength).

3 Methods

3.1 Induction of AL-PCD in Arabidopsis Cells In Vitro

The cell cultures that we use for the techniques described in this chapter were obtained from the Department of Plant Sciences at the University of Oxford. Suspension cell cultures were established from callus obtained from stem explants of Arabidopsis ecotype Landsberg erecta [12].

3.1.1 Cell Culture, Subculturing, and Growth Conditions

Cultures are maintained in Arabidopsis suspension cell MS medium. Subculture cells once every 7 days. This is carried out by pipetting 10 mL of a 7-day-old culture of cells into 90 mL of MS media in a 250-mL conical flask. Flasks are then placed on a rotary shaker at 110 rpm (5 cm rotation) under a constant temperature (22 °C) and light regime (6 μmol/m^2/s). Suspension cultures used for

isolation of mitochondria were subbed as previously described but grown in complete darkness for 7 days prior to isolation.

3.1.2 Heat Treatment of Cells

A short heat treatment [4–6] is an effective inducer of AL-PCD in Arabidopsis suspension cultures. In order to obtain enough mitochondrial protein for cytochrome c Western blotting, 2×100 mL 7-day-old cultures (per treatment) are transferred to a water bath with an orbital shaker (at 90 rpm) that is preheated to the appropriate temperature for experimentation. In this system the cultures were treated for 10 min at 54 °C. However, the timing and temperature need to be predetermined in your laboratory (*see* **Note 1**). After the heat treatment, cultures can be used immediately for mitochondrial isolation or, if carrying out a time course, transferred to normal growing conditions (as in Subheading 3.1.1) for the appropriate length of time, prior to mitochondrial isolation. To test for the induction of AL-PCD, a small aliquot is removed from the treated culture prior to mitochondrial isolation and transferred to a sterile petri dish, incubated in normal growing conditions, and scored for viability after 6–24 h (6 h results in maximal protoplast condensation which facilitates scoring for rates of AL-PCD but you can score this morphology up to 24 h after heat treatment).

3.2 Induction of AL-PCD in Arabidopsis Root Hairs In Vivo

The method described is adapted from [7] and has been previously described by Kacprzyk et al. [8].

3.2.1 Growth of Arabidopsis Seedlings

Arabidopsis seeds are sterilized in the laminar flow hood using aseptic techniques. One milliliter of sterilizing solution is added to seeds in a 1.5-mL microcentrifuge tube. Seeds are incubated in the sterilizing solution for 20 min with occasional mixing by inversion. The sterilizing solution is removed by pipetting and seeds are washed four times with sterile distilled water. Seeds are sown in 2–3 rows on solid agar growth medium using 200-μL cutoff pipette tips. Plates are sealed with Parafilm and seeds vernalized in the dark at 4 °C for 1–3 days. Seeds are germinated at 22 °C, in constant light, in a vertical position, which allows the roots to grow down, and on, the agar surface. Seedlings are used for experiments when 5–6 days old.

3.2.2 Induction of AL-PCD in Arabidopsis Seedlings

5–6-Day-old Arabidopsis seedlings can be conveniently treated in 24-well culture plates. Here, we present a protocol for two types of cell death inducing treatments: heat and SA. For the heat treatment, each well of a 24-well culture plate is filled with 1 mL of sterile distilled water. Arabidopsis seedlings are transferred to individual wells using a forceps and the plate sealed with Leucopore tape. The heat treatment is carried out by allowing the culture plate to float on the surface of the water bath set to the selected temperature, with no

shaking/mixing. After the heat shock, seedlings are incubated in the light at 22 °C until scoring for PCD rates or analysis of mitochondrial swelling. Mitochondrial swelling is a relatively early event in plant PCD and can be detected soon after cell death induction (*see* **Note 2**). Typical rates of AL-PCD induced 24 h after 10-min heat shock (49–51 °C) range between 30 and 60 % (*see* **Note 1**). For the SA treatment, the SA stock is diluted in distilled water and wells of the multiwell plate filled with 1 mL of SA solution. Seedlings are subjected to the stress treatment by transferring them to the SA solution using forceps (one seedling per well) and incubating in the light at 22 °C until scoring for PCD rates or analysis of mitochondrial swelling. Typical rates of AL-PCD induced after 24-h treatment with 60–75 μM SA range between 30 and 70 % (*see* **Note 1**).

3.3 Microscopy

3.3.1 Fluorescein Diacetate Staining of Cells/Root Hairs

Fluorescein diacetate (FDA) is a hydrophobic compound that passively enters the cell where it is cleaved by cytoplasmic enzymes [4]. When cleaved it becomes charged, which prevents it from exiting the cell. When exposed to light at a wavelength of 490 nm, viable cells which have been treated with FDA fluoresce bright green while dead cells do not fluoresce. When required, the stock of FDA is diluted in fresh MS medium (for examination of suspension cells) or distilled water (for examination of root hairs) at a ratio of 1:50 (10/500 μL of media or distilled water). For examination of cells, an equal volume of cell suspension and diluted FDA are pipetted onto a microscope slide and covered gently. For examination of root hairs, whole seedlings are stained in 50 μL of FDA solution directly on the microscope slide and covered gently with the coverslip. Cells or root hairs can then be immediately examined under a phase-contrast microscope with an FITC filter and an attached fluorescence lamp.

3.3.2 Scoring of Cells/Root Hairs for AL-PCD Morphology

Cells/root hairs that have undergone PCD show a characteristic retraction of the protoplast away from the cell wall and do not cleave FDA. The retraction of the protoplast creates a gap between the wall and the plasma membrane that is observable under a light microscope [4] (*see* **Note 2**). Cells/root hairs that die via necrosis do not display this retraction and cannot cleave FDA (Fig. 1).

3.3.3 In Vivo Analysis of Mitochondrial Swelling in Arabidopsis Root Hairs

The method for measuring mitochondrial swelling has been adapted from [8]. MTG FM is a fluorescent dye, which covalently binds to mitochondrial proteins regardless of the membrane potential, and hence can be used to stain the mitochondrial masses [13]. Seedlings are incubated in 70 nM MTG solution in distilled water in the dark, at room temperature, for 30 min directly prior to confocal imaging (*see* **Note 3**). Seedlings are carefully transferred to a microscope slide and mounted in approximately 40 μL of distilled water. Strips of electrical tape are placed between the microscope slide and the coverslip in order to prevent damaging

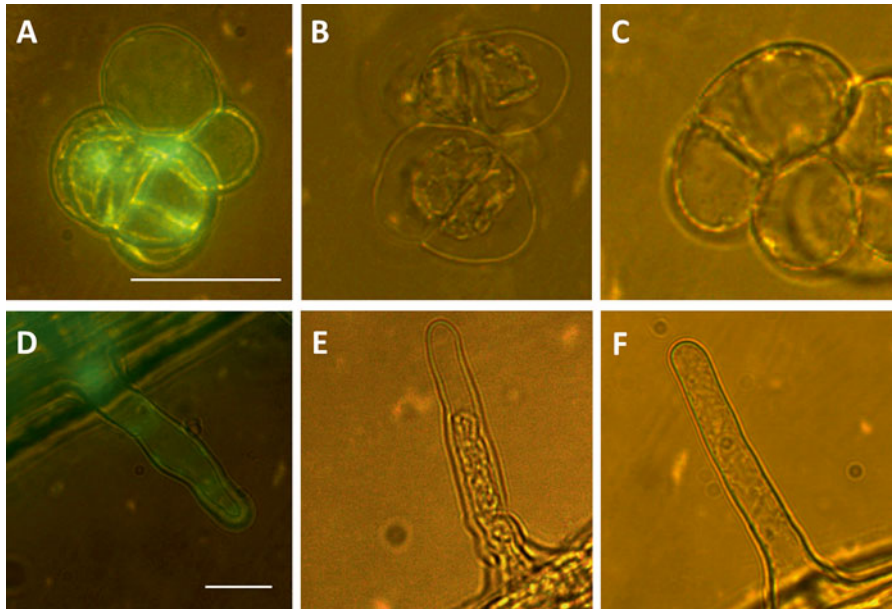

Fig. 1 AL-PCD morphology in suspension cells and root hairs of Arabidopsis. (**a**, **d**) Living cells/root hair stained with fluorescein diacetate (FDA) and viewed under white and fluorescent light. (**b**, **e**) AL-PCD cells/root hair showing condensation of the cytoplasm and no fluorescence after FDA staining. (**c**, **f**) Necrotic cells/root hair showing no protoplast retraction and no fluorescence after FDA staining. Scale bars: 40 μm for (**a**–**c**) and 10 μm for (**d**–**f**)

the seedling during imaging. Electrical tape can also be used to firmly secure the coverslip before confocal imaging (optional). Seedlings are typically imaged using a 60× immersion oil objective of Olympus Fluoview FV1000 microscope. MTG is excited with an argon laser (488 nm) and detected at 515–520 nm. Mitochondrial swelling can be further analyzed by determining the average area of an individual MTG signal, which corresponds to the average size of a mitochondrial cross-section area. The MTG signal is typically round or oval in shape and its approximate area can be determined by manually measuring its short and long diameter and calculating the area of the resulting ellipse on the basis of collected values, taking into account the magnification factor (Fig. 2). Simple graphical programs (such as Microsoft Paint) allow relatively easy measurements of the diameters of MTG signal (expressed in pixels). Typically, the average size of 10–15 mitochondria per root hair is recorded and 2–3 root hairs per seedling are analyzed. Mitochondrial swelling is indicated by a significant increase in the average MTG signal area.

3.4 Isolation of Mitochondria

Steps 1 and **2** are carried out in a cold room at 4 °C. Keep all centrifuge and homogenization tubes on ice. Centrifugation steps are carried out at 4 °C.

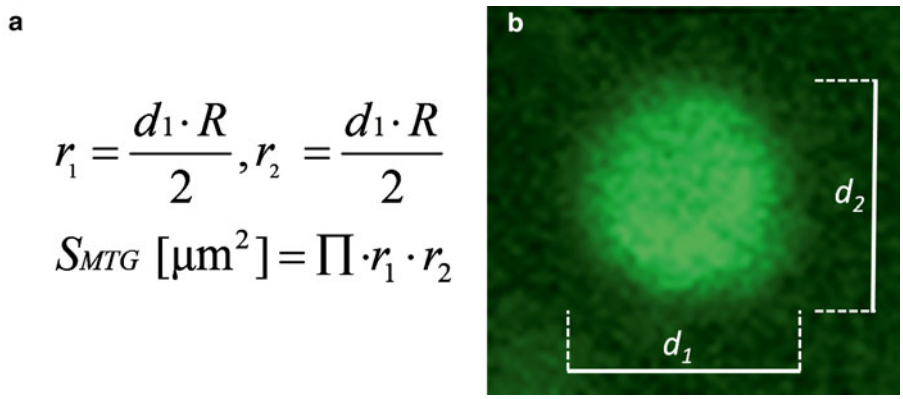

Fig. 2 Determination of the surface area of MTG signal. The surface area of individual MTG signal (S_{MTG}) is calculated according to the presented formula (**a**), where d_1, d_2—diameters of MTG signal, expressed in number of pixels, measured in graphical program (i.e., Microsoft Paint) (**b**), r_1, r_2—radii of the ellipse, and R—the actual pixel's dimension [μm/pixel], calculated using the image properties stored by software used for confocal imaging (i.e., image size in pixels and actual size of the image in μm)

1. Filter 200 mL of heat-shocked or control (untreated) dark-grown Arabidopsis suspension cells through one layer of Miracloth lining a Buchner funnel under gentle (water tap) vacuum.
2. Homogenize the cell suspension in homogenization buffer containing glass beads (acid washed, 425–600 μm diameter) using a mortar and pestle (*see* **Note 4** for alternative homogenization method suggestion), for ~3 times for 4 min or until ~80 % of cells are disrupted. In order to monitor cell disruption, examine an aliquot of cells using a light microscope after each homogenization step (*see* **Note 5**). Only add enough homogenization buffer to achieve a thick "soup-like" consistency. Filter cell suspensions through two layers of Miracloth each time as in **step 1** adding fresh buffer.
3. Add the homogenized cell extract to a 40-mL plastic tube and bring the volume of each tube up to 30 mL with homogenization buffer.
4. Centrifuge extracts at 2,000 × *g* for 10 min to remove debris.
5. Carefully transfer supernatant to a 15-mL Corex glass tube and centrifuge the supernatant at 13,000 × *g* for 15 min.
6. At this stage the supernatant (cytosolic fraction) can be stored at −70 °C if required for further analysis.
7. Resuspend the crude mitochondrial pellet in 2 mL wash buffer and homogenize gently and briefly using a Potter-Elvehjem pestle and 5-mL glass tube to remove any clumps.
8. Centrifuge suspensions until rotor reaches ~7,000 × *g* and then stop rotor.

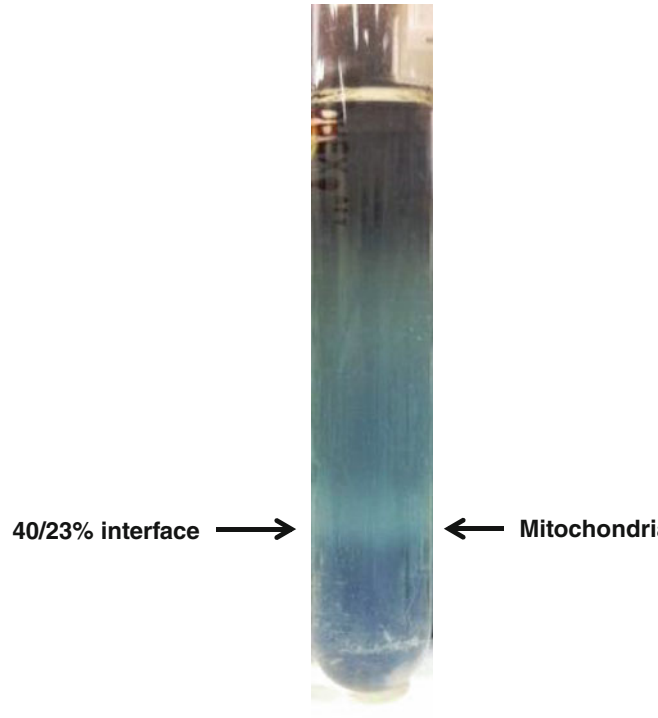

Fig. 3 Appearance of the mitochondrial band on the Percoll density gradient. Mitochondria appear as a diffuse whitish band at the interface of the 40/23 % Percoll layers

9. Transfer the supernatant to a fresh tube and recentrifuge at 13,000 × *g* for 15 min.
10. Re-homogenize the resuspended pellet, as in **step 7**, in order to remove clumps and carefully load onto a 40, 23, and 18 % (v/v) Percoll step gradient (in 0.3 M mannitol, 10 mM TES, pH 7.5, and 0.1 % BSA) (*see* **Note 6**).
11. Centrifuge the gradients at 40,000 × *g* for 45 min with the centrifuge brake off.
12. Remove the upper layer of the gradient by aspiration and collect the purified mitochondria at the 23–40 % interface (will be a diffuse whitish band—*see* Fig. 3) using a 1-mL pipette. Transfer to a 15-mL Corex tube, bring volume up to 10 mL with wash buffer, and then centrifuge four times for 5 min at 10,000 × *g*. The mitochondria will not pellet the first or second time due to residual Percoll, so be careful when removing buffer after the first and second centrifugation steps.
13. Resuspend mitochondria in 1 mL of wash buffer and perform one centrifugation step at 10,000 × *g* for 5 min in a 1.5-mL microcentrifuge tube.

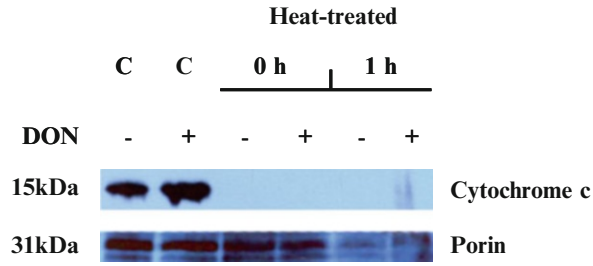

Fig. 4 Western blot showing release of cytochrome c after heat shock in Arabidopsis suspension cells. Cytochrome c remains associated with the mitochondrial fraction of non-heat-treated control cell samples (±DON). However, cytochrome c release from the mitochondrial fraction was induced immediately following a 10-min heat treatment at 54 °C (0 h ± DON). VDAC/porin remained associated with the mitochondrial fraction in all samples. *C* control samples. Figure taken from [6]

14. Finally, resuspend pellet in approximately 30 μL of wash buffer (*see* **Note 7**).
15. Determine the mitochondrial protein concentration using the Bradford protein determination method and add 2× SDS loading buffer (*see* **Note 8**). Use immediately or store samples at −70 °C prior to Western blot analysis.

3.5 Western Blot Analysis

3.5.1 15 % SDS-PAGE

Protein (40 μg) is separated on a 15 % SDS-PAGE [14] using the Bio-Rad Mini-PROTEAN 3 Cell system as per the manufacturer's instructions and transferred to nitrocellulose (Optitran BA-S 83, 0.2-μm, Schleicher and Schuell) using the Bio-Rad Mini TransBlot Electrophoretic Transfer Cell system as per the manufacturer's instructions. Western blotting is performed using the ECL Western blotting detection system as per the manufacturer's instructions. Antibodies to cytochrome c 7H8.2C12 (BD Pharmingen, Oxford, UK) or VDAC/porin (Sigma) were diluted 1:1,000 and HRP-conjugated anti-mouse (Pierce) or rabbit IgG (Sigma) were also diluted 1:1,000 (*see* **Note 9**) (Fig. 4).

4 Notes

1. Prior to carrying out the mitochondrial isolation from heat-treated cells or analyzing mitochondrial swelling, you need to determine the temperature and time of the heat treatment which results in maximal AL-PCD in your culture. In order to achieve this, subject the required culture volume to a range of heat treatments over a time course. If the heat stress is too low the majority of cells will survive rather than undergoing

AL-PCD. When the heat stress is too high there will be too many cells in the culture dying via necrosis. *See* ref. [2] for a detailed description of routine heat curve analysis in suspension cells. In case of root hair system, especially while studying modulation of AL-PCD rates by chemical agents or in mutant/transgene background, it is preferable to use levels of stress inducing moderate rates of AL-PCD (30–70 %) in root hairs of control seedlings. Such levels of death induced in control cell enable detection of both pro-survival and pro-death effect of chemical modulator/genetic modification. As with the cell suspension system, the choice of stress level to be used (temperature for heat shock or concentration of SA) can be facilitated by preparing a heat curve or concentration curve. *See* ref. [7] for example of heat curve analysis in the root hair system.

2. AL-PCD morphology in Arabidopsis root hairs is characterized by a readily recognizable gap between the condensed protoplast and cell wall. Typically, this gap is present at the tip of the root hair; however, sometimes it can also be identified in the middle part of the root hair or close to its base. Occasionally, condensed cytoplasm can split into several units.
3. It is important to carefully select the time point at which the mitochondrial swelling is analyzed after the cell death induction. Mitochondrial swelling is a relatively early event during plant PCD, sometimes considered "a point of no return" of the PCD pathway and can precede loss of viability by several hours [9]. From our experience, mitochondrial swelling can be detected as early as 1.5 h following 65 μM SA treatment, followed by 30-min staining with MTG.
4. An alternative to the mortar and pestle, if available in your laboratory, is the Waring Blender as described in ref. [15].
5. This step is the most crucial for obtaining good yields of mitochondria. The monitoring of cells using the light microscope is important, as it is easy to overestimate how much you have homogenized. You need to experiment a bit with the consistency of the homogenate each time and the amount of glass beads you use. Sometimes an extra step is necessary depending on the efficiency of the homogenization in the mortar and pestle. If you add too much buffer at any stage it is pointless to carry on with homogenization, just re-filter, and start again.
6. We used a 9 mL Percoll gradient and prepared it by pipetting 3 mL of the most dense solution (40 %) slowly down the side of a 15-mL Corex glass tube and then very slowly and carefully pipetting the 23 % solution on top of the 40 % solution cushion, allowed to equilibrate, and then added the 18 % solution in the same manner. The Percoll gradients can be prepared during centrifuge steps.

7. The concentration of mitochondrial protein obtained using this method should be in the range of 10–15 μg/μL.
8. We found that adding freshly made up DTT to the 2× loading dye greatly improves the sharpness of the cytochrome c bands on the Western blot.
9. For the detection of VDAC/porin as a marker of mitochondrial membrane integrity, we ran two gels simultaneously containing identical amounts of mitochondrial protein and performed two Western blots. Alternatively, we have also "stripped" the cytochrome c blot and re-probed with VDAC/porin using commercially available products but found the bands on the "stripped" blot to look more diffuse.

References

1. Lam E (2004) Controlled cell death, plant survival and development. Nat Rev Mol Cell Biol 5:305–315
2. Reape TJ, Molony EM, McCabe PF (2008) Programmed cell death in plants: distinguishing between different modes. J Exp Bot 59:435–444
3. Reape TJ, McCabe PF (2008) Apoptotic-like programmed cell death in plants. New Phytol 180:13–26
4. McCabe PF, Leaver CJ (2000) Programmed cell death in cell cultures. Plant Mol Biol 44:359–368
5. Burbridge E, Diamond M, Dix PJ, McCabe PF (2006) Use of cell morphology to evaluate the effect of a peroxidase gene on cell death induction thresholds in tobacco. Plant Sci 171:139–146
6. Diamond M, Reape TJ, Rocha O, Doyle SM, Kacprzyk J, Doohan F, McCabe PF (2013) The Fusarium mycotoxin deoxynivalenol can inhibit plant apoptosis-like programmed cell death. PLoS One 8(7):e69542
7. Hogg BV, Kacprzyk J, Molony EM, O'Reilly C, Gallagher TF, Gallois P, McCabe PF (2011) An in vivo root hair assay for determining rates of apoptotic-like programmed cell death in plants. Plant Methods 7:45
8. Kacprzyk J, Devine A, McCabe PF (2014) The root hair assay facilitates the use of genetic and pharmacological tools in order to dissect multiple signalling pathways that lead to programmed cell death. PLoS One 9(4):e94898
9. Scott I, Logan DC (2008) Mitochondrial transition morphology is an early indicator of subsequent cell death in Arabidopsis. New Phytol 177:90–101
10. Balk J, Leaver CJ, McCabe PF (1999) Translocation of cytochrome *c* from the mitochondria to the cytosol occurs during heat-induced programmed cell death in cucumber plants. FEBS Lett 463:151–154
11. Balk J, Chew SK, Leaver CJ, McCabe PF (2003) The intermembrane space of plant mitochondria contains a DNase activity that may be involved in programmed cell death. Plant J 34:573–583
12. May MJ, Leaver CJ (1993) Oxidative stimulation of glutathione synthesis in *Arabidopsis thaliana* suspension cultures. Plant Physiol 103:621–627
13. Pendergrass W, Wolf N, Poot M (2004) Efficacy of MitoTracker Green™ and CMX rosamine to measure changes in mitochondrial membrane potentials in living cells and tissues. Cytometry A 61A:162–169
14. Laemmli UK (1970) Cleavage of structural proteins during the assembly of the head of bacteriophage T4. Nature 227:680–685
15. Sweetlove LJ, Taylor NL, Leaver CJ (2007) Isolation of intact, functional mitochondria from the model plant *Arabidopsis thaliana*. In: Leister D, Hermann JM (eds) Methods Mol Biol, vol 372. Humana, Totowa, NJ, pp 125–136

Chapter 16

Imaging and Analysis of Mitochondrial Dynamics in Living Cells

Sanjaya B. Ekanayake, Amr M. El Zawily, Gaël Paszkiewicz, Aurélia Rolland, and David C. Logan

Abstract

One of the most striking features of plant mitochondria when visualized in living tissue is their dynamism. The beauty of cytoplasmic streaming, driving, and being driven by the motility of mitochondria and other small organelles belies the complexity of the process. Equally, capturing that dynamism and investigating the genes, proteins, and mechanisms underpinning the processes using molecular cell biology and bioimaging is a complex process. It requires the generation of fluorescent protein constructs, stable transgenic plants sometimes expressing multiple fusions, and generation of mutants, even before one is ready for analytical experimentation. Here, we describe some of the key tools and methods necessary to investigate plant mitochondrial dynamics.

Key words Mitochondria, Image analysis, Microscopy, Deconvolution, Tracking, Motility, Colocalization, Live cell imaging

1 Introduction

Plant mitochondrial dynamics research is defined as the study of the genes, proteins, and mechanisms involved in the control, or modulation, of mitochondrial shape, size, number, and motility. While researchers have been fascinated by the morphology and movement of mitochondria in plant cells for over 100 years [1], it was the development of green fluorescent protein (GFP) as a reporter for gene expression [2–4] that led to a cell biological renaissance during which cellular compartments such as mitochondria [5] could be lit up by GFP, thereby enabling visualization of their dynamics in living tissues in real time. The development of GFP technology was paralleled by advances in biological imaging

Electronic supplementary material: Supplementary material is available in the online version of this chapter at 10.1007/978-1-4939-2639-8_16.

James Whelan and Monika W. Murcha (eds.), *Plant Mitochondria: Methods and Protocols*, Methods in Molecular Biology, vol. 1305, DOI 10.1007/978-1-4939-2639-8_16,

and analysis so that researchers could take advantage of the power of GFP as a noninvasive probe that requires no cofactors and only molecular oxygen to catalyze the cyclization necessary to form the protein's fluorophore [6]. Improved versions of GFP were developed [7, 8], new color variants based on GFP were generated by mutation (e.g., yellow fluorescent protein (YFP) and cyan fluorescent protein (CFP) [9]), and novel fluorescent proteins (FPs) were identified from diverse organisms, such as the red FP DsRed from a *Discosoma* sp. coral [10]. In turn, DsRed was used as mutation substrate to generate a new range of red, orange, and yellow fluorescent proteins with improved structures, spectral characteristics, stability, and decreased sensitivity as a fusion partner [11, 12]. Similarly, GFPs were generated that were photoactivatable [13], while other FPs were discovered that were photoconvertible [14]. As each new FP was developed, plant biology researchers were quick to generate plasmid vectors for the expression and targeting of these new FPs to the cellular compartment of interest such that now there is a vast array of FP-based plasmids and transgenic plants described in the literature.

Researchers interested in mitochondrial dynamics and interactions of mitochondria with other organelles have, therefore, both the genetic resources and technical tools at their disposal to support their enquiries. However, the technology is only enabling; it does not guarantee image quality or accuracy and therefore the extent of data mining and quantification that is possible from imaging data. As with most experimentation, an apparently simple result, e.g., a single image, hides a great deal of optimization and hard work. The purpose of this chapter is to lighten the workload by providing some advice and basic protocols.

2 Materials

2.1 Microscope

The choice between using a wide-field epifluorescence microscope (WFM) or laser scanning confocal microscope (LSCM) should be made according to specific experimental requirements. Generally, we prefer to use a WFM due to its potentially increased sensitivity (*see* **Note 1**) and thus lower necessary intensity of illumination, and because a whole frame (field-of-view, FOV) is captured simultaneously: this can be very important when imaging fast-moving mitochondria. To be able to use an LSCM to faithfully capture mitochondria moving at high speeds (e.g., 10 μm/s) [15], it is necessary to increase the scanning speed (and likely the zoom factor) which typically necessitates using low resolutions such as 512×512 or 256×256 pixels. As a result of the low resolution, and lack of averaging, image quality is poor and fine detail is lost. A very important point to note for LSCMs is that fast scan speeds mean that "pixel dwell time" (the duration that the laser is illuminating each pixel)

will be decreased proportionately and therefore the illumination power will have to be increased which can cause bleaching of the fluorophore or phototoxicity to the specimen. However, the LSCM is the machine of choice for generating *z*-stacks, reducing out-of-focus blur, and for simultaneous capture of multiple fluorescence emission from the specimen. For many applications in mitochondrial dynamics a spinning disk confocal microscope (SDCM) may offer the best option; however relatively few laboratories or central microscopy facilities are equipped with SDCMs.

2.2 General Configuration of a Wide-Field Epifluorescence Microscope

There are a number of different WFM systems. The first is an Olympus BX61 microscope with motorized objective nosepiece and filter wheel. Illumination is provided by an X-Cite white light source (Lumen Dynamics) with adjustable output in 1 % steps and images are captured with a QImaging Rolera-MGi + EMCCD camera (*see* **Note 2**). The system is controlled by Metamorph software running on a Dell workstation. The Rolera MGi+ camera is very sensitive but the payoff is a relative small 512 × 512 chip with a pixel size of 16 μm. However, the combination of light source and camera allows very low illumination levels and short exposure times that in part compensates for the speed of the filter wheel motor when performing multichannel experiments.

The second WFM is a Zeiss Axio Imager Z2 with motorized objectives, filter wheel, and x–y stage. Illumination is provided by a Colibri-2 LED unit, or HXP 120 white light source, and images are captured with a Hamamatsu ORCA-Flash 4.0 V2 sCMOS camera. There are two major benefits provided by the Zeiss system relative to the Olympus: (1) fast switching between LEDs allows multiband filter cubes to be used and, (2) the latest generation sCMOS camera which combines sensitivity with resolution (2,048 × 2,048 pixels of 6.5 μm) to give fine details often sought after when imaging mitochondrial dynamics. Ideal objectives for imaging are a 20× for identifying an appropriate area of tissue and a 100× N.A. = 1.4 oil immersion objective for analytical work. For high-quality image capture, high N.A. oil immersion 40× or 63× is sufficient since digital zoom can be applied; however in order to observe by the eye pieces it is better to have a 100× lens. In addition, optical magnification is preferable to digital zoom and the shallower depth of field offered by a higher magnification lens limits blur from above and below the focal plane.

2.3 Filter Cubes

The most important consideration for imaging mitochondrial dynamics and fluorescent probes in general in plant cell biology is the choice of filter cubes. Plant tissues present particular problems when it comes to capturing fluorescence and these are not always appreciated by those running central imaging facilities and likely never considered by the purchaser of the WFM you may be using if its primary purpose was for imaging non-plant samples.

Plant tissues often show autofluorescence when illuminated with blue light (as used for GFP) and although chlorophyll is the most common source of difficulty, other plant tissues (including seeds) are also highly autofluorescent. This is much more of a problem with WFMs than with LSCMs: LSCMs offer optical sectioning so that autofluorescence from other optical planes can be excluded, line switching between channels can help if cross talk is a problem, or, in the ideal situation, the LSCM may be capable of spectral imaging and unmixing. With a WFM, options are limited: LED illumination helps narrow the excitation wavelength but if the problem is a wide-emission spectrum then it is the emission filter that must be optimized. For example, GFP cubes are sometimes long-pass filters allowing light of wavelengths longer than 510 nm to pass—illuminating plant leaves with such a cube would lead to excitation and detection of chlorophyll to such an extent that the GFP signal would be almost invisible and of course inseparable by a monochrome camera. Better, therefore, to choose a band-pass filter (e.g., Zeiss filter set 38: Ex BP 470/40, DM 495, EM BP 525/50; *see* **Note 3**). However, the biggest problem is with the detection of red fluorescent proteins (RFP). These were not developed with plant imaging in mind and off-the-shelf cubes typically use an emission filter too far into the red spectrum which makes imaging RFP (such as mRFP1 or mCherry) impossible in leaves due to chlorophyll autofluorescence. For example, Zeiss filter set 63 uses an emission filter of 629/62 nm, while the Semrock mCherry-B-0000 cube uses EM 641/75 nm; neither of these are optimal for leaves; if possible change the emission filter to a 593/40 or similar (*see* **Note 4**). Similarly, dual-band cubes will likely need to be modified for imaging RFP (*see* **Note 5**).

2.4 Plant Material

Stable transgenic Arabidopsis (*Arabidopsis thaliana*) lines (*see* **Note 6**) expressing GFP in the matrix, using the targeting signal from the *Nicotiana plumbaginifolia* beta-ATPase subunit [5] have typically been the material of choice for analysis of mitochondrial dynamics [16–20] and despite the generation of lines expressing mito-FP of different colors (CFP, YFP, mRFP1, and mCherry), GFP is still the fluorophore of choice if there are no experimental reasons for choosing an alternative. Mito-GFP is the brightest for observing mitochondrial dynamics using a WFM without using a camera since it best suits the color sensitivity of the human eye and visualization by eye is strongly encouraged at the start of new investigations since it provides a larger FOV than the camera and the readout is instantaneous. While quantification requires image capture and processing, the human eye and brain are the best for getting an overall view of anything out of the ordinary in new mutants, or caused by novel treatments. Despite GFP being the protein of choice, when generating plants expressing

multiple fluorescent fusions labeling different organelles or cellular compartments, alternative mito-FPs may need to be used to ensure compatibility. This choice is frequently dependent on the availability of stable lines expressing a fusion for the additional organelle or compartment. For example, we have generated double transgenics expressing mito-CFP and YFP-HDEL using YFP-HDEL plants produced by Teh and Moore [21] for mitochondria and ER labeling, or mito-mCherry and GFP-EB1b using plants produced by Mathur et al. [22] for investigations of mitochondria and the plus ends of microtubules. However, where use of mito-GFP is predetermined, for example, when using EMS-generated mutants in a mito-GFP background [16] then investigations of mitochondrial interactions with other cellular structures require use of RFPs for the best spectral separation. In addition to matrix-localized single-wavelength FPs, we have generated a line expressing matrix-localized mEosFP green-to-red photoconvertible FP [19] and have lines expressing FPs at the outer membrane using fusions to BIGYIN [17] and NMT [16], e.g., GFP-BIGYIN and NMT-GFP or NMT-mCherry fusions (Logan, unpublished).

Generating dual- and triple-labeled stable transgenic lines is one of the most challenging steps in the study of mitochondrial dynamics due to silencing issues (*see* **Note 7**). Whenever possible, it is best to generate new lines expressing multiple fusion constructs by genetic crossing of good evenly expressing lines of each individual fusion rather than by retransformation. Such an approach means that antibiotic resistance conferred by the T-DNA is not an issue since screening of the F_1 and F_2 lines will be performed solely on the basis of FP expression and not by antibiotic resistance. In addition to ER/mitochondria and microtubule plus-end/mitochondria lines, we have successfully generated lines expressing mCherry-mTalin and mito-GFP for visualizing mitochondria and F-actin, mCherry-MAP4 and mito-GFP for visualizing microtubules and mitochondria, and lines expressing mito-GFP/mito-mCherry and YFP-gammaTIP for visualizing mitochondria and the tonoplast.

Until recently all of our fusion constructs were driven by the CaMV 35S promoter but in an attempt to reduce silencing in multicolored lines, and obtain expression in tissues where the 35S promoter is less active, we have generated a new suite of mito-FPs (GFP, YFP, CFP, mCherry, and mEosFP) using the ubiquitin promoter Gateway® vectors engineered by Grefen et al. [23]. These new constructs use the same, tried and tested, N-terminal mitochondrial targeting sequence from the *N. plumbaginifolia* beta subunit of the mitochondrial ATPase [5, 24, 25]. The F_2 seed of these lines has only recently become available and while expression is excellent we have yet to determine their behavior in plants expressing other fluorescent fusions.

2.5 Solutions and Media

2.5.1 Plant Growth

1. 80 % (v/v) ethanol.
2. 30 % (v/v) bleach—domestic grade.
3. Sterile deionized or reverse osmosis purified water.
4. 0.5× Murashige and Skoog (MS) agar plates: 0.5× MS medium, 0.8 % (w/v) M type agar, 1 % (w/v) sucrose, 0.05 % (w/v) MES buffer, pH 5.8.
5. Benomyl (fungicide).
6. Plant growth chamber with temperature and light control.

2.5.2 Visualization of Fluorescent Proteins

1. 60 % (v/v) glycerol.
2. Double-sided adhesive tape.
3. 0.1 % (w/v) plant-certified agar (*see* **Note 8**).
4. 30 mM Oryzalin in 100 % ethanol.
5. 10 mM Nocodazole in DMSO.
6. 2 mM Latrunculin-B (lat-B) in 100 % ethanol.

3 Methods

3.1 Seed Germination and Plating

1. Surface sterilize seeds by mixing for 7 min in 80 % (v/v) ethanol, followed by 7 min in 30 % (v/v) household bleach. Wash seeds three times in sterile water.
2. Prepare 0.5× strength MS agar plates containing sucrose (*see* **Notes 8** and **9**). If contamination with fungi is a problem add 5 ppm Benomyl to the molten media before plating [26] (*see* **Note 10**).
3. Unless screening plants for antibiotic resistance there is no need to add antibiotics to the media. Stratify the seeds by storing plates in a refrigerator at 4 °C for 3 days in order to synchronize germination.
4. After this stratification step, transfer Petri dishes to a growth chamber (16-h light at 100 μmoles/s/m^2, 8-h dark cycle, 23 °C).

3.2 Mounting Tissue for Screening Plants to Identify Lines Expressing Fluorescent Protein Fusions

Remove a small piece of one of the first true leaves of a 14-day-old seedling growing on 0.5 % MS agar using small scissors (*see* **Note 11**). It is convenient if the seedlings are arranged in an array on the Petri dish to facilitate removal of pieces of leaf and enable correspondence to be made between leaf piece on the slide and the plant on the plate. Nine leaf pieces can be arranged asymmetrically on a glass slide to ensure correct orientation with respect to the seedlings on the Petri dish.

If screening for double- or triple-expressing plants, it is recommended to mount leaf pieces from only five plants due to the prolonged time taken to identify co-expressing cells (*see* **Note 7**).

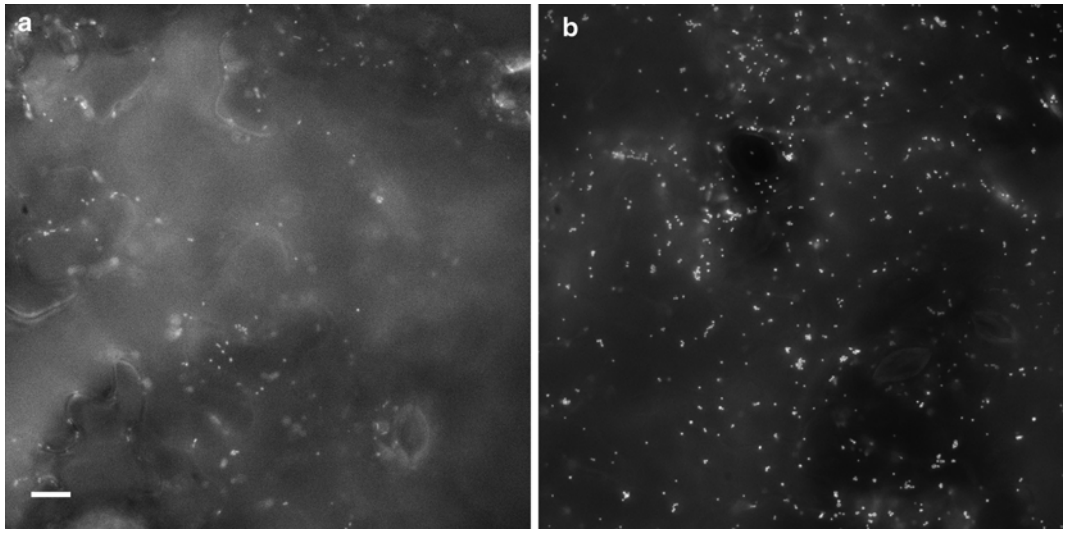

Fig. 1 Effect of mounting in 60 % (v/v) glycerol. (**a**) A piece of leaf of a 14-day-old Arabidopsis seedling expressing mito-EosFP (green channel) mounted simply between slide and coverslip in water. (**b**) Piece of leaf from the same plant as in (**a**) but this time mounted in 60 % (v/v) glycerol. Scale bar = 10 μm

Apply a small amount of pressure onto the micro coverslip (24 × 50 mm) to release air bubbles and to allow the adherence between coverslip and leaf. Leaf pieces can also be mounted in 60 % (v/v) glycerol facilitating good contact between the irregular leaf surface and the coverslip which is essential for imaging (Fig. 1).

Keep track of the number (i.e., 1–9) of plants expressing the fusion(s) and once finished with each slide discard non-expressing lines and keep expressing seedlings for transfer to compost.

3.3 Analysis of Fluorescent Proteins in Root Tissue

1. Place previously sterilized seeds on 0.5× MS agar plate using a micropipette (0.1–2 μL, Eppendorf Research Pro). This pipette is suited to the job since the width of the tip point allows a single seed to attach by suction. Plate seeds in one or two rows while being careful to leave space between two rows to allow proper root growth. Time taken at this plating stage is recovered by not having to handle the seedlings again before experimentation, thereby reducing damage to the delicate roots and root hairs.
2. Stratify seeds and incubate the plates as in Subheading 3.1. Orientate the plates in an upright position once in the growth chamber to allow the seedlings to grow roots on the surface of the plate rather than into the agar that could otherwise lead to damage during seedling removal.
3. It is important to be consistent with plant age and sampling area when observing and comparing mitochondrial dynamics in plants. For root samples we use root hairs and root epidermal cells in the differentiation zone of 10-day-old seedlings.

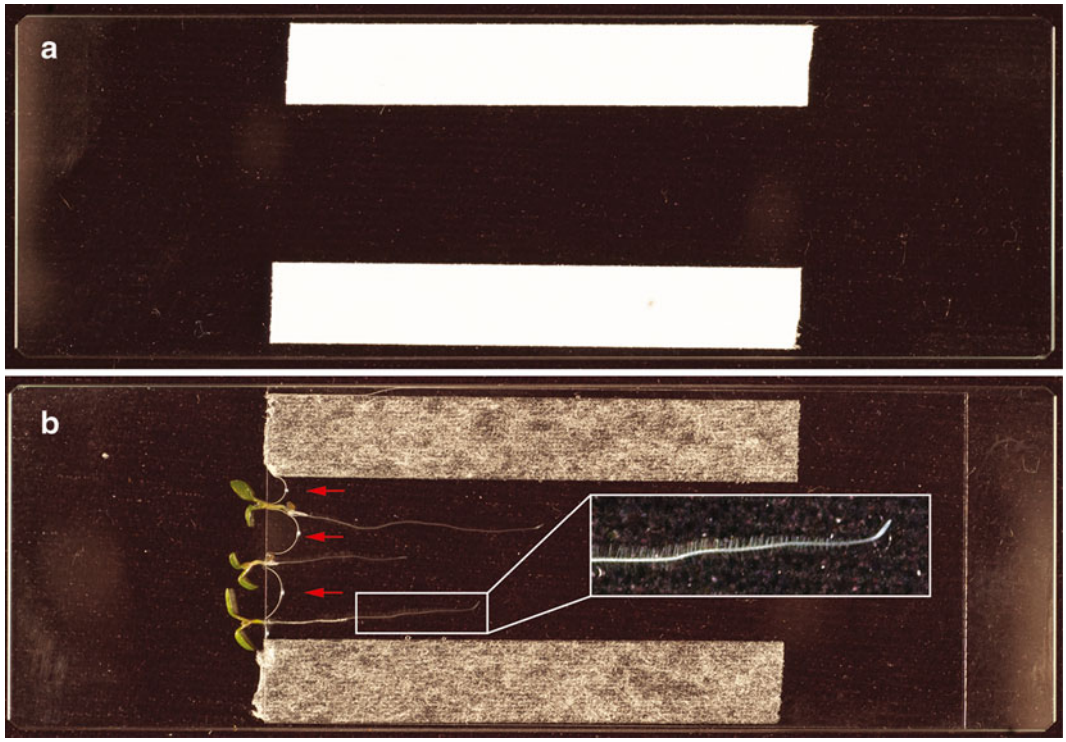

Fig. 2 Mounting whole Arabidopsis seedlings for imaging of roots and root hairs. (**a**) Chambered slide prepared using ultrathin double-sided adhesive tape (*see* Note 12). (**b**) Top adhesive protection removed, and three 10-day-old seedlings mounted under a coverslip in 0.1 % (w/v) agar Type M (*see* Note 8). If water evaporates, or mounting is not complete (*red arrows*), more agar solution or water can be added to fill chamber. The inset is a magnified region showing the regular arrangement of roots hairs that are well orientated for imaging

4. Prepare a chambered glass slide (Fig. 2) by placing using two strips of ultrathin double-sided adhesive tape (*see* **Note 12**) lengthwise along a regular glass slide (75 × 25 mm, 1 mm thick).
5. Fill the chamber between the two strips of tape with 0.1 % (w/v) plant-certified agar (*see* **Note 8**).
6. Pick up a seedling from the plate using fine forceps taking care to lift the seedling by supporting the leaves within the forceps tips rather than clasping the leaves directly. Take care not to damage the root system.
7. Place the seedling immediately onto the prepared slide, try to keep the root as straight as possible, and place the seedling so that the differentiation zone of the root is close to the middle of the slide (Fig. 2b).
8. Finally mount the cover glass (cover glass No. 1) on top of the tapes (be careful to avoid air bubbles); this should perfectly seal the slide and in our experience should last at least an hour

without detrimental evaporation (depending on the level of humidity in the air; if the water is evaporating quickly refill by adding sterile water to an open edge of the cover glass).

3.4 Analysis of Fluorescent Proteins in Leaf Tissue

1. Small pieces of leaf of 7–14-day-old plants can be mounted directly between coverslip and slide in water, or chambered slides can be prepared as described above which prevent the coverslip from moving with the objective when using oil immersion. The adhesive tape method is also very well suited to imaging protoplasts since it prevents the sheer forces between coverslip and slide from bursting the protoplasts.
2. Frequently, poor images arise due to lack of contact between the leaf and the coverslip. It is therefore useful to mount in 0.1 % (w/v) agar or in 60 % (v/v) glycerol (*see* Subheading 3.2).

3.5 General Image Acquisition and Analysis

1. Place the prepared slide on the stage of the microscope, and select the region of interest. Choose location to be imaged using a low-power objective and via the eyepieces first before switching to the objective to be used for image capture and fine-tuning in the *x*, *y*, and *z* planes via the camera using image capture software.
2. When capturing *z*-stacks (for 3D imaging) the optimal distance between each plane is generally set using the software's suggestion since this will take into account the objective lens (magnification and N.A.) and the immersion medium (*see* **Note 13**).
3. The camera exposure time depends on the illumination and detector settings (*see* **Note 14**). In general, this should be set to as low a value as possible, especially when multichannel images are to be captured using a WFM. In our experience, the best microscope setup has illumination by LEDs since fast switching is possible between excitation wavelengths allowing the use of dual-band cubes. It is also possible to use white light illumination, but unless fast filter wheels are available, the limiting time factor for fast acquisition is the time taken for the filter wheel to switch to each single-band cube or switch excitation filter only if a suitable dual-band dichroic and emission filter is used.
4. Set up the microscope to switch off the LED or close the shutter on the white light source after capture of each image. This is especially important in longer experiments, for example when capturing mitochondrial movement on the actin cytoskeleton.
5. For time-lapse capture, set the time interval between image capture according to experimental requirements (the minimum interval will be limited by exposure time, number of channels, and speed of switching between channels).

6. It is good practice to add basic annotations to images before finishing a microscope session since this will save time in the long run, for example, adding scale bars and *z*-position or time to *z*-stacks and time-lapse movies, respectively. Often these can be added to captured images in batch mode. Most acquisition software save metadata with the image, so make sure that your files are saved in a mode that allows this so that all imaging information is available to the analysis software in subsequent steps.
7. Image analysis naturally depends on the nature of the experiment and a number of powerful image analysis software programs are available (*see* **Note 15**). The choice of these is likely down to availability and personal preference. We have used software (BitPlane) and FIJI/ImageJ [27] for analysis and AutoQuant (Media Cybernetics) for deconvolution (Fig. 3). Additional vector graphic annotations (arrows etc.) are best added in Adobe Illustrator.
8. To date we have found that the most useful analyses are particle (e.g., mitochondrial) number and size (performed with the Analyze Particles command in ImageJ), quantification of movement (Subheading 3.6), and tracking of mitochondria (Subheading 3.7).

3.6 Quantification of Mitochondrial Movement

A convenient graphic method to represent motility of mitochondria and/or other organelles is to overlay two images captured at defined time points (e.g., 1-s apart). Each image is false colored with contrasting color (e.g., green and red) before overlay such that movement is evident from the appearance of organelles of both colors (either red or green) while lack of movement is evident from the merged color (yellow in this instance). An example of this is shown in Fig. 4a–c. This method is also easily amenable to colocalization quantification.

Several image analysis programs (for instance, Imaris, ImageJ, and AutoQuant) can be used to quantify movement using colocalization of the differently colored pixels in the two images generated as above. Here we present the steps required to use AutoQuant to calculate the colocalization of pixels within more than one region of interest (ROI) instead of the entire image (Fig. 4d).

1. Import the merged image or z-stack into AutoQuant X3, if using AutoQuant X2, and then install the colocalization plug-in. We prefer using the original image without deconvolution (which might affect the accuracy of the colocalization data).
2. Go to "Analysis" icon in the toolbar and select "Colocalization."
3. A colocalization preview image will appear and a screen with a 2D histogram will appear on the right-hand side.
4. On the top of the preview colocalization image or window, click on the shapes icon (square or circle) and then draw the required ROI. You can select more than one ROI.

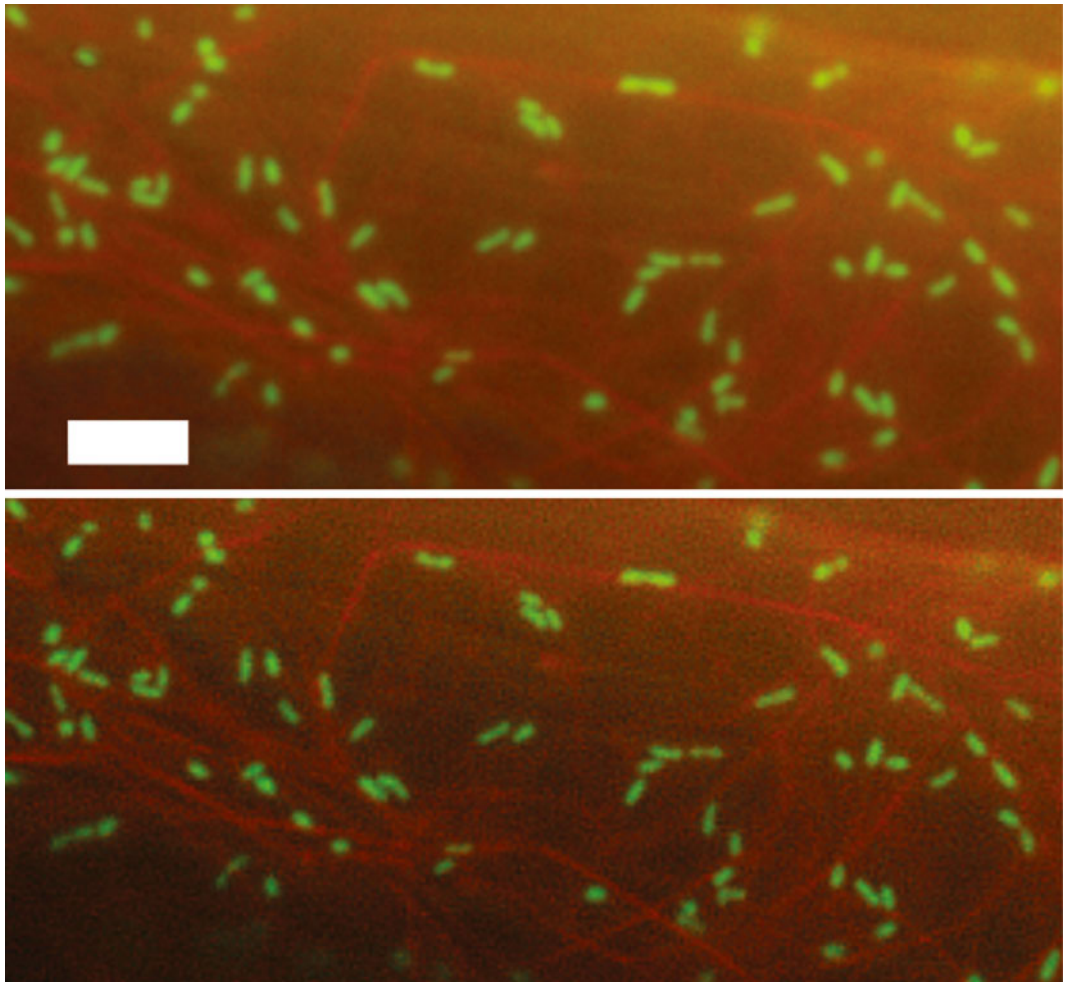

Fig. 3 Improving image clarity by deconvolution. A single frame of a time-lapse series captured by WFM of mitochondria and actin in a root epidermal cell of a mito-GFP/mCherry-mTalin stable double-transgenic line. The image was subjected to deconvolution using AutoQuant *X*2 (high noise, adaptive (blind), theoretical PSF, 100 iterations) and additional parameters dictated by the microscope setup (Olympus BX61, 100× Plan Apo N.A. = 1.4 objective) and the camera (QImaging Rolera-MGi+). Scale bar = 5 μm

5. Adjust the threshold on the 2D histogram and change histogram settings according to your chosen parameters.
6. Activate an ROI on the preview colocalization image that was selected by clicking on it, and then select the "Add ROI" button on the "Colocalization Analysis" screen on the right-hand side to calculate the statistical values including percent of colocalization as well as Pearson's Correlation Coefficient and Manders' Overlap Coefficient values for the selected ROI.
7. To calculate colocalization within a second or subsequent ROI, repeat **step 6**.

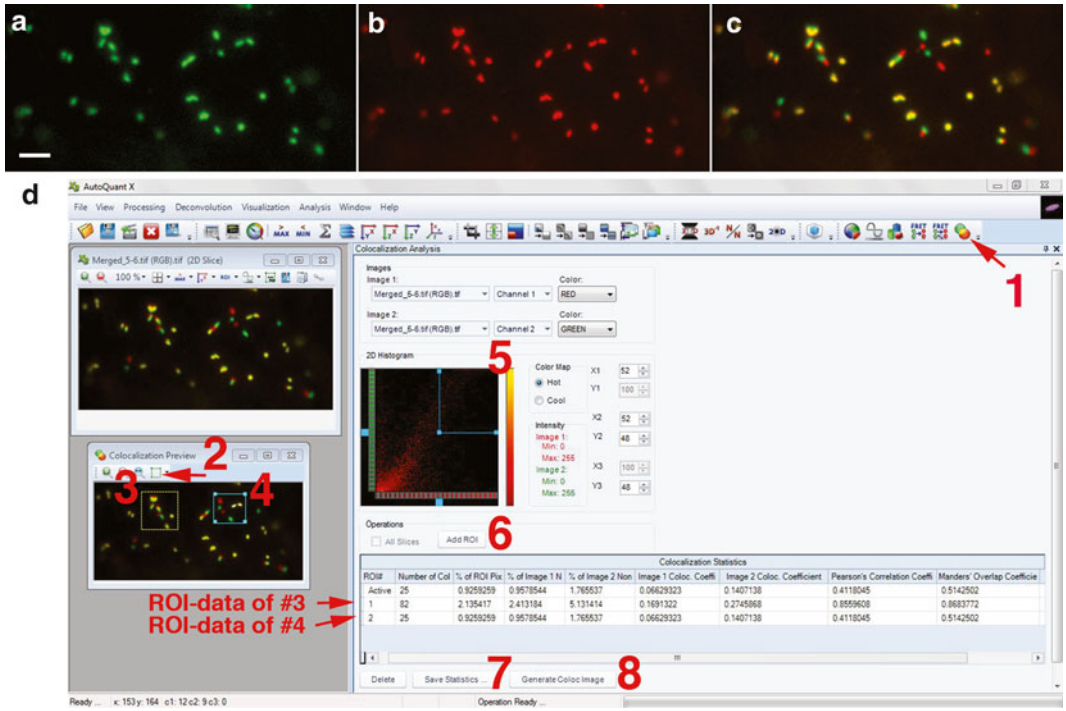

Fig. 4 False coloring of sequential time-lapse images to display mitochondrial motility. (**a**) The first image, in this instance of mitochondria in an Arabidopsis leaf epidermal cell, is false-colored green. (**b**) A second image, captured 1 s later, is false-colored red. (**c**) Overlap of (**a**) and (**b**) created in Fiji/ImageJ. Scale bar = 5 μm. (**d**) Screen grab of the process of quantifying motility by colocalization: Click on the "Analysis" drop-down menu and click on "colocalization." Instead, you can also find the colocalization icon in the toolbar (#1). In the "Preview Colocalization" window, you will find the shapes that can be used to specify the ROI (#2). Draw ROI(s) (# 3 and 4) and adjust the threshold (#5). After activating an ROI, click "Add ROI" (#6). The statistical data will appear in the table below that can be exported by click on "Save Statistic" (#6). Finally, generate a colocalization image (#8)

8. To export the statistical data to a Microsoft Excel file, click on "Save Statistics."
9. To generate a colocalization image, click on "Generate Coloc Image."

3.7 Tracking

Here we describe methods used to acquire 3D-rendered images, track individual mitochondrion, or clusters, and finally generate numerical representations of mitochondrial dynamics in live root epidermal cells from 10-day-old plants.

1. Prepare the root sample on a standard glass slide as detailed in Subheading 3.3.
2. Choose location to be imaged by the eyepieces first and fine-tune via the camera using image capture software. Select an FOV such that mitochondria in the chosen display more horizontal movement (x, y) than vertical movement (z).

3. Set up time-lapse settings according to the speed of movement, brightness of the fluorophore, sensitivity of the camera, and number of channels to be imaged. Ideally, one uses a stored multidimensional acquisition program, thereby allowing minor, and thus quick, tailoring to the specific experimental requirements.
4. Collect an image series for 2–10 min according to the experiment (supplementary movie). Longer times often lead to out-of-focus images due to movement of the sample and the chance of artifacts.
5. Use AutoQuant to deconvolute images using the 3D-blind deconvolution algorithm with adaptive PSF, low noise, and ten iterations (default settings). Set up suitable modality settings according to the microscope used.
6. Open deconvoluted image stack using Imaris software (Fig. 5a), then add new "spots" in surpass mode, and, using the step-by-step wizard, select "track spots over time" to identify individual mitochondrion.

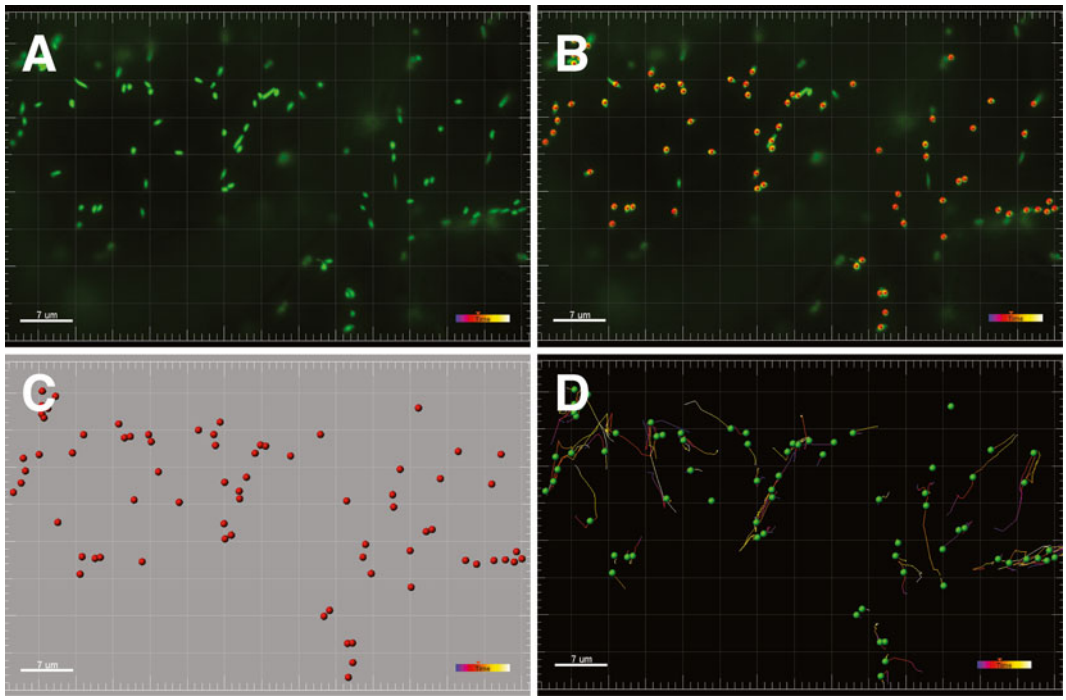

Fig. 5 Tracking mitochondria using Imaris. (**a**) A representative image of a time series of mitochondria expressing mito-GFP after deconvolution using AutoQuant and visualized using Imaris 7.4.2 software (Bitplane). (**b**) *Red dots* highlight mitochondria identified using "spot" detection with the mitochondria in green (Supplementary Movie 1, see Extras.springer.com). (**c**) Representation of mitochondria as *red spots* with the image removed. (**d**) Representation of identified mitochondria (as *green spots*) with "tracks" of movement; each track is color-coded to show the specific time point (color key: *blue* is 0 s, white is 30 s; Supplementary Movie 2, see Extras.springer.com). Scale bar = 7 μm

7. Use the source channel with 0.5 μm as estimated "spot" (mitochondria) diameter (as an approximate diameter of plant mitochondria) to identify individual mitochondria (Fig. 5b).
8. Use the background subtraction threshold filter ("Quality") to eliminate unspecific background mitochondria/"spots."
9. Manually add or delete mitochondria (spots) that were not recognized (or falsely detected) by the automatic detection (Fig. 5c) (*see* **Note 16**).
10. Use Autoregressive motion as the tracking algorithm to track the identified spots (mitochondria).
11. If one particular mitochondrion disappeared within consecutive time-lapse images (e.g., the mitochondrion had moved out of the FOV), set the detection algorithm to search for it in five consecutive frames within a maximum radius of 2 μm from its last spot. Given that the average mitochondrial speed in wild-type Arabidopsis leaves is below 5 μm/s and using an image capture rate of 1 fps, we found that there is a high tendency for errors with a radius of more than 5 μm. Enable the "Fill gaps with all detected objects" function to identify and link the mitochondria that are reappearing within five frames with each respective mitochondrion before its temporary disappearance.
12. After this step, the moving mitochondrion at each time point will be linked to a single track by means of automatic track detection (Fig. 5d); falsely linked mitochondria can be disconnected manually using the "edit track" function.
13. Mitochondria which were present continually for more than 16 s (or frames) within a total 30-s sampling time will be used (selected using "Track Duration" filter) for further statistical analysis to avoid sampling mitochondria that were only transiently in the FOV, likely due to movement deeper into the tissue.
14. Mitochondrial clusters can be identified using a similar algorithm with different parameters for spot size, for example, using a filter for "Number of Voxels" above 10.000, and "Volume" above 4.000 μm^3 to filter out normal mitochondria.
15. Resulting tracking data statistics can be exported as a Microsoft Excel spread sheet for statistical analysis purposes.

3.8 Example Experiment: Mitochondria and the Cytoskeleton

In order to study the interrelationships between mitochondria, actin filaments, and microtubules, we have used double-transgenic lines expressing mCherry-mTalin and mito-GFP or mCherry-MAP4 and mito-GFP to visualize mitochondria and F-actin or microtubules, respectively. Various drugs can also be deployed to disrupt the actin or microtubule cytoskeleton (e.g., lat-B to sequester G-actin; and oryzalin and nocodazole which bind to tubulin dimers). It is best to use candidate drugs when plants are younger

(5–10 days old) so that the tissues are relatively thin and also because cytoskeleton-directed FP fusions are often silenced in older tissue. A range of drug concentrations and treatment durations are advised meaning that the experiment becomes complex due to the multiple parameters involved and thus careful planning is a must.

In fact, timing is one of the key difficulties when performing microscopy since it invariably takes longer than one first imagines to find suitably expressing cells that are also well orientated in the FOV. It is therefore essential that the experiments are well planned and that sufficient time is provided between incubation steps. For example, do not plan to capture images of the effects of lat-B after 30-min incubation and again at 45 min from seedlings added to the test solution at time zero. Instead, stagger the incubation start times as suggested in the following protocol:

1. Dilute oryzalin to 10–30 μM, nocodazole to 10 μM, and lat-B to 2 μM with water before use.
2. Prepare control solutions of ethanol and DMSO to the same concentration. When experiments are performed with different concentrations, the lowest dilution factor of the solvent is used as a control.
3. Start your day by adding seedlings of the control lines into the required number of small glass Petri dishes (4–6 seedlings per dish) containing 0.5× MS and the appropriate concentration of ethanol or DMSO. Label each plate according to the incubation time required for the control treatment.
4. 30 min after incubating the control seedlings, add seedlings to be treated with drugs to dishes containing 0.5× MS.
5. For example, at 9 a.m. add control seedlings to different plates and label them 1, 2, 3 h, etc., and then at 9:30 a.m., add all seedlings to be treated with drugs on several plates and label them as 1, 2, 3 h, etc. Thus, after 1 h, the first control seedlings will be ready for microscopy, and 30 min later, the first drug-treated seedlings will be ready. This 30-min time interval is sufficient to screen seedlings of each plate in a relaxed manner. Leaving a 1-h period between each drug treatment concentration will result in a productive day with many replications possible.
6. Gently mount the entire seedling onto the slide if root cells are to be imaged (Subheading 3.3) or mount one leaf.
7. Metamorph (running our Olympus BX61) or Zen Blue (running our Zeiss Axio Imager Z2) can be programed for multidimensional image capture since both microscopes feature motorized components. Illumination intensity and camera exposure times can be programed based on tests performed before the experiment is started. Ideally illumination will be low (e.g., 1–4 % for either the X-Cite source or LEDs) but still allowing relatively short exposure times of 40–200 ms.

As such, it is possible to program capture intervals (i.e., the time between two images in the same channel) of 1 s or even less when a dual-band cube and LED switching are employed.

8. It is also preferable to capture movies even if the intention is to present multiple single time point images. In this way a selection of images are available to choose from.

4 Notes

1. Sensitivity depends on the camera. Many WFMs are not equipped with the best cameras to give high sensitivity and speed without sacrificing resolution too much.
2. The camera must be monochrome since color cameras do not offer the sensitivity and hence speed of capture required.
3. EM = emission, DM = dichroic mirror, EX = excitation. Bandpass excitation and emission filters are referred to by their center wavelength separated from the bandwidth by "/." Thus, a 470/40 nm excitation filter transmits between 450 and 490 nm.
4. Semrock FF01-593/40-25: The emission maximum of mRFP1 is 607 nm while that of mCherry is 610 nm. This filter is also ideal for imaging the mitochondrial membrane potential probe, TMRM.
5. For example in the off-the-shelf dual-band cube from Semrock, GFP/DsRed-A-000, change the EM to FF01-523/610-25.
6. Almost all our research on mitochondrial dynamics uses stable transgenics. We believe that the results are less prone to artifact, allow investigation of a large range of cell types, and of course enable the generation of stable lines expressing multiple FP fusions by means of crossing.
7. When screening double-transgenic lines expressing GFP and mRFP1 fusions it is best to screen for mRFP1 first and then for GFP since mRFP1 is a poor fusion partner and expression is often seen to be mistargeted.
8. Type-M agar from Sigma (A4800) or another plant tissue culture-certified agar.
9. We have recently removed sucrose from our Arabidopsis media with observable no ill effects.
10. Benomyl is an especially useful addition to selection media when plating thousands of T1 seed on larger Petri dishes for screening after transformation of Arabidopsis since fungal contamination is often a problem despite surface sterilization.

11. Vannas spring scissors can be relatively expensive; however cheaper "student" versions are perfect, e.g., product 91500–09 from www.finescience.de.
12. Product TP005: www.crafterscompanion.co.uk/search/tp005.
13. If capturing z-stacks that will be compared (e.g., control versus treated; mutant versus wild type) be sure to use identical imaging parameters including the distance between each slice and the number of slices captured. You should also ensure that the starting point of the stack is the same so that the same area of plant material is optically sectioned.
14. If images are to be compared try to ensure that the imaging parameters are identical. This is less critical for analyses of movement but for morphological comparisons and in cases where pixel intensity/number will be quantified the imaging parameters must be identical for all images. In addition, ensure that the detector is not saturated and that there is background in the image so that the dynamic range of the detector/camera is not compromised.
15. All image analysis should be performed on a copy of the original image and the original image should be archived in a form that contains the metadata. Images for presentation should be TIFFs and any image compression is to be avoided if possible. When performing analyses or annotating images it is advisable to duplicate the image regularly (particularly in ImageJ where it is often not possible to reverse steps).
16. According to our experience some relatively long mitochondria tend to be identified as two or more separate spots; hence it is necessary to manually edit spots after the automatic detection. There is often a similar issue with automatic track detection.

Acknowledgements

The Olympus microscope system in the Logan lab at the University of Saskatchewan, Canada, was purchased with a Canada Foundation for Innovation LOF grant to DCL. Imaris and AutoQuant were purchased with an NSERC RTI award to DCL. The Zeiss microscope system in Angers, France, was purchased by SFR QUASAV as part of the Campus Végétal project. Thanks to David Macherel for supporting my move to Angers and his continued support thereafter, and for alerting me to the ultrathin tape. AME was supported by an NSERC Discovery grant to DCL, by the Department of Biology at the UofS, and UGF and GTF awards. DSBE was supported by NSERC Discovery grants to DCL and Dr. Chris Todd (Biology, UofS).

References

1. Cavers F (1914) Chondriosomes (mitochondria) and their significance. New Phytol 13:96–106
2. Haseloff J, Siemering KR, Prasher DC, Hodge S (1997) Removal of a cryptic intron and subcellular localization of green fluorescent protein are required to mark transgenic Arabidopsis plants brightly. Proc Natl Acad Sci U S A 94:2122–2127
3. Chalfie M, Tu Y, Euskirchen G et al (1994) Green fluorescent protein as a marker for gene expression. Science 263:802–805
4. Sheen J, Hwang S, Niwa Y et al (1995) Green-fluorescent protein as a new vital marker in plant cells. Plant J 8:777–784
5. Logan DC, Leaver CJ (2000) Mitochondria-targeted GFP highlights the heterogeneity of mitochondrial shape, size and movement within living plant cells. J Exp Bot 51:865–871
6. Heim R, Prasher DC, Tsien RY (1994) Wavelength mutations and posttranslational autoxidation of green fluorescent protein. Proc Natl Acad Sci U S A 91:12501–12504
7. Heim R, Cubitt AB, Tsien RY (1995) Improved green fluorescence. Nature 373:663–664
8. Siemering KR, Golbik R, Sever R, Haseloff J (1996) Mutations that suppress the thermosensitivity of green fluorescent protein. Curr Biol 6:1653–1663
9. Tsien RY (1998) The green fluorescent protein. Annu Rev Biochem 67:509–544
10. Matz MV, Fradkov AF, Labas YA et al (1999) Fluorescent proteins from nonbioluminescent Anthozoa species. Nat Biotechnol 17:969–973
11. Shaner NC, Campbell RE, Steinbach PA et al (2004) Improved monomeric red, orange and yellow fluorescent proteins derived from Discosoma sp. red fluorescent protein. Nat Biotechnol 22:1567–1572
12. Campbell RE, Tour O, Palmer AE et al (2002) A monomeric red fluorescent protein. Proc Natl Acad Sci U S A 99:7877–7882
13. Patterson GH and Lippincott-Schwartz J (2002) A photoactivatable GFP for selective photolabeling of proteins and cells. Sci (New York, NY) 297:1873–1877
14. Wiedenmann J, Ivanchenko S, Oswald F et al (2004) EosFP, a fluorescent marker protein with UV-inducible green-to-red fluorescence conversion. Proc Natl Acad Sci U S A 101: 15905–15910
15. Zheng M, Beck M, Müller J et al (2009) Actin turnover is required for myosin-dependent mitochondrial movements in Arabidopsis root hairs. PLoS One 4:e5961
16. Logan DC, Scott I, Tobin AK (2003) The genetic control of plant mitochondrial morphology and dynamics. Plant J 36:500–509
17. Scott I, Tobin AK, Logan DC (2006) BIGYIN, an orthologue of human and yeast FIS1 genes functions in the control of mitochondrial size and number in Arabidopsis thaliana. J Exp Bot 57:1275–1280
18. Scott I, Logan DC (2008) Mitochondrial morphology transition is an early indicator of subsequent cell death in Arabidopsis. New Phytol 177:90–101
19. Mathur J, Radhamony R, Sinclair AM et al (2010) mEosFP-based green-to-red photoconvertible subcellular probes for plants. Plant Physiol 154:1573–1587
20. Yao N, Eisfelder BJ, Marvin J, Greenberg JT (2004) The mitochondrion—an organelle commonly involved in programmed cell death in Arabidopsis thaliana. Plant J 40:596–610
21. Teh O-K, Moore I (2007) An ARF-GEF acting at the Golgi and in selective endocytosis in polarized plant cells. Nature 448:493–496
22. Mathur J, Mathur N, Kernebeck B et al (2003) A novel localization pattern for an EB1-like protein links microtubule dynamics to endomembrane organization. Curr Biol 13: 1991–1997
23. Grefen C, Donald N, Hashimoto K et al (2010) A ubiquitin-10 promoter-based vector set for fluorescent protein tagging facilitates temporal stability and native protein distribution in transient and stable expression studies. Plant J 64:355–365
24. Boutry M, Chua NH (1985) A nuclear gene encoding the beta subunit of the mitochondrial ATP synthase in Nicotiana plumbaginifolia. EMBO J 4:2159–2165
25. Chaumont F, de Castro Silva Filho M, Thomas D et al (1994) Truncated presequences of mitochondrial F1-ATPase β subunit from Nicotiana plumbaginifolia transport CAT and GUS proteins into mitochondria of transgenic tobacco. Plant Mol Biol 24:631–641
26. Paul A-L, Semer C, Kucharek T, Ferl RJ (2001) The fungicidal and phytotoxic properties of benomyl and PPM in supplemented agar media supporting transgenic Arabidopsis plants for a Space Shuttle flight experiment. Appl Microbiol Biotechnol 55:480–485
27. Schindelin J, Arganda-Carreras I, Frise E et al (2012) Fiji: an open-source platform for biological-image analysis. Nat Methods 9: 676–682

Chapter 17

Analysis of Plant Mitochondrial Function Using Fluorescent Protein Sensors

Stephan Wagner, Thomas Nietzel, Isabel Aller, Alex Costa, Mark D. Fricker, Andreas J. Meyer, and Markus Schwarzländer

Abstract

Mitochondrial physiology sets the basis for function of the organelle and vice versa. While a limited range of in vivo parameters, such as oxygen consumption, has been classically accessible for measurement, a growing collection of fluorescent protein sensors can now give insights into the physiology of plant mitochondria. Nevertheless, the meaningful application of these sensors in mitochondria is technically challenging and requires rigorous experimental standards. Here we exemplify the application of three genetically encoded sensors to monitor glutathione redox potential, pH, and calcium in the matrix of mitochondria in intact plants. We describe current methods for quantitative imaging and analysis in living root tips by confocal microscopy and discuss methodological limitations.

Key words Plant mitochondria, Fluorescent protein sensors, In vivo imaging, Confocal microscopy, Respiratory physiology, roGFP, Cameleon, cpYFP

1 Introduction

While much of the mitochondrial respiratory machinery is known in molecular detail [1], knowledge of the physiological context that it operates in in vivo is still very limited. This is an important issue to overcome if we are to understand how individual or populations of mitochondria function *in planta*. Hallmarks of mitochondrial physiology, such as pH or membrane potential, are not only set by the mitochondrial machinery, but they also control the function of those systems, either through direct regulation or indirectly as signals [2].

Mitochondria maintain a physiological status that differs markedly from the surrounding cytosol and other compartments (e.g. for thiol redox status [3], pH [4], calcium [5], or ATP levels [6]). Both mitochondrial membranes that separate the organelle from the cytosol allow distinct physiological identities of the respective spaces to be maintained. The inner mitochondrial membrane

James Whelan and Monika W. Murcha (eds.), *Plant Mitochondria: Methods and Protocols*, Methods in Molecular Biology, vol. 1305, DOI 10.1007/978-1-4939-2639-8_17,

provides a particularly selective barrier with a pronounced proton motive force allowing the matrix to establish its distinct physiological status. Considering the specific physiology of mitochondria and their sub-compartments separately from other parts of the cell is therefore critical and necessitates a mitochondria-specific readout in the context of the living plant cell.

Fluorescent protein sensors are well suited for measuring mitochondrial physiology and inferring function. As proteins they can be genetically targeted to specific subcellular locations with high accuracy, and their fluorescence allows nondestructive measurements from living cells and tissues of physiological parameters along with and mitochondrial morphology, motility, and localization. Here we provide a guideline for the application of fluorescent protein sensors to explore the specific physiological status in the matrix of plant mitochondria using confocal microscopy. We focus on one sensor for each, glutathione redox potential (E_{GSH}), pH, and free calcium, that have proven adequate for measurements in the mitochondrial matrix [5, 7, 8]. However, the principles of the approach described can be generalized to other fluorescent protein sensors, other physiological parameters, other submitochondrial compartments, or other tissues.

2 Materials

2.1 Sensors, Constructs, and Plant Lines

For all three sensors comprehensive in vitro characterization is available, including a reliable account of their respective spectroscopic characteristics, specificities, and sensitivity ranges (Table 1; *see* **Notes 1–6**). This is a critical prerequisite for their use *in planta*, although it cannot be ruled out that their behavior may alter in the complex in vivo environment. Constructs for Agrobacterium-based plant transformation and stable transgenic lines in Arabidopsis Col-0 (*Arabidopsis thaliana* ecotype Columbia-0) background with confirmed mitochondrial sensor localization (*see* **Notes 7** and **8**) are available upon request [5, 7, 8].

2.2 Plant Culture

Young seedlings (2–5 days after germination) are convenient for mitochondrial imaging due to a high mitochondrial density (and maximal sensor signal in turn), thin tissue layers, and cell walls that are still relatively permeable to external treatments. Whole young seedlings can be used, which avoids cutting tissue, and subsequent potential effects on plant or tissue physiology. Seedlings are cultured on vertical medium plates [0.5× MS medium, pH 5.8 (with KOH), 0.8 % (w/v) phytagel] with the root growing along the medium surface. This allows transfer of the whole seedling with minimal mechanical stress (*see* **Note 8**).

Table 1
Characteristics of three sensors for mitochondrial glutathione redox status (E_{GSH}), pH, and free calcium concentration, and Arabidopsis lines expressing the sensors

Parameter	E_{GSH}	pH	Ca^{2+}
Sensor and line name	mt-roGFP2-Grx1	mt-cpYFP	4mt-YC3.6
Targeting peptide (*see* **Note 7**)	1× SHMT (Arabidopsis)	1× β-ATPase (Nicotiana)	4× COX8 (human)
Promoter (*see* **Note 5**)	UBQ10 (Arabidopsis)	35S (CaMV)	35S (CaMV)
Antibiotic selection in plants (*see* **Note 8**)	Kanamycin	Hygromycin	Hygromycin
50 % response (purified protein)	−280 mV (E_{GSH})	8.7 (pH; at 488 nm excitation)	250 nM [Ca^{2+}]
Physiological range of reliable sensitivity (*see* **Note 1**)	−240 to −320 mV (at pH 7.0)	7–10	50 nM to 1 μM
pH sensitivity (pH 6.5–8.2)	Negligible	Very strong	Minor
Ratioing principle (*see* **Note 3**)	Dual excitation, single emission	Dual excitation, single emission	Single excitation, dual emission (FRET)
FP basis	EGFP	cpYFP	CFP, cpVenus
Excitation maximum	400 nm, 490 nm	418 nm, 494 nm	436 nm
Excitation laser line for microscopy	405 nm, 488 nm	405 nm, 488 nm	442 nm or 458 nm
Emission maximum	511 nm	515 nm	476 nm, 527 nm
Emission range for microscopy	505–530 nm	505–530 nm	475–500 nm, 525–540 nm
Spectroscopic dynamic range (purified protein)	~12	~50 (pH 7–10)	~7
Spectroscopic dynamic range (in Arabidopsis root tip mitochondria)	~5 (Fig. 3)	~20 (pH 7–10; Fig. 3)	>4 (*see* **Note 11**)
References	[7, 13, 15, 22]	[8, 16, 23, 24, 27]	[5, 25, 26]

2.3 Assay Media

Culture medium: 0.5× MS, 10 mM MES, pH 5.8.

Calcium measurement medium: 5 mM KCl, 10 mM $CaCl_2$, 10 mM MES, pH 5.8 [5].

2.4 Imaging Chamber

Live imaging of plant physiology benefits from minimal perturbation to the tissue during measurement. While it is impossible to achieve that entirely, practical compromises can be reached to avoid mechanical stress. A simple imaging chamber is used allowing sufficient space for the tissue between microscope slide and coverslip using 1–3 layers of insulating tape as spacers to match the tissue thickness and to build a hydrophobic barrier for the medium

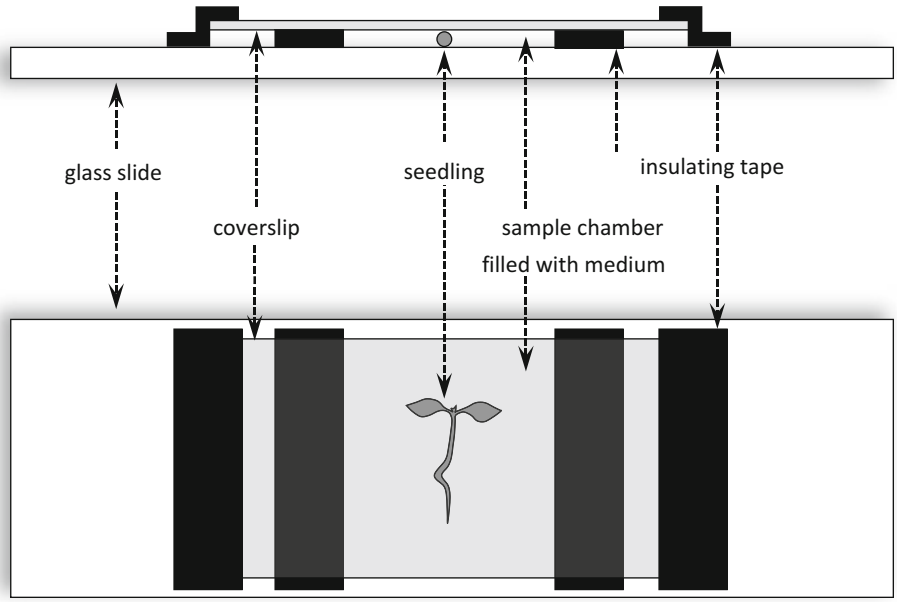

Fig. 1 Schematic side and top view of simple chamber for live imaging

(Fig. 1). Systems for medium exchange or continuous perfusion can be highly useful for dynamic stimulus application and kinetic analysis [9] (*see* **Note 4**) but will not be covered here.

2.5 Confocal Microscope and Laser Settings

A state-of-the-art (upright or inverted) confocal microscope is required for the measurements described here. The method is described for a Zeiss LSM780 confocal system (Carl Zeiss Microscopy GmbH, Jena, Germany), but can be applied at other setups. Laser lines for 405 and 488 nm excitation are required for roGFP2-Grx1 and cpYFP imaging, while a single 442 or 458 nm line is needed for YC3.6 imaging.

2.6 Image Analysis

Careful ratiometric image analysis is critical to extract quantitative data. We have developed a custom MatLab (The MathWorks, Natick, MA) analysis suite that integrates the different analysis and visualization steps via a clear user interface. The program and a detailed user manual are available upon request from Mark D. Fricker, University of Oxford, UK (mark.fricker@plants.ox.ac.uk).

3 Methods

A straightforward procedure is presented here to compare E_{GSH}, pH, and free calcium levels in the mitochondrial matrix at steady state in root tips of young Arabidopsis seedlings between two conditions (e.g. treatment *vs.* control). The aim is to illustrate the principal steps and considerations for routine measurement, which

can then be transferred to other systems and different or more complex tasks, such as monitoring of dynamic changes in the physiology in individual mitochondria [10] or across the mitochondrial populations of whole tissues [5, 11].

3.1 Sample Mounting

1. Gently lift a seedling off the plate using a pair of featherweight forceps and place it in a drop of culture medium (~50 μL) on the microscope slide between the two strips of insulating tape (Fig. 1).
2. Gently place a coverslip on top, avoid air bubbles, and fix it with tape on both sides.
3. If the resulting chamber is not completely filled with medium, carefully top up by pipetting additional medium to one of the open sides.
4. Mount the slide onto the microscope stage. For calcium and pH measurements let the sample rest for 15 min to allow potential touch-induced transients to settle.
5. Choose a lens and add the appropriate immersion liquid. A 25× lens (water immersion, NA 0.8) allows coverage of the entire root tip up to the elongation zone; a 40× lens (water immersion, NA 1.2) allows individual mitochondria to be resolved. Water immersion is best suited optically for plant in vivo imaging, while oil immersion lenses with large numerical aperture can provide good results for tissue layers just below the coverslip at high resolution.
6. Identify the root tip in bright-field mode, and then check for sensor expression using fluorescent light in combination with a green fluorescent protein (GFP) or yellow fluorescent protein (YFP) filter (*see* **Notes 5** and **6**).
7. Use the first specimen to set up the confocal microscope and to optimize the instrument settings. Then start the data collection with a separate set of individuals.

3.2 General Confocal Settings

1. For the roGFP2-Grx1 and cpYFP sensors set up two channels with excitation at 405 and 488 nm, with a dichroic mirror for both excitation wavelengths. Line switching, rather than frame switching, between channels should be used, as mitochondria can be very motile in plants. Sensor fluorescence is detected at 505–530 nm. For the 405 nm channel the emission signal at 430–470 nm is also collected which may be used to correct for autofluorescence. Autofluorescence of cell wall or vacuolar contents can be significant in this channel. For the YC3.6 sensor one channel is set up with excitation at 458 nm (or 442 nm if available for more efficient excitation closer to the CFP excitation maximum (Table 1) [12]) and fluorescence is collected at 475–500 nm (CFP) and 525–540 nm (cpVenus) (Fig. 2a).
2. A non-confocal transmission image is collected in parallel as a bright-field-like reference (Fig. 2a; *see* **Note 9**).

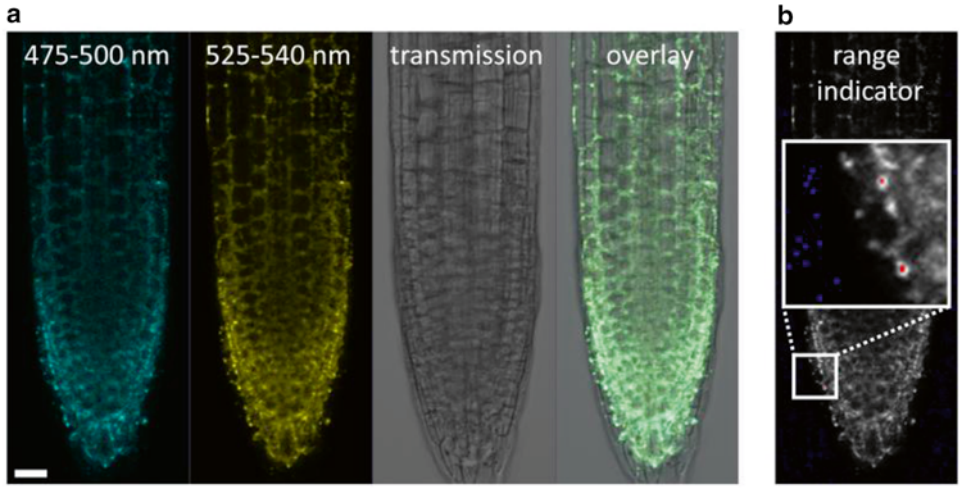

Fig. 2 (**a**) Imaging 4mt-YC3.6 in an Arabidopsis root tip. Channels displayed in *cyan* and *yellow* show emission intensity at 475–500 nm (CFP) and 525–540 nm (cpVenus), respectively, upon excitation at 458 nm using a 25× lens (water immersion, NA 0.8). Size bar = 20 μm. (**b**) Channel showing emission intensity of cpVenus in range indicator mode. Oversaturated and zero pixels are displayed in *red* or *blue*, respectively

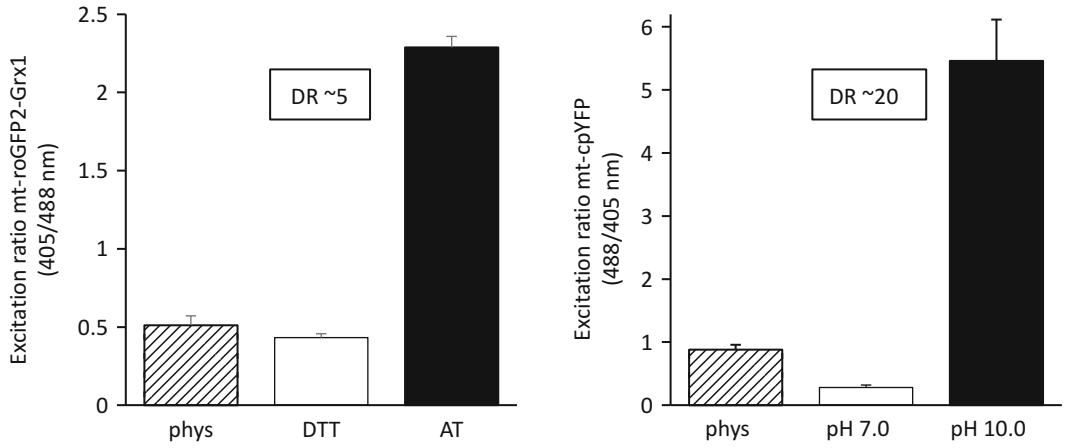

Fig. 3 Exemplary assessment of matrix E_{GSH} and pH in vivo using the mt-roGFP2-Grx1 and mt-cpYFP sensor in root tips of Arabidopsis seedlings. The empirical dynamic spectroscopic range (DR) of the sensors upon in vivo calibration treatments is shown in *insets*. *phys* physiological state, *DTT* 10 mM dithiothreitol, *AT* 2 mM aldrithiol-2. $n \geq 3$, error bars: SD

3.3 Specific Adjustments for Sensor Imaging

1. Set laser power to ≤30 μW (405 nm) and ≤7 μW (488 nm) for exciting mt-roGFP2-Grx1 and mt-cpYFP, and ≤5 μW (442/458 nm) for 4mt-YC3.6 at the objective. This should be determined empirically with a light meter as there can be large discrepancies between nominal laser power, adjusted output percentage, and the actual power that the sample is exposed

to. Keeping laser exposure low avoids sensor bleaching and minimizes photooxidative stress of the tissue, which can itself affect mitochondrial physiology.

2. Use a detector gain within the linear detector range (≤800). If required the photon yield may be increased at the expense of z-resolution by opening the pinhole up to three Airy units.
3. Select scan speed, pixel resolution, averaging, and digital zoom to generate an image of reasonable visual quality with sufficient signal-to-noise ratio to allow for quantitative measurements.
4. Use simple lookup tables such as the range indicator to adjust the amplifier offset value to completely capture the background signal. This is achieved when only very few zero pixels are apparent in the range indicator mode (Fig. 2b).
5. Avoid pixel saturation as this prevents analysis. This is particularly relevant for mitochondrial localized sensors as the fluorescence signal is highly concentrated in small volumes that can easily reach saturation (Fig. 2b).
6. Choose settings to allow the intensities to change between different images without reaching the detector limits. Anticipate variation in signal intensities due to both differences in sensor expression between individuals, physiologically induced ratio changes, or the full probe response during calibration (*see* **Note 10**).
7. Once optimized, keep the settings strictly constant for a given experiment. Any change of settings will directly impact on the measured ratio.

3.4 Data Collection and Quantitative Image Analysis

1. The simplest type of experiment is to monitor the steady-state effect of a treatment compared to its control condition after a fixed time of exposure. Typically single images are collected for >3 individual root tips per treatment ($n = 10$ recommended). It is helpful if all individuals show comparable sensor expression levels although the ratio approach can compensate for variation in sensor abundance. Images should be recorded at similar tissue depths. Individual root tips that show particularly high autofluorescence signals in the 405 nm channel (for roGFP2-Grx1 and cpYFP) should be avoided.
2. To calibrate the sensor, incubate control seedlings in the respective calibration medium (Table 2), typically for >15 min before image collection, and mount in calibration medium (*see* **Notes 10**–**13**). Collect images for >3 individual root tips per calibration point ($n = 10$ recommended).
3. Load the individual image files into the MatLab-based analysis software and perform the analysis steps in the order set by the program. These include sub-pixel channel alignment, noise reduction and pixel binning, background measurement and

Table 2
Calibration regimes

Sensor	Point 1	Point 2
mt-roGFP2-Grx1	2–5 mM aldrithiol-2, 0.5× MS, 10 mM MES, pH 5.8 (KOH)	10 mM DTT, 0.5× MS, 10 mM MES, pH 5.8 (KOH)
mt-cpYFP	100 mM MOPS-Tris, 40 mM K_2SO_4, 5 µM CCCP, 0.5× MS, pH 7.0	100 mM CHES-Tris, 40 mM K_2SO_4, 5 µM CCCP, 0.5× MS, pH 10.0
4mt-YC3.6 (*see* **Note 11**)	n/a	n/a

subtraction, autofluorescence measurement and subtraction (in case of high autofluorescence in the 405 nm channel), calculation and calibration of the ratio image on a pixel-by-pixel basis, and generation of a pseudo-color representation. Images can be saved in windows .avi format for time series or .tif/.jpg/.png for single images.

4. If required, regions of interest (ROIs) can be manually defined to analyze particular areas and spatial differences. The analysis follows the same sequence as for the generation of the ratio image except that calculations are based on the average intensities in the entire image (or ROI) and provide better signal-to-noise as more pixels are averaged before calculation of the ratio value. The ratio values can be calibrated for conversion to redox potential or pH values (*see* **Note 14**). Export the ratio values as a spreadsheet file (.xls), or a complete output of the graphical data and images as an enhanced metafile (.emf).

4 Notes

1. The sensor must be chosen carefully depending on the hypothesis to be tested. The sensitivity range of the sensor must match the conditions to be assessed. For matrix E_{GSH}, pH, and free calcium levels under control conditions that means that the midpoint potential, pK_a and K_d of the sensor, should be close to −350 mV (note that this value is pH adjusted for matrix pH [13]), 7.8 (our own observation), and 100–200 nM [5, 14], respectively. A number of different variants of the sensors described here are available, but the physiological range they can report is still incomplete.
2. The specificity of the sensor should be well defined, based on in vitro characterization, and ideally be supported by a clear mechanistic understanding of the sensor behavior.

3. The sensor should respond in a ratiometric manner, which allows internal normalization and quantitative measurements independent of sensor expression levels and optical path length variations.
4. The sensor response should be rapid and fully reversible with a known underlying reaction mechanism to ensure a meaningful dynamic readout. For example in the case of roGFPs, fusion to the human glutaredoxin Grx1 increases and standardizes their response kinetics based on a defined reaction mechanism independent of the local intracellular environment of the sensor [15].
5. The sensor should be bright as compared to other components in the plant tissue with similar fluorescence properties, to allow for a high signal-to-noise ratio. This is achieved by a high-fluorescence quantum yield of the sensor as well as reasonable expression levels in the plant cell.
6. The expression of the sensor itself must not affect mitochondrial physiology in any major way. Sufficiently high expression levels are required for a reliable readout with a high signal-to-noise ratio, but each sensor molecule represents an artificial addition to the matrix protein inventory. Matrix homeostasis may be affected by either the high abundance of the additional protein or adding additional buffering capacity for the physiological parameter to be assessed. While there is no consistent empirical indication for the former (many lines overexpressing fluorescent proteins have been produced without any detectable phenotype, e.g. [16]), the latter should be assessed for each specific sensor class and plant line. For instance, the pH active tyrosine of mt-cpYFP contributes to the pH buffering capacity in the physiological range of the matrix. However, one might expect the contribution of mt-cpYFP to matrix pH buffering negligible, given the abundance of endogenous matrix proteins and metabolites. An analogous argument applies for calcium binding by YC3.6 and matrix calcium buffering. Mt-roGFP2-Grx1 expression provides additional protein surface thiols to the matrix, as well as ectopic glutaredoxin activity. For the impact of the sensor on glutathione redox buffering to be minor, the relative abundance of sensor needs to be low as compared to local glutathione concentration, and electron flux through the glutathione pool. This is likely to be the case considering that the estimated sensor expression levels are in the low μM range (our observation), about three orders of magnitude below the estimated matrix glutathione levels (low mM range across the plant cell [17] with indications for even higher levels in the matrix [18]). Nevertheless, interaction of the additional glutaredoxin with endogenous targets cannot be ruled out.

7. Correct localization of the sensor in the mitochondria must be unambiguous. Mis-localization in the cytosol or in the plastids is not uncommon for strongly expressed fluorescent proteins and must be either ruled out by selection of appropriate lines or considered appropriately in the experiment [7].
8. Silencing of sensor expression giving rise to tissue with patchy expression or absent fluorescence can be problematic and often increases over generations. Preselection of individuals to be used for experiments by fluorescence, rather than antibiotic resistance, is advisable. Depending on the question, tissues with patchy sensor expression may be still usable for data collection as long as parts of the image contain clear signal.
9. If images are collected in green tissues a channel should be added to monitor chlorophyll fluorescence (excitation 405, 442, 458, or 488 nm; emission 640–700 nm) and to make sure that chlorophyll signal does not bleed through into any of the channels used for ratioing. This is particularly relevant if stress treatments are applied which may affect the chloroplast fluorescence spectrum.
10. In vivo sensor calibration by a standardized regime is an important, yet not always straightforward, element of a meaningful experiment. It (a) ensures that the sensor construct responds in a manner that is comparable to its in vitro behavior, (b) sets the maximal spectroscopic dynamic range within which the sensor can respond under the present conditions, and (c) allows calculation of absolute concentrations from the ratio data (*see* **Note 14**). The minimal requirement for an in vivo calibration is to drive the sensor to its two extremes with high confidence (i.e., fully protonated/deprotonated, oxidized/reduced, occupied/free binding site). Ideally, a full titration through the midpoint would be valuable, but can be difficult to achieve for routine measurements. Here we describe calibration regimes for mitochondrial pH and E_{GSH}.
11. In vivo calibration of 4mt-YC3.6 has been attempted using 5 mM EGTA and 10 mM $CaCl_2$, respectively, in the presence of the calcium ionophores ionomycin or A23187, but the sensor could not be driven to the expected extreme ratios (our own observations). Since the sensor responds to calcium stimuli nevertheless, it is likely that the ionophores do not reach the relevant membranes *in planta*. Currently no reliable calibration regime for mitochondrial YC3.6 is available for intact plant tissues.
12. Full oxidation of roGFP2 sensors can be achieved with 10–100 mM H_2O_2 [13, 19]. While that regime drives the sensor into oxidation, it can lead to partial sensor bleaching, formation of oxygen bubbles that interfere with imaging, and cell

death. In addition its efficient detoxification by the antioxidant defense machinery of the plant cell can leave doubts if the sensor has really been fully oxidized. This can be avoided by specific thiol oxidation with aldrithiol-2 (2,2′-dipyridyl disulfide) [20, 21] as suggested here.

13. In young seedlings tissue penetration by the calibration agents suggested here has been found unproblematic. This is likely to differ for other tissues and requires optimization.
14. Based on the calibration and the midpoint redox potential, pK_a and K_d (and Hill coefficient) of the sensor, respectively, an absolute value of redox potential, pH, or calcium concentration can be calculated. This value will not only depend on accurate calibration values, but also on additional parameters. For instance, the redox potential depends on the local pH environment, which needs measurement or estimation. In addition an assumption has to be made that the midpoint potential of the sensor does not differ between in vitro and in vivo conditions. While this is a reasonable assumption for a lot of fluorescent protein sensors, unexpected behavior in a complex in vivo situation can not be fully ruled out. Nevertheless a relative comparison between samples is possible without further transformation of the ratio values and avoids potential calibration-related artifacts.

Acknowledgement

M.S. was supported by the Deutsche Forschungsgemeinschaft through the Emmy Noether Programme (SCHW1719/1-1).

References

1. Baradaran R, Berrisford JM, Minhas GS et al (2013) Crystal structure of the entire respiratory complex I. Nature 494:443–448
2. Schwarzländer M, Finkemeier I (2013) Mitochondrial energy and redox signaling in plants. Antioxid Redox Signal 18:2122–2144
3. Schwarzländer M, Fricker MD, Sweetlove LJ (2009) Monitoring the in vivo redox state of plant mitochondria: effect of respiratory inhibitors, abiotic stress and assessment of recovery from oxidative challenge. Biochim Biophys Acta 1787:468–475
4. Poburko D, Santo-Domingo J, Demaurex N (2011) Dynamic regulation of the mitochondrial proton gradient during cytosolic calcium elevations. J Biol Chem 286:11672–11684
5. Loro G, Drago I, Pozzan T et al (2012) Targeting of Cameleons to various subcellular compartments reveals a strict cytoplasmic/mitochondrial Ca^{2+} handling relationship in plant cells. Plant J 71:1–13
6. Imamura H, Nhat KP, Togawa H et al (2009) Visualization of ATP levels inside single living cells with fluorescence resonance energy transfer-based genetically encoded indicators. Proc Natl Acad Sci U S A 106:15651–15656
7. Albrecht SC, Sobotta MC, Bausewein D et al (2014) Redesign of genetically encoded biosensors for monitoring mitochondrial redox status in a broad range of model eukaryotes. J Biomol Screen 19:379–386
8. Schwarzländer M, Logan DC, Fricker MD et al (2011) The circularly permuted yellow fluorescent protein cpYFP that has been used as a superoxide probe is highly responsive to pH but not superoxide in mitochondria: implications

for the existence of superoxide 'flashes'. Biochem J 437:381–387

9. Behera S, Krebs M, Loro G et al (2013) Ca^{2+} imaging in plants using genetically encoded Yellow Cameleon Ca^{2+} indicators. Cold Spring Harb Protoc 2013:700–703
10. Schwarzländer M, Logan DC, Johnston IG et al (2012) Pulsing of membrane potential in individual mitochondria: a stress-induced mechanism to regulate respiratory bioenergetics in Arabidopsis. Plant Cell 24:1188–1201
11. Loro G, Costa A (2013) Imaging of mitochondrial and nuclear Ca^{2+} dynamics in Arabidopsis roots. Cold Spring Harb Protoc 2013:781–785
12. Costa A, Candeo A, Fieramonti L et al (2013) Calcium dynamics in root cells of *Arabidopsis thaliana* visualized with selective plane illumination microscopy. PLoS One 8:e75646
13. Schwarzländer M, Fricker MD, Müller C et al (2008) Confocal imaging of glutathione redox potential in living plant cells. J Microsc 231: 299–316
14. Logan DC, Knight MR (2003) Mitochondrial and cytosolic calcium dynamics are differentially regulated in plants. Plant Physiol 133:21–24
15. Gutscher M, Pauleau AL, Marty L et al (2008) Real-time imaging of the intracellular glutathione redox potential. Nat Methods 5:553–559
16. Logan DC, Leaver CJ (2000) Mitochondria-targeted GFP highlights the heterogeneity of mitochondrial shape, size and movement within living plant cells. J Exp Bot 51: 865–871
17. Fricker MD, May M, Meyer AJ et al (2000) Measurement of glutathione levels in intact roots of Arabidopsis. J Microsc 198:162–173
18. Zechmann B, Mauch F, Sticher L et al (2008) Subcellular immunocytochemical analysis detects the highest concentrations of glutathione in mitochondria and not in plastids. J Exp Bot 59:4017–4027
19. Marty L, Siala W, Schwarzländer M et al (2009) The NADPH-dependent thioredoxin system constitutes a functional backup for cytosolic glutathione reductase in Arabidopsis. Proc Natl Acad Sci U S A 106:9109–9114
20. Dooley CT, Dore TM, Hanson GT et al (2004) Imaging dynamic redox changes in mammalian cells with green fluorescent protein indicators. J Biol Chem 279:22284–22293
21. Ostergaard H, Tachibana C, Winther JR (2004) Monitoring disulfide bond formation in the eukaryotic cytosol. J Cell Biol 166: 337–345
22. Meyer AJ, Brach T, Marty L et al (2007) Redox-sensitive GFP in *Arabidopsis thaliana* is a quantitative biosensor for the redox potential of the cellular glutathione redox buffer. Plant J 52:973–986
23. Nagai T, Sawano A, Park ES et al (2001) Circularly permuted green fluorescent proteins engineered to sense Ca^{2+}. Proc Natl Acad Sci U S A 98:3197–3202
24. Wang W, Fang H, Groom L et al (2008) Superoxide flashes in single mitochondria. Cell 134:279–290
25. Nagai T, Yamada S, Tominaga T et al (2004) Expanded dynamic range of fluorescent indicators for Ca^{2+} by circularly permuted yellow fluorescent proteins. Proc Natl Acad Sci U S A 101:10554–10559
26. Filippin L, Abad MC, Gastaldello S et al (2005) Improved strategies for the delivery of GFP-based Ca^{2+} sensors into the mitochondrial matrix. Cell Calcium 37:129–136
27. Schwarzländer M, Wagner S, Ermakova YG et al (2014) The 'mitoflash' probe cpYFP does not respond to superoxide. Nature 514(7523):E12–E14. doi:10.1038/nature13858

Chapter 18

In Planta Analysis of Leaf Mitochondrial Superoxide and Nitric Oxide

Marina Cvetkovska and Greg C. Vanlerberghe

Abstract

Superoxide (O_2^-) and nitric oxide (NO) are produced within plant mitochondria and may have signaling functions within the cell. Here we describe semiquantitative fluorescence imaging-based approaches to estimate the mitochondrial amount of these reactive and short-lived species within intact leaf tissue. We also outline a biochemical method using oxyhemoglobin to measure NO within a whole leaf tissue extract. This quantitative method, while not specifically evaluating mitochondrial localized NO, does nonetheless provide another independent measure of NO that can be useful.

Key words DAF-FM, Fluorescence confocal microscopy, Leaf tissue, Mitochondria, MitoSOX, Nitric oxide (NO), Oxyhemoglobin, Superoxide (O_2^-)

1 Introduction

A secondary consequence of plant mitochondrial electron transport chain (ETC) activity is the leakage of single electrons to O_2, producing the superoxide radical anion (O_2^-). This reactive oxygen species (ROS) may then be converted to other ROS such as H_2O_2 and the hydroxyl radical [1]. There is accumulating evidence that plant mitochondria are also a source of reactive nitrogen species (RNS) [2]. For example, electron leakage from the ETC to nitrite can produce nitric oxide (NO). NO may then react with O_2^-, producing another RNS, peroxynitrite.

It seems that plant cells can use mitochondrial ROS and RNS as signaling molecules to control diverse plant processes [3–5]. However, there are major challenges to studying these signaling functions. Methods are required to evaluate the concentration and subcellular localization of these short-lived and reactive species. Further, methods are required that better distinguish between the different specific species of ROS and RNS within the cell. Further, the investigator must strive to maintain physiological conditions as much as possible during such measurements. For example, while

James Whelan and Monika W. Murcha (eds.), *Plant Mitochondria: Methods and Protocols*, Methods in Molecular Biology, vol. 1305, DOI 10.1007/978-1-4939-2639-8_18,

isolated mitochondria have been instrumental in determining the general mitochondrial metabolic conditions that promote ROS generation by the ETC [1], they would not be an appropriate system to elucidate a broader signaling function of these ROS within the intact cell or tissue and in response to particular internal or external (environmental) conditions.

In the case of mitochondria, O_2^- and NO are species of particular interest since these are the ROS and RNS that are immediate by-products of ETC activity. Since NO is volatile, methods for its detection and quantification can be divided into those that attempt to directly measure the dissolved *in planta* tissue concentration of NO and those that attempt to indirectly estimate tissue concentration by measuring the NO being released to the atmosphere [6]. Classic early experiments that demonstrated the presence and biological significance of NO in plant tissues made use of an oxyhemoglobin-based biochemical assay to measure the NO [7, 8].

The concentrations of NO and O_2^- in intact cells and tissues can be evaluated using cell-permeable small-molecule probes, combined with live cell imaging by fluorescence microscopy [9, 10]. Compartment-specific O_2^- probes such as the mitochondrion-localizing fluorescent probe MitoSOX (Invitrogen), provide a means to directly establish the local concentration of this ROS [11]. Such an analysis is aided by the inability of O_2^- to readily cross membranes, hence minimizing its potential to relocate elsewhere following generation within the mitochondrion. We provide below a protocol to assess mitochondrial O_2^- in the mesophyll cells of near-intact tobacco leaf (lower epidermis removed) using MitoSOX. Unlike O_2^-, NO readily crosses biological membranes, complicating efforts to understand its localized concentration, as well as its site(s) of synthesis [2]. We provide below two methods to examine NO in tobacco leaf. An oxyhemoglobin-based biochemical assay provides a direct *in planta* measure of total NO in a leaf homogenate. Meanwhile, the cell-permeable small-molecule probe DAF-FM (Invitrogen) [12] combined with fluorescence confocal microscopy provides an independent measure of NO concentration in the near-intact leaf. In this case, double-labeling experiments utilizing DAF-FM and a mitochondrion-localizing fluorescent probe such as MitoTracker (Invitrogen), followed by colocalization analyses of their fluorescent signals, provide one means to evaluate the local (mitochondrial) concentration of NO.

2 Materials

2.1 Reagents and Equipment for Fluorescence Imaging of O_2^- and NO

1. MitoSOX Red mitochondrial superoxide indicator (Life Technologies, Invitrogen #M36008) is stored at –20 °C as a desiccated stock and protected from light. A 5 mM stock solution is made by dissolving the reagent in dimethyl sulfoxide

(DMSO) (*see* **Note 1**). A working solution (3 μM in distilled water) is prepared fresh on the day of use and kept in the dark.

2. 4-Amino-5-methylamino-2′7′-difluorofluorescein diacetate (DAF-FM diacetate, Invitrogen #D23844) is stored at –20 °C as a desiccated stock and protected from light. A 5 mM stock solution is made by dissolving the reagent in DMSO (*see* **Note 1**). A working solution [10 μM in a DAF-FM loading and wash buffer (10 mM KH_2PO_4, pH 7.4)] is prepared fresh on the day of use and kept in the dark.
3. MitoTracker Red (Invitrogen #M22425) and MitoTracker Green (Invitrogen #M7514) are stored at –20 °C as desiccated stocks and protected from light. A 1 mM stock of each is prepared by adding DMSO (*see* **Note 1**). When using MitoTracker Green in double-labeling experiments with MitoSOX Red, a working solution of MitoTracker Green (0.35 μM in distilled water) is prepared fresh on the day of use and kept in the dark. When using MitoTracker Red in double-labeling experiments with DAF-FM diacetate, a working solution of MitoTracker Red (0.35 μM in 10 mM KH_2PO_4, pH 7.4) is prepared fresh on the day of use and kept in the dark.
4. Standard microscope slides and coverslips.
5. Flat-end tweezers and scalpel blades.
6. Sealing grease: We use Dow Corning high-vacuum silicone grease (Sigma-Aldrich, St. Louis, MO, USA).
7. Confocal laser scanning microscope with appropriate filter combinations: We use an LSM510 Meta confocal microscope (Carl Zeiss, Oberkochen, Germany).
8. Software for image processing and analysis: We use ImageJ (open source) with the JACoP plug-in for colocalization analyses.
9. The cell-permeable O_2^- scavenger superoxide dismutase-polyethylene glycol (SOD-PEG) (Sigma-Aldrich #S9549), the cell-permeating NO scavenger 2-(4-carboxyphenyl)-4,4,5,5-tetramethylimidazoline-1-oxyl-3-oxide (cPTIO) (Sigma-Aldrich #C221), the NO donor sodium nitroprusside (SNP) (Sigma-Aldrich #S0501), and the mitochondrial Complex III inhibitor antimycin A (Sigma-Aldrich #A8674).

2.2 Reagents and Equipment for NO Quantification Using Oxyhemoglobin

1. Hemoglobin: We use lyophilized hemoglobin from bovine blood (Sigma-Aldrich #H2500).
2. Tris buffer (50 mM Tris, pH 7.0).
3. Sodium hydrosulfite ($Na_2S_2O_4$).
4. Sephadex G-25 column: We use prepackaged disposable PD-10 desalting columns (GE Healthcare, Cooksville, ON, Canada).

5. Source of pure O_2.
6. Extraction buffer: 100 mM KH_2PO_4 pH 7.0, 0.6 % (w/v) insoluble PVP (added after autoclaving).
7. Powdered activated carbon.
8. Catalase: We use catalase from bovine liver supplied as an aqueous solution, >30,000 U/mg protein (Sigma-Aldrich #C3155).
9. Superoxide dismutase (SOD): We use SOD from bovine erythrocytes, supplied as a lyophilized powder, 2,500–7,000 U/mg protein (Sigma-Aldrich #S2515).
10. Spectrophotometer to measure absorbance at 401 and 421 nm.

3 Methods

All of the methods have been optimized for use with tobacco plants (*Nicotiana tabacum* L. cv Petit Havana SR1). The plants are grown in controlled-environment growth chambers (Model PGR-15, Conviron, Winnipeg, Canada) with a 16-h photoperiod, a temperature of 28/22 °C (light/dark), a relative humidity of 60 %, and at an irradiance of 130–150 μmol/m^2/s. Examples of published work utilizing the methods can be found elsewhere [13–16].

3.1 Detection of O_2^- and NO Using Fluorescence Confocal Microscopy

1. Obtain fresh leaf tissue and use flat-end tweezers to gently peel off the lower epidermis.
2. Using a scalpel blade, cut a section of leaf (~5-mm square) from the tissue lacking lower epidermis and place it in one of the working solutions of probe (as described in Subheading 2.1, **items 1–3**). Ensure that the side of the leaf lacking lower epidermis is in contact with the solution (*see* **Note 2**). For small samples, it is convenient to use 0.5 mL of solution in a 2-mL microcentrifuge tube, while for larger samples, a 5 mL solution in a small dish works fine also.
3. Incubate the samples for 30 min in the dark at room temperature (RT) to allow for loading of the probe into the tissue.
4. Transfer the samples from the working solutions to the same solution but without probe (distilled water or 10 mM KH_2PO_4, pH 7.4) to wash the sample. Several washes may be necessary to remove probe that has not been loaded into cells (*see* **Note 3**). Protect the sample from light during these washes.
5. Apply a uniformly thin layer of sealing grease to the edges of a coverslip and add several drops of the washing solution directly on the coverslip. Place the leaf sections in this solution, ensuring that the side without epidermis is facing down against the coverslip. Carefully place a microscope slide atop the coverslip while ensuring that no air bubbles become trapped in the sample.

6. The prepared slides should be protected from light and viewed under the microscope as soon as possible.
7. The microscope should be adjusted to the appropriate excitation/emission settings (MitoSOX Red, 488/585–615 nm; MitoTracker Green, 488/500–530 nm; MitoTracker Red, 543/585–615 nm; DAF-FM diacetate, 488/500–530 nm) (*see* **Note 4**). A recent study suggests that the excitation/emission settings for MitoSOX may be further optimized [17]. However, regardless of the settings used, it is critical to verify their suitability through a series of control experiments (*see* **steps 8** and **9** below).
8. It is critical to perform a series of controls prior to starting a new experiment in order to confirm the validity of the images being obtained. To ensure no confounding effects due to sample autofluorescence, obtain images of unlabeled plant tissue (prepared as above but without probe) using the same acquisition settings and longest exposure times being used for labeled samples. Chlorophyll autofluorescence should be detected at higher wavelengths (>630 nm) but not in the 585–615 and 500–530 nm range. Further, examine the fluorescence of a cell-free mixture of probe and loading/washing solution over an extended period of time to confirm no rise in fluorescence signal resulting from auto-oxidation of probe. Finally, in cases where the tissue is being double-labeled with two probes, establish that there is no significant bleed-through and cross talk between channels using a single-labeled experiment.
9. It is critical that additional positive and negative controls are used to ensure that the signals resulting from MitoSOX Red and DAF-FM labeling are due to the presence of O_2^- and NO, respectively, in the sample tissue. This is most effectively confirmed by preincubating leaf segments (with lower epidermis removed) with various donors, inducers, and scavengers of O_2^- and NO. In our experiments, we treated leaf segments with antimycin A (10 μM, 1 h, RT), which is known to increase the production of mitochondrial O_2^-, prior to loading with MitoSOX Red. This treatment dramatically elevated MitoSOX Red fluorescence. Further, a co-treatment (1 h, RT) with both antimycin A and SOD-PEG (100 U/mL) strongly reduced the subsequent MitoSOX Red signal. Alternatively, pretreatment with SNP (2 mM, 1 h, RT, 130 μmol/m^2/s) dramatically increased subsequent DAF-FM fluorescence, while a co-treatment (1 h, RT, 130 μmol/m^2/s) with both SNP and cPTIO (200 μM) could strongly reduce the subsequent DAF-FM signal.
10. Establish clear criteria for selecting cells for image acquisition and subsequent analysis. Special care should be taken to follow these criteria throughout the experiment as the

mesophyll cells are irregular in shape. Confirm that the sample has similar fluorescence signal throughout by observing many fields of view.

11. All images within an experiment should be acquired using the same microscope settings. It is necessary to take separate images in all channels in double-labeling experiments.
12. Using a choice of image analysis software, overlay images taken in different channels. For example, overlay MitoTracker Red fluorescence images collected in the red channel with DAF-FM fluorescence images collected in the green channel (*see* **Note 5**).
13. Threshold each channel to differentiate between the presence of the fluorophore and background fluorescence. Image quality is critical to successfully establish the spatial relationship between two fluorophores in double-labeling experiments, so it is important to eliminate noise (background fluorescence, reflection from cell walls, low-level autofluorescence, etc.) from the images.
14. Colocalization between two fluorophores (for example, colocalization of MitoTracker Red and DAF-FM) can be evaluated using a variety of methods and coefficients, depending on the software used. We have used the Pearson's coefficient, where a value of 1 corresponds to absolute colocalization of the two fluorophores, a value of 0 indicates random localization, and a value of −1 indicates an absolute mutual exclusion of the two signals. We have also used the Manders' coefficient, which represents the fraction of red pixels in the one fluorescence channel that overlap with green pixels in the second fluorescence channel. This coefficient will range from 0 (random localization) to 1 (complete colocalization). We recommend using at least two methods of colocalization analysis when examining the relationship between two fluorophores.

3.2 Detection of NO Using the Oxyhemoglobin Method

1. The method was adapted from that described to measure NO in animal tissues [18].
2. Condition the Sephadex G-25 column by filling the column with Tris buffer and allowing the solution to penetrate the packing bed fully. The conditioning procedure should be repeated at least four times and the flow-through discarded. The column should be used immediately.
3. On the day of use, gently dissolve 25 mg of hemoglobin in 2 mL of Tris buffer in a 4 mL glass vial. When fully dissolved, the solution should be dark red or brown.
4. Add ~4 mg of sodium hydrosulfite and swirl gently. The solution should turn dark purple.

5. Cover the open vial with Parafilm and blow a gentle stream of O_2 into the vial for 5–10 min with gentle shaking. The color of the solution should change to bright red indicating a change from methemoglobin to oxyhemoglobin (*see* **Note 6**).
6. Add ~1.5 mL of the oxyhemoglobin solution directly to the Sephadex G-25 column and wait until the solution penetrates the packing bed completely. Then add ~1 mL of Tris buffer.
7. Elute the sample with ~4 mL of Tris buffer. Collect the eluate in a glass vial and then close the vial with a cap and intact septum. Care should be taken to avoid the leading and trailing ends of the eluate (*see* **Note 7**). The eluate (oxyhemoglobin stock solution) should now be kept on ice and in the dark. A syringe through the septum should be used to sample from the stock.
8. Determine the concentration of the stock oxyhemoglobin by diluting an aliquot 100× in Tris buffer and measuring its absorbance at 415 nm. Calculate the concentration using the extinction coefficient of 131/mM/cm. For best results, the solution should be used as soon as possible.
9. Grind leaf tissue under liquid nitrogen.
10. Transfer 150 mg of leaf powder to a 1.5-mL microcentrifuge tube. Add 1 mL of extraction buffer and vortex thoroughly (30 s).
11. Add powdered activated carbon (~100 mg) and vortex again (30 s).
12. Centrifuge the sample (11,000 × *g*, 10 min, 4 °C).
13. Remove the supernatant to a fresh tube and repeat **steps 10** and **11** until the sample is clear (i.e., no green).
14. Transfer an aliquot of the clear supernatant (~700 uL) to a fresh tube. To each sample add 100 U of catalase and 50 U of SOD. Briefly mix the sample and incubate at RT for 5 min (*see* **Note 8**).
15. Add 10 μM of the freshly prepared oxyhemoglobin to the sample, briefly vortex the sample, and incubate at RT for 5 min.
16. Measure the absorbance of the sample at 401 nm and 421 nm. Calculate the NO concentration by subtracting the absorbance at 421 nm from the absorbance at 401 nm, and using the extinction coefficient of 77/mM/cm (*see* **Note 9**).

4 Notes

1. MitoSOX Red and DAF-FM stock solutions in DMSO can be stored at −20 °C in the dark for up to 1 month. MitoTracker stock solutions in DMSO are stable for up to 3 months when stored at −20 °C in the dark.

2. For good image quality, it is critical not to damage the mesophyll layer during these steps. Be careful not to touch this layer with tweezers or a scalpel blade at any time.
3. The number and duration of the washes should be determined empirically. The goal of these washes is to obtain a sample that shows clear and defined fluorescence signals, by limiting the amount of nonspecific fluorescence arising due to the presence of excess probe. The majority of our experiments did not require extensive washing.
4. The testing and use of appropriate excitation/emission combinations is critical due to the autofluorescence inherent in plant tissues. The detection range for each probe should be as narrow as possible in order to avoid collecting fluorescence signal that is not due to the probe.
5. If the experiment involves the acquisition of z-stacks, make sure that you are analyzing a single image layer at a time. This is as opposed to analyzing a maximum intensity projection of the entire stack which might not reflect spatial relationships between the two fluorophores.
6. The conversion from methemoglobin to oxyhemoglobin can also be achieved with a stream of air (rather than pure O_2) but this procedure takes a longer time and does not give as high oxyhemoglobin yields.
7. The hemoglobin solution should be desalted quickly to avoid conversion of oxyhemoglobin to methemoglobin. After passing through the Sephadex G-25 column, the color of the solution should remain bright red. A stream of O_2 can be used if the solution begins to turn brown.
8. Catalase and SOD are added to scavenge H_2O_2 and O_2^-, which could otherwise react with the oxyhemoglobin.
9. A test can be performed to check the sensitivity of the assay. SNP can be dissolved in 10 mM KH_2PO_4 (pH 7.4) to different final concentrations (0.5, 1, 2.5, 5, and 10 mM). These samples are incubated under light (400 μmol/m^2/s) for 1 h at RT to facilitate NO release. Under these conditions, 1 mM SNP releases ~5 μM NO [19]. The samples are then treated with catalase and SOD prior to the addition of 10 μM oxyhemoglobin and the measurement of NO concentration (as described above). This test is useful to estimate the range of plant NO concentrations that the assay might be expected to measure. If the NO concentrations in plant samples do not fall within this measurable range, then a possible solution is to empirically adjust the oxyhemoglobin concentration being used.

References

1. Møller IM (2001) Plant mitochondria and oxidative stress: electron transport, NADPH turnover, and metabolism of reactive oxygen species. Annu Rev Plant Physiol Plant Mol Biol 52:561–591
2. Gupta KJ, Fernie AR, Kaiser WM et al (2010) On the origins of nitric oxide. Trends Plant Sci 16:160–168
3. Gleason C, Huang S, Thatcher LF et al (2011) Mitochondrial complex II has a key role in mitochondrial-derived reactive oxygen species influence on plant stress gene regulation and defense. Proc Natl Acad Sci U S A 108: 10768–10773
4. Cvetkovska M, Alber NA, Vanlerberghe GC (2013) The signaling role of a mitochondrial superoxide burst during stress. Plant Signal Behav 8:e22749
5. Schwarzländer M, Finkemeier I (2013) Mitochondrial energy and redox signaling in plants. Antioxid Redox Signal 18: 2122–2144
6. Mur LAJ, Mandon J, Cristescu SM et al (2011) Methods of nitric oxide detection in plants: a commentary. Plant Sci 181:509–519
7. Delledonne M, Xia YJ, Dixon C et al (1998) Nitric oxide functions as a signal in plant disease resistance. Nature 394:585–588
8. Clarke A, Desikan R, Hurst RD et al (2000) NO way back: nitric oxide and programmed cell death in *Arabidopsis thaliana* suspension cells. Plant J 24:667–677
9. Sandalio LM, Rodriguez-Serrano M, Romero-Puertas MC et al (2008) Imaging of reactive oxygen species *in vivo* in plant tissues. Method Enzymol 440:397–409
10. Swanson SJ, Choi W-G, Chanoca A et al (2011) In vivo imaging of Ca^{2+}, pH, and reactive oxygen species using fluorescent probes in plants. Annu Rev Plant Biol 62:273–297
11. Robinson KM, Janes MS, Beckman JS (2008) The selective detection of mitochondrial superoxide by live cell imaging. Nat Protoc 3:941–947
12. Kojima H, Urano Y, Kikuchi K et al (1999) Fluorescent indicators for imaging nitric oxide production. Angew Chem Int Ed 38:3209–3321
13. Cvetkovska M, Vanlerberghe GC (2012) Alternative oxidase modulates leaf mitochondrial concentrations of superoxide and nitric oxide. New Phytol 195:32–39
14. Cvetkovska M, Vanlerberghe GC (2012) Coordination of a mitochondrial superoxide burst during the hypersensitive response to bacterial pathogen in *Nicotiana tabacum*. Plant Cell Environ 35:1121–1136
15. Cvetkovska M, Vanlerberghe GC (2013) Alternative oxidase impacts the plant response to biotic stress by influencing the mitochondrial generation of reactive oxygen species. Plant Cell Environ 36:721–732
16. Cvetkovska M, Dahal K, Alber NA, Jin C, Cheung M, Vanlerberghe GC (2014) Knockdown of mitochondrial alternative oxidase induces the "stress state" of signaling molecule pools in *Nicotiana tabacum*, with implications for stomatal function. New Phytol 203(2):449–461
17. Nazarewicz RR, Bikineyeva A, Dikalov SI (2013) Rapid and specific measurements of superoxide using fluorescence spectroscopy. J Biomol Screen 18:498–503
18. Murphy ME, Noack E (1994) Nitric oxide assay using hemoglobin method. Methods Enzymol 233:240–250
19. Pasqualini S, Meier S, Gehring C et al (2009) Ozone and nitric oxide induce cGMP-dependent and -independent transcription of defense genes in tobacco. New Phytol 181: 860–870

Chapter 19

Databases and Informatics Resources for Analysis of Plant Mitochondria

Reena Narsai

Abstract

As more omics data is generated from various plant species, it is becoming increasingly possible to carry out a range of in silico analyses to gain insight into mitochondrial function in plants. From the use of software tools for DNA motif analyses and transcript expression visualization to proteomic and subcellular localization resources, it is possible to carry out significant in silico analyses that are highly informative to researchers and can help to guide experimental design for further mitochondrial study. Databases specific to plant mitochondrial analyses have been developed in recent years, revealing mitochondria-specific information. This chapter outlines the databases and informatics resources that are useful for plant mitochondrial studies, with specific examples presented to indicate how these resources can be used to gain insight into plant mitochondrial function(s).

Key words Mitochondria, Database, In silico, Subcellular localization, Gene expression, Co-expression

1 Introduction

The compartmentalization of the cell, including the development of the mitochondria, has enabled specialized functions to be carried out at specific locations. Mitochondria represent a major site for energy production in the form of ATP, via the respiratory pathway. In addition to this, mitochondria are also the site for various other functions including vitamin biosynthesis, photorespiration, transcription, RNA editing, and translation of mitochondrial encoded genes in plants. To date, the most well-characterized plant mitochondrial proteome exists for Arabidopsis (*Arabidopsis thaliana*), with ~1,000 mitochondrial proteins identified to date [1, 2], representing only half of the approximate number of proteins predicted to be mitochondrial on the basis of the aforementioned range of mitochondrial functions. However, with increasing characterization of biochemical pathways in mitochondria, it has become possible to carry out various predictions on the basis of the sequence and function data that has been gathered to date.

James Whelan and Monika W. Murcha (eds.), *Plant Mitochondria: Methods and Protocols*, Methods in Molecular Biology, vol. 1305, DOI 10.1007/978-1-4939-2639-8_19,

As more omics data is generated across different plant species, specific software tools are being developed to carry out various in silico analyses. Many studies have shown the efficient use of computational tools to significantly increase our understanding of mitochondria, as well as other cellular functions [3, 4]. The results from the use of such tools can also be helpful in guiding or directing projects by providing information at the DNA, RNA, and proteins levels. For example, tools and databases for the prediction of protein subcellular location can be useful in projects involving experimental confirmation of protein subcellular localization or even in guiding predicted protein function given predicted subcellular location [5, 6]. Additionally, carrying out phylogenetic analyses using specialized software has been useful in revealing relationships between gene/protein family members [5, 6]. Similarly, revealing patterns of co-expression can be insightful for understanding genes encoding proteins of unknown function [3]. These represent just a few examples of how software tools can be used to generate knowledge and contribute to more efficient experimental design. When used properly and in combination, these also present a powerful way to gain insight into mitochondrial function.

In this chapter, databases and tools designed for analyses at the DNA, RNA, and protein levels are shown and it is demonstrated how these can be combined to maximize our understanding of possible mitochondrial function(s), even for genes/proteins with unknown function. While many tools are specific to Arabidopsis, a range of non-species-specific resources are also presented here, as well as tools for determining orthology between different species. Various databases and informatics resources for analyzing plant mitochondria are presented, with specific examples given to reveal how these can be used to advance knowledge of mitochondrial function in plants.

2 Materials

2.1 Software Tools and Databases

For all of the tools and informatics resources presented, computer access and an Internet connection are typically the only requirements (*see* **Note 1**). The resources described in this chapter represent several commonly used in silico analysis methods for examining the regulation and function of plant mitochondria. Table 1 lists all the informatics resources cited, including databases for extracting DNA, RNA, and protein sequence data [such as TAIR [7], RGAP [8], Gramene [9]]; resources for RNA analyses including motif, co-expression, and microRNA (miRNA) analyses [such as Genevestigator [10], BAR [11], Rice DB [12], ATTED-II [13], AthaMap [14], AGRIS [15], MEME SUITE [16], PlantRNA [17], miRBase [18]), RNAhybrid [19], sRNA2 [20] and OrganelleGenomeDRAW [21]]; tools for protein analyses

Table 1
Databases and informatics resources for analysis of plant mitochondria

Database	Site address
Sequence retrieval	
[7] *TAIR*: the Arabidopsis information resource	www.arabidopsis.org
[8] *RGAP*: rice genome annotation project	http://rice.plantbiology.msu.edu/
[9] *Gramene*: a comparative resource for plants	http://www.gramene.org
DNA/RNA expression analysis	
[10] *Genevestigator*: microarray database and analysis toolbox	https://www.genevestigator.com/gv/
[11] *The botany array resource*: expression angling, and promoter analyses	http://bbc.botany.utoronto.ca
[12] *Rice DB*: an Oryza information portal	http://ricedb.plantenergy.uwa.edu.au/
[13] *ATTED-II*: identify co-expressed genes and *cis-elements*	http://atted.jp/
[14] *AthaMap*: in silico transcription factor-binding site resource in Arabidopsis	http://www.athamap.de
[15] *AGRIS*: Arabidopsis gene regulatory information server	http://arabidopsis.med.ohio-state.edu
[16] *MEME SUITE*: tools for motif discovery and searching	http://meme.nbcr.net
[17] *PlantRNA*: a database for tRNAs of photosynthetic eukaryotes	http://plantrna.ibmp.cnrs.fr/
[18] *miRBase*: annotating high-confidence microRNAs using deep seq. data	http://www.mirbase.org/
[19] *RNAhybrid*: microRNA target prediction	http://bibiserv.techfak.uni-bielefeld.de/rnahybrid/
[20] *sRNA 2*: small RNA database	http://mpss.udel.edu/rice_sRNA2/
[21] *OrganellarGenomeDRAW*: maps of plastid and mitochondrial genomes	http://ogdraw.mpimp-golm.mpg.de/
Protein analysis	
[22] *ATP*: ambiguous targeting prediction	http://www.cosmoss.org/bm/ATP
[23] *Mitoprot*: mitochondrial location predictor	http://ihg.gsf.de/ihg/mitoprot.html
[24] *Predotar*: a tool for screening proteomes for N-terminal targeting sequences	https://urgi.versailles.inra.fr/predotar/predotar.html
[25] *TargetP*: subcellular location predictor	http://www.cbs.dtu.dk/services/TargetP/
[2] *SUBA3*: SUBcellular location of proteins in Arabidopsis	http://www.suba.bcs.uwa.edu.au
[26] *MitoP2*: an integrated database for Mitochondrial proteins	http://www.mitop2.de

(continued)

Table 1
(continued)

Database	Site address
[12] *Rice DB*: an Oryza information portal	http://ricedb.plantenergy.uwa.edu.au/
[27, 28] *GelMap*: the protein complex proteome of Arabidopsis mitochondria	https://gelmap.de/arabidopsis_mito
[29] *GelMap*: Mito. complex I of Arabidopsis: subunits resolved by 3D PAGE	https://gelmap.de/arabidopsis-3d-complex-i/
[30] *GelMap*: the mitochondrial complexome of *Medicago truncatula*	https://gelmap.de/medicago/
[31] *MPIC*: the mitochondrial protein import component database	http://www.plantenergy.uwa.edu.au/applications/mpic/
[32] *Expasy*: compute pI/Mw	http://web.expasy.org/compute_pi/
[33] *InterPro*: protein sequence analysis and classification	https://www.ebi.ac.uk/interpro/
Orthology	
[34] *BLAST*: basic local alignment search tool	http://blast.ncbi.nlm.nih.gov/Blast.cgi
[35] *InParanoid 7*: new algorithms and tools for eukaryotic orthology analysis	http://InParanoid.sbc.su.se
[36] *OrthoMCL*: assign orthology or cluster proteomes into new orthologue groups	http://orthomcl.org/orthomcl/
[37] *MEGA5*: molecular evolutionary genetics analysis software version 5.0	http://www.megasoftware.net
Microscopy	
[38] *LIPS*: a microscopic image DB of intracellular structures in AT guard cells	hasezawa.ib.k.u-tokyo.ac.jp/lips/images.html
[39] *PODB3*: the plant organelles database 3: integrating electron micrographs	http://podb.nibb.ac.jp/Organellome/

including subcellular localization determination and identification of putative functional domains [such as ATP [22], Mitoprot [23], Predotar [24], TargetP [25], SUBA3 [2], MitoP2 [26], Rice DB [12], GelMap [27–30], MPIC [31], Compute pI/Mw [32], InterPro [33]]; methods for determining orthology between different species [including BLAST [34], InParanoid 7 [35], OrthoMCL [36], MEGA5 [37]); as well as resources for viewing organelle morphology through microscopy [such as LIPS [38] and PODB3 [39]]. Each of these resources can be accessed via the presented hyperlinks in Table 1. For some of the analyses, there may be other tools able to perform similar tasks (*see* **Note 2**); however, this selection is presented on the basis of their use in previously published studies, particularly those examining plant mitochondria.

3 Methods

3.1 Sequence Data

Most informatics tools (including those listed in Table 1) require sequence data as the input information in order to carry out in silico predictions. These tools often involve the use of an algorithm(s) designed to analyze one or more sequences for putative motifs that may be present in the DNA/protein sequence(s). Thus, the first step of in silico analyses is often the extraction of sequence data. If possible, this should be extracted in FASTA format (*see* **Note 3**). For Arabidopsis, rice (*Oryza sativa*), and several other cereal species, sequence data can be extracted from TAIR [7], RGAP [8] or RAP-DB [40], and Gramene [9], respectively.

3.2 Protein Analyses

When considering mitochondrial function, often researchers work in different areas of specialization from organelle transcriptomics to mitochondrial complex proteomics. For example, after carrying out microarrays or RNA sequencing to examine transcript abundance, it may be useful to determine if a set of genes showing a specific expression pattern are encoding mitochondrial proteins. Alternatively, after carrying out proteomic analyses and identifying proteins on whole-cell extracts, a researcher may also want to determine whether any of the proteins identified are mitochondrial. Thus, the first step of many mitochondrial studies involves confirmation that the proteins of interest are in fact mitochondrial.

3.2.1 Determining Subcellular Localization

Most mitochondrial proteins are nuclear encoded and thus are translated in the cytosol and targeted to the mitochondria [41]. Given that targeting to mitochondria often relies on the presence of specific motifs present in the terminal regions of the protein sequence, it is possible to predict whether a protein is mitochondrial by examining the protein sequence(s) [24, 25]. This forms the basis of most targeting prediction software, such as ATP [22], Mitoprot [23], Predotar [24], and TargetP [25], which have been developed using learning sets of known targeting sequences. Each of these prediction tools (*see* **Note 4**) has a search box, in which a set of protein sequences in FASTA format can be entered, and once this is searched, an output is presented that shows the predicted subcellular localization and a measure of confidence in this prediction. For example, Fig. 1ai illustrates the Predotar output when the rice arginase (LOC_Os04g01590.1) protein sequence is searched, and a confidence score of 0.68 is given for mitochondrial localization, where 1.0 would indicate the highest confidence of mitochondrial localization [24]. While this can be useful as a guide and to shortlist the more likely mitochondrial candidates for experimental analysis [5, 6], it does produce a significant number of false positives, which was observed when all proteins encoded in the rice genome were examined [12].

For species such as Arabidopsis and more recently rice, there are a number of large-scale proteomic studies analyzing isolated mitochondria as well as individual studies involving fluorescent protein targeting [5, 6, 42]. Databases such as SUBA (for Arabidopsis) [2], MitoP2 (also for Arabidopsis) [26], and Rice DB (for rice) [12] have collated this information in parallel to precomputed subcellular localization prediction outputs so that researchers can quickly and easily determine if their protein of interest has been shown to be mitochondrial by both prediction and/or experimental means. For the rice arginase, when this is searched in Rice DB [12], the output in the flat file is shown for this protein indicating the predicted localization based on a number of predictors, as well as the manually collated table showing the experimentally confirmed localization, experimental method [green fluorescent protein (GFP) targeting or organelle isolation and mass spectrometry identification], and publication relevant to this (Fig. 1aii). Note that Rice DB [12] also shows phenotype information (e.g., from mutant studies) for proteins with experimentally confirmed organelle localizations (Fig. 1aii). MitoP2 [26] and Rice DB [12] have also integrated homology searches, displaying the presence of orthologues in other species. For example, a search for many of the mitochondrial import components in Rice DB [12] will reveal these to be predicted to be mitochondrial, with many having no experimental confirmation of a mitochondrial localization. However, clicking on orthology in the Rice DB [12] output will reveal that several of these have close orthologues in Arabidopsis that have been experimentally confirmed to be mitochondrial, with links presented for the relevant publications and SUBA [2]. While these resources are useful, it is essential to confirm subcellular localization for all proteins of interest by experimental means before considering a protein to be mitochondrial (Fig. 1aiii).

Tools and databases like these have proven to be useful in several previous studies, whereby computational predictors were used to examine lists of genes for targeting studies [5, 6], or to confirm that a set of genes showing a specific expression pattern are enriched in genes encoding mitochondrial proteins [3].

3.2.2 *Mitochondria-Specific Databases*

Mitochondrial studies often involve the isolation of plant mitochondria to allow for a more intensive analysis of proteins. For Arabidopsis in particular, various studies have carried out high-resolution analyses on isolated mitochondria, revealing information about the function of individual proteins and protein complexes [28, 43–45]. For some of these studies, this information is housed in databases that allow users to interact with and download data that may be specific to a researcher's protein of interest [28, 31].

For example, the GelMap portal presents the output after mitochondrial isolation and protein separation by two-dimensional

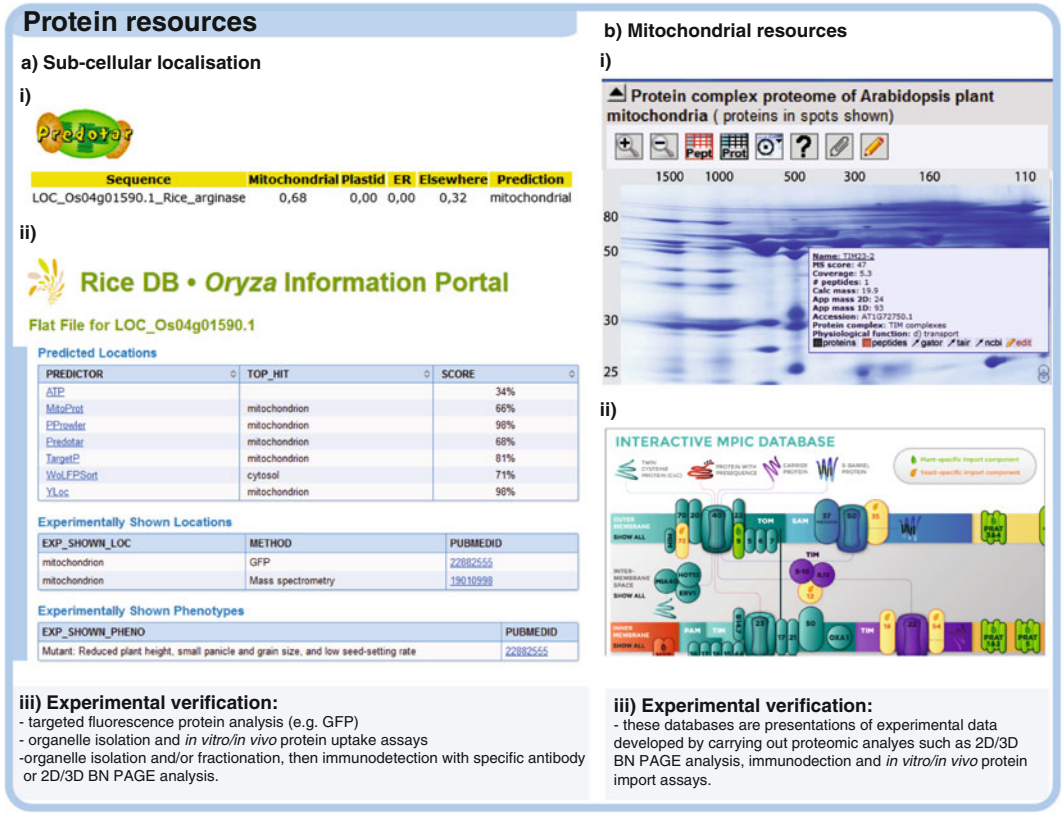

Fig. 1 Schematic representation of the tools and outputs available for in silico protein analyses. (**a**) Subcellular localization tools including the following: (*i*) computational predictors of subcellular localization such as Predotar, output shown for rice arginase after FASTA sequence of this protein (LOC_Os04g01590.1) was searched for predicted localization, and (*ii*) the output after a search in Rice DB, which shows both predicted localization (using several predictors) and manually collated information on experimental determination of localization for the rice arginase. (*iii*) Experimental means of verifying the findings from the tools presented in (*i*) and (*ii*). (**b**) Mitochondrial specific resources such as (*i*) the Arabidopsis mitochondrial proteome GelMap, showing an example of the output for the translocase of the mitochondrial inner membrane TIM23-2 (At1g72750.1), showing the MS score, protein properties, size, subcellular location, physiological function, and association with a complex, where relevant, and (*ii*) the interactive diagram from the Mitochondrial Import Components Database (MPIC) that allows users to click on proteins of interest and view details of protein domains, orthology, expression, and protein properties. (*iii*) Experimental means of verifying the findings from the tools presented in (*i*) and (*ii*)

blue native/sodium dodecyl sulfate-polyacrylamide (2D BN-PAGE) gel electrophoresis, where this is combined with tandem mass spectrometry and the latest software technology to present an interactive portal for researchers to examine their protein(s) of interest within this mitochondrial protein complex proteome (Fig. 2bi) [27–30]. At the GelMap portal [27], it is possible to examine the mitochondrial proteome of Arabidopsis, rice, *Cyclamen persicum*, *Medicago truncatula*, as well as a high-resolution analysis of the mitochondrial respiratory Complex I

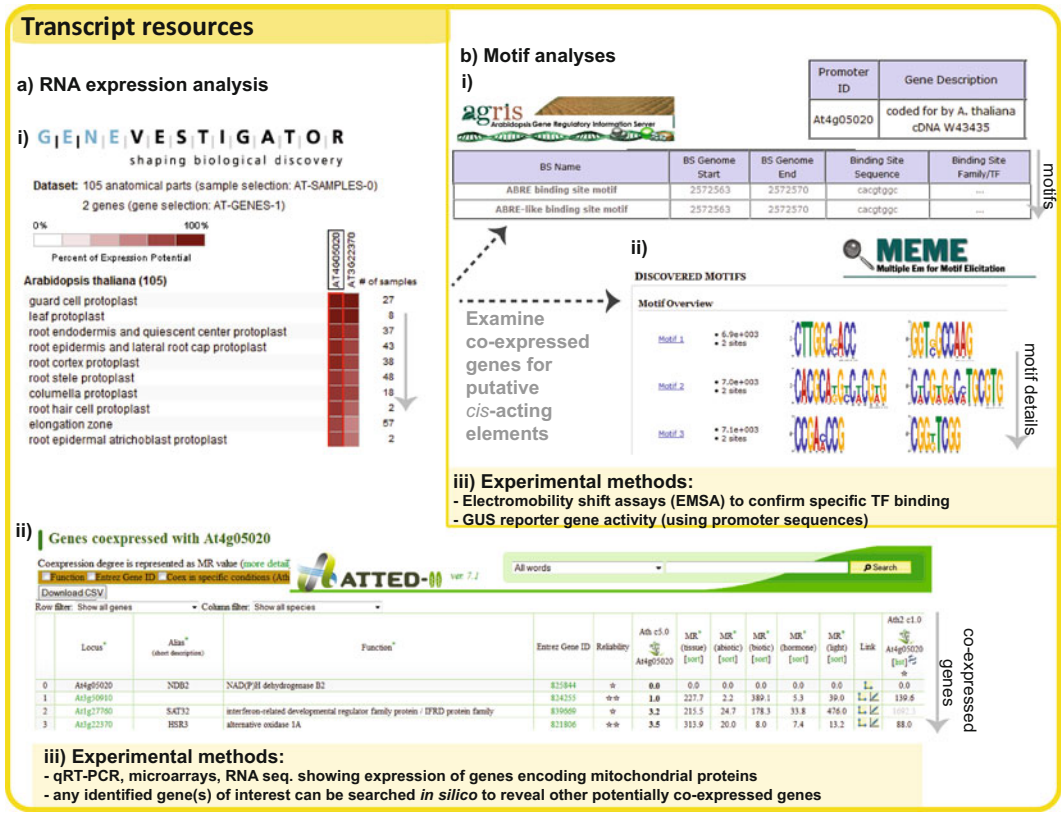

Fig. 2 Schematic representation of the tools and outputs available for in silico transcriptomic analyses. (**a**) RNA expression analysis resources: (*i*) As an example of the visualization tools available for gene expression, the GENEvestigator output is shown for the Arabidopsis genes encoding *NDB2* and *AOX1a*. (*ii*) For co-expression analysis, the ATTED-II output is shown when *NDB2* is searched. Note that *AOX1a* was recognized as one of the top co-expressed genes with *NDB2*. (*iii*) Experimental means of verifying the findings from the tools presented in (*i*) and (*ii*). (**b**) Motif analysis: (*i*) As an example of the tools that search for known *cis*-acting elements in Arabidopsis, the output is shown for two (of the many) motifs returned when the 1 kb upstream sequence of the *NDB2* gene is searched. Note that these motifs are presented as they were also present in the promoter of *AOX1a*. (*ii*) As an example of one of the methods for identifying putative motifs (in any species), the output from the MEME motif tool is also shown. (*iii*) Experimental means of verifying the findings from the tools presented in (*i*) and (*ii*)

from Arabidopsis. This software can be applied to a user-supplied 2D gel image as well, allowing users to contribute to this database as well as make this data more accessible to researchers.

When a GelMap image is opened, the gel image is shown and users can click on the "spots," which may contain one or more proteins, or hover over to view the name(s) of the protein(s) and MS reliability score (Fig. 1bi). Alternatively, clicking on the protein table icon allows users to view details including spot number, protein name, dedicated protein complex, MS reliability score, calculated molecular weight, and TAIR AGI. Figure 1bi shows the GelMap image after clicking on the protein spot for the translocase

of the inner mitochondrial membrane TIM23-2 from the Arabidopsis mitochondrial GelMap [28]. Thus, researchers can gain insight into mitochondrial proteins or mitochondrial protein complexes by using this software. Detailed information into each of the GelMaps can be found in the respective publications linked to each (Table 1) [27–30].

Mitochondrial import components make up a significant number of proteins in the mitochondrial proteome and several studies have revealed the evolution of plant-specific import components, as well as the expansion of gene families for those encoding import components [45]. Thus, a database was recently developed to house information on the plant Mitochondrial Protein Import Components (MPIC) [31]. This searchable database, featuring an interactive diagram, allows users to analyze and examine detailed information on the mitochondrial import components across 24 species (including 15 plant species) (Fig. 1bii). Details including protein properties, such as functional domains, isoelectric point (pI), and molecular weight (Mw), as well as orthology and gene expression can be viewed within MPIC [31], facilitating analysis of mitochondrial import components at an unparalleled level.

It is important to note that the existing mitochondrial GelMaps [27–30] and the MPIC database [31] are resources that house and have reanalyzed experimental information already generated for specific species (Fig. 1biii). Thus, for other species, alternative resources need to be utilized in order to gain an insight into proteins. One of the most extensively used resources is the Expasy Bioinformatics Portal [32], which presents a range of software tools for protein analysis, from domain and secondary structure predictions to prediction of other protein properties such as molecular weight. Similarly, the InterPro database can be used to reveal the presence of putative functional domains within a protein sequence (Table 1) [33]. Most tools at the Expasy Bioinformatics Portal and the InterPro database require the search input to be protein sequence data (in FASTA format). For example, entering protein sequences into the "Compute pI and Mw" tool (Table 1) produces an output that shows the predicted pI and Mw for the input protein sequences. Additionally, if a researcher is working with a relatively newly sequenced plant genome, it is possible to use the "Translate" tool (within the Expasy Bioinformatics Portal) to convert a DNA sequence into the predicted translated protein sequence, which facilitates the use downstream of software that require protein sequence data as input.

3.3 DNA and RNA Analysis

Using the aforementioned protein analysis software/databases, it is possible to generate a list of putative mitochondrial proteins for further analysis. Alternatively, if a researcher is interested in a specific mitochondrial protein complex or set of mitochondrial proteins, it can be useful to consider other factors in addition to

protein subcellular localization, such as the possible co-expression of genes. By analyzing the expression of a set of genes encoding mitochondrial proteins, any similarities in the transcriptomic responses between these genes can be revealed, which would support a hypotheses suggesting that these may function together. For example, it has been shown that the genes encoding the mitochondrial ALTERNATIVE OXIDASE 1A (*AOX1a*) and the internal NADPH dehydrogenase (*NDB2*) in Arabidopsis are co-expressed [46], often showing similarities in their respective transcriptomic responses (*see* **Note 5**). Additionally, examining the expression of a set of putative mitochondrial genes can help to guide experimental design by providing a basis for selection of a particular genes/proteins for further analysis. For example, there are three genes encoding each of the translocases of the mitochondrial inner membrane 17 and 23, respectively, and the genes showing highest expression represent the most abundance protein isoform throughout vegetative development [31, 47]. However, it is important to point out that while this will not always be the case, it does help guide further experiments when a long list of putative mitochondrial proteins are being examined.

To date, many tools have been developed to visualize gene expression. One of the most informative methods is to use the tool that presents a large (or largest) number of expression datasets that have been normalized collectively, taking into account batch differences. Among these, Genevestigator [10], the BAR [11], and Rice DB [12] are all tools that allow users to view expression data by heatmap. A list of gene identifiers can be entered into these, and the expression levels for these genes can be visualized as a heatmap using publically available datasets examining the response to stress and/or over the course of plant development. Figure 2ai shows examples of the top section of a heatmap output using GENEvestigator [10] to examine *NDB2* and *AOX1a* gene expression in Arabidopsis.

Using GENEvestigator [10] or other independent tools, such as the BAR [11] or Rice DB [12], to examine gene expression often reveals patterns of co-expression, whereby a set of genes appear to have similarities in their transcriptomic responses (as shown for *NDB2* and *AOX1a* in Fig. 2ai). Another to comprehensively identify co-expression for rice and Arabidopsis is to enter the identifier for a gene of interest into the search box within the ATTED-II database [13], which would return a list of co-expressed genes with the entered gene of interest. For example, when At4g05120 (identifier for *NDB2* in Arabidopsis) was entered into ATTED-II, the output showed *AOX1a* as the third most highly co-expressed gene (Fig. 2aii). However, it is important to note that even when co-expression is detected by these resources, it is essential to experimentally confirm these findings (Fig. 2aiii). Furthermore, it is also useful to consider the role of possible

co-regulation when tight patterns of co-expression are observed. To do this, co-expressed genes can be analyzed in silico by examining the upstream DNA promoter sequences of these genes and then searching for possible common *cis*-acting elements, such as putative transcription factor-binding sites that may be responsible for this regulation.

Motif analysis tools such as Athamap [14] and AGRIS [15] allow researchers to search for experimentally confirmed *cis*-acting elements when a gene(s) of interest is entered. For example, when the 1 kb upstream promoter sequence of the Arabidopsis *NDB2* gene was entered into AGRIS [15], the output revealed an abscisic acid-responsive element (ABRE) was present (Fig. 2bi), among other experimentally known *cis*-acting elements. The experimentally confirmed motifs compiled in AGRIS and Athamap are also incorporated into Rice DB [12], allowing users to discover whether a set of rice genes contain known transcription factor-binding sites in their respective promoters. In addition, Rice DB [12] also allows users to search for genes containing a putative promoter motif by simply entering the motif, as a DNA sequence into the search box. Alternatively, the presence of all 4,096 possible hexamer sequences can be searched for a list of genes of interest, whereby the output presents the percentage occurrence of these motifs in the promoters of the entered gene list versus the percentage occurrence in the promoters of all genes in the rice genome using Rice DB (*see* **Note 6**). This is very similar to the motif analysis tool at TAIR [7] for Arabidopsis, which also presents these putative hexamer occurrences in comparison to the occurrence of these in the promoters of all genes in the Arabidopsis genome. Thus, in this way, it is possible to search and find putative *cis*-acting elements in a given set of genes.

While these tools are useful for rice and Arabidopsis, other tools need to be employed for non-model plant species. For example, the MEME SUITE [16] allows users to enter promoter sequences from any gene set, across any species, to reveal possible *cis*-acting elements (*see* **Note 7**). The output from the MEME motif tool [16] is shown when the Arabidopsis *NDB2* and *AOX1a* promoter sequences were entered (Fig. 2bii). Notably, Motif 2 shows similarities with the ABRE motif recognized by AGRIS to be present in the *NDB2* promoter (Fig. 2bii). Overall, these tools are useful for providing an indication of putative *cis*-acting elements, which can help to target specific experiments to confirm the functionality of these motifs (Fig. 2biii).

In addition to resources that are informative at an mRNA expression level, several resources have also been developed to provide insight into putative transfer RNAs (tRNAs) and miRNAs, even within mitochondrial encoded genes in plants. For example, the PlantRNA database compiles tRNA information from nuclear and organelle encoded sequences from 11 species, including

five flowering plants, providing a useful resource for identifying mitochondrial encoded tRNAs [17]. Similarly, several resources for miRNA analyses have also been developed, incorporating the option of searching within the mitochondrial genome. The miRBases database annotates high-confidence miRNAs for a range of species including many different plant species [18]. miRBase allows miRNA accessions to be searched, as well as DNA sequences, and the results indicate whether the input sequences represent miRNAs/miRNA precursors (with E-values indicated). Complementing this are tools that reveal possible miRNA targets for a given miRNA. For example, co-expressed genes may be searched for possible regulation by common miRNA and to do this, the RNAhybrid tool [19] may be used as this facilitates miRNA target prediction. For Arabidopsis, Medicago, *Brassica napus*, and *Chlamydomonas reinhardtii*, the RNAhybrid output has already been computed and analyzed for all genes in each of the respective genomes [48, 49]. Similarly, for rice, putative miRNA targets are annotated in the sRNA2 database [20], allowing the user to search if a particular gene is a known miRNA target. Known targets based on sRNA2 [20] can also be searched within Rice DB [12]. Alternatively, for any plant species, it is possible to use a combination of the miRBase [18] and RNAhybrid [19] tools to determine if one or more mitochondrial genes of interest or nuclear genes encoding mitochondrial proteins are possible targets of miRNA-mediated regulation.

When analyzing organelle genomes, such as the mitochondrial genome, it is important to use the informatics resources that are designed to allow for these as input. One such tool is the OrganelleGenomeDRAW tool for drawing organelle genome maps and visualizing organelle-encoded gene expression [21]. Thus, after carrying out transcriptomic analysis of organelle expression whether by sequencing or quantitative real-time PCR, it is possible to visualize this expression using OrganelleGenomeDRAW [21]. Additionally, when working with a non-model species, it is useful to have a way to generate a high-quality image showing the physical map of the mitochondrial genome. Collectively, the tools for expression visualization, motif analysis, possible miRNA regulation, annotation of tRNAs, and organelle genome annotation can be very useful to answer significant questions about mitochondrial biology, and this is even more informative when combined with the protein resources. Figure 3 provides an overview of the scientific questions often asked in mitochondrial studies, as well as the databases and informatics resources currently available to help answer these questions.

3.4 Determining Orthology

As more plant genomes are sequenced, current informatics tools are being advanced to incorporate these newly sequenced species. However, there are still many plant species that have not been sequenced or for which the informatics tools have not been

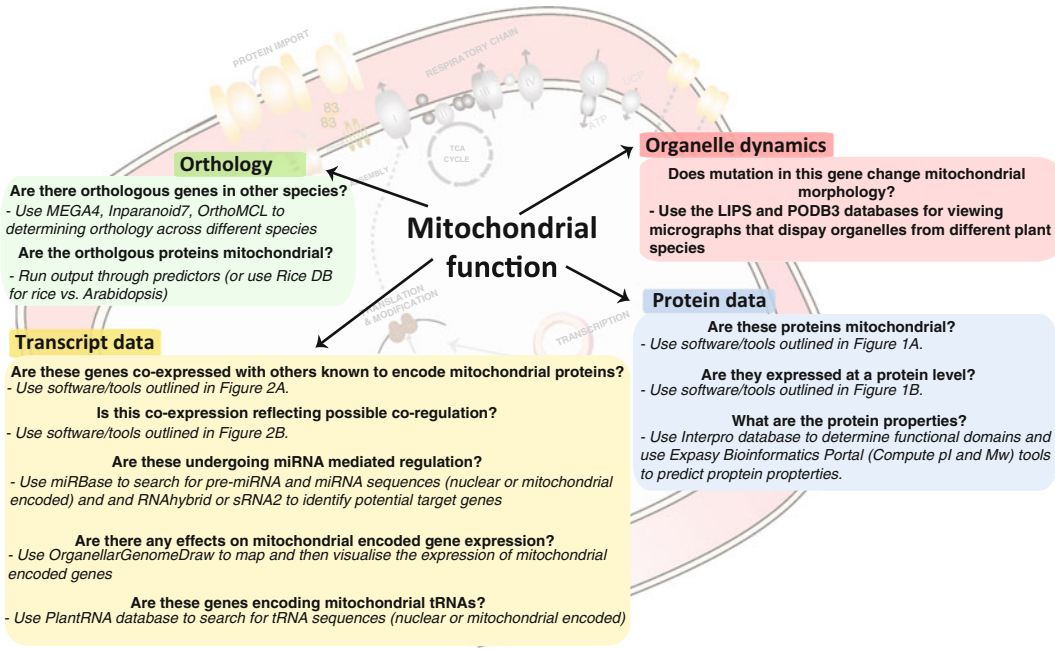

Fig. 3 Overview of the databases and informatics resources for analysis of plant mitochondria. Questions that can be addressed using informatics tools are shown; combining these with experimental methods can help to answer these and gain insight into plant mitochondria

developed to the extent possible in Arabidopsis or rice. Additionally, for comparison between species and evolutionary analyses, it is useful to examine orthologous genes in other species. For example, the mitochondrial proteome in Arabidopsis is the most advanced compared to other plant species [1]; thus it can be highly informative to use orthology to determine if a gene of interest from another species has an Arabidopsis orthologue that is known to be mitochondrial. This knowledge can then be used to subsequently guide the selection of experiments to determine function for a protein of interest in the species being examined.

One of the most well-known ways to determine orthology is to use the BLAST tool [34], whereby selecting the species and entering sequence data results in an output showing possible orthologues and associated E-values to indicate confidence. In addition to BLAST, other databases such as InParanoid7 [35] and OrthoMCL [36] can also be used to facilitate orthologue identification. Specifically, the InParanoid database allows the search and download of precomputed orthologous groups between two species, thus allowing users to have a set of all orthologous genes (in the whole genome) for the two selected species [35]. Similarly, OrthoMCL presents orthologous groups for two or more species/genomes, allowing identification of species-specific genes [36]. Viewing orthologous relationships is also possible using the MEGA5 software [37]; however, this software is designed more

specifically to enable comprehensive phylogenetic analyses between species. Hence, in the MPIC database [31], both BLAST [34] and the MEGA5 software [37] were used in combination to identify orthologous mitochondrial import components, as well as identify the phylogenetic relationship between these, revealing the existence of several plant-specific mitochondrial import components.

3.5 Organelle Morphology

In addition to resources presenting molecular information, databases housing microscopy images of organelles have also emerged, allowing researchers to efficiently examine these intracellular structures, and, where relevant, comparing these with user-generated images. One of these databases is the LIPS database, which presents optical-section images of intracellular structures, including mitochondria in Arabidopsis guard cells [38]. Similarly, the PODB3 database presents images and movie data of plant organelles, including mitochondria, in various tissues over the course of development in various plant species [39]. The PODB3 database is also structured into smaller databases according to the data presented, allowing users to specifically search for electron micrographs, movies, time-lapse images, organelles visualized with fluorescent or nonfluorescent probes, as well as protocols for plant organelle research [39].

Thus, by using the various informatics tools and resources from DNA motif analyses and transcript expression to specific mitochondrial databases, it is possible for researchers to gain maximum insight into mitochondrial function in plants (Fig. 3).

4 Notes

1. While most of these tools work online in a web browser, often a certain amount of memory is required to run these, particularly for long queries. For some tools it is possible to download the software on your machine; it is useful to do this if many/long queries are to be run.
2. Other tools may be available, in addition to those presented here; however, it is important to confirm the accuracy of these tools and to ensure that the tool/software is designed to handle your input data.
3. Most tools accept or even require sequences do be entered in FASTA format. An example of the FASTA format is shown here:
   >LOC_Os01g01010.1 protein
   MSSAAGQDNGDTAGDYIKWMCGAGGRAGGAMANL
   QRGVGSLVRDIGDPCLNPSP
4. Many of these subcellular localization predictors have limits on the number of sequences that can be entered at a time; often there is a limit of 2,000 sequences that can be entered.

If more are required to be searched, this can either be run in batches or the software can be downloaded (for those that allow it) and run on the user's machine.

5. Co-expression refers to the same "direction" of change in the transcriptomic response. For example, in Arabidopsis while *AOX1a* and *NDB2* encoding genes are both upregulated in response to specific stresses, this induction is not necessarily of equal magnitude. Thus co-expression refers to a common pattern of expression and not only the magnitude of the responses specifically.
6. For the 4,096 possible hexamers in rice promoter sequences, Rice DB [12] accepts a limited number of genes for analysis (less than 100 genes).
7. The MEME SUITE [16] has a 100,000-character limit for sequences entered (also less than 100 genes typically); thus users must be sure to only enter a shortlisted number of promoter sequences for motif over-representation analysis.

References

1. Lee CP, Taylor NL, Millar AH (2013) Recent advances in the composition and heterogeneity of the Arabidopsis mitochondrial proteome. Front Plant Sci 4:4. doi:10.3389/fpls.2013.00004
2. Tanz SK, Castleden I, Hooper CM, Vacher M, Small I, Millar HA (2013) SUBA3: a database for integrating experimentation and prediction to define the SUBcellular location of proteins in Arabidopsis. Nucleic Acids Res 41(Database issue):D1185–D1191
3. Narsai R, Law SR, Carrie C, Xu L, Whelan J (2011) In-depth temporal transcriptome profiling reveals a crucial developmental switch with roles for RNA processing and organelle metabolism that are essential for germination in Arabidopsis. Plant Physiol 157(3): 1342–1362
4. Shingaki-Wells R, Millar AH, Whelan J, Narsai R (2014) What happens to plant mitochondria under low oxygen? An omics review of the responses to low oxygen and re-oxygenation. Plant Cell Environ 37:2260–2277. doi:10.1111/pce.12312
5. Xu L, Carrie C, Law SR, Murcha MW, Whelan J (2013) Acquisition, conservation, and loss of dual-targeted proteins in land plants. Plant Physiol 161(2):644–662
6. Xu L, Law SR, Murcha MW, Whelan J, Carrie C (2013) The dual targeting ability of type II NAD(P)H dehydrogenases arose early in land plant evolution. BMC Plant Biol 13:100
7. Huala E, Dickerman AW, Garcia-Hernandez M, Weems D, Reiser L, LaFond F, Hanley D, Kiphart D, Zhuang M, Huang W, Mueller LA, Bhattacharyya D, Bhaya D, Sobral BW, Beavis W, Meinke DW, Town CD, Somerville C, Rhee SY (2001) The Arabidopsis Information Resource (TAIR): a comprehensive database and web-based information retrieval, analysis, and visualization system for a model plant. Nucleic Acids Res 29(1):102–105
8. Kawahara Y, de la Bastide M, Hamilton JP, Kanamori H, McCombie WR, Ouyang S, Schwartz DC, Tanaka T, Wu J, Zhou S, Childs KL, Davidson RM, Lin H, Quesada-Ocampo L, Vaillancourt B, Sakai H, Lee SS, Kim J, Numa H, Itoh T, Buell CR, Matsumoto T (2013) Improvement of the Oryza sativa Nipponbare reference genome using next generation sequence and optical map data. Rice (N Y) 6(1):4. doi:10.1186/1939-8433-6-4
9. Monaco MK, Stein J, Naithani S, Wei S, Dharmawardhana P, Kumari S, Amarasinghe V, Youens-Clark K, Thomason J, Preece J, Pasternak S, Olson A, Jiao Y, Lu Z, Bolser D, Kerhornou A, Staines D, Walts B, Wu G, D'Eustachio P, Haw R, Croft D, Kersey PJ, Stein L, Jaiswal P, Ware D (2014) Gramene 2013: comparative plant genomics resources. Nucleic Acids Res 42(Database issue):D1193–D1199. doi:10.1093/nar/gkt1110
10. Zimmermann P, Hirsch-Hoffmann M, Hennig L, Gruissem W (2004) GENEVESTIGATOR.

Arabidopsis microarray database and analysis toolbox. Plant Physiol 136(1):2621–2632

11. Toufighi K, Brady SM, Austin R, Ly E, Provart NJ (2005) The botany array resource: e-Northerns, expression Angling, and promoter analyses. Plant J 43(1):153–163
12. Narsai R, Devenish J, Castleden I, Narsai K, Xu L, Shou H, Whelan J (2013) Rice DB: an Oryza Information Portal linking annotation, subcellular location, function, expression, regulation, and evolutionary information for rice and Arabidopsis. Plant J 76(6):1057–1073
13. Obayashi T, Kinoshita K, Nakai K, Shibaoka M, Hayashi S, Saeki M, Shibata D, Saito K, Ohta H (2007) ATTED-II: a database of co-expressed genes and cis elements for identifying co-regulated gene groups in Arabidopsis. Nucleic Acids Res 35(Database issue):D863–D869
14. Steffens NO, Galuschka C, Schindler M, Bulow L, Hehl R (2004) AthaMap: an online resource for in silico transcription factor binding sites in the Arabidopsis thaliana genome. Nucleic Acids Res 32(Database issue):D368–D372. doi:10.1093/nar/gkh017
15. Davuluri RV, Sun H, Palaniswamy SK, Matthews N, Molina C, Kurtz M, Grotewold E (2003) AGRIS: Arabidopsis gene regulatory information server, an information resource of Arabidopsis cis-regulatory elements and transcription factors. BMC Bioinformatics 4:25. doi:10.1186/1471-2105-4-25
16. Bailey TL, Boden M, Buske FA, Frith M, Grant CE, Clementi L, Ren J, Li WW, Noble WS (2009) MEME SUITE: tools for motif discovery and searching. Nucleic Acids Res 37(Web Server issue):W202–208. doi:10.1093/nar/gkp335
17. Cognat V, Pawlak G, Duchene AM, Daujat M, Gigant A, Salinas T, Michaud M, Gutmann B, Giege P, Gobert A, Marechal-Drouard L (2013) PlantRNA, a database for tRNAs of photosynthetic eukaryotes. Nucleic Acids Res 41(Database issue):D273–D279
18. Kozomara A, Griffiths-Jones S (2014) miRBase: annotating high confidence microRNAs using deep sequencing data. Nucleic Acids Res 42(Database issue):D68–D73
19. Kruger J, Rehmsmeier M (2006) RNAhybrid: microRNA target prediction easy, fast and flexible. Nucleic Acids Res 34(Web Server issue):W451–454. doi:10.1093/nar/gkl243
20. Jeong DH, Park S, Zhai J, Gurazada SG, De Paoli E, Meyers BC, Green PJ (2011) Massive analysis of rice small RNAs: mechanistic implications of regulated microRNAs and variants for differential target RNA cleavage. Plant Cell 23(12):4185–4207
21. Lohse M, Drechsel O, Kahlau S, Bock R (2013) OrganellarGenomeDRAW--a suite of tools for generating physical maps of plastid and mitochondrial genomes and visualizing expression data sets. Nucleic Acids Res 41(Web Server issue):W575–581
22. Mitschke J, Fuss J, Blum T, Hoglund A, Reski R, Kohlbacher O, Rensing SA (2009) Prediction of dual protein targeting to plant organelles. New Phytol 183(1):224–235
23. Claros MG, Vincens P (1996) Computational method to predict mitochondrially imported proteins and their targeting sequences. Eur J Biochem 241(3):779–786
24. Small I, Peeters N, Legeai F, Lurin C (2004) Predotar: a tool for rapidly screening proteomes for N-terminal targeting sequences. Proteomics 4(6):1581–1590
25. Emanuelsson O, Brunak S, von Heijne G, Nielsen H (2007) Locating proteins in the cell using TargetP, SignalP and related tools. Nat Protoc 2(4):953–971
26. Prokisch H, Ahting U (2007) MitoP2, an integrated database for mitochondrial proteins. Methods Mol Biol 372:573–586. doi:10.1007/978-1-59745-365-3_39
27. Rode C, Senkler M, Klodmann J, Winkelmann T, Braun HP (2011) GelMap-a novel software tool for building and presenting proteome reference maps. J Proteomics 74(10):2214–2219
28. Klodmann J, Senkler M, Rode C, Braun HP (2011) Defining the protein complex proteome of plant mitochondria. Plant Physiol 157(2):587–598. doi:10.1104/pp. 111.182352
29. Peters K, Belt K, Braun HP (2013) 3D Gel Map of Arabidopsis Complex I. Front Plant Sci 4:153
30. Kiirika LM, Behrens C, Braun HP, Colditz F (2013) The Mitochondrial Complexome of Medicago truncatula. Front Plant Sci 4:84
31. Murcha MW, Narsai R, Devenish J, Kubiszewski-Jakubiak S, Whelan J (2014) MPIC: a mitochondrial protein import components database for plant and non-plant species. Plant Cell Physiol 56:e10
32. Artimo P, Jonnalagedda M, Arnold K, Baratin D, Csardi G, de Castro E, Duvaud S, Flegel V, Fortier A, Gasteiger E, Grosdidier A, Hernandez C, Ioannidis V, Kuznetsov D, Liechti R, Moretti S, Mostaguir K, Redaschi N, Rossier G, Xenarios I, Stockinger H (2012) ExPASy: SIB bioinformatics resource portal. Nucleic Acids Res 40(Web Server issue):W597–603
33. Hunter S, Jones P, Mitchell A, Apweiler R, Attwood TK, Bateman A, Bernard T, Binns D, Bork P, Burge S, de Castro E, Coggill P, Corbett M, Das U, Daugherty L, Duquenne L,

Finn RD, Fraser M, Gough J, Haft D, Hulo N, Kahn D, Kelly E, Letunic I, Lonsdale D, Lopez R, Madera M, Maslen J, McAnulla C, McDowall J, McMenamin C, Mi H, Mutowo-Muellenet P, Mulder N, Natale D, Orengo C, Pesseat S, Punta M, Quinn AF, Rivoire C, Sangrador-Vegas A, Selengut JD, Sigrist CJ, Scheremetjew M, Tate J, Thimmajanarthanan M, Thomas PD, Wu CH, Yeats C, Yong SY (2012) InterPro in 2011: new developments in the family and domain prediction database. Nucleic Acids Res 40(Database issue):D306–D312

34. Altschul SF, Gish W, Miller W, Myers EW, Lipman DJ (1990) Basic local alignment search tool. J Mol Biol 215(3):403–410
35. Ostlund G, Schmitt T, Forslund K, Kostler T, Messina DN, Roopra S, Frings O, Sonnhammer EL (2010) InParanoid 7: new algorithms and tools for eukaryotic orthology analysis. Nucleic Acids Res 38(Database issue):D196–D203
36. Fischer S, Brunk BP, Chen F, Gao X, Harb OS, Iodice JB, Shanmugam D, Roos DS, Stoeckert CJ Jr. (2011) Using OrthoMCL to assign proteins to OrthoMCL-DB groups or to cluster proteomes into new ortholog groups. Curr Protoc Bioinformatics Chapter 6:Unit 6 12 11–19
37. Tamura K, Peterson D, Peterson N, Stecher G, Nei M, Kumar S (2011) MEGA5: molecular evolutionary genetics analysis using maximum likelihood, evolutionary distance, and maximum parsimony methods. Mol Biol Evol 28(10):2731–2739
38. Higaki T, Kutsuna N, Hasezawa S (2013) LIPS database with LIPService: a microscopic image database of intracellular structures in Arabidopsis guard cells. BMC Plant Biol 13:81
39. Mano S, Nakamura T, Kondo M, Miwa T, Nishikawa S, Mimura T, Nagatani A, Nishimura M (2014) The plant organelles database 3 (PODB3) update 2014: integrating electron micrographs and new options for plant organelle research. Plant Cell Physiol 55(1):e1. doi:10.1093/pcp/pct140
40. Sakai H, Lee SS, Tanaka T, Numa H, Kim J, Kawahara Y, Wakimoto H, Yang CC, Iwamoto M, Abe T, Yamada Y, Muto A, Inokuchi H, Ikemura T, Matsumoto T, Sasaki T, Itoh T (2013) Rice annotation project database (RAP-DB): an integrative and interactive database for rice genomics. Plant Cell Physiol 54(2):e6. doi:10.1093/pcp/pcs183
41. Welchen E, Garcia L, Mansilla N, Gonzalez DH (2014) Coordination of plant mitochondrial biogenesis: keeping pace with cellular requirements. Front Plant Sci 4:551. doi:10.3389/fpls.2013.00551
42. Scott I, Logan DC (2008) Mitochondrial morphology transition is an early indicator of subsequent cell death in Arabidopsis. New Phytol 177(1):90–101
43. Duncan O, Taylor NL, Carrie C, Eubel H, Kubiszewski-Jakubiak S, Zhang B, Narsai R, Millar AH, Whelan J (2011) Multiple lines of evidence localize signaling, morphology, and lipid biosynthesis machinery to the mitochondrial outer membrane of Arabidopsis. Plant Physiol 157(3):1093–1113
44. Huang S, Taylor NL, Narsai R, Eubel H, Whelan J, Millar AH (2009) Experimental analysis of the rice mitochondrial proteome, its biogenesis, and heterogeneity. Plant Physiol 149(2):719–734
45. Murcha MW, Wang Y, Narsai R, Whelan J (2014) The plant mitochondrial protein import apparatus - the differences make it interesting. Biochim Biophys Acta 1840(4):1233–1245
46. Clifton R, Lister R, Parker KL, Sappl PG, Elhafez D, Millar AH, Day DA, Whelan J (2005) Stress-induced co-expression of alternative respiratory chain components in Arabidopsis thaliana. Plant Mol Biol 58(2):193–212
47. Wang Y, Carrie C, Giraud E, Elhafez D, Narsai R, Duncan O, Whelan J, Murcha MW (2012) Dual location of the mitochondrial preprotein transporters B14.7 and Tim23-2 in complex I and the TIM17:23 complex in Arabidopsis links mitochondrial activity and biogenesis. Plant Cell 24(6):2675–2695
48. Alves L Jr, Niemeier S, Hauenschild A, Rehmsmeier M, Merkle T (2009) Comprehensive prediction of novel microRNA targets in Arabidopsis thaliana. Nucleic Acids Res 37(12):4010–4021
49. Lenz D, May P, Walther D (2011) Comparative analysis of miRNAs and their targets across four plant species. BMC Res Notes 4:483. doi:10.1186/1756-0500-4-483

Chapter 20

Expression and Crystallization of the Plant Alternative Oxidase

Benjamin May, Catherine Elliott, Momi Iwata, Luke Young, Julia Shearman, Mary S. Albury, and Anthony L. Moore

Abstract

The alternative oxidase (AOX) is an integral monotopic membrane protein located on the inner surface of the inner mitochondrial membrane. Branching from the traditional respiratory chain at the quinone pool, AOX is responsible for cyanide-resistant respiration in plants and fungi, heat generation in thermogenic plants, and survival of parasites, such as *Trypanosoma brucei*, in the human host. A recently solved AOX structure provides insight into its active site, thereby facilitating rational phytopathogenic and antiparasitic drug design. Here, we describe expression of recombinant AOX using two different expression systems. Purification protocols for the production of highly pure and stable AOX protein in sufficient quantities to facilitate further kinetic, biophysical, and structural analyses are also described.

Key words Alternative oxidase, AOX, Trypanosomal alternative oxidase (TAO), Monotopic membrane protein, *Sauromatum guttatum*

1 Introduction

The alternative oxidase (AOX) is an integral monotopic protein located on the inner surface of the inner mitochondrial membrane, branching from the traditional respiratory chain at the point of the quinone pool [1]. AOX is present in all plants in addition to some fungi, protists, and proteobacteria [2]. Crucially, higher mammals such as humans lack the AOX and in recent years, the AOX has been identified as a potential important chemotherapeutic target in several human parasites including *Trypanosoma brucei* [3], *Cryptosporidium parvum* [4], and *Blastocystis hominis* [5]. Compounds such as ascofuranone have proven to be effective specific inhibitors against the trypanosomal alternative oxidase (TAO) [6], providing safer and more efficient treatments when compared to existing therapeutic strategies for treating

James Whelan and Monika W. Murcha (eds.), *Plant Mitochondria: Methods and Protocols*, Methods in Molecular Biology, vol. 1305, DOI 10.1007/978-1-4939-2639-8_20,

trypanosomal diseases such as Nagana in cattle and African sleeping sickness in humans [7]. AOX is also emerging as an increasingly important fungicide target in several organisms including the opportunistic human pathogen *Candida albicans* [8, 9], the wheat pathogen *Septoria tritici* [10], and most recently *Chalara fraxinea*, the fungal pathogen that causes ash dieback (http://oadb.tsl.ac.uk/?p=729).

Functionally, AOX is a non-proton motive [11] terminal oxidoreductase which catalyzes the reduction of oxygen through to water via the oxidation of quinol [1, 12]. In thermogenic plants, the free energy generated by this reaction does not contribute to the generation of a proton gradient for ATP synthesis but is released as heat, which is used to volatilize aromatic compounds to attract pollinating insects [13, 14]. In non-thermogenic tissues however, AOX expression is upregulated when the organism is subject to stress such as ageing [15] or exposure to respiratory chain inhibitors [16]. Furthermore, AOX activity is stimulated by α-keto acids such as pyruvate [17, 18]. In the parasite *Trypanosoma brucei*, TAO is upregulated in its active bloodstream form and acts as the sole terminal oxidase under these conditions, thereby facilitating the reoxidation of cytosolic glycerol-3-phosphate [19].

Despite the fact that the AOX has been studied for decades, a structure from the AOX family has only been solved recently [20]. This is in part due to difficulties in obtaining protein in sufficient purity and quantity, in addition to the observed instability of the AOX proteins when purified from native tissues [1]. In order to overcome this problem and allow for further detailed elucidation of the kinetic, catalytic, and structural nature of the AOX, recombinant AOX has been expressed in several different systems, namely in yeast *Schizosaccharomyces pombe* [21], the haem-deficient *Escherichia coli* strains [17, 22–25], and more recently in mammalian HeLa cells [26]. The activity and functionality of recombinant AOX can best be identified using the *S. pombe* system with an activity assay and Western blotting to confirm mitochondrial location [21]. However, due to the low levels of protein expression, the *S. pombe* system is not suitable for the large-scale production of pure AOX for structural and biophysical studies. Bacterial systems are better suited for overexpression of membrane proteins [22–25]. While *E. coli* systems such as C41 and C43 are specialized in overexpression of membrane-bound proteins [27], the advantage of the SASX41B and FN102 systems in relation to the expression of AOX is the lack of expression of other terminal respiratory oxidases, thereby resulting in a more accurate attribution of AOX activity during activity assays. Finally, expression of recombinant AOX in HeLa cells serves as a proof of principle for the expression of a nonmammalian recombinant protein in a mammalian system [26].

X-ray crystallography is one of the most powerful methods to determine a protein structure at atomic level. Structure determination of a membrane protein is time consuming and labor intensive due to technical difficulties in comparison to soluble proteins. Crystallization is a major bottleneck of X-ray crystallography, since it necessitates not only screening and optimization of crystallization conditions but may also require modification of the target proteins. Although the process relies on empirical methods, we are beginning to understand the critical factors, such as stability and monodispersity, and how to solve these challenges [28, 29]. Membrane proteins are often destabilized following detergent solubilization and tend to aggregate. Even if the aggregation is mild and no visible precipitation is observed, since this type of aggregation cannot be detected by SDS-PAGE or an activity assay, the protein is still unlikely to crystallize. The choice of detergent plays a crucial role in membrane protein crystallization [30]. Generally membrane proteins are more stable in detergents with low critical micelle concentration (CMC) values, such as n-dodecyl β-d-maltoside (DDM). "Large" detergents such as DDM form large. Micelles, which better protect hydrophobic surfaces of membrane proteins whereas "small" detergents with higher CMCs are more advantageous for crystallization. This is due to the fact that membrane proteins are more exposed in small micelles, and therefore more likely to form better crystal contacts. It is important to take these two factors into account when selecting an appropriate detergent while attempting crystallization of membrane proteins.

Size-exclusion chromatography (SEC) is widely used as the final step in the purification protocol to evaluate protein quality factors, such as aggregation and stability [31]. This technique shows direct and reliable indication of the protein quality used for crystallization. Effectiveness of crystallization screens can be improved by use of a crystallization robot and an observation system. An automated system improves efficiency by reducing volume of sample necessary and time required for setting up screening plates. An automatic observation system, which is usually composed of an incubator with a camera connected to a database, allows quick and efficient evaluation and analysis of protein crystals.

The protocols defined in this chapter provide a robust expression and purification system for recombinant AOX, which may further be applied to other monotopic membrane proteins such as the plastid terminal oxidases (PTOX [2]).

2 Materials

All chemicals should be of reagent grade and made up in double-deionized (DDI) water, with autoclaving where appropriate and storage at room temperature unless indicated.

2.1 Transformation and Growth of Recombinant Sauromatum guttatum AOX (rSgAOX) in S. pombe

For *S. pombe*, Subheading 2.1 or 3.1, the wild-type and mutant transformation and consequential grow ups are prepared alongside each other.

1. Use *S. pombe* strain sp.011 (*ade*6–704, *leu*1–32, *ura*4-D18, *h*$^-$) and plasmid pREP1-AOX (*see* **Note 1**) [21, 32].
2. Autoclaved yeast extract supplement (YES) medium: 5 g/L yeast extract, 30 g/L glucose, 225 mg/L adenine, 225 mg/L histidine, 225 mg/L leucine, 225 mg/L uracil, and 225 mg/L lysine hydrochloride.
3. 50× autoclaved salt stock: 53.5 g/L $MgCl_2{\cdot}6H_2O$, 0.74 g/L $CaCl_2{\cdot}2H_2O$, 50 g/L KCl, 2 g/L Na_2SO_4.
4. 1,000× autoclaved vitamins: 1 g/L Na pantothenate, 10 g/L nicotinic acid, 10 g/L inositol, 10 mg/L biotin.
5. 1,000× autoclaved minerals: 5 g/L H_3BO_3, 5 g/L $MnSO_4$, 4 g/L $ZnSO_4{\cdot}7H_2O$, 2 g/L $FeCl_2{\cdot}6H_2O$, 0.4 g/L $H_2MoO_4{\cdot}H_2O$, 1 g/L KI, 0.4 g/L $CuSO_4{\cdot}5H_2O$, 10 g/L citric acid.
6. Autoclaved pombe minimal medium (PM medium): 3 g/L potassium hydrogen phthalate, 2.2 g/L Na_2HPO_4, 5 g/L NH_4Cl, 20 g/L D-glucose, 20 mL salt stock (50×), 1.0 mL vitamin stock (1,000×), 0.1 mL mineral stock (1,000×). Add supplements as appropriate: 75 mg/L adenine, 75 mg/L. uracil, 75 mg/L leucine. For sp.011, use PM media plus adenine, uracil, and leucine (PM + AUL). For transformants, use PM media plus adenine and uracil (PM + AU).
7. Autoclaved pombe minimal agar: PM medium with 2 % (w/v) New Zealand agar.
8. Autoclaved 0.1 M lithium acetate/TE: 10 mM Tris–HCl pH 7.6, 1 mM EDTA.
9. 50 % (w/v) PEG 3350 in lithium acetate/TE: Make up fresh and filter sterilize using a 0.45-μm filter unit.
10. Zymolyase-20 T (MPBIO, 08320921): Use at 7.5 mg/g fresh cell weight.
11. Lysing enzyme (Sigma: L-1412): Use at 15 mg/g fresh cell weight.
12. Autoclaved spheroplast buffer (SB): 1.35 M sorbitol, 1 mM EGTA, 10 mM citrate/Na_2HPO_4 pH 5.8.
13. Autoclaved spheroplast wash buffer (SW): 0.75 M sorbitol, 0.4 M mannitol, 10 mM MOPS pH 6.8.
14. Autoclaved mannitol wash buffer (MW): 0.65 M mannitol, 2 mM EGTA, 10 mM MOPS pH 6.8.

2.2 Transformation, Growth, and Harvest of FN102 E. coli Cells Expressing rSgAOX

1. LB-broth and LB-agar: 10 g/L tryptone peptone, 10 g/L NaCl, 5 g/L yeast extract. Add 15 g/L agar for LB-agar prior to autoclaving. Supplement with 50 μg/mL kanamycin, 100 μg/mL ampicillin, and 50 μg/mL 5-aminolevulinic acid (ALA).
2. Autoclaved 0.1 M $CaCl_2$.
3. Autoclaved glycerol/$CaCl_2$ mixture: 10 % (v/v) glycerol and 0.075 M $CaCl_2$.
4. FN102 cells and recombinant DNA (including a 6-histidine tag).
5. Autoclaved K-broth: 10 g/L tryptone peptone, 5 g/L yeast extract, 5 g/L casamino acid, 10.4 g/L K_2HPO_4, 3 g/L KH_2PO_4, 0.74 g/L trisodium citrate, 2.5 g/L $(NH_4)_2SO_4$, 2 g/L glucose.
6. Supplement A: 0.05 g/L $MgSO_4$, 0.025 g/L $FeSO_4$, 0.025 g/L $FeCl_3$, and 0.1 g/L carbenicillin (to be added to the K-broth after autoclaving and before use).
7. 1 M Tris buffer with pyruvate: 50 mM Tris–HCl, 10 mM pyruvate, pH 7.5.
8. 1 M Isopropylthio-β-galactoside (IPTG).
9. Protease Inhibitor Cocktail tablets (Roche Complete, mini: 11836145001): One tablet per 50 mL of Tris–HCl buffer with pyruvate.

2.3 Solubilization and Purification of rSgAOX from E. coli Strain FN102

1. Solubilization buffer: 50 mM Tris–HCl pH 7.5, 10 mM pyruvate, 1 % (w/v) DDM, 20 % (v/v) glycerol.
2. HIS-Select® Cobalt Affinity Gel (Sigma, catalogue number: H8162) (*see* **Note 2**).
3. Equilibration buffer: 50 mM Tris–HCl pH 7.5, 10 mM pyruvate, 0.5 % (w/v) DDM, 0.5 % (w/v) octylglucoside, 20 % (v/v) glycerol, 100 mM $MgSO_4$, 20 mM imidazole.
4. Wash buffer: 50 mM Tris–HCl pH 7.5, 10 mM pyruvate, 0.5 % (w/v) DDM, 0.5 % (w/v) octylglucoside, 20 % (v/v) glycerol, 100 mM $MgSO_4$, 20 mM imidazole.
5. Elution buffer: 50 mM Tris–HCl pH 7.5, 10 mM pyruvate, 0.5 % (w/v) DDM, 0.5 % (w/v) octylglucoside, 20 % (v/v) glycerol, 100 mM $MgSO_4$, 250 mM imidazole.

2.4 Activity Assay of Mitochondrial and Membrane-Bound rSgAOX Samples: Rank Oxygen Electrode (Rank Brothers, Cambridge)

1. Membrane-bound rSgAOX assay buffer: 50 mM Tris–HCl, 10 mM pyruvate, pH 7.5.
2. Yeast mitochondrial assay buffer: 0.65 M mannitol, 1 mM $MgCl_2$, 5 mM K_2HPO_4, 10 mM KCl, 20 mM MOPS pH 6.8.
3. Stock solution 0.1 M NADH.
4. Stock solution 1 mg/mL antimycin A.
5. Stock solution 100 mM KCN—make fresh.

2.5 Activity Assay of Solubilized and Purified rSgAOX Samples: Spectrophotometric Assay

1. 50 mM Tris–HCl, 10 mM pyruvate, pH 7.5 assay buffer.
2. Stock solution 50 mM Q_1H_2—keep under an inert atmosphere.

2.6 Size-Exclusion Chromatography Analysis

1. Detergent stock solutions: Dissolve a choice of detergent in water with a concentration of ten times CMC. The stock solutions can be stored in −20 °C. Stock concentrations of detergents are as follows:

   1.5 mM n-Dodecyl β-D-maltopyranoside (DDM).

   200 mM Octyl glucoside (OG).

   18 mM n-Decyl-β-D-maltoside (DM).

   10 mM β-D-Lauryldimethylamine N-oxide (LDAO).

   0.1 mM Decyl maltose neopentyl glycol (DMNG).

   10.2 mM Octyl glucose neopentyl glycol (OGNG).

   65 mM n-Nonyl-β-D-glucoside (NG).

   1.7 mM n-Octyl β-D-maltoside (OM).

   5.6 mM 6 Cyclohexyl-β-D-maltoside (CYMAL-6) (Affymetrix, CA, USA, or GLYCON, Germany).
2. Prominence HPLC system (Shimadzu, UK) is used for SEC analysis (*see* **Note 3**).
3. Running buffer: pH 7.5, 20 mM Tris–HCl, 150 mM NaCl, 10 % (v/v) glycerol, 0.03 % (w/v) DDM. The solution is filtered and degassed prior to use.
4. SEC column: Superose-6 10/300GL or Superdex-200 (GE Healthcare). The column is equilibrated with the running buffer prior to use.

2.7 Crystallization of AOX

1. Mosquito (TTP Labtech, UK) crystallization robot is used to set up the crystallization plates. The 96-well MRC Crystallization Plates (Molecular Dimensions: MD11-00U-100) format is used. Plates are stored and observed at 20 and 4 °C with a Thermo Rhombix Cs750i.
2. Running buffer: pH 7.5, 20 mM Tris–HCl, 150 mM NaCl, 5 % (v/v) glycerol, 0.03 % (w/v) DDM (or a choice of detergent based on the SEC analysis above; here DDM is used as example, and detergent concentration is 2–3 times its CMC). The solution is filtered and degassed prior to use. SEC is ideally run at 4 °C.

3 Methods

3.1 Transformation, Growth, and Mitochondrial Harvest of S. pombe Cells Expressing rSgAOX

All stages, until directed otherwise, should be carried out under sterile conditions.

1. Set up a starter culture by inoculating a single sp.011 colony into 5 mL of YES media and grow for 2–3 days, at 30 °C with shaking at 180 rpm, to a density of $3–5 \times 10^7$ cells/mL.
2. Use the starter culture to inoculate 100 mL of PM + AUL in a 250-mL conical flask and grow overnight, at 30 °C with shaking at 180 rpm, to a density of $0.5–1 \times 10^7$ cells/mL (typically use 0.8–1.5 mL of starter culture).
3. Collect cells by centrifugation at $1{,}900 \times g$ for 5 min at room temperature.
4. Discard supernatant, wash cells in 50 mL sterile distilled water, and then centrifuge at $1{,}900 \times g$ for 5 min at room temperature.
5. Resuspend cells in lithium acetate/TE to a concentration of 1×10^9 cells/mL. Dispense into 0.1 mL aliquots in microcentrifuge tubes.
6. Incubate cells at 30 °C for 1 h with occasional mixing.
7. Add 1–2 μg DNA and 290 μL 50 % (w/v) PEG to each aliquot. Mix thoroughly.
8. Incubate tubes at 30 °C for 1 h with occasional mixing.
9. Place tubes in a water bath and heat shock at 43 °C for 15 min.
10. Pellet cells at $15{,}000 \times g$ for 20 s. Remove supernatant and gently resuspend pellet in 100 μL lithium acetate/TE.
11. Plate the resuspended cells on PM + AU agar plates. Incubate for 3–5 days at 30 °C.

    Step 12 *onwards: Instructions are for a single sample and need to be repeated for second sample*, i.e., *wild type and mutant.*

12. Restreak a single transformant onto PM + AU agar plates. Incubate for 3–5 days at 30 °C.
13. Set up a starter culture by inoculating a single colony from the freshly streaked transformant into 100 mL PM + AU broth. Incubate for 3 days at 30 °C with shaking at 180 rpm in order to obtain a density of $5–7 \times 10^7$ cells/mL.
14. Use the starter culture to inoculate PM + AU broth in order to obtain a density of 1×10^7 cells/mL after incubation overnight at 30 °C with shaking at 180 rpm. Typically we use 20–35 mL per 1 L. Inoculate cells into 2×1 L PM + AU in 2-L conical flasks and incubate overnight at 30 °C with shaking at 180 rpm (*see* **Note 4**).

The following stages do not require sterile conditions.

15. Harvest cells by centrifugation at 2,000 × *g* for 5 min.
16. Wash cells in 300 mL distilled water and combine pellets. Harvest cells by centrifugation at 2,000 × *g* for 5 min. Measure the weight of cell pellet. In our experience 7–8 g is sufficient for isolation of mitochondria.
17. Into a microcentrifuge tube weigh out an appropriate amount of Zymolyase-20 T (7.5 mg/g fresh cell weight) and dissolve in 1 mL SB (*see* **Note 5**).
18. Using a paintbrush resuspend cells in 90 mL SB and transfer to a 250-mL conical flask. Add the Zymolyase-20 T solution.
19. Incubate at 30 °C for 15 min with shaking at 180 rpm.
20. Into a microcentrifuge tube weigh out an appropriate amount of lysing enzymes (15 mg/g fresh cell weight) and dissolve in 1 mL SB.
21. Add lysing enzyme solution to the cell suspension.
22. Incubate at 30 °C for a further 45 min with shaking at 180 rpm.
23. Assess formation of spheroplasts. Dilute a 10 μL sample 100× in (1) SB and (2) distilled water and measure absorbance at A_{800}. Spheroplast formation is achieved when there is a 75–80 % reduction in absorbance between samples in SB and distilled water. Spheroplast formation can also be examined under the microscope. Place 5 μL of cell suspension on a hemocytometer slide and add 5 μL water. The cells should become round and will eventually lyse if the cell wall has been removed.

The following steps are all carried out on ice using chilled solutions.

24. Dilute spheroplasts to 200 mL with SW and divide between 4 × 50-mL conical centrifuge tubes. Harvest spheroplasts at 400 × *g* for 10 min at 4 °C. If available, use a swinging bucket rotor.
25. Rinse each pellet with 50 mL SW at 4 °C and spin cells as before. In our experience there is no need to resuspend cells.
26. Resuspend each of the four pellets in 3–4 mL MW, pool, and transfer to a 50-mL loose-fitting glass homogenizer. Homo genize gently to resuspend pellet and cause lysis.
27. Dilute to 300 mL MW to complete lysis and divide between 6 × 50-mL conical centrifuge tubes.
28. Spin suspension at 400 × *g* for 10 min at 4 °C. Pour off supernatant carefully in order to avoid dislodging the loose pellet. Divide the supernatant between 8 × 50-mL centrifuge tubes (*see* **Note 6**).

29. A mitochondrial pellet is obtained by centrifugation of the supernatant at 17,700 × *g* for 10 min at 4 °C.
30. Remove the supernatant and use a fine paintbrush to transfer all pellets into a single 50-mL centrifuge tube. Resuspend the combined samples in 5–10 mL MW. Resuspend the mitochondria by drawing the paintbrush repeatedly through the pellets. Dilute to 40 mL and centrifuge at 12,000 × *g* for 10 min at 4 °C.
31. Use the fine paintbrush to resuspend the pellet in 0.5–1 mL MW and transfer the mitochondrial suspension to a 2-mL microcentrifuge tube. If necessary, the sample may be diluted further before assaying. The activity of AOX expressed in yeast mitochondria decreases with time; therefore assays for AOX activity should be performed on the same day or samples should be fast-frozen immediately and stored at –80 °C. Samples can also be stored at –20 °C for protein estimation and Western blot.

3.2 Transformation, Growth, and Harvest of FN102 Cells Expressing rSgAOX

All stages, until directed otherwise, should be carried out under sterile conditions.

1. Plate out FN-102 Δ-haem *E. coli* onto LB-agar containing 100 μg/mL kanamycin and 50 μg/mL ALA only. Incubate for 12 h at 37 °C.
2. Inoculate 5 mL of LB-broth containing 50 μg/mL kanamycin and 50 μg/mL ALA, with a single colony from plate. Incubate overnight at 37 °C.
3. Inoculate 100 mL LB-broth, with 50 μg/mL kanamycin and 50 μg/mL ALA, with 1 mL of culture. Incubate at 37 °C until $A_{650} = 0.45–0.6$.
4. Chill on ice for 10 min.
5. Transfer 100 mL culture to sterile centrifuge tubes and harvest cells via centrifugation at 1,900 × *g* for 5 min at 4 °C.
6. Resuspend cell pellet in 25 mL 0.1 M $CaCl_2$. Leave resuspended cells on ice for 20–30 min, then repeat the centrifugation stage, and gently resuspend (as cells are fragile at this stage) in 5 mL glycerol/$CaCl_2$ mixture. Cells are now competent.
7. For each transformation, aliquot 200 μL of competent FN102 cells into a chilled microcentrifuge tube and add 0.3 μg of DNA. For a negative control, use sterile DDI water in place of the DNA.
8. Incubate the cells on ice for 30 min.
9. Heat shock the cells by placing them in a water bath at 42 °C for 2 min.
10. Immediately incubate the cells on ice for 20 min.
11. Add 800 μL of LB-broth and incubate at 37 °C for 1 h with shaking up to 180 rpm.

12. Pellet cells at 15,000 × *g* for 2 min, remove 750 μL of the supernatant, and resuspend the cells in the remaining 150 μL LB-broth.
13. Plate out the suspension on LB-agar plates containing 100 μg/mL ampicillin, 50 μg/mL kanamycin, and 50 μg/mL ALA and incubate the plates overnight at 37 °C.
14. Streak out a single colony of transformed FN102 cells onto plate of LB-agar containing 100 μg/mL ampicillin, 50 μg/mL kanamycin, and 50 μg/mL ALA and incubate at 37 °C for 12 h.
15. Prepare two sterile flasks containing 50 mL of K-broth supplemented with 100 μg/mL ampicillin, 50 μg/mL kanamycin, and 50 μg/mL ALA. Inoculate each flask with one loop of cells from the agar plate prepared in **step 14**. Incubate the flasks at 37 °C for 8 h at 160 rpm.
16. In order to remove the ALA from the starter culture media, transfer the starter cultures from **step 15** into sterile centrifuge tubes and centrifuge at 3,000 × *g* for 10 min in a fixed-angle rotor at 4 °C.
17. Pour off the supernatant, resuspend the pellet in 1–2 mL fresh LB-broth (without supplements) using a paintbrush, and repeat the centrifugation step. Once again discard supernatant and resuspend into one tube in 1–2 mL LB-broth.
18. Determine the absorbance (at 650 nm) of the resuspended cell solution and add a sufficient volume of cell suspension to each of the four 2-L conical flasks containing sterile K-broth with supplement A to ensure that A_{650} is 0.01 OD in each flask.
19. Incubate the flasks at 30 °C in an orbital shaker at 160 rpm.
20. When A_{650} reaches 0.1 OD, induce the expression of AOX with 25–100 μM IPTG (*see* **Note 7**) and incubate the cultures at 30 °C with shaking at 160 rpm for 14 h.

The following stages do not require sterile conditions.

21. Transfer the cultures into 500-mL centrifuge tubes and centrifuge in a precooled rotor at 8,000 × *g*, 4 °C, for 8 min.
22. Discard the supernatant and determine the wet weight of the cells. Add 2.5 mL of chilled Tris–HCl buffer with pyruvate per gram of wet weight.
23. Add Protease Inhibitor Cocktail tablets into the cell suspension.
24. Homogenize the samples in a tight-fitting glass homogenizer and pool samples into one chilled beaker.
25. Lyse the cells using two passes through a French Press (Thermo Scientific) at 10,000 psi.
26. Remove the cell debris via centrifugation of the lysed cells at 40,000 × *g*, 4 °C, for 15 min.

27. Decant the supernatant into ultracentrifuge tubes and centrifuge at 200,000 × *g*, 4 °C, for 1 h.
28. Discard the supernatant and using a small spatula, scrape the membrane pellet off the side of the centrifuge tube and transfer into a precooled tight-fitting glass homogenizer. Ensure complete transfer of any residual membrane pellet by addition of Tris–HCl buffer with pyruvate to the ultracentrifuge tubes with gentle agitation, and transfer into homogenizer with solid membrane pellet. If homogenate is viscous, add additional Tris–HCl buffer with pyruvate until a liquid consistency is achieved.
29. Samples should then be stored at –20 °C for 1 h before being transferred to –80 °C for longer term storage.

3.3 Solubilization and Purification of Membrane-Bound rSgAOX Expressed in FN102 Cells

1. Add equal volumes of membrane-bound rSgAOX sample to the solubilization buffer in a drop-wise manner while agitating the sample.
2. Incubate the mixture at 4 °C for 1 h, with gentle mixing.
3. Transfer the sample to ultracentrifuge tubes and centrifuge at 200,000 × *g*, 4 °C, for 1 h.
4. Decant the supernatant (the soluble fraction) into a tube. The pellet should be resuspended in a minimal volume of Tris buffer with pyruvate to ascertain what proportion of the rSgAOX has been successfully solubilized.
5. Prepare a suitable bed volume (we typically use an equivalent volume to the solubilized protein sample as recommended by the manufacturer's guidelines) of HIS-Select Cobalt Affinity Resin (Sigma). The ethanol is removed from the slurry through gentle centrifugation (1 min at 2,000 × *g*) followed by aspiration of the ethanol from the top of the beads.
6. Equilibrate the resin in 3× bed volume of chilled equilibration buffer via inversion mixing at 4 °C for 1 h.
7. Transfer the equilibrated resin to a small polypropylene or glass chromatography column (*see* **Note 8**) and allow the equilibration buffer to elute.
8. Carefully add the solubilized sample to the top of the column and allow the solubilized protein sample to pass through the resin (*see* **Note 9**). Retain the eluted liquid as the flow-through fraction.
9. Gently add 10× bed volume of wash buffer and allow to pass through the column. Collect this eluate as the wash fraction.
10. Add 3× bed volume of equilibration buffer, allow to pass through the column, and collect the eluted liquid as a single eluate fraction. Alternatively collect eluate in several 1 mL fractions to allow for improved protein concentration.

11. The flow-through, wash, and eluate fractions should be retained on ice immediately and assayed as soon as possible. They can be stored at −20 °C for up to 1 month or −80 °C for up to 1 year without significant loss of activity [25].

3.4 Activity Assay of Mitochondrial and Membrane-Bound rSgAOX Samples: Oxygen Electrode

1. Add a suitable volume of assay buffer to an oxygen electrode chamber (dependent upon the volume of the chamber, we routinely use 400 μL in a 1-mL electrode chamber) and use this to establish a baseline for oxygen concentration in solution, and zero baseline with addition of a few grains of sodium dithionite. Rinse chamber several times and replace with fresh assay buffer.
2. Add mitochondrial or membrane-bound rSgAOX sample to chamber, place plunger into chamber in order to reduce surface area of the assay buffer in contact with air, and then allow oxygen concentration to settle in order to establish any background auto-oxidation levels.
3. Add (to a final concentration of) 1 μg/mL antimycin A and 1 mM KCN into the chamber using a syringe.
4. Finally, add the substrate (typically final concentration of 1.25 mM NADH or 150 μM Q_1H_2) and continue recording until an initial rate has been established.

3.5 Activity Assay of Solubilized and Purified rSgAOX Samples: Spectrophotometric Assay

1. Add a suitable volume of assay buffer (Tris buffer with pyruvate) to a cuvette and use this to establish a baseline for single wavelength (278 nm if using Q_1H_2 $\varepsilon = 15{,}000/M/cm$) by performing an absorbance versus time scan, preferably using a spectrophotometer with a stirrer.
2. Add the substrate and record the trace in order to establish any background auto-oxidation levels.
3. An AOX-specific inhibitor may then be added to the cuvette if desired and the subsequent rate recorded.
4. Finally, add the purified rSgAOX and record the data until the initial rate has been determined (typically 1 min).
5. To ascertain specific (and therefore total) activity, use the slope of the graph corresponding to the initial rate and subtract any slope value corresponding to auto-oxidation of substrate.

3.6 Preparing Purified rSgAOX Protein for Circular Dichroism

1. In order to replace the elution buffer present in the eluate fraction, concentrate one or more eluate fractions by adding a 50 % (w/v) PEG-6000 solution in a drop-wise manner until the solution becomes turbid.
2. Centrifuge the solution at 13,000 × *g* for 30 min at 4 °C and gently aspirate the supernatant.
3. The pellets should then be stored at −80 °C as soon as possible and the pellets should be resuspended in 0.04 % (w/v) DDM before use for circular dichroism experiments (*see* **Note 10**).

3.7 Size-Exclusion Chromatography Analysis

1. In order to provide a minimum of 1.5 mg/mL purified protein, concentrate several pooled and purified eluate fractions from Subheading 3.3, **step 10**, by adding a 50 % (w/v) PEG-6000 solution in a drop-wise manner until the solution becomes turbid.
2. Centrifuge the solution at 13,000 × *g*, 4 °C, for 30 min and gently aspirate the supernatant.
3. Resuspend in 50 mM Tris–HCl, 10 mM pyruvate, and 100 mM magnesium sulfate 0.03 % (w/v) DDM, pH 7.5 (*see* **Note 11**) for crystallographic screening.
4. Place 105 μL of the protein sample into a microcentrifuge tube and add 45 μL of the detergent stock solution for each detergent to be tested. The final concentration of the detergents is 3× the CMC. A sample with DDM should be always included as reference.
5. Incubate overnight with gentle mixing at 4 °C.
6. The concentrated sample is centrifuged, 10,000 × *g*, 4 °C, for 15 min. Remove precipitant if necessary.
7. Load the sample onto the column via a 0.5-mL injection loop. The elution condition is as follows: with a flow rate of 0.3–0.4 mL/min, the elution volume is equivalent to one column volume (~24 mL). The eluate is collected by a fraction collector (0.4 mL/tube). The sample should be tested in order of instability: that is, the sample incubated with the smallest detergent is tested first and with the largest detergent last. A typical flow rate is 0.3–0.4 mL/min; elute with one column volume (24 mL).
8. Analyze the profile of the chromatograms as indicated in Fig. 1.

3.8 Crystallization of AOX

1. Concentrate the purified sample from Subheading 3.3, **step 10**, to 0.5 mL using an Amicon Ultra-4 (MWCO 50 kDa).
2. The concentrated sample is centrifuged for 15 min 10,000 × *g*, at 4 °C. Remove precipitant if present.
3. Load the sample onto an SEC column. Analyze the peak fractions corresponding to rSgAOX by SDS-PAGE and decide which fraction to use. Combine and pool the fractions.
4. Determine the protein concentration.
5. The pooled sample is concentrated to the desired concentration (>5 mg/mL) with an Amicon Ultra-4 (MWCO 50 kDa). The optimum concentration is protein dependent; however 10 mg/mL is a good starting point if possible.
6. The concentrated sample is centrifuged for 15 min at 10,000 × *g* at 4 °C. Remove precipitant if present.

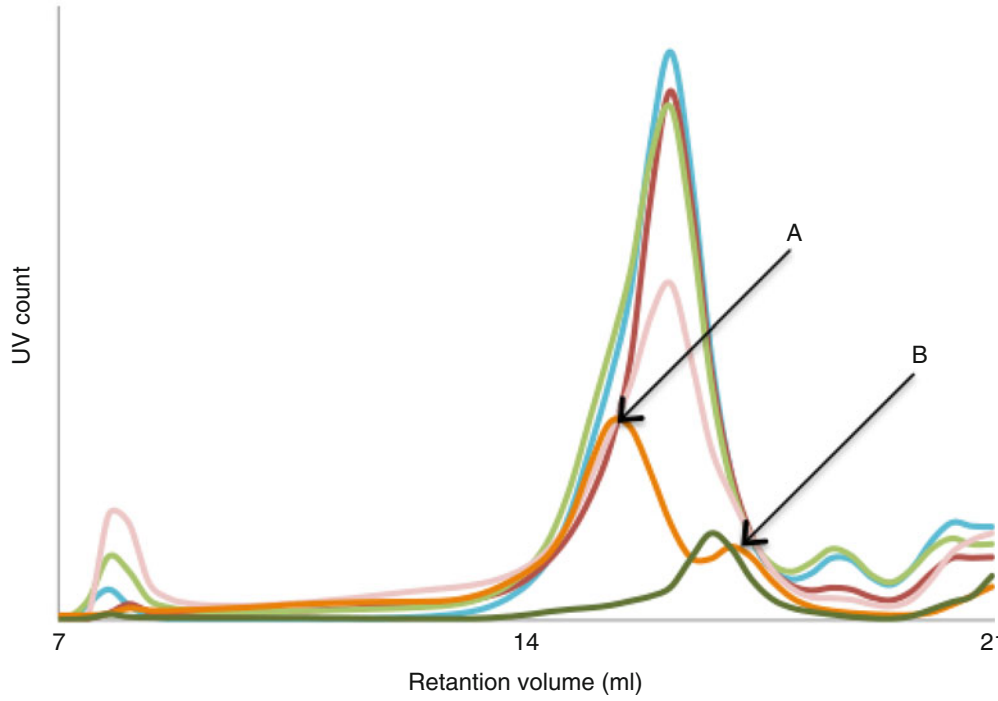

Fig. 1 Overlaid chromatograms of SEC runs of purified SgAOX samples incubated with various detergents at 4 °C. DDM → LDAO, DMNG, DM → OGNG, OG. SgAOX was eluted from 12 to 15 mL. Peaks around 8.5 mL indicate some aggregation. From the shapes and the peak heights, SgAOX is reasonably stable in DDM, LDAO, and DMNG. Two peaks (*see arrows* **A** and **B**) in the profile with OGNG suggest that two SgAOX species exist. These might represent dimer and monomer or some degraded molecules. The chromatogram showed clear differences between detergents which can be used to evaluate the relative stability of the sample in other detergents outlined in this method

7. Each of the 96 wells in an MRC plate is filled with 85 μL of each screening solution from a choice of commercially available crystallization screening kits.
8. Set up a crystallization screen plate with a mosquito robot. Follow the standard protocol of the machine. The plate prepared in **step 7** is set on the mosquito and the protein sample is dispensed to the designated place on the plate. The robot first aspirates the protein solution, dispense 0.1 μL to each top well, then aspirates 0.1 μL of the bottom solutions, and dispenses to the top well where the protein and bottom solutions are mixed. The MRC plate is removed from the robot and sealed with a transparent film. The plate is stored in an observation system and observed immediately after the setting up, followed by further observations after 1 day, 2 days, 5 days, 1 week, 2 weeks, and 1 month (*see* **Note 12**).

3.9 Homology Modeling of the AOX

1. In order to construct a homology model of the AOX, the protein sequence (the target sequence, in FASTA format) should first be aligned to a template sequence of a closely related protein with known structure (such as TAO; Q26710 and 3VV9) using a multiple alignment program such as Clustal Omega.[1]
2. The alignment should then be manually appraised to ensure a high-quality matching of conserved regions.
3. The alignment may then be submitted to a homology modeling program or server, such as SWISS-MODEL,[2] using the alignment project mode.
4. Following the modeling output and automatic evaluation, the structure should then be further evaluated both heuristically and using an algorithm such as ProSA-web.[3]
5. The model may then be viewed in a molecular viewing program such as PyMOL[4] (Fig. 2).

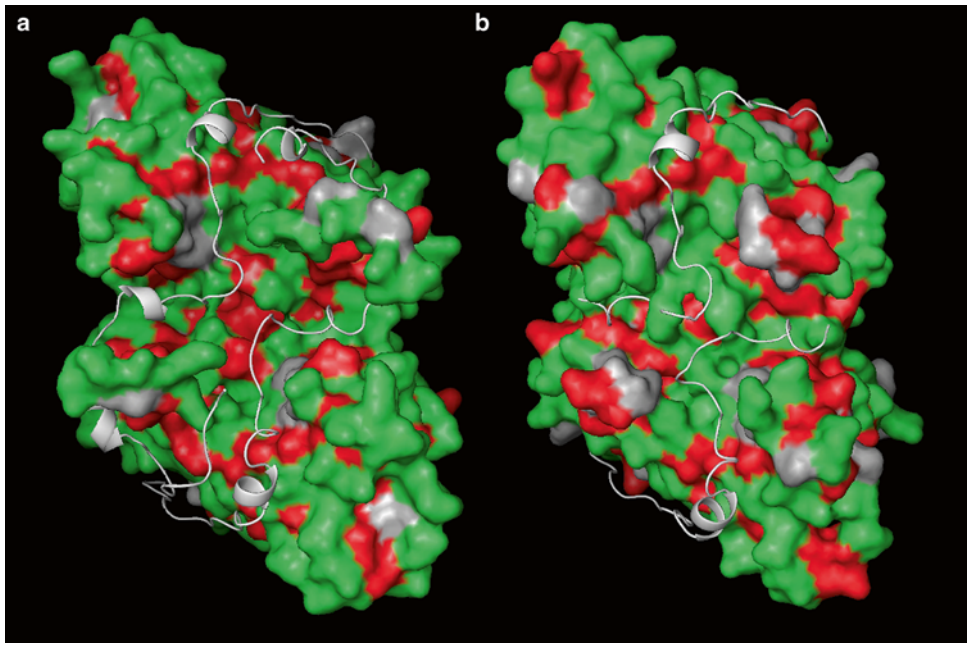

Fig. 2 A comparison of the structure of the trypanosomal and *Sauromatum* AOX. (**a**) Represents TAO, pdb 3VV9, and (**b**) represents subsequent homology model of *S. guttatum* AOX, P22185, created using the protocol defined in Subheading 3.9. In these representations, the solvent-facing surface is shown, with *green* indicating hydrophilic residues and *red* hydrophobic residues. The unstructured N-terminal regions of each monomer for both TAO and the *S. guttatum* homology model are shown in *white*. These diagrams were created using PyMOL

[1] http://www.ebi.ac.uk/Tools/msa/clustalo/
[2] http://swissmodel.expasy.org/
[3] https://prosa.services.came.sbg.ac.at/prosa.php
[4] http://www.pymol.org/

6. Ideally, the process should be repeated with a number of different template sequences to ascertain which is the best template from which to create an accurate homology model (*see* **Note 13**).

4 Notes

1. All AOX *S. pombe* constructs are based on pREP1 with selection for leucine prototrophy.
2. As an alternative to cobalt affinity resin, nickel affinity resin may be used if it is more practical. Both resins performed equally efficiently when purifying the 6-histidine-tagged recombinant *S. guttatum* AOX expressed in FN102.
3. Regarding the chromatography system, any standard system may be used; however, an auto-sampler speeds up these experiments. Ideally, the experiment is performed in a cold room, in particular when many samples are tested or the protein is unstable.
4. It is advisable to examine cells under the microscope to check for contamination before setting up large 1 L cultures.
5. Batches of Zymolyase-20 T can vary in activity, so it may be necessary to adjust mg/g.
6. Use clean tubes that have not been washed in detergent.
7. The time taken for the culture flasks to reach the correct optical density will vary from isoform to isoform, depending on how efficient each isoform is at "rescuing" the haem-deficient cells. Extra time should be allowed for underactive isoforms which may be predicted to have reduced activity. Furthermore, different recombinant AOX isoforms required different IPTG concentrations for efficient induction; therefore, it is recommended that IPTG concentrations (25 μM for SgAOX and 100 μM for TAO) should be screened when attempting to purify a recombinant AOX for the first time.
8. This process may be carried out at room temperature if the protein is stable. It is recommended that a 4 °C environment is used if the protein stability is unknown.
9. If the recombinant protein is not binding to the resin (i.e., most of the protein activity is present in the flow-through fraction, rather than the eluate fraction), the column may be mixed by gentle inversion where practical, at 4 °C, for up to 1 h.
10. While 0.04 % (w/v) DDM proved to be the best buffer for circular dichroism experiments using rSgAOX, other buffers may be used, provided that the protein retains its conformational shape. *See* ref. 33 for a comprehensive guide to preparing protein samples for circular dichroism spectroscopy and for an account of CD data analysis of membrane proteins [34].

11. While 50 mM Tris–HCl, 10 mM pyruvate, 100 mM magnesium sulfate, and 0.03 % (w/v) DDM, pH 7.5 have proved to be the best buffer for crystallographic screening in the case of rSgAOX, other buffers may be used provided that the protein remains active and stable. One recommendation is that the detergent concentration should be kept to a minimum in order to increase the likelihood of producing stable, diffraction-quality crystals. *See* ref. 35 for a review for SEC, ref. 36 on the challenges and solutions for the production of membrane protein crystals, as well as ref. 20, 37 for previous successful crystal production with small monotopic membrane proteins.
12. It is highly recommended that two identical plates be set up which can be stored at 20 °C and 4 °C, respectively, for each screening kit. In this experiment, 12 μL of the protein solutions is required to complete one plate. Hence the purification volume will need to be scaled up based upon the estimation of the protein sample required. A plate can be set up manually with multichannel pipettes with a larger dispensing volume and observed under a light microscope. Plates incubated at 4 °C should be observed in the cold room as temperature changes introduce condensation.
13. In the case of AOX, structural data was not available until 2013 [20]. In lieu of structural data, homology models were constructed using members of the closely related di-iron carboxylate family as templates, such as Δ^9-desaturase [38–40].

Acknowledgements

M.I. is supported by Wellcome Trust [099165/Z/12/Z] whereas A.L.M. gratefully acknowledges BBSRC and the University of Sussex for financial support. L.Y. and B.M. gratefully acknowledge the University of Sussex and J.S. the BBSRC (CASE Award) for studentship support.

References

1. Moore AL, Shiba T, Young L et al (2013) Unraveling the heater: new insights into the structure of the alternative oxidase. Annu Rev Plant Biol 64:637–663
2. McDonald AE, Vanlerberghe GC (2006) Origins, evolutionary history, and taxonomic distribution of alternative oxidase and plastoquinol terminal oxidase. Comp Biochem Physiol Part D Genomics Proteomics 1:357–364
3. Chaudhuri M, Hill GC (1996) Cloning, sequencing and functional activity of the *Trypanosoma brucei brucei* alternative oxidase. Mol Biochem Parasitol 83:125–129
4. Suzuki T, Hashimoto T, Yabu Y et al (2004) Direct evidence for cyanide-insensitive quinol oxidase (alternative oxidase) in apicomplexan parasite *Cryptosporidium parvum*: phylogenetic and therapeutic implications. Biochem Biophyl Res Commun 313:1044–1052
5. Standley DM, van der Giezen M (2012) Modeling the alternative oxidase from the human pathogen Blastocystis using automated hybrid structural template assembly. Res Rep Biochem 2:1–8
6. Yabu Y, Yoshida A, Suzuki T et al (2003) The efficacy of ascofuranone in a consecutive

treatment on *Trypanosoma brucei brucei* in mice. Parasitol Int 52:155–164

7. Philips MA (2012) Stoking the drug target pipeline for human African trypanosomiasis. Mol Microbiol 86:10–14
8. Veiga A, Arrabaça JD, Loureiro-Dias MC (2003) Cyanide-resistant respiration, a very frequent pathway in yeast. FEMS Yeast Res 3:239–245
9. Yan L, Li M, Cao Y et al (2009) The alternative oxidase of *Candida albicans* causes reduced fluconazole susceptibility. J Antimicrob Chemother 64:764–773
10. Affourtit C, Heaney SP, Moore AL (2000) Mitochondrial electron transfer in the wheat pathogenic fungus *Septoria triciti*—on the role of alternative respiratory enzymes in fungicide resistance. Biochim Biophys Acta 1459:291–298
11. Moore AL, Bonner WD, Rich PR (1978) The determination of the proton-motive force during cyanide-insensitive respiration in plant mitochondria. Arch Biochem Biophys 186: 298–306
12. Moore AL, Siedow JN (1991) The regulation and nature of the cyanide-resistant alternative oxidase of plant mitochondria. Biochim Biophys Acta 1059:121–140
13. Meeuse BJD (1975) Thermogenic respiration in Aroids. Annu Rev Plant Physiol 26:117–126
14. Meeuse BJD, Raskin I (1988) Sexual reproduction in the arum lily family, with emphasis on thermogenicity. Sex Plant Reprod 1:3–15
15. Hiser C, McIntosh L (1990) Alternative oxidase of potato is an integral membrane protein synthesized *de novo* during aging of tuber slices. Plant Physiol 93:312–318
16. Finnegan PM, Soole KL, Umbach AL (2004) Alternative mitochondrial electron transport proteins in higher plants. In: Day DA, Millar AH, Whelan J (eds) Plant Mitochondria: from genome to function. Kluwer Academic Publishers, London, pp 163–20l
17. Umbach AL, Ng VS, Siedow JN (2006) Regulation of plant alternative oxidase activity: a tale of two cysteines. Biochim Biophys Acta 1757:135–142
18. Carré JE, Affourtit C, Moore AL (2011) Interaction of purified plant alternative oxidase from *Arum maculatum* with pyruvate. FEBS Lett 585:397–401
19. Chaudhuri M, Ott RD, Hill GC (2006) Trypanosome alternative oxidase: from molecule to function. Trends Parasitol 22:484–491
20. Shiba T, Kido Y, Sakamoto K et al (2013) Structure of the trypanosome cyanide-insensitive alternative oxidase, a promising drug target. Proc Natl Acad Sci U S A 110:4580–4585
21. Albury MS, Dudley P, Watts FZ et al (1996) Targeting the plant alternative oxidase protein to *Schizosaccharomyces pombe* mitochondria confers cyanide-insensitive respiration. J Biol Chem 271:17062–17066
22. Kumar AM, Söll D (1992) *Arabidopsis* alternative oxidase sustains *Escherichia coli* respiration. Proc Natl Acad Sci U S A 89:10842–10846
23. Berthold DA (1998) Isolation of mutants of the *Arabidopsis thaliana* alternative oxidase (ubiquinol:oxygen oxidoreductase) resistant to salicylhydroxamic acid. Biochim Biophys Acta 1364:73–83
24. Kido Y, Sakamoto K, Nakamura K et al (2010) Purification and kinetic characterisation of recombinant alternative oxidase from *Trypanosoma brucei brucei*. Biochim Biophys Acta 1797:443–450
25. Elliott C, Young L, May B et al (2014) Purification and characterisation of recombinant DNA encoding the alternative oxidase from *Sauromatum guttatum*. Mitochondrion 19 Pt B:261–8. doi:10.1016/j.mito.2014.03.002
26. Kakizaki Y, Ito K (2013) Engineering plant alternative oxidase function in mammalian cells: substitution of the motif-like sequence ENV for QDT diminishes catalytic activity of *Arum concinnatum* AOX1a expressed in HeLa cells. Appl Biochem Biotechnol 170:1229–1240
27. Miroux B, Walker JE (1996) Over-production of proteins in *Escherichia coli*: mutant hosts that allow synthesis of some membrane proteins and globular proteins at high levels. J Mol Biol 260:289–298
28. Carpenter EP, Beis K, Cameron AD et al (2008) Overcoming the challenges of membrane protein crystallography. Curr Opin Struct Biol 18:581–586
29. Hunte C, von Jagow G, Schagger H (2003) Strategies and techniques. In: Membrane protein purification and crystallisation. A practical guide, 2nd edn. Academic, New York, p 365
30. Ostermeier C, Michel H (1995) Crystallisation of membrane proteins. Curr Opin Struct Biol 7:697–701
31. Healthcare GE (2007) Purifying challenging proteins. GE Healthcare Bio-Science AB, Sweden
32. Albury MS, Affourtit C, Moore AL (1998) A highly conserved glutamate residue (Glu-270) is essential for plant alternative oxidase activity. J Biol Chem 273:30301–30305
33. Greenfield NJ (2006) Using circular dichroism spectra to estimate protein secondary structure. Nat Protoc 1:2876–2890
34. Wallace BA, Lees JG, Orry AJW et al (2003) Analyses of circular dichroism spectra of membrane proteins. Protein Sci 12:875–884

35. Kawate T, Gouaux E (2006) Fluorescence-detection size-exclusion chromatography for precrystallisation screening of integral membrane proteins. Structure 14:673–681
36. Morares I, Evans G, Sanchez-Weatherby J et al (2014) Membrane protein structure determination—the next generation. Biochim Biophys Acta 1838:78–87
37. Iwata M, Lee Y, Yamashita T et al (2012) The structure of the yeast NADH dehydrogenase (Ndi1) reveals overlapping binding sites for water- and lipid-soluble substrates. Proc Natl Acad Sci U S A 109:15247–15252
38. Lindqvist Y, Huang W, Schneider G et al (1996) Crystal structure of Δ^9 stearoyl-acyl carrier protein desaturase from castor seed and its relationship to other di-iron proteins. EMBO J 15:4081–4092
39. Andersson ME, Nordlund P (1999) A revised model of the active site of alternative oxidase. FEBS Lett 449:17–22
40. Berthold D, Andersson ME, Nordlund P (2000) New insight into the structure and function of the alternative oxidase. Biochim Biophys Acta 1460:241–254

INDEX

James Whelan and Monika W. Murcha (eds.), *Plant Mitochondria: Methods and Protocols*, Methods in Molecular Biology, vol. 1305, DOI 10.1007/978-1-4939-2639-8, © Springer Science+Business Media New York 2015

E

F

G

H

I

K

L

M

N

O

P

R

S

T

U

V